Immunomodulatory Effects of Adenoviral CTLA4-EGFP Transfected Dendritic Cells in Allotransplantation.

Ashley Newland

Transplantation Immunology Laboratory
The Queen Elizabeth Hospital

Date of Submission: January 2006

This thesis is submitted in fulfilment of the requirements of the award of PhD in Medicine at The University of Adelaide.

Table of Contents

List of Figures VIII
Publications X
Presentations XI
Declaration XII
Acknowledgements XIII
Abbreviations XIV
Summary XVII

Chapter 1: Review of Literature

1.1. Introduction 2
1.2. T Cell Activation 2
1.3. The Immunological Synapse 3
1.4. The CD28 Costimulatory Pathway 4
1.4.1. CD28 Expression and Function 4
1.4.2. CD28 Biochemical Pathways 5
1.5. CTLA4 Expression, Structure and Function 6
1.5.1 Regulation of CTLA4 expression and distribution 6
1.5.2. The Molecular Structure of CTLA4 8
1.5.3. Functional Characteristics of CTLA4 9
1.5.3.1. The "Proximal Competition" Model of CTLA4 Induced Antagonism 10
1.5.3.2. The "Distal Signaling" Model of CTLA4 Induced Antagonism 11
1.5.3.3. The "Threshold" Model of CTLA4 Induced Antagonism 11
1.5.3.4. The "Attenuation" Model of CTLA4 Induced Antagonism 12
1.5.4. CTLA4 Signaling Pathways 12
1.6. Expression of CD80 and CD86 Ligands 13
1.6.1. CD80 and CD86 Expression 13
1.6.2. CD80 and CD86 Binding to CD28 and CTLA4 14
1.7. Other Regulators of CD28 Costimulation 16
1.8. Interleukin 10 (IL10) Expression, Structure and Function 17
1.8.1. Interleukin 10 Expression 17
1.8.2. The Molecular Structure of IL10 18
1.8.3. The Interleukin 10 Receptor (IL10R) 18
1.8.4. The Functional Characteristics of IL10 19
1.8.5. Viral IL10 20
1.8.6. IL10 Signaling Pathways 21
1.9. Immunology of Transplant Rejection 22
1.9.1. Direct and Indirect Pathways of Allorecognition 22
1.9.2. The Involvement of the Th1/Th2 Paradigm in Transplantation 22
1.10. Mechanisms of Alloreactive T Cell Hyporesponsiveness 24
1.10.1. Anergy 24
1.10.2. Apoptosis and Activation Induced Cell Death (AICD) 25
1.10.3. Generation of and interactions with regulatory T cells 25

1.11. Current Immunosuppressive Treatments to Prevent Transplant Rejection 26
1.12. Inhibition/Blockade of the CD28 Costimulatory Pathway in Transplantation 29
1.12.1. Generation of Soluble CTLA4-Ig Fusion Proteins 29
1.12.2. Blockade of the CD28 Costimulatory Pathway 29
1.12.3. The Effects of CTLA4-Ig on Th1/Th2 Pathways in Allotransplantation 31
1.12.4. IL10 and Transplantation 31
1.12.5. Limitations of Systemic CTLA4-Ig and IL10 Treatments 32
1.13. Dendritic Cells as Gene Therapy Targets to Induce Transplantation Tolerance 33
1.13.1. The Role of Dendritic Cells in Transplantation 33
1.13.2. Genetic Modification of Dendritic Cells 34
1.13.3. Genetically Engineered Dendritic Cells in Tolerance Induction 37
1.14. Targeting Multiple Dendritic Cell Pathways in Allotransplantation 38
1.15. The Ovine Model of Renal Transplantation 40
1.16. Project Aims 42

Chapter 2: General Materials and Methods

2.1. Materials 45
2.1.1. Antibodies 45
2.1.1.1. Anti-Human Antibodies 45
2.1.1.2. Anti-Ovine Antibodies 45
2.1.1.3. Control Antibodies 46
2.1.1.4. Secondary Antibodies 46
2.1.1.5. Other Antibodies 46
2.1.2. Cell Lines 47
2.1.2.1. Bacterial Cell Lines 47
2.1.2.2. Cell Culture Cell Lines 47
2.1.3. Cytokines and Recombinant Proteins 47
2.1.4. Radiochemicals 48
2.1.5. Flow Cytometry Reagents 48
2.1.6. Tissue Culture Reagents 48
2.1.7. Histological Reagents 49
2.1.8. Molecular Biology Reagents 49
2.1.9. Plasmid Vectors 51
2.1.10. Immunoprecipitation Reagents 51
2.1.11. Other Reagents 52
2.2. Solutions and Buffers 53
2.2.1. Agarose Gel Electrophoresis Buffers and Solutions 53
2.2.2. RNA Extraction Buffers and Solutions 53
2.2.3. Cloning and Transfection Buffers and Solutions 54
2.2.4. Tissue Culture Buffers and Solutions 56
2.2.5. Immunoprecipitation Buffers 57
2.2.6. Flow Cytometry Buffers and Solutions 60
2.2.7. Dephosphorylation Buffers and Solutions 60

2.2.8. ELISA Solutions 60
2.2.9. Immunohistology Solutions 61

2.3. General Methods **62**
2.3.1. Cell Culture ***62***
2.3.1.1. Ovine and Human PBMC Extraction 62
2.3.1.2. Human Monocyte Derived Dendritic Cells 62
2.3.1.3. Nylon Wool Isolation of T Cells 63
2.3.1.4. Mixed Lymphocyte Reaction 63
2.3.1.5. Cell Lines 64
2.3.2. Molecular Biology Methods ***64***
2.3.2.1. Total RNA Extraction 64
2.3.2.2. Reverse Transcription (RT) 65
2.3.2.3. Polymerase Chain Reaction (PCR) 65
2.3.2.4. Agarose Gel Electrophoresis 66
2.3.2.5. Endonuclease Resriction Digestion of DNA 67
2.3.2.6. Agarose Gel Purification of Restriction Digest Products 67
2.3.2.7. Ultraclean™ Purification of DNA 68
2.3.2.8. Ligation of DNA Fragments into Cloning Vectors 68
2.3.2.9. Dephosphorylation of DNA Fragments 68
2.3.2.10. Preparation of Competent *E. Coli* TGF1α and DH10β Cells 69
2.3.2.11. Transformation of Competent *E.Coli* Cells 69
2.3.2.12. Plasmid Mini-preparation (Mini-prep) 70
2.3.2.13. Plasmid Midi-preparation (Midi-prep) 70
2.3.2.14. DNA Sequencing 71
2.3.2.15. Transfection of CHO cells with Purified Plasmids 71
2.3.3. Adenoviral Methods ***72***
2.3.3.1. Preparation of Electrocompetent BJ5183 Cells 72
2.3.3.2. Electrotransfection of BJ5183 Cells 72
2.3.3.3. Screening of Colonies for Homologous Recombination 73
2.3.3.4. Transformation of DH10β *E.Coli* cells 73
2.3.3.5. Lipofectamine Transfection of Adenoviral Constucts into HEK-293 Cells 74
2.3.3.6. Preparation of Adenoviral HEK-293 Cell Lysates 74
2.3.3.7. Infection of HEK-293 Cells and Scale-up Viral Production 75
2.3.3.8. Caesium Chloride (CsCl) Density Gradient Purification of Adenoviral Particles 75
2.3.3.9. Dialysis of CsCl Purified Adenoviral Particles 76
2.3.3.10. Cytopathic Effect Assay (CPE) Quantitation of Adenoviral Titers 77
2.3.4. Flow Cytometry ***77***
2.3.4.1. Cell Surface Staining 77
2.3.4.2. FITC-Dextran Assay 78
2.3.5. Histochemistry ***78***
2.3.5.1. Biopsy Preparation 78
2.3.5.2. Hematoxylin and Eosin Staining 79
2.3.5.3. Immunohistochemistry 79
2.4. Centifuges **80**

Chapter 3: Immunomodulation of the Human DC-MLR by Combined IL10 and CTLA4-Ig Treatment

3.1. Introduction ***82***
3.2. Materials and Methods ***84***
3.2.1. Preparation of Cell Populations 84
3.2.2. Monoclonal Antibodies and Flow Cytometry 85
3.2.3. Proliferation Assays 85
3.2.4.Restimulation Assay 86
3.2.3. CFSE-MLR 86
3.3. Results ***87***
3.3.1. Phenotype of Human Monocyte-Derived DC and Associated Function 87
3.3.2. Immunomodulatory Properties of IL10 and CTLA4-Ig 87
3.3.3. Combined Treatment with IL10 and CTLA4-Ig in the DC-MLR Induces T Cell Hyporesponsiveness 89
3.3.4. $CD4^+$ and $CD8^+$ T cell Proliferation is Inhibited by IL10 and CTLA4-Ig in the CFSE-MLR 89
3.3.5. T Cells Stimulated by DC in the Presence of CTLA4-Ig in Combination with IL10 are Hyporesponsive to Restimulation 90
3.3.6. IL10 and CTLA4-Ig Mediated Inhibition of the DC-MLR is not Dependent on $CD4^+CD25^+$ Regulatory T Cells 90
3.3.7. NK Cells are Required for the Inhibition of T Cell Proliferation by Sub-Optimal Doses of IL10 and CTLA4-Ig 91
3.3.8. NK Cells Influence DC Function 92
3.3.9. NK Cells Prime $CD4^+$ T Cell Proliferation in a CTLA4-Ig Sensitive Manner 93
3.4. Discussion ***94***

Chapter 4: Isolation and Characterisation of Ovine DC Derived from Afferent Lymph

4.1. Introduction ***103***
4.1.1. Isolation of Ovine Dendritic Cells from Lymph Nodes Draining the Skin 103
4.1.2. *In vivo* Properties of Dendritic Cells 104
4.2. Materials and Methods ***107***
4.2.1. Cannulation 107
4.2.2. Metrizamide Purification of Ovine DC from Lymph 107
4.2.3. Flow Cytometry 108
4.2.4. Dendritic Cell Mixed Lymphocyte Reaction 108
4.2.5. PKH26 Labeling 109
4.2.6. Normal Lymphocyte Transfer Reaction 109
4.2.7. Immunohistological Analysis of Skin Biopsies 110
4.2.8. RNA Extraction from Skin Biopsies and PCR analysis of IL-2 mRNA Expression 110

4.2.9. Mitomycin C Treatment of PBMC 110
4.2.10. Sensitisation Assay 111
4.3 Results ***112***
4.3.1. Phenotype of Ovine Pseudo-Afferent Derived DC 112
4.3.2. Stimulatory Capacity of Ovine DC 112
4.3.3. Dendritic Cells Rapidly Migrate to the Draining Lymph Node 113
4.3.4. Intradermal Injection of Allogeneic DC and PBMC Elicits a Strong NLT Response 113
4.4. Discussion ***115***

Chapter 5: Generation of an Adenoviral Ovine CTLA4-EGFP Construct and the Immunomodulatory of Transduced DC

5.1. Introduction ***120***
5.2. Methods ***124***
5.2.1. Cloning of the Extracellular Domain of Ovine CTLA4 124
5.2.2. Generation of Adenoviral Constructs 124
5.2.3. Preparation of CTLA4-EGFP Fusion Proteins 125
5.2.4. Immunoprecipitation from Infected Fibroblasts 125
5.2.5. Quantification of EGFP and CTLA4-EGFP Fusion Proteins by ELISA 126
5.2.6. CTLA4-EGFP Binding Assay 127
5.2.7. Two-Way Mixed Lymphocyte Reaction 128
5.2.8. Genetically Modified DC as Stimulators in the MLR 128
5.3. Results ***129***
5.3.1. Generation and Characterisation of Fusion Protein Constructs 129
5.3.2. Generation and Characterisation of Adenoviral Constructs 129
5.3.3. Adenoviral Transfection of Ovine Fibroblasts 130
5.3.4. Secretion and Function of Ovine CTLA4-EGFP from Adenovirally Infected Fibroblasts 131
5.3.5. Binding of CTLA4-EGFP to Ovine and Human DC 131
5.3.6. Adenoviral CTLA4-EGFP Transfected DC have Reduced Allostimulatory Capacity 132
5.4. Discussion ***134***

Chapter 6: Immunomodulatory Function of Ovine DC Transfected with Adenoviral CTLA4-EGFP in a Reconstituted NOD-*scid* Model of Ovine Skin Rejection

6.1. Introduction ***141***
6.2. Methods ***144***
6.2.1. NOD-*scid* mice 144
6.2.2. Harvesting of Ovine Skin 144
6.2.3. Grafting of Ovine Skin 144
6.2.4. Intraperitoneal Challenge with Allogeneic Ovine PBMC and DC 145
6.2.5. Adenoviral Transfection of Ovine DC 146
6.2.6. ELISA Quantification of CTLA4-EGFP and EGFP 146

6.2.7. Histological Analysis of Skin Biopsies 146
6.2.8. Rejection Scores 147
6.3. Results ***148***
6.3.1. Ovine Skin Engraftment in NOD-*scid* Mice 148
6.3.2. Injection of Allogeneic DC and PBMC Provokes Rejection of Ovine Skin Allografts 148
6.3.3. Dendritic Cells Transfected with Adenoviral Vectors Migrate to the Skin Graft after Intraperitoneal Injection 149
6.3.4. Injection of Donor-Specific Ovine DC Transfected with Adenoviral CTLA4-EGFP Protects Ovine Skin Grafts from Rejection 149
6.4. Discussion ***151***

Chapter 7: Concluding Remarks
7.1. Concluding Remarks and. Future Directions ***157***

Appendices
Appendix 1. Primers 165
Appendix 2. Adenoviral Vectors 166
Appendix 3. Ovine CTLA4 Sequence from CTLA4-EGFP 167
Appendix 4. Ovine CTLA4-Ig Sequence 168
Appendix 5. Ovine IL10 Sequence from IL10-DsRED2 169

Reference List: **170**

List of Figures

Chapter 1

Figure 1.1. CD28 costimulatory interactions and the involvement of CTLA4 in T cell regulation
Figure 1.2. Integrated and divergent intracellular signaling pathways of the TCR and CD28
Figure 1.3. The CD80/86 binding domain of CTLA4 is distal to the dimer interface
Figure 1.4. Two Models of CTLA4 Antagonism of T Cell Activation
Figure 1.5. Influence of CTLA4 intracellular signaling pathways on TCR and CD28 signals
Figure 1.6. Influence of IL10 on T cell receptor signaling pathways
Figure 1.7. Direct and Indirect Pathways of Allorecognition
Figure 1.8. Regulation of Th1 and Th2 cells and influence of exogenous IL10
Table 1.1. Current immunosuppressive drugs, their targets and specific side-effects
Table 1.2. Advantages and disadvantages of gene therapy techniques

Chapter 3

Figure 3.1. Characterisation of human monocyte-derived dendritic cells
Figure 3.2. Titration of CTLA4-Ig and IL10
Figure 3.3. CTLA4-Ig blockade is reversed by treatment with anti-CTLA4 mAb
Figure 3.4 The effect of CTLA4-Ig and IL10 on the differentiation of DC from monocytes.
Figure 3.5 Effect of CTLA4 and IL10 on TNFα induced DC maturation.
Figure 3.6 Combined treatment of the DC-MLR with IL10 and CTLA4-Ig.
Figure 3.7 CTLA4 and IL10 inhibit proliferation of CFSE labeled T cells in the DC-MLR
Figure 3.8 T cells cultured with IL10 and CTLA4-Ig in the primary DC-MLR are hypo-responsive to restimulation.
Figure 3.9 $CD4^+CD25^-$ T cells are unresponsive to sub-optimal IL10 and CTLA4-Ig treatment and are not influenced by repletion with $CD4^+CD25^+$ T_{reg} cells.
Figure 3.10 Isolation of $CD4^+$ T cells and $CD56^+$ NK cells
Figure 3.11 NK cells restore the capacity of CTLA4-Ig and IL-10 to inhibit $CD4^+$ responder cells in the MLR.
Figure 3.12: NK cells stimulate allogeneic DC lysis, activation and sensitivity to sub-optimal doses of CTLA4-Ig/IL10
Figure 3.13 NK cells prime CD4 T cell proliferation.

Chapter 4

Figure 4.1. Characterisation of ovine DC obtained by pseudo-afferent cannulation
Figure 4.2. Ovine DC stimulate the proliferation of alloreactive PBMC
Figure 4.3. Intradermally injected DC rapidly migrate to the draining lymph node
Figure 4.4. The Allogeneic NLT reaction induces an indurated lesion at the site of injection
Figure 4.5. Quantification of lesion induration in the NLT reaction.

Figure 4.6. The allogeneic NLT reaction is characterised by extensive lymphocyte infiltration
Figure 4.7. Infiltrates of the allogeneic NLT reaction consist of both $CD4^+$ and $CD8^+$ cells.
Figure 4.8. The NLT Reaction results in a systemic sensitisation to NLT donor antigen

Chapter 5

Figure 5.1. Schematic representation of adenoviral CTLA4-EGFP construction
Figure 5.2. Cloning of ovine CTLA4-EGFP
Figure 5.3. Cloning of ovine CTLA4-Ig
Figure 5.4. Conditioned media from CTLA4-EGFP and CTLA4-Ig Electroporated cells in the ovine two-way MLR
Figure 5.5. *Pac*I Restriction Digest Screening of Clones for Homologous Recombination Between pShuttleCMV and pAdEasy1 Vectors.
Figure 5.6. Assessment of the fluorescence of AdCTLA4-EGFP and AdEGFP transduced ovine fibroblasts.
Figure 5.7. Immunoprecipitation of CTLA4-EGFP from infected fibroblast
Figure 5.8. Dose-response inhibition of a two-way MLR by CTLA4-EGFP
Figure 5.9. Binding of ovine CTLA4-EGFP to ovine and human DC
Figure 5.10. AdCTLA4-EGFP Transduced ovine and human DC inhibit the MLR
Figure 5.11. Effect of adenoviral transfection on human DC cell-surface marker expression

Chapter 6

Figure 6.1. Schematic representation of skin grafting and immune reconstitution of NOD-*scid* mice.
Figure 6.2. Ovine Skin Engraftment onto NOD-*scid* Mice
Figure 6.3. Lymphocyte Infiltrate after Autologous and Allogeneic Immune Reconstitution.
Figure 6.4. Lymphocyte infiltrates of ovine skin after autologous and allogeneic challenge of NOD-*scid* mice consist of $CD4^+$ and $CD8^+$ T cells.
Figure 6.5. Quantitative analysis of lymphocyte infiltrates in ovine skin exposed *in vivo* to autologous or allogeneic challenge
Figure 6.6. ELISA quantification of CTLA4-EGFP and EGFP from transfected DC and serum from NOD-*scid* mice treated with transfected DC
Figure 6.7. Adenoviral CTLA4-EGFP transfected ovine DC migrate to the ovine skin allograft in NOD-scid mice
Figure 6.8. Ovine skin from NOD-*scid* mice treated with AdCTLA4-EGFP transfected ovine DC demonstrate reduced lymphocyte infiltration compared with AdEGFP transfected control DC.
Figure 6.9. Quantitative analysis of lymphocyte infiltration in ovine skin exposed *in vivo* to allogeneic challenge and treated with AdCTLA4-EGFP or AdEGFP transfected ovine DC.

Publications

- **Newland A.M.**, Russ G., Krishnan R. (2006). NK cells prime the responsiveness of autologous $CD4^+$ T cells to CTLA4-Ig and IL10 mediated inhibition in an allogeneic dendritic cell-MLR. *Immunology (Accepted for publication 16/01/06).*

- **Newland A.M.**, Kireta S., Russ G., Krishnan R. (2004). Ovine Dendritic Cells Transduced with an Adenoviral $CTLA4_e$EGFP Fusion Protein Construct Induce Hyporesponsiveness to Allostimulation. *Immunology.* **113:** 310-317.

- **Newland A.M.**, Russell C., Russ G., Krishnan R. (2004). The Normal Lymphocyte Transfer Reaction in a Large Animal Model to Investigate in-vivo Alloreactivity. *Immunology and Cell Biology.* **82:** (suppl.) A19.

- **Newland A.M.**, Russ G., Krishnan R. (2004). Synergistic Inhibition of Costimulatory Pathways as a Strategy to Inhibit Allograft Rejection. *Transplantation.* **78:** 539.

Presentations

2005

- Transplantation Society of Australia and New Zealand Annual Scientific Meeting (Canberra, Australia), "B7 COSTIMULATORY BLOCKADE COMBINED WITH IL10 AUGMENTS DENDRITIC CELL MEDIATED HYPORESPONSIVENESS IN T CELLS."

2004

- XX International Congress of the Transplantation Society (Vienna, Austria), "SYNERGISTIC INHIBITION OF COSTIMULATORY PATHWAYS AS A STRATEGY TO INHIBIT ALLOGRAFT REJECTION."

- Transplantation Society of Australia and New Zealand Annual Scientific Meeting (Canberra, Australia), "THE NORMAL LYMPHOCYTE TRANSFER REACTION IN A LARGE ANIMAL MODEL TO INVESTIGATE *IN-VIVO* ALLOREACTIVITY."

2003

- The Queen Elizabeth Hospital Research Day (Adelaide, Australia), "THE NORMAL LYMPHOCYTE TRANSFER REACTION AS A MODEL OF *IN-VIVO* ALLOREACTIVITY."

- Australian Society of Medical Research National Conference (Adelaide, Australia), "THE NORMAL LYMPHOCYTE TRANSFER REACTION AS A MODEL OF *IN-VIVO* ALLOREACTIVITY."

2002

- Australasian Society of Immunology Student Awards (Adelaide, Australia), "SYNERGISTIC INHIBITION OF ALLOIMMUNITY WITH CTLA4-EGFP AND IL-10: GENE THERAPY APPLICATIONS IN A RENAL TRANSPLANT MODEL."

- The Queen Elizabeth Hospital Research Day (Adelaide, Australia), "SYNERGISTIC INHIBITION OF COSTIMULATORY PATHWAYS AS A STRATEGY TO INHIBIT ALLOGRAFT REJECTION"

- AusBiotech National Conference (Melbourne, Australia), "STUDIES OF THE IMMUNOMODULATORY EFFECTS OF AN OVINE CTLA4-EGFP FUSION PROTEIN USING ADENOVIRAL VECTORS."

Declaration

This work contains no material which has been accepted for the award of any other degree or diploma in any university or other tertiary institution and, to the best of my knowledge and belief, contains no material previously published or written by another person, except where due reference has been made in the text.

I give consent to this copy of my thesis, when deposited in the University Library, being available for loan and photocopying.

Ashley Newland

Acknowledgments

First I would like to acknowledge my supervisors Doctor Ravi Krishnan and Associate Professor Graeme Russ. In particular to Ravi for his guidance and for always making himself available to bounce ideas off or discuss relevant papers.

I am also grateful to all the staff and students in the Transplantation Immunology Laboratory at TQEH for their support. In particular to Svjetlana and Emma for their patience and willingness to help.

I am exceptionally appreciative of Kidney Health Australia (formally known as the Australian Kidney Foundation) for providing me with a biomedical research scholarship.

Dr Chris Russell is particularly noted and thanked for providing her time and expertise to operate on my wooly patients, performing numerous cannulations and providing me with valuable ovine DC. Geoff Dandy is also acknowledged for sharing his experience with cannulations and helping us trouble-shoot problems.

Thanks also to Adrian from TQEH Animal House for taking good care of my sheep, providing me with almost limitless blood for experiments and for the removal of numerous lymph nodes.

I would also like to thank my family and friends for their support throughout the whole PhD and in particular to Nicole for her patience throughout the write-up process.

Abbreviations

µF	Micro Farrads
aa	Amino acid
Ad(prefix)	Adenoviral
APC	Antigen Presenting Cell
bp	Base Pair
cDNA	Complementary DNA
CDR	Complementarity Determining Region
CHO	Chinese Hamster Ovary
Ci	Curie
CIP	Calf Intestinal Phosphatase
Con A	Concanavalin A
CPM	Counts Per Minute
CTL	Cytotoxic T Lymphocyte
CTLA4	Cytotoxic T Lymphocyte Associated Antigen 4
DC	Dendritic Cell
DNA	Deoxyribonucleic Acid
dNTP	Deoxynucleotide Triphosphate
E.	*Eschericia*
EDTA	Ethylenediaminetetraacetic Acid
EGFP	Enhanced Green Fluorescent Protein
FCS	Foetal Calf Serum
FITC	Fluoroscein Isothiocyanate
g	gravities (Centrifugal Force)
GFP	Green Fluorescent Protein
GM-CSF	Granulocyte/Macrophage Colony Stimulating Factor
h	hour
hr(prefix)	Human Recombinant….
Hu	Human
IL-	Interleukin-

Ig	Immunoglobulin
Kb	Kilobase
kDa	Kilodaltons
L	Ligand
LB	Luria Broth
M	Molar
MCS	Multiple Cloning Site
MHC	Major Histocompatibility Complex
min	Minute
µl	Microlitre
ml	Millilitre
MLR	Mixed Lymphocyte Reaction
MMLV	Moloney Monkey Leukaemia Virus
MOI	Multiplicity of Infection
mRNA	Messenger RNA
NF-κβ	Nuclear Factor κβ
NK	Natural Killer
nm	Nanometre
OD	Optical Density
O/N	Overnight
Ov	Ovine
PBMC	Peripheral Blood Mononuclear Cells
PBS	Phosphate Buffered Saline
PCR	Polymerase Chain Reaction
r	Recombinant
RNA	Ribonucleic Acid
rpm	Revolutions per minute
RT	Reverse Transcription
SDS-PAGE	Sodium Dodecyl Sulphate-Polyacrylamide Gel Electrophoresis
sec	Second
sH_2O	Sterile water

siRNA	Short-interfering RNA
S/R	Stimulator/Responder
TCR	T Cell Receptor
TNF	Tumour Necrosis Factor
U	Units
UV	Ultraviolet
V	Volt
w/v	Weight to Volume ratio
vs	Versus
v/v	Volume to Volume ratio

Summary

T cell activation occurs by the recognition of antigens presented by antigen presenting cells in the presence of sufficient CD28 costimulation. CTLA4 fusion proteins and interleukin 10 (IL10) are able to abrogate CD28 costimulation and therefore T cell activation. This thesis investigates the combined activity of these agents on allo-immunity and characterises the development of a gene therapy strategy utilising dendritic cells (DC) as a cellular vehicle to deliver CTLA4 fusion proteins.

Chapter 3 describes the effect of combined treatment of the DC-MLR with suboptimal doses of CTLA4-Ig and IL10. Inhibition of the MLR was augmented using the combination of the agents and interestingly a key role for Natural Killer (NK) cells in sensitising both DC and T cells to the inhibitory function of CTLA4-Ig and IL10 at low concentrations was highlighted.

Chapter 4 details the isolation and characterisation of ovine DC obtained by cannulation of the afferent lymphatics of the prefemoral lymph node of sheep. Importantly the isolated DC were potent allo-stimulators of the DC-MLR *in vitro* and were able to rapidly migrate to secondary lymphoid tissues upon *in vivo* administration. Moreover the intradermal injection of allogeneic DC and lymphocytes provoked a strong cutaneous reaction, confirming *in vivo* function and supporting the use of these cells for genetic manipulation to induce alloreactive T cell hyporesponsiveness.

Chapter 5 describes the generation of an adenoviral construct encoding a fusion of the extracellular domain of ovine CTLA4 and the gene for Enhanced Green Fluorescent Protein (EGFP). The adenoviral vector was able to infect both fibroblasts

and dendritic cells allowing production of CTLA4-EGFP proteins and detection of CTLA4-EGFP expression in transfected cells by virtue of the inherent fluorescence of EGFP. CTLA4-EGFP was able to bind to the CD80/86 ligands expressed on DC resulting in alloreactive T cell hyporesponsiveness. Moreover both ovine and human DC transfected with the adenoviral CTLA4-EGFP construct were able to inhibit the DC-MLR providing *in vitro* proof of concept and supporting the assessment of adenoviral CTLA4-EGFP transduced DC in an *in vivo* model of alloreactivity.

In **Chapter 6** an immunocompromised NOD-*scid* model of vascularised ovine skin transplantation was used to test the ability of adenoviral CTLA4-EGFP transduced DC to modify ovine skin allograft rejection after challenge with allogeneic ovine lymphocytes. Adenoviral CTLA4-EGFP transduced DC were able to migrate to the skin allograft and in comparison to DC transfected with the adenoviral vector blank control, inhibited rejection of the skin allograft. Moreover the inhibition of rejection was not associated with detectable levels of CTLA4-EGFP in circulation, indicating that adenoviral CTLA4-EGFP transduced DC are able to inhibit alloreactivity without the requirement of systemic immunosuppression. These data indicate that CTLA4-EGFP transduced DC are able to induce alloreactive T cell hyporesponsiveness *in vitro* and *in vivo* and supports further investigation in a preclinical ovine model of renal transplantation.

Chapter 1
Literature Review

1.1. Introduction

The CD28 costimulatory pathway facilitates a major signaling mechanism required for T cell activation. Modulation or ablation of this pathway can inhibit T cell activation which when applied to allogeneic immune responses has the potential to induce tolerance and promote allograft acceptance. The fusion protein, CTLA4-Ig and the cytokine, Interleukin 10 (IL-10) are proteins each capable of modulating the CD28 costimulatory pathway. This review of the literature will provide a background to the structure, expression and immune functions of both proteins with particular focus on how they relate to the CD28 costimulatory pathway and the allostimulatory function of dendritic cells. Since the focus of this thesis is on the application of CTLA4-Ig and IL-10 in the transplantation setting an overview of established and novel immunomodulatory therapies used in particular to prolong allograft transplant acceptance is also depicted.

1.2. T-Cell Activation

Full activation of T cells requires two separate but complementary signals (1). Antigen presenting cells (APC) are able to present antigens in association with Major Histocompatibility Complex (MHC) molecules to T cells. Recognition of these MHC/Antigen complexes by the T cell receptor (TCR) provides the first signal, however this alone is not sufficient for T cell activation. The second signal is provided by interactions between costimulatory molecules on the APC and the T cells including the CD28, CD40, ICOS and OX40 costimulatory molecules. Costimlulatory molecule interactions can reduce the number of engaged TCR required by more than 80% (2), thereby reducing the threshold required for T cell activation. The cross-linking interactions

between CD28 and CD80/CD86 costimulatory molecules provide one of the most important costimulatory pathways. Notably TCR engagement in the absence of sufficient costimulation leads to T cell anergy, which is defined as a state in which the T cell is viable but fails to display functional responses such as proliferation or production of interleukin 2 (IL-2) in response to its specific antigen (3, 4).

Prolonged engagement between the APC and T cell is required to facilitate TCR engagement and costimulation, leading to full T cell activation (5, 6). This requirement is met by the formation of an immunological synapse.

1.3. The Immunological Synapse

The immunological synapse is a term used to describe the complex and highly structured interface between APC and T cells, which facilitates prolonged molecular interactions. The physical organisation of the immunological synapse is characterised by a ring of adhesion molecules, including CD2, CD48, LFA-1 and ICAM-1 molecules which form the peripheral supramolecular activation cluster (p-SMAC) around a central cluster of TCR–peptide–MHC molecules (c-SMAC)(7, 8). The immunological synapse acts to prolong the duration of T cell/APC interactions and associate the necessary signaling molecules to an intimate core (8-10). The importance of the immunological synapse is demonstrated by interference of key molecules including ICAM-1, LFA-1, CD48 and CD2, the disruption of any of which prevents T cell activation (11-13).

1.4. The CD28 Costimulatory Pathway

1.4.1. CD28 Expression and Function

The CD28 costimulatory pathway represents the most potent and best-characterised costimulatory pathway. The functional role played by the CD28 costimulatory pathway is highlighted in CD28 knockout mice. T cells isolated from $CD28^{-/-}$ mice have severely reduced proliferative capacity to allostimulation, antibody stimulation directed against the TCR, and specific antigen stimulation (14-16). *In vivo*, CD28 deficiency also results in reduced immune responses to allograft antigens, graft-versus-host disease and autoimmune disorders, including experimental allergic encephalomyelitis (EAE) and arthritis (17, 18).

CD28 is a membrane-bound glycoprotein constitutively expressed on all murine T cells and on 80% of human T cells (19, 20). CD28 binds to its ligands CD80 and CD86 (**figure 1.1.a**), which are expressed on the surface of APC including monocytes, B lymphocytes and dendritic cells (21). CD28 is able to engage CD80/86 within the central cluster of the immunological synapse (8, 22) and thus acts in close proximity with TCR engagement (9). Despite sharing structural and binding similarities to adhesion molecules (23), CD28 has been shown to offer no additional support to the adhesion of the immunological synapse or directly support TCR engagement, thus its primary purpose appears to be that of costimulation (24). CD28 costimulation lowers the threshold for T cell activation by reducing the number of TCR-MHC interactions required, promotes clonal expansion by upregulation of IL-2, controls T cell differentiation by monitoring IL-4 production (25, 26) and increases T cell survival by up-regulation of the anti-apoptotic protein $Bcl\text{-}_{XL}$ expression (27). CD28 costimulation also upregulates the expression of other

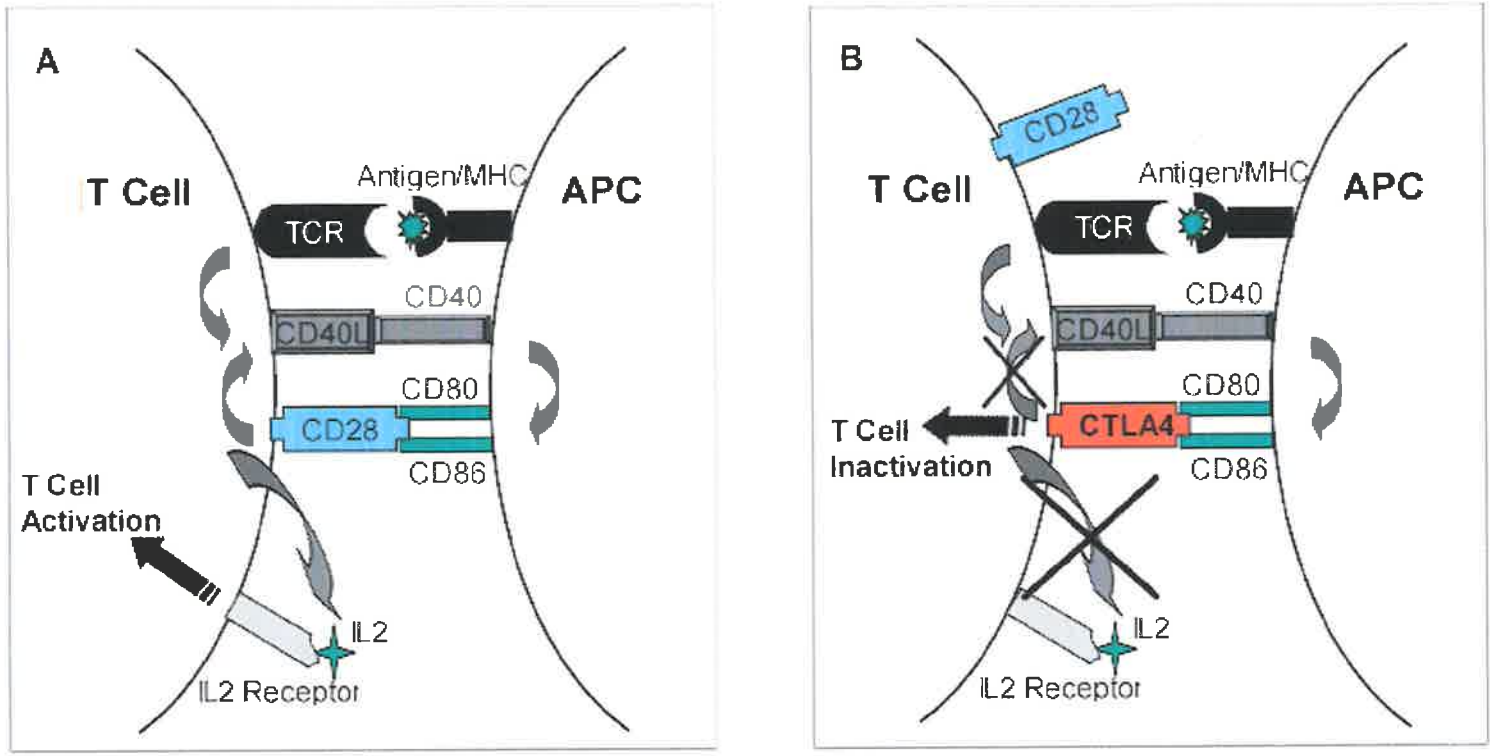

Figure 1.1. CD28 Costimulatory Interactions and the Involvement of CTLA4 in T Cell Regulation

A. Recognition of the antigen/MHC complex by the T cell receptor up-regulates the expression of the CD40 Ligand on the T cell. Subsequent costimulatory interactions between CD40 and the CD40 Ligand up-regulates the expression of CD80 and CD86 molecules on the antigen presenting cell (APC). This facilitates binding to CD28 resulting in the increased production of the CD40 ligand and IL2 by the T cell. IL2 is then able to bind in an autocrine manner activating the T cell.

B. Once expressed on the T cell, CTLA4 binds to CD80 and CD86 in place of CD28 due to its higher binding affinity and inhibits T cell proliferation.

costimulatory molecules such as CD40 ligand and ICOS, which, through the engagement with their respective receptors further enhance the immune response (28, 29).

1.4.2. CD28 Biochemical Pathways

While the biological activity of CD28 costimulation has been well characterised, the precise signal transduction pathways of CD28 remain to be defined. Current literature indicates that CD28 is able to mediate multiple intracellular signals, some of which converge with TCR signaling pathways synergising the induction of multiple transcription factors. These include the activation of the JUN-kinase pathway, the recruitment of phosphatidylinositol-3-kinase (PI3K), the pleckstrin homology domain containing tyrosine kinase Itk, and the activation of the Src family kinase Lck (30-33). CD28-mediated activation of PI3K further induces the recruitment of PKC-θ to the central cluster of the immunological synapse in addition to the nuclear localization of NF-κβ, and upregulation of IL-2 transcription (34). The integration of CD28 costimulatory pathways and TCR signaling are shown in **figure 1.2**.

CD28 costimulation also acts to remove TCR antagonists. Cbl-b proteins, which are negative regulators of tyrosine kinase signaling, bind to the TCR preventing signaling (35, 36). Engagement of CD28 promotes signals which degrade cbl-b on the TCR abrogating its suppressive activity (37). Conversely CTLA4 engagement (**section 1.5**) functions to induce the re-expression of cbl-b which may then retarget the signaling domains of the TCR (37).

While the exact signaling mechanisms of CD28 costimulation are still under investigation, it is clear that CD28 engagement in conjunction with TCR signaling leads to

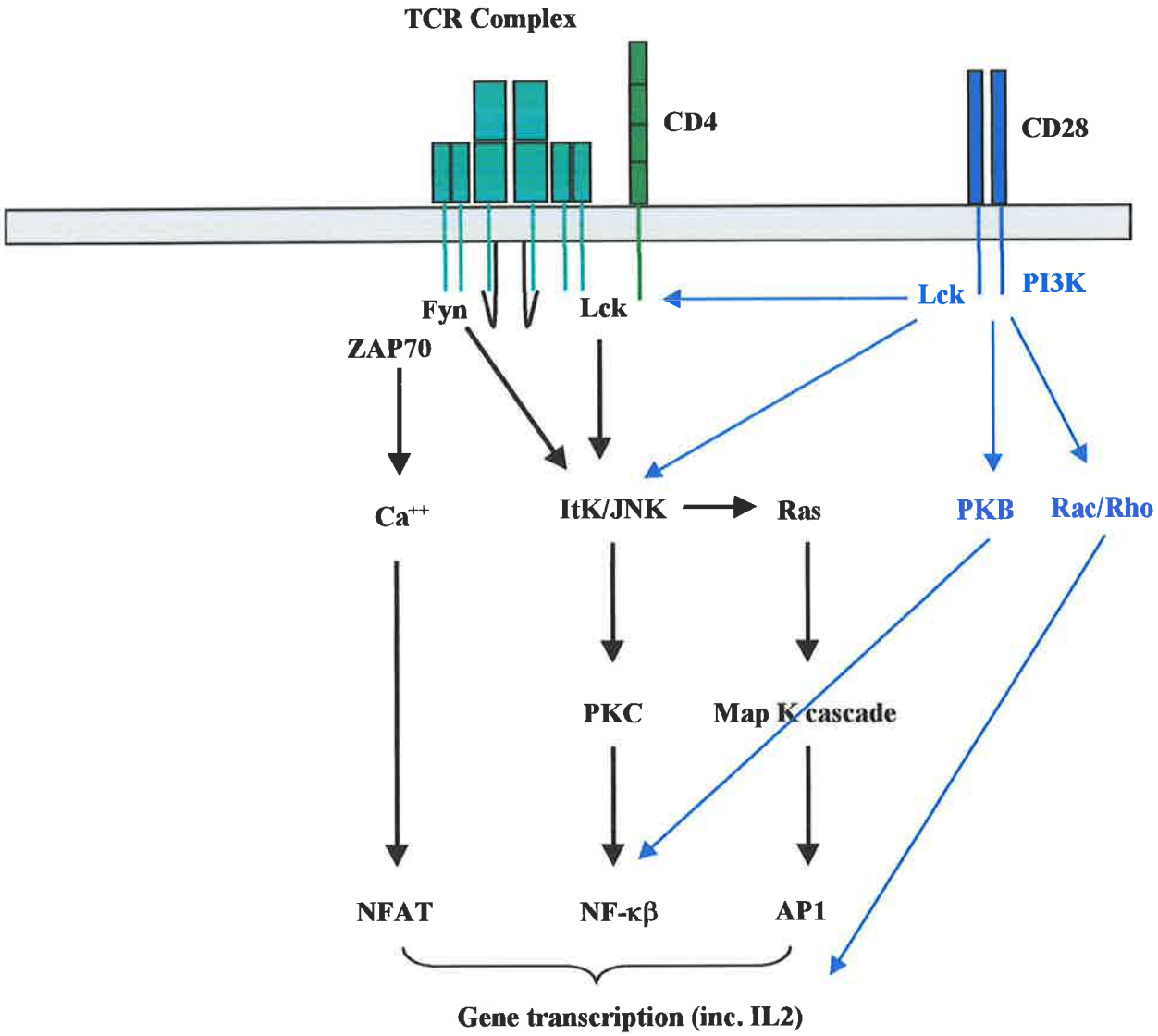

Figure 1.2. Integrated and divergent intracellular signaling pathways of the TCR and CD28 Engagement of the TCR and CD28 costimulatory molecules on T cells leads to complex signaling pathways resulting in the transcription of cytokines able to potentiate T cell activation. Illustrated above are the key signaling pathways of CD28 some of which integrate with and strengthen TCR signaling as well as TCR independent pathways.

the rapid expansion of antigen-specific T cells. However unregulated T cell expansion can lead to lethal T cell hyperproliferative disorders (38). CTLA4, which is a negative regulator of T cell activation, provides the required down-regulatory mechanism to keep T cell proliferation under control. **Figure 1.1** provides an outline of the CD28 costimulatory interactions and the involvement of CTLA4.

1.5. CTLA4 Expression, Structure and Function

CTLA4 was the fourth cDNA found in a search for genes specifically expressed in cytotoxic T cells and was thus named "Cytotoxic T Lymphocyte Associated Antigen" (39). Its subsequent characterization has made it one of the most important negative regulators of immune responses and has been exploited to prolong allograft acceptance, and attenuate rheumatoid arthritis and autoimmunity.

1.5.1. Regulation of CTLA4 Expression and Distribution

CTLA4 expression is limited to activated T lymphocytes including $CD8^+$ (cytotoxic) T cells as well as both Th_1 and Th_2 $CD4^+$ (helper) T cell subsets (40). Expression is regulated primarily by IL-2, produced in response to CD28 costimulation (41) and therein is limited to those T cells which co-express CD28 (42). The importance of CD28 in CTLA4 induction is demonstrated by the rapid up-regulation of CTLA4 expression after cross-linking the CD28 molecule with antibodies (42), while significantly less CTLA4 is expressed in CD28 knockout mice (43). The human CTLA4 gene is located on Chromosome 2 (44) and the transcriptional regulation is controlled by a promoter

located 335bp upstream of the CTLA4 gene which contains a number of conserved regulatory elements involved in positive and negative gene regulation (40).

While CTLA4 mRNA expression can be detected within 1 h of TCR engagement, peaking between 24 and 36 h (42), up-regulation of the CTLA4 protein expression peaks between 48 and 72 h after T cell activation (43). Even at peak expression, however, the majority of CTLA4 is located in vesicles within the cell from where it is trafficked to the plasma membrane at the site of TCR engagement (45).

Upon T cell activation, the majority of CTLA4 is localized in intracellular vesicles in close proximity to the microtubule-organizing center (MTOC), which are rapidly repositioned close to the immunological synapse upon TCR engagement (45, 46). Moreover the translocation of CTLA4 to the cell surface is promoted by the strength of TCR signaling.

Expression of CTLA4 on the cell surface is modulated by calcium flux and direct phosphorylation of its intracellular domain (45-47). This intracellular domain has been identified as the tyrosine-based localisation motif (YVKM) (48, 49). Surface expression of CTLA4 on T cells may be transient as the YVKM motif, in an unphosphorylated state, interacts with the medium chain of the AP-2 clathrin-coated pit adapter protein, resulting in rapid endocytosis and intracellular accumulation (41, 47, 50). Conversely phosphorylation of Tyr^{201} results in the stabilization of CTLA4 expression on the cell surface. These factors partially account for the 30 to 50 fold lower surface expression of CTLA4 compared to CD28 even at peak T cell activation. (51). Memory T cells which typically possess greater quantities of intracellular CTLA4 than naïve T cells also demonstrate prolonged surface expression of CTLA4 (52).

1.5.2. The Molecular Structure of CTLA4

CTLA4 is a membrane bound glycoprotein consisting of single extracellular, transmembrane and cytoplasmic domains and is a member of the immunoglobulin (Ig) superfamily (39). Other members of the Ig superfamily include MHC class I and II products, the immunoglobulins and numerous T cell receptors including CD4, CD8, ICAM1/2, VCAM, CD2, CD28, CD80 and CD86 (53). Characteristic of a number of immunoglobulin superfamily proteins, CTLA4 consists of a single Ig variable-region-like (V-like) domain flanked by 2 hydrophobic regions (39).

CTLA4 is a structural homologue of CD28 and is able to bind to the ligands of CD28, namely CD80/86 (54). This binding effect is at least in part due to a hydrophobic MYPPPY hexapeptide motif, which is conserved in CTLA4 and CD28 from most species (55, 56). The only exceptions are ovine and bovine CD28 in which the methionine residue is replaced by a leucine residue (57). The MYPPPY motif makes up the Complementarity Determining Region 3 (CDR3) -like binding domain which is important for binding to CD80/86 (58). Although the MYPPPY motif is the primary motif involved in CD80/86 ligation, analogous regions to the CDR1-like binding domain have been shown to potentiate the different binding affinities of CTLA4 and CD28 (59).

Both CTLA4 and CD28 form disulphide-linked homodimers. Unlike most v-type immunoglobulin domains such as the TCR, the formation of the CTLA-4 homodimer places the CD80/86 binding sites distal to the dimer interface allowing each CTLA4 dimer to bind 2 ligands (58) (**figure 1.3**). This potentially allows a very stable multi-meric lattice organisation which may disrupt the assembling of components of the immunological synapse, thereby preventing optimal CD28 and TCR signaling (60-62).

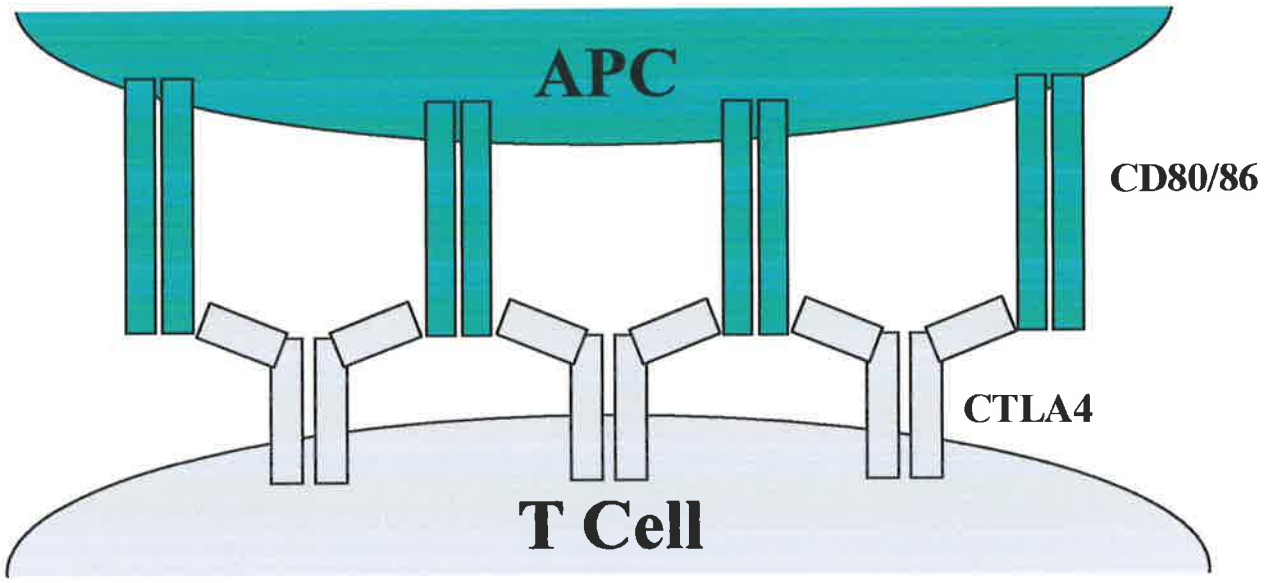

Figure 1.3 The CD80/86 binding domain of CTLA4 is distal to the dimer interface
Contrary to many members of the immunoglobulin family, the binding domain of CTLA4 is located distal to the dimer interface and hence each molecule is able to bind two CD80 or CD86 ligands resulting in a stable multi-meric lattice organisation.

1.5.3. Functional Characteristics of CTLA4

CTLA4 acts as a negative regulator of T cell proliferation. The vital role played by CTLA4 is demonstrated by lethal lymphoproliferative disorders in mice deficient in CTLA4 as a result of unchecked polyclonal $CD4^+$ T cell expansion (63, 64). In these mice virtually all peripheral T lymphocytes demonstrated an activated phenotype, with a four-fold increase in the proportion of T cells in active cell cycle (38, 63). The lymphoproliferative disorder is a direct function of unchecked interactions between CD28 and CD80/86, as CTLA4-Ig treatment of $CTLA4^{-/-}$ mice attenuates T cell activation (65). The inhibition of proliferation was dependent on continual CTLA4-Ig administration as cessation of the treatment rapidly restored T cell activation (66). Given that $CTLA4^{-/-}$ mice have normal thymocyte development (64), these observations implied that CTLA4 plays an important role in the regulation of peripheral T cell tolerance and homeostasis.

CTLA-4 engagement with CD80/86 inhibits IL-2 (the primary T cell growth factor) production and the expression of CD69 (an early marker of T cell proliferation), restricting progression of the cell cycle from G1 to S phase (67). CTLA4 engagement can also lead to the production of transforming growth factor-β (TGF-β) by T cells (68). The importance of TGF-β in CTLA4-mediated T cell inactivation was demonstrated by CTLA4 engagement of TGF-$\beta1^{-/-}$ T cells in a proliferation assay, with only 38% suppression compared to 95% for wild-type T cells (68). In other studies CTLA4 engagement has also been shown to augment anti-tumor immunity (69) and regulate autoimmune diabetes (70).

While CTLA4 engagement regulates T cell activity, the precise biological outcome appears to depend on the state of T cell activation. Although expressed at low levels on

resting $CD4^+$ T cells, cross-linking of CTLA4 with agonistic antibodies blocks the transition from G_0 to G_1 and induces Bcl-xL, preventing apoptosis (71, 72). Conversely activated $CD4^+$ T cells treated in this manner induce Fas-independent cell death (71). These differences reflect the roles of CTLA4 in both the regulation of activated T cells and in the maintenance of peripheral tolerance.

A number of models have been proposed to explain some of the salient features of CTLA4 with regard to the inhibition of T cell activation. The first two models were proposed in 1997 with both likely to contribute to varying degrees. The models are the "proximal competition" model and the "distal signaling" model (26) and are outlined in **Figure 1.4.** These were followed by the "threshold" and "attenuation" models reported in 2001 which focus on different aspects of CTLA4 function (73).

1.5.3.1. The "Proximal Competition" Model of CTLA4 Induced Antagonism

CTLA4 binds to CD80/86 molecules with greater binding affinity than CD28 (74, 75). In this model CTLA4 purely out competes CD28 with respect to CD80/86 binding, reducing CD28 mediated costimulation. This model does not attribute any regulatory function to CTLA4 signaling. In support of this model Masteller (49), demonstrated that the introduction of a mutant form of CTLA4 lacking the cytoplasmic domain into CTLA4 deficient mice partially rescued the lethal lymphoproliferative disorder associated with CTLA4 knockout mice. Further studies also support a role for CTLA4-mediated inhibition in the absence of cytoplasmic signaling (75-77).

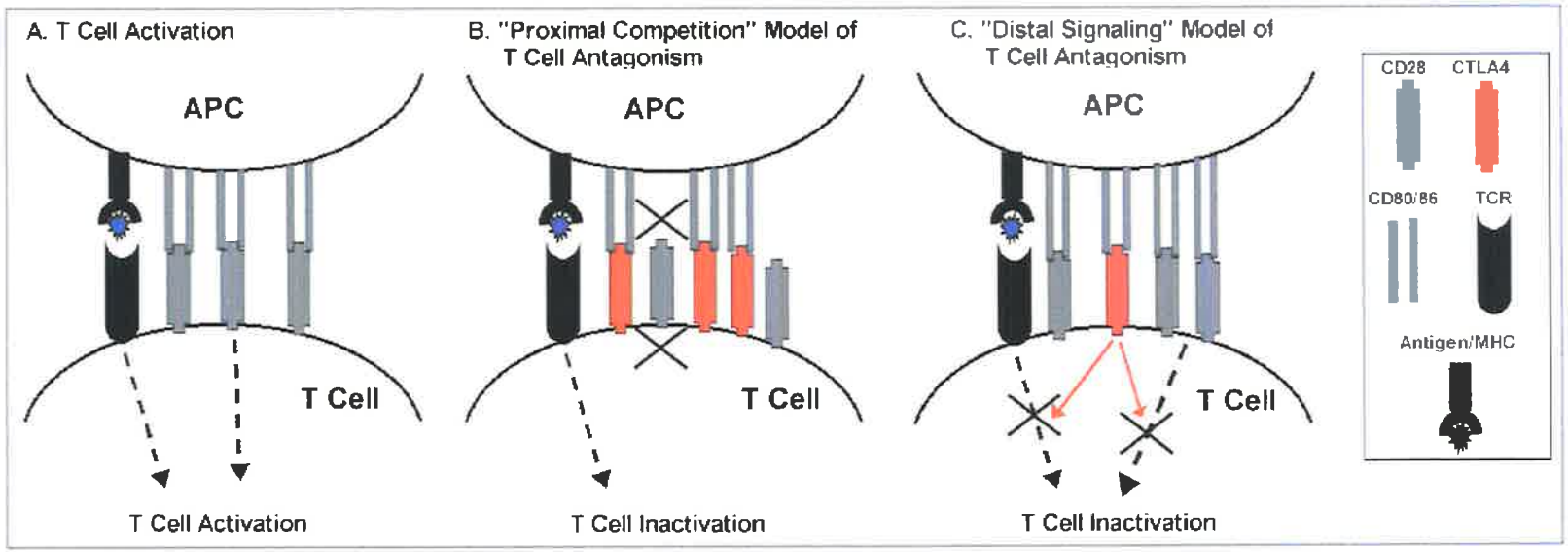

Figure 1.4. Two Models of CTLA4 Antagonism of T Cell Activation
A. T cell activation requires two signals. The first signal is provided by the interactions between the TCR and the antigen/MHC complex. The second signal is provided by costimulatory molecule interactions. The CD28 and CD80/86 interactions provide one of the strongest costimulatory pathways. The presence of both signals permits T cell activation.
B. In the "proximal competition" model, CTLA4 is expressed at sufficient levels to sequester CD80 and CD86 from CD28 by virtue of its high binding affinity. CD28 is therefore unable to bind to CD80/86 and subsequently no costimulatory signal is produced. In the absence of sufficient costimulation the T cell becomes inactivated. In this model no functional activity is attributed to CTLA4 mediated signaling.
C. In the "distal signaling" model, CD28 ligation to CD80 and CD86 molecules is not inhibited, however CTLA4 engagement with its ligands facilitates CTLA4 mediated intracellular signaling which interferes with TCR and CD28 signaling pathways, resulting in T cell inactivation.

1.5.3.2. The "Distal Signaling" Model of CTLA4 Induced Antagonism

In the distal signaling model, T cell inactivation occurs as a result of negative signaling by the CTLA4 molecule. The importance of CTLA4 intracellular signaling is illustrated by the 100% conservation of the cytoplasmic domain between species, implying a strong intracellular signaling function maintained by evolutionary pressure (44). In the "distal signaling" model CTLA4, once bound to CD80/86, antagonises the CD28 and/or TCR pathways by intracellular mechanisms the precise nature of which are not entirely understood. Supporting this model, cross-linking of the CTLA4 receptor on purified T cells with antibodies in conjunction with CD3 and CD28 cross-linking resulted in a significant reduction of T cell proliferation (78). This provided strong evidence for the inhibitory signaling properties of CTLA4 given the absence of ligand competition between CTLA4 and CD28 in the experiment. Furthermore CTLA4 is able to mediate inhibitory effects in CD28 deficient mice (79). Recent data also support this model by the observations that a CD80/86-nonbinding CTLA4 mutant was still able to inhibit T cell proliferation, cytokine production and TCR-mediated ERK activation (80).

Both models play a role in T cell antagonism although the extent of their influence appears to be related to the level of CD80/86 expression. As CTLA4 is expressed at much lower levels than CD28 (51), the "proximal competition" model is likely to operate most efficiently under conditions of low CD80/86 while the "distal signaling" model is likely to be more prevalent under conditions of high CD80/86 expression (75).

1.5.3.3. The "Threshold" model of CTLA4 induced antagonism

In situations of low expression of CD80/86 ligands, the constitutive intracellular pool of CTLA4 may translocate to the immunological synapse within hours of TCR engagement

(45, 81). By virtue of its higher binding affinity (74), the low levels of CTLA4 from within the intracellular pool may be sufficient to prevent T cell activation by raising the threshold for T cell activation. This is likely to play a vital role in the maintenance of peripheral tolerance. Thus in the threshold model, CTLA4 may restrict the clonal representation of T cells reacting to an APC with TCR signaling above a designated threshold.

1.5.3.4. The "Attenuation" model of CTLA4 induced antagonism

The attenuation model is derived from the observation that CTLA4 preferentially regulates T cells which have strong and stable engagement of the TCR (82). In this model, CTLA4 expression is rapidly upregulated as a consequence of strong TCR and costimulatory molecule signaling, as high levels of CD80/86 on APC are likely to overcome the initial CTLA4 pools. Therefore in activated T cells, CTLA4 functions to broaden the repertoire of T cells clonally expanding, by restricting the domination by any one antigen-specific T cell clone (82).

1.5.4. CTLA4 Signaling Pathways

The precise nature of CTLA4 signaling pathways remains elusive however experimental data indicates that CTLA4 ligation is able to modulate early TCR and CD28 signaling events and also events further downstream.

Engagement of CTLA4 on the cell-surface is able to inhibit TCR signaling by utilizing the tyrosine phosphatase SHP-2 to dephosphorylate the TCR-ζ chain (83, 84). CTLA4 also associates with PI3K, which is an important protein for CD28 signaling pathways (85). Therefore CTLA4 may sequester PI3K, thereby restricting CD28 signaling.

Through the decreased accumulation of nuclear factor of activated T cells (NFAT) and activator protein 1 (AP-1) in the nucleus, CTLA4 is also able to inhibit CD3 and CD28 mediated IL-2 production (86). Furthermore CTLA4 engagement increases Iκβ-α (an inhibitor of NFκβ) and a decrease in RelA translocation to the nucleus, which downregulates the production of cytokines including IL-2, IL-3, IL-4, IL-10 and IFN-γ (87, 88). The influence of CTLA4 engagement on TCR and CD28 signaling is shown in **figure 1.5**. Moreover CTLA4 ligation provokes the re-expression of cbl-b which antagonises TCR signaling (37).

1.6. Expression and Function of CD80 and CD86 Ligands

CD80 (alternatively termed B7.1) was identified in 1982 (89), but it wasn't until 1987 that it was identified as the ligand for CD28 (90). The search for a second ligand for CD28 on APC was undertaken after it was shown that while CTLA4-Ig could effectively block primary T cell responses, antibodies against CD80 were not effective (91). Moreover CTLA4-Ig was able to bind to B cells from $CD80^{-/-}$ mice implying a second ligand also recognised by CTLA4 (91). CD86 (also known as B7.2) was subsequently identified as the second ligand for CD28 in 1993 (92).

1.6.1. CD80 and CD86 Expression

Although CD80 and CD86 only share 25% amino acid similarity, they share a similar secondary structure, namely, a single IgV- and a IgC domain with 4 conserved cysteine residues which allow the formation of disulphide bonds between the two Ig domains. CD86 is however thought to be expressed on the cell surface as a monomer (93,

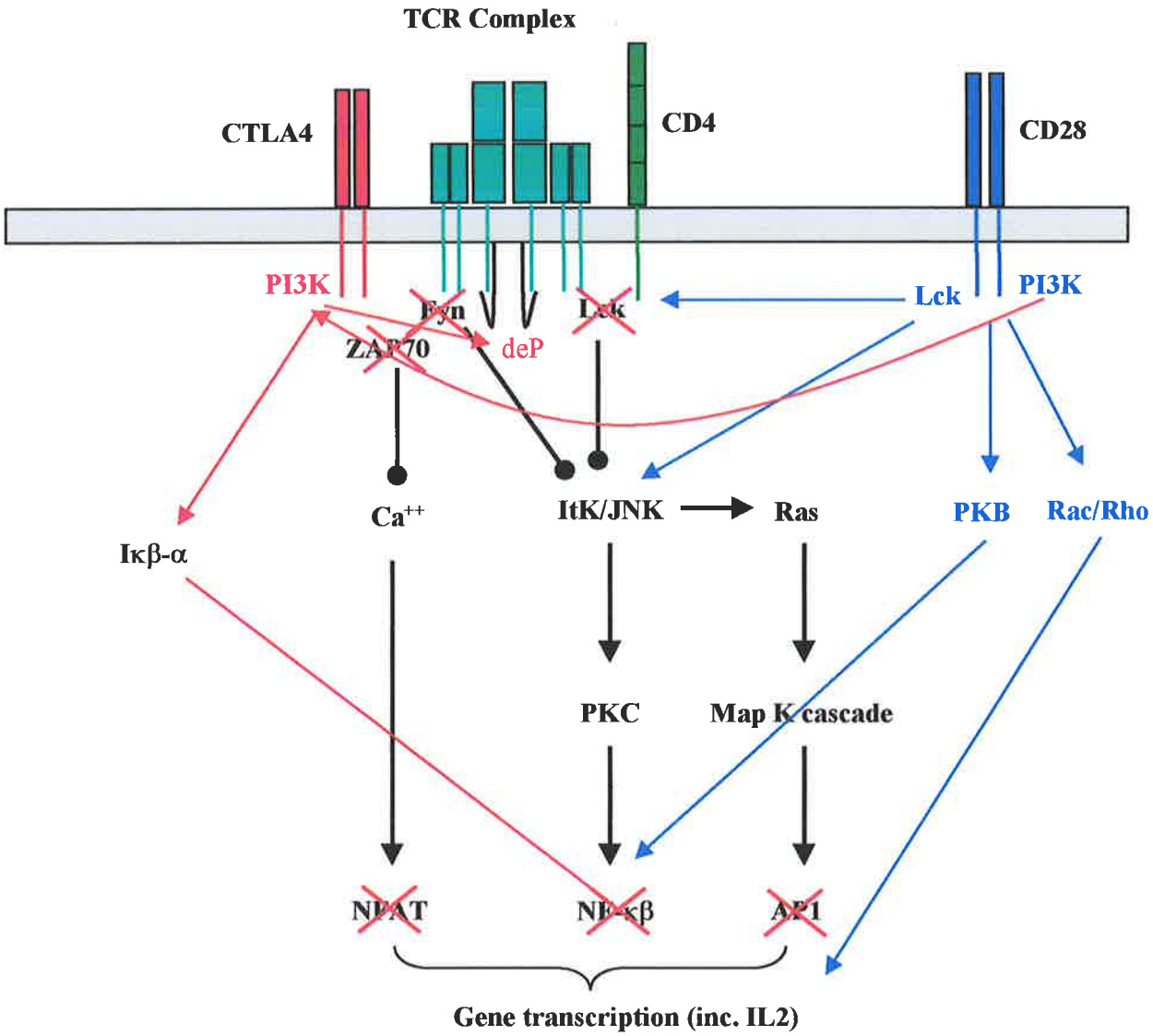

Figure 1.5. Influence of CTLA4 intracellular signaling pathways on TCR and CD28 signals Contrary to CD28, CTLA4 acts to attenuate T cell activation. Current literature indicates that CTLA4 dephosphorylates the TCR ζ chain, preventing TCR signaling and sequesters PI3K, restricting CD28 signaling. Moreover CTLA4 is able to target TCR and CD28 stimulated NF-κβ. CTLA4 mediated effects are shown in red.

94) while CD80 has been shown to form a bivalent homodimer (61). Importantly both CD80 and CD86 are able to bind to CD28 and CTLA4 (95). A particular difference between CD80 and CD86 lies in their different kinetics of expression. CD86 is expressed on APC at low levels and is rapidly up-regulated upon activation, while CD80 is absent on resting APC and has delayed expression kinetics (95). Up-regulation of both CD80 and CD86 expression is augmented by CD40/CD40L costimulation (96, 97).

1.6.2. CD80 and CD86 Binding to CD28 and CTLA4

CTLA4 is able to bind to CD80 and CD86 with 10 fold greater affinity than CD28, however both CTLA4 and CD28 demonstrate differential binding affinities to each ligand. CD80 binds to CTLA4 13-fold stronger than CD86, while CD28 binds to CD86 with 2 to 3 -fold higher affinity than CD80 (74, 93). Taken with the delayed onset of CD80 expression, which closely matches that of CTLA4, this supports a biased influence of CD80 over CD86 on inhibitory function. Moreover the recruitment of CTLA4 to the immunological synapse is highly dependent on CD80, in contrast to CD28 which is primarily dependent on CD86 (98). This does not however preclude CD80 from playing a strong stimulatory role in the absence of CTLA4 as CD80 augments CD86 costimulation. In particular in the absence of CD80 expression, insufficient levels of IL-2 are produced to mediate T cell activation (99). CD80 and CD86 may also play different roles in transplant rejection as blockade of CD86 at the time of transplantation with mAb prolongs allograft acceptance in mice while blocking CD80 had no effect (100, 101). Furthermore CD80 mAb blockade in CD28 deficient mice shortened the duration of allograft acceptance, potentially by blocking interactions with CTLA4 (102).

CD80 and CD86 also play an important role in the homeostasis of regulatory T (T_{reg}) cells. CD80/86 interactions with CD28 on T_{reg} cells have also been shown to be vital for T_{reg} cell viability (103, 104), while ligation of CTLA4 on T_{reg} cells with CD80/86 on responder T cells downregulates their immune responsiveness (105).

While engagement of CD80/86 was originally thought to induce unidirectional signals to the T cell, evidence now exists to the contrary. Cross-linking of CD80/86 expressed on DC with CTLA4-Ig or membrane bound CTLA4 (including from T_{reg} cells) can stimulate IFN-γ production, which, in an autocrine or paracrine manner can induce DC production of 2,3-dioxygenase (IDO), that in turn degrades tryptophan to byproducts able to inhibit T cell proliferation (106-108). The importance of IDO in the mode of action of CTLA4-Ig came by the abrogation of CTLA4-Ig protection by pharmacologically inhibiting IDO (106). In comparison to the tolerogenic properties after CTLA4 binding, CD28 engagement of CD80/86 on DC was stimulatory, resulting in increased expression of IL6 and IFNγ with an inhibition of tryptophan catabolism (109). Bidirectional signaling also occurs between T cells and memory B cells as CD80 and CD86 expressed on memory B cells are able to interact with CD28 on T cells, stimulating both T cell activation and increased IgG1 and IgE production by the B cells (110, 111).

CD28 clearly provides a critical costimulatory pathway and can reduce the threshold of TCR triggering required for T cell activation, while CTLA4 plays a vital role in the maintenance of peripheral tolerance by restricting T cell reactivity to weak or self-antigens. While CTLA4 acts as a critical regulator of the CD28 costimulatory pathway, there are a number of other factors that can restrict CD28 costimulation.

1.7. Other regulators of CD28 Costimulation

While the CD28 costimulatory pathway is negatively regulated by competition with CTLA4 for binding to CD80/86 and inhibitory intracellular signaling by CTLA4 engagement, other receptor-ligand interactions and factors are able to modulate the expression and function of CD28 costimulation and subsequent T cell activation. Programmed death-1 (PD1) is another member of the immunoglobulin superfamily, which is expressed on activated CD4 and CD8 T lymphocytes (112). Engagement with its ligand (PDL), expressed by macrophages and DC (113), is able to inhibit the early stages of T cell activation. In addition to promoting apoptosis (112), PD-1 blocks CD28-mediated activation of PI3K, abrogating the effects of CD28 and inhibiting T cell proliferation (114). In combination with anti-CD154, PDL fusion proteins were able to induce long-term survival of islet allograft transplantation (115). Other recently identified cell-surface molecules including B7-H3, B7-H4 and BTLA are able to inhibit T cell activation although their influence on CD28 signaling has not been investigated (116).

Age has been shown to influence CD28 expression with significant down-regulation of CD28 expression and increased T cell apoptosis in the elderly (118, 119). In this regard the expression of the pro-inflammatory cytokine TNF-α is upregulated in the elderly and rheumatoid arthritis patients and has been shown to reduce CD28 expression on T cells (120). Moreover ligation of Fas (CD95) on T cells results in reduced CD28 mRNA expression (121, 122). Taken together these factors account for the decreased ability to mount effective immune responses in aging populations. The HIV virus is also able to down-regulate CD28 expression, partially mediating immune deficiency associated with AIDS (123, 124). While down-regulation of CD28 expression and signaling appears to

correlate with disease progression, applied to allograft transplantation, therapeutic effects may be achieved. Notably glucocorticoids and Cyclosporin A, which are used in current immunosuppressive regimes, inhibit CD28-mediated production of IL-2 and activation-induced CD28 expression (125, 126). Endogenous or exogenous interleukin 10 (IL-10) is able to mediate numerous effects on the immune system including disruption to the CD28 costimulatory pathway and is the focus of the next section of this literature review.

1.8. Interleukin 10 (IL-10) Expression, Structure and Function

Interleukin 10 is a potent cytokine that is expressed by a range of cells with pleotropic properties. A particular feature of IL-10 is its ability to mediate immune responses by the modulation of CD28 costimulation. IL-10 was discovered during a search for a cytokine produced by Th2 cells which could inhibit proliferation, effector function and the development of Th1 cells (127, 128). Thus IL-10 was initially known as the cytokine synthesis inhibitory factor (CSIF). The cDNA for mouse and human IL-10 cDNA were subsequently discovered (129, 130).

1.8.1. Interleukin 10 Expression

IL-10 is expressed by B cells, DC, T helper cells, monocytes and macrophages (131, 132). The expression of IL-10 appears to be tightly regulated, as extremely low levels of constitutive expression in resting cells are observed. The expression of IL-10 is increased during differentiation of naïve T cells to Th2 cells, while IL-10 is silenced in committed Th1 cells (133). IL-10 is typically expressed late after cell activation compared to other cytokines and is influenced by various pathways including IFNγ which inhibits the

expression of IL-10 (134). Further attenuation of IL-10 expression results from CD28 costimulation (135).

Transcription of the IL-10 gene requires promoter activity of a TATA-box (77 bases upstream of the ATG start codon) and up to 150 additional 5' nucleotides (136). The IL-10 promoter is also influenced by two informative microsatellites, IL-10.G and IL-10.R, 1.2 kb and 4 kb upstream of the transcription start site (137) and contains several transcription factor responsive elements (138). IL-10 mRNA expression can be regulated by transcription factors Sp1 and Sp3, which are constitutively expressed by several cell types (139), while post-transcriptional regulation is controlled by mRNA destabilizing motifs AUUUA and related sequences found in the 3'-untranslated region (UTR) of IL-10 mRNA (140).

1.8.2. The Molecular Structure of IL-10

Human IL-10 and viral IL-10 are 17-18kDa peptides, devoid of N-glycosylation (141) which exist as acid-sensitive, noncovalent homodimers (142, 143). IL-10 is a member of the four α-helix bundle family of cytokines (144). The mouse IL-10 and human IL10 genes are both located on mouse and human chromosome 1 and are encoded by five exons (145). The amino acid and nucleotide sequences of human and murine IL-10 both have a high degree of homology with the open reading frame of the Epstein-Barr virus genome (129, 130, 146).

1.8.3. The Interleukin 10 Receptor (IL-10R)

The IL-10 receptor is composed of a heterodimer of IL-10R1 and IL-10R2. IL-10R1 is expressed primarily on hemopoietic cells including non-activated T cells,

monocytes, macrophages, B cells and DC (147). IL-10R1 incorporates the IL-10 binding region while IL-10R2, which is constitutively expressed on a wider range of cells and tissues, doesn't appear to be influenced by the cells state of activation (148). IL-10R2 doesn't play a significant role in IL-10 binding but instead plays an accessory subunit role for the initiation of signaling by the recruitment of a Jak kinase (149, 150). The importance of the IL-10R2 subunit is evident in IL-10R2$^{-/-}$ mice, which develop chronic enterocolitis, similar to IL-10$^{-/-}$ animals (141).

During T cell activation the expression of IL-10R1 is significantly downregulated, rendering the activated T cell resistant to the inhibitory effects of IL-10 (147) and may account for the insensitivity of memory T cells to IL-10. As most cells and tissues constitutively express IL-10R2, IL-10R1 expression and binding is the rate-limiting step, which determines the reactivity of cells to IL-10 (148, 151). Furthermore IL-10R1 expression on DC diminishes upon DC maturation (152) which correlates with the observation that mature DC are resistant to the effects of IL-10 (153).

1.8.4. The Functional Characteristics of IL-10

The main role of IL-10 is to control and limit the magnitude of an immune response, as demonstrated in mice lacking IL-10 which exhibit spontaneous enterocolitis and other symptoms similar to Crohn's disease (154). Moreover IL-10 deficient mice have increased Th1 responses (155) resulting in enhanced clearance of infection (156) and elevated levels of asthmatic and allergic responses (157, 158).

IL-10 is a pleotropic cytokine able to exert positive and negative effects on a range of cells. While IL-10 is able to have a direct inhibitory effect on CD4^{+} T cells, the prime mechanism of inhibition is via the modulation of APC including monocytes and dendritic

cells. Contrary to these inhibitory effects IL-10 is able stimulate mast cells, $CD8^+$ T cells, thymocytes and B cells (130, 159-163).

The effects of IL-10 on APC include the blocked secretion of the inflammatory cytokine IL-12 (164) and down-regulation of costimulatory molecule expression including the CD80/86 (165, 166) and CD40 molecules (167, 168). Moreover IL-10 is able to block DC maturation (153, 169-171). A further inhibitory function of IL-10 on DC has been recently discovered as IL-10 upregulates the cell-surface expression of the inhibitory receptor LIR-2 on DC (172). These effects on APC down-regulate their stimulatory capacity, preventing T cell proliferation. IL-10 can also act directly on CD4+ T cells by impairing cellular function by inhibiting IL-2, TNF and IL5 production (173, 174). The incidence of IL-10 directly influencing T cell proliferation in the complete absence of APC may be low, however, anti-CD3 proliferation assays have demonstrated a concomitant requirement for CD28 costimulation (175). IL-10 can also act to restore the expression of TGF-βR2 on activated T cells which would otherwise be TGF-β insensitive, promoting further inhibitory potential (176).

The activation or inhibition of $CD8^+$ T cells depends largely on the presence of APC. While IL-10 has been shown to directly induce $CD8^+$ T cell activation (162, 177), $CD8^+$ T cell inhibition can occur indirectly via IL-10 treated APC (163).

1.8.5. Viral IL-10

Viral homologues of IL-10 have been identified in a number of viral genomes including Epstein Barr Virus (EBV) and cytomegalovirus (CMV) which are expressed during the lytic viral phase (178). CMV-IL-10 shares only 27% homology to hIL-10 (179) while EBV-IL-10 has 84% homology at the amino acid level (129). The primary disparity between hIL-10 and EBV-IL-10 (vIL-10) is an amino acid substitution at position 87,

which prevents vIL-10 from stimulating mast cells and B cells while its immunosuppressive properties on DC and T cells are retained (180).

1.8.6. IL-10 Signaling Pathways

IL-10 exerts its effects by the activation of the Jak/STAT pathway of signal transduction (141). By this means IL-10 is capable of inhibiting the production of pro-inflammatory cytokines and chemokines (134) including IL-1 and TNF which have synergistic activity on inflammatory pathways as well as inhibiting endogenous IL-10 production (181). IL-10 binding also results in an inhibition of the tyrosin phosphorylation of CD28 (175). Furthermore ligation of the IL-10R prevents the binding of the p85 subunit of phosphatidyl-inositol 3-kinase (PI3-K) to CD28 thus blocking another CD28-signaling pathway (182). **Figure 1.6** illustrates the salient inhibitory functions of IL-10 with regard to TCR and CD28 signaling pathways in T cells.

IL-10 is able to inhibit NFκβ in CD4+ T cells and monocytes by firstly inhibiting IKK activity, which subsequently inhibits NFκβ translocation and secondly by blocking NFκβ DNA binding within the nucleus (141, 183, 184). A number of proinflammatory cytokines, chemokines, adhesion molecules, antigen-presentation and costimulatory molecules expression are all regulated by NFκβ, which may explain the wide-acting inhibitory effects of IL-10 (185, 186) although IL-10 can stimulate NFκβ activation in CD8+ T cells (162).

1.9. Immunology of Transplant Rejection

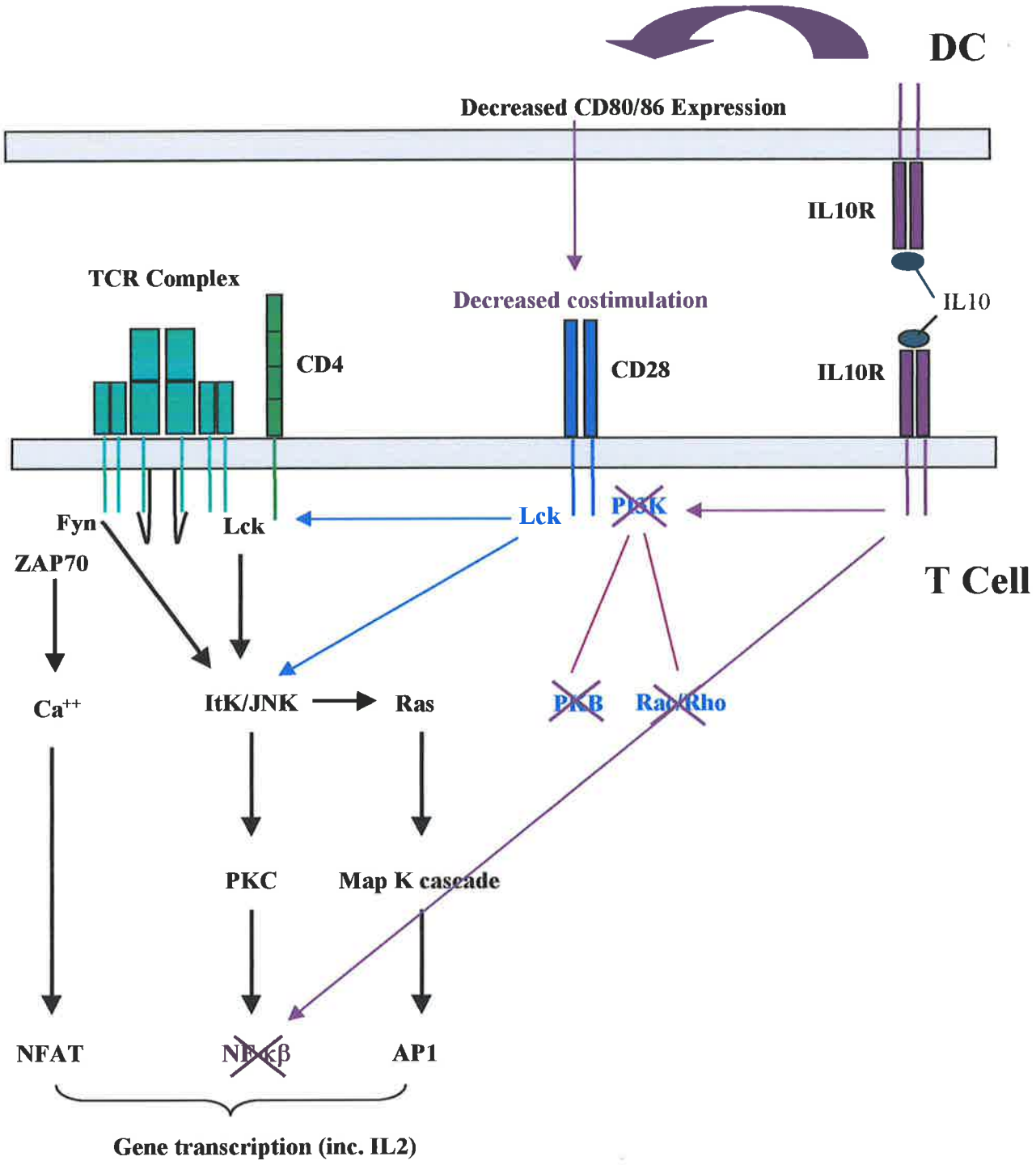

Figure 1.6. Influence of IL10 on T cell receptor signaling pathways
IL10 receptor engagement on T cells results in the inactivation of PI3K, thereby significantly attenuating CD28 signaling. Moreover IL10 engagement also inhibits NF-κβ. As APC also express the IL10 receptor, the engagement of which results in the down-regulation of CD80/86 expression, IL10 can also reduce the level of CD28 engagement further attenuating CD28 costimulatory signals. IL10 mediated effects are shown in purple.

1.9.1. Direct and Indirect Pathways of Allorecognition

T cells play an essential role in the initiation and co-ordination of the immune response (187). Allografts are rejected following recognition by T cells of donor MHC molecules on donor APC (direct allorecognition) or processed donor MHC antigens presented by recipient APC (indirect allorecognition). The direct and indirect pathways are illustrated in **Figure 1.7**. The direct pathway of allorecognition is believed to be the primary cause of acute rejection while chronic rejection has been attributed to the indirect pathway (188). Transplanted organs have been shown to contain "passenger leukocytes" which migrate from the organs to the lymphoid tissue of the organ recipient within two days of transplantation (189, 190). This efficiently exposes donor antigen presenting cells to the recipient's immune system, facilitating direct allorecognition.

There are 100 fold more T cells capable of participating in the direct allorecognition pathway than the indirect pathway (188), making the direct pathway an important target in the prevention of allograft rejection. More recent research using immunospot techniques has demonstrated that during acute murine skin allograft rejection, 90% of the T cell repertoire was directed against intact MHC molecules while only 10% was indirectly presented by host APC (191).

1.9.2. The Involvement of the Th1/Th2 Paradigm in Transplantation

$CD4^+$ T helper (Th) cells can be divided into two distinct functional subsets (Th1 and Th2) each able to produce their own set of cytokines and direct T cell differentiation (192). Th1 cells specifically produce IL-2 and IFN-γ and are associated with cell-mediated immunity. Th2 cells specifically produce IL-4 and IL-10 and initiate the humoral response. As demonstrated by **Figure 1.8** Th1 and Th2 cells are reciprocally regulated.

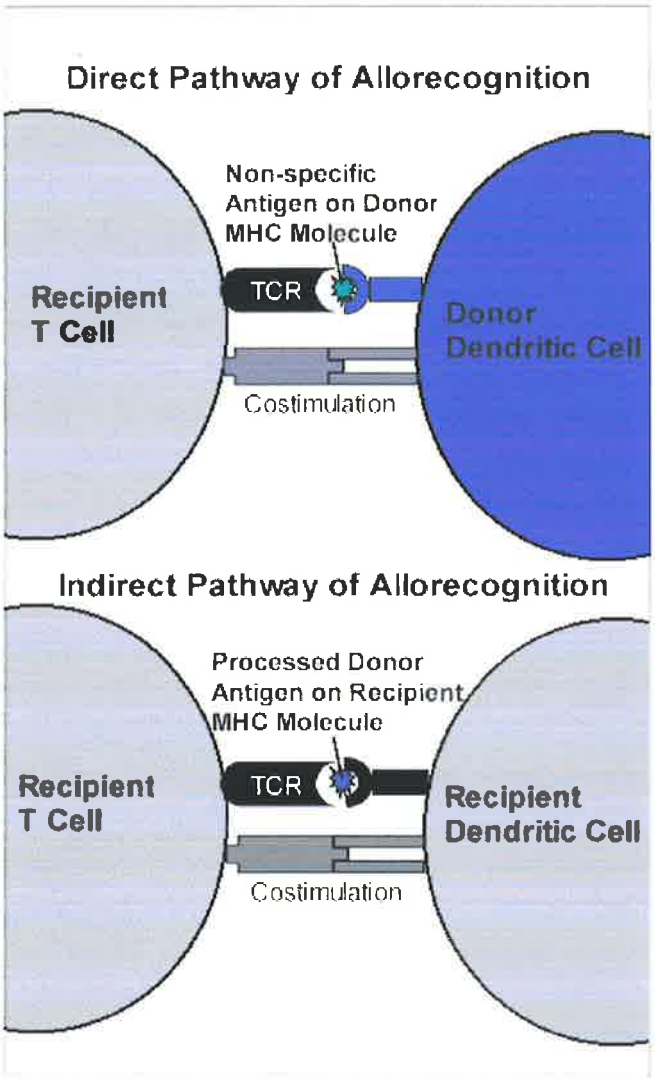

Figure 1.7. Direct and Indirect Pathways of Allorecognition
In the direct pathway of allorecognition T cells are activated by donor antigen presenting cells. Antigen presenting cells such as dendritic cells are normally resident in transplanted organs and rapidly migrate to lymphoid tissues. Recognition is facilitated by MHC molecule polymorphisms between individuals. The indirect pathway involves the capture and processing of donor antigens by recipient antigen presenting cells and presentation on recipient MHC molecules.

Figure adapted from Coates *et al.* 2001.

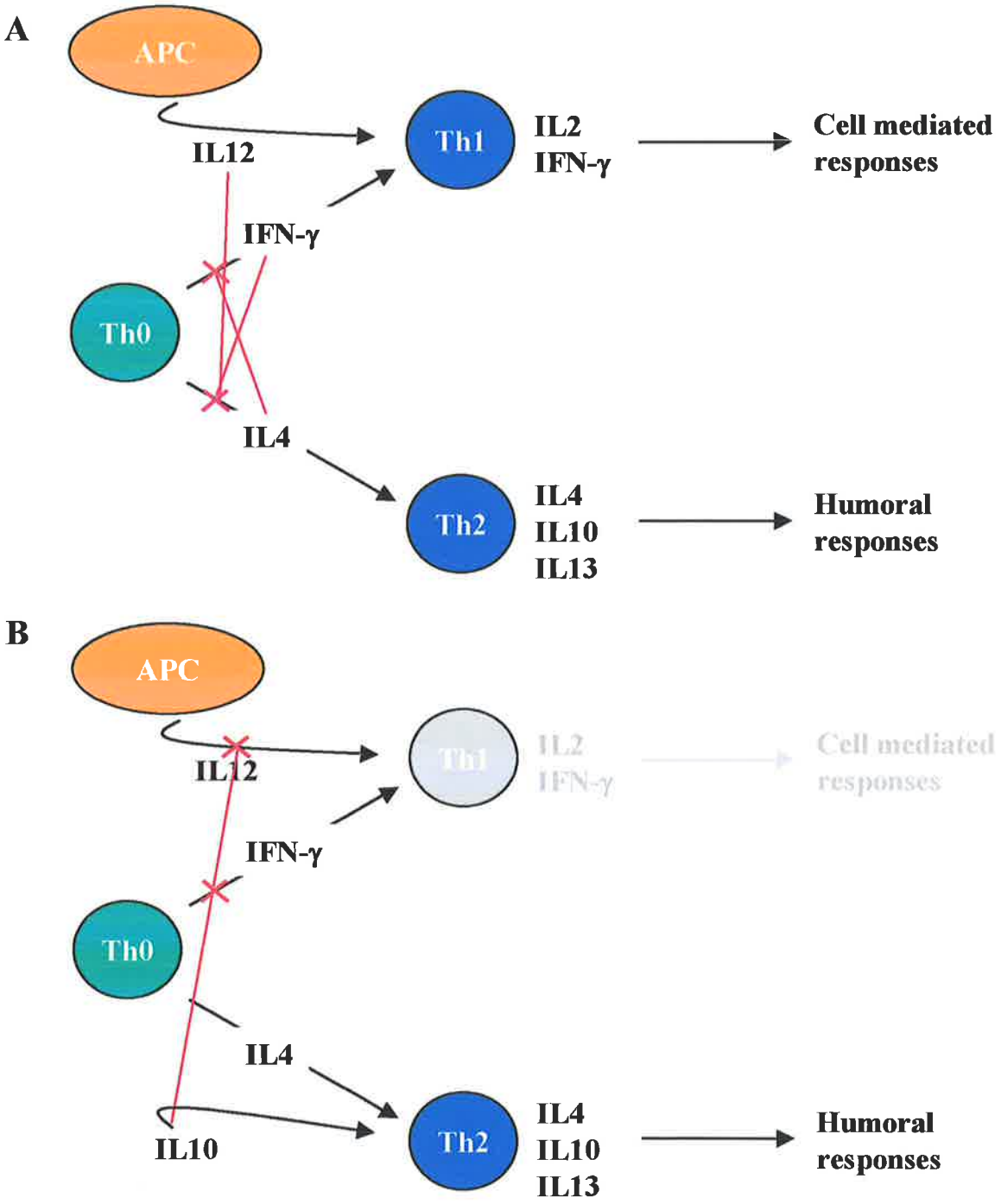

Figure 1.8. Regulation of Th1 and Th2 cells and influence of exogenous IL10
A) Th1 and Th2 cells secrete a number of common cytokines. However the function and characterisation of the subsets is defined by the expression of cytokines unique to each subset as shown above. Of particular note the Th1 cytokine IFNγ, inhibits the development of Th2 cells from the Th0 state and conversely the Th2 cytokine IL4 inhibits the development of Th1 cells. IL12 secreted by APC also promotes Th1 development. Th1 and Th2 cells are thought to modulate the cell mediated and humoral immune responses respectively.
B) Addition of IL10 skews the differentiation of Th0 cells to a Th2 phenotype by inhibiting IL12 production by APC, abrogating the effect of IFNγ and supporting the function of IL4.

Th1 cells have been implicated in the rejection of transplants while Th2 cells are thought to induce and maintain tolerance in transplantation models. This is supported by the expression of the Th2 cytokines IL-4 and IL-10 in grafts of tolerant animals; while rejected grafts were found to high levels of the Th1 cytokine IFN-γ (193).

The precise role of CD28 and CTLA4 on the Th1 and Th2 balance remains elusive and variable conclusions can be made depending on the model used. CD28 engagement has been shown to control the production of IL-4 by a 3-phosphoinositide-dependent protein kinase 1 dependent manner, which can drive Th2 development (194). However CD28 ligation can also increase IL-2 secretion and IL-12 receptor expression promoting a Th1 response (25, 195). Conversely CTLA4 engagement has been shown to inhibit $CD4^+$ T cells irrespective of their Th profile (88), although CTLA4 has been shown to preferentially promote resistance to activation induced cell death (AICD) in Th2 cells (196). Whether CD28 engagement leads to Th1 or Th2 differentiation may depend on other signals leading to a preferential release of IL-4 or IL-12.

The role of IL-10 on the Th1/Th2 balance is more clearly defined and notably IL-10 is currently used as a drug to treat chronic Th1-related diseases (197). IL-10 can directly inhibit both Th1 and Th2 T cells although the effect is targeted stronger against Th1 cells (198). Alternatively IL-10 can operate indirectly on the T cells by inhibiting IFNγ and IL-12 production by DC, while promoting Th2 cytokine production (164, 199-202). Furthermore inhibition of IL-10 production by DC using siRNA leads to the promotion of Th1 responses associated with high IL-12 expression (168).

1.10. Mechanisms of Alloreactive T cell Hyporesponsiveness

As T cells are the main effector cells of rejection of allografts, much research has been conducted to elucidate the various mechanisms by which T cells can induce immunity or tolerance. T cell immunity as described in **Section 1.2** involves recognition of antigen in the presence of sufficient costimulation and results in the clonal expansion of the reactive cells. There is however a number of mechanisms through which T cell tolerance can be induced which occur naturally to prevent autoreactive T cell activation. These mechanisms include T cell anergy, apoptosis, activation induced cell death (AICD) and the generation of or interaction with regulatory T cells.

1.10.1. Anergy

T cell anergy is defined as 'a tolerance mechanism in which the lymphocyte is intrinsically functionally inactivated following an antigen encounter, but remains alive for an extended period of time in the hyporesponsive state' (203).

T cell anergy has been demonstrated by antigen presentation in the absence of costimulation. The absence or blocking of CD80/86 with CTLA4-Ig upon antigen presentation to T cells results in the inability of clones to proliferate or produce IL-2 upon rechallenge (204). Thus the CD28 costimulatory pathway represents a vital signaling mechanism, which prevents the induction of anergy. Anergy can typically be overcome by the inhibition of anergic factors (205) or as a result of cell-cycle progression through production of growth factors such as IL-2 (206). An essential function of the ability of CD28 to circumvent anergy appears to be the induction of IL-2 secretion as anergy induced by the blockade of CD28 costimulation can be overcome by the addition of IL-2 (207, 208), although in some circumstances TCR activation must also occur (209). Signaling through

CTLA4 on the other hand can induce 'division arrest' anergy which is a state unable to be restored by IL-2 (207).

1.10.2. Apoptosis and Activation Induced Cell Death (AICD)

As immune cells are not shed, a process must be in place to restrict the number of lymphocytes in circulation and permit regular turnover of cells. This process is known as programmed cell death or apoptosis. Apoptosis is characterised by shrinkage of the cell, collapse of the nucleus and phagocytosis by macrophages prior to cell lysis, to minimise inflammatory responses (210). CD28 costimulation facilitates the expression of anti-apoptotic proteins, including Bcl-XL, which promote cell survival (27). Evidence also exists to support the induction of Bcl-XL by CTLA4 crosslinking (72). It therefore stands to reason that blockade of CD80/86 with CTLA4-Ig promotes T cell apoptosis and has been shown to be FasL independent (211).

Activation induced cell death (AICD) is another form of apoptosis which occurs as a result of activation via the TCR. AICD plays a vital role in both central and peripheral tolerance preventing the induction of autoimmune disease and is mediated by the expression and engagement of Fas/FasL molecules or TNF activity (212).

1.10.3. Generation of and interactions with regulatory T cells

While the concept of regulatory or suppressor T cells was introduced in the 1970s (213), it wasn't until the availability of sufficient cell-surface markers in the 1990s that permitted the characterisation of the $CD4^{+}CD25^{+}$ phenotype of these cells (214). Notably since 2001 there have been at least 500 publication each year characterising regulatory T cells (215).

Three types of regulatory T cells have been discovered in humans and mice. These are the naturally occurring thymus-derived regulatory T (T_{reg}) cells as well as induced Tr1 cells and Th3 in the periphery. T_{reg} cells act to prevent harmful immune responses to self and nonself antigens and play a vital role in autoimmune homeostasis (214). Thymus generated T_{reg} cells are $CD4^+$ T cells which constitutively express CD25, the α-chain of the IL-2 receptor (214), and are contact dependent in their mode of action. $CD4^+CD25^+$ T_{reg} also express the transcription factor Foxp3 (forkhead box P3) (216), and have constitutive CTLA4 cell-surface expression (217). T_{reg} cells are also able to induce 'infectious tolerance' by converting naïve T cells into suppressive cells (218-220). These converted suppressive T cells mediated their inhibitory actions by IL-10 (221) or TGF-β (222) production.

In contrast Tr1 and Th3 regulatory T cells do not express the CD25 marker or Foxp3 but maintain high levels of IL-10 and TGF-β expression respectively, to which their inhibitory function is attributed (223-225).

1.11. Current Immunosuppressive Treatments to Prevent Transplant Rejection

To prevent rejection of allografts, a cohort of immunosuppressive drugs is used each targeting different stages of immune responses, including T cell activation, cytokine production and clonal expansion (226). These drugs act in a non-specific manner thereby reducing immune responses against the transplant and also against infectious pathogens. Therefore patients undergoing immunosuppressive therapy become more susceptible to opportunistic infection (227, 228) and cancer formation (229, 230) in addition to drug

specific side-effects such as those detailed in **table 1.1**. Current immunosuppressive regimes involve combinations of immunosuppressive drugs to lower the individual side-effects of each drug, whilst maintaining sufficient immunosuppression. Although these drug regimes have vastly improved one-year survival rates, they do not induce tolerance and over 50% of kidney transplants are still subject to chronic rejection within 10 years (231-233). Tolerance in the context of allografts is defined as donor-specific unresponsiveness without the need for continual immunosuppression (234) and is the ultimate goal of transplant treatments. Therefore there is a large scope for the introduction of new agents which act in a more specific manner with less side-effects, or new techniques to induce allo-antigen specific tolerance.

Drug Name	Biological Target	Pharmalogical Side Effects	References
Steroids	APC and cytokines General anti-inflammatory agent	Cushingoid Syndrome, Cataracts, Hypertension, Bone necrosis, Hyperglycemia, Hyperlipidemia, Growth retardation	(235)
Azathioprine	De novo purine biosynthesis. Prevents mitosis of fast-dividing cells.	Leukopenia Thrombocytopenia Megaloblastic anemia	(236, 237)
Cyclosporin	Blocks IL-2 production by inhibiting calcineurin	Renal damage Hypertension Vascular arteriosclerosis	(238, 239)
Tacrolimus	Inhibits calcineurin by targeting the corticoid receptor	Renal damage Hypertension Vascular arteriosclerosis	(239, 240)
Mycophenolate Mofetil (MMF)	Inhibits purine synthesis and the type II isomer of inosine monophosphate dehydrogenase thereby inhibiting activated lymphocytes	Minimal side-effects but must be used as an adjuvant	(241, 242)
Rapamycin	Blocks IL-2 activation and phosphorylation of 70 S6 kinase, inhibiting T cell progression from the G to S phase of cell cycle		(243, 244)

Table 1.1. Current immunosuppressive drugs, their targets and specific side-effects
A number of immunosuppressive agents with different targets are used alone or in combination to treat allograft rejection. However these drugs, while prolonging allograft survival, are systemic and non-discriminatory in their mode of action and thereby can increase the patients risk of opportunistic infections and cancer formation. In addition a number of these drugs have specific pharmacological side-effects as listed above.

1.12. Inhibition/Blockade of the CD28 Costimulatory Pathway in Transplantation

1.12.1. Generation of Soluble CTLA4-Ig Fusion Proteins

Soluble CTLA4 fusion proteins (CTLA4-Ig) have been generated by fusing the extracellular portion of CTLA4 to the hinge and CH2/CH3 regions of human IgG1 (54). As CTLA4-Ig maintains the high binding affinity of native CTLA4 to CD80/86 (54) it is able to prevent CD28 mediated costimulation in a similar manner to the "proximal competition" model (**Figure 1.4**). Moreover binding of CTLA4-Ig to CD80/86 on DC can induce IDO expression, further enhancing the immunosuppressive effect. LEA29Y which is a high affinity variant of CTLA4-Ig is currently in stage II clinical trials as a calcineurin sparing agent in organ transplantation (245).

1.12.2. Blockade of the CD28 Costimulatory Pathway

While treatment of DC with antibodies or antisense oligodeoxyribonucleotides directed against the CD80 and CD86 ligands inhibits the proliferation and cytokine secretion of T cells (246-248) the majority of experiments designed to block CD28 costimulation have utilised the duel specificity of CTLA4-Ig to both ligands.

The strong inhibitory effects of CTLA4-Ig on T cells have been demonstrated *in vitro* and *in vivo* (54). CTLA4-Ig treatment at the time of transplantation has been efficacious in prolonging allograft survival in murine models of cardiac (249, 250), corneal (251), renal (252), islet (253) and skin allografts (254). Although CTLA4-Ig has prolonged

allograft survival in a number of animal models and in some cases induced tolerance, the exact mechanisms of how this occurs are still unclear. In most cases CTLA4-Ig administration at the time of transplantation prolonged allograft survival marginally but did not induce tolerance. However delayed administration of CTLA4-Ig by 48h combined with the addition of donor splenocytes at the time of transplantation induced long-term (< 100 days) allograft survival (255, 256). These experiments illustrate the importance of the presentation of donor antigen early in the immune response for CTLA4-Ig to act effectively. The benefits of the delayed administration of CTLA4-Ig may be a function of the migration of passenger leukocytes from the organ or may indicate a requirement for partial T cell activation prior to costimulatory blockade. Sayegh (255) demonstrated that the major effect of the donor splenocytes administered in association with CTLA4-Ig was due to the direct presentation of donor antigen as opposed to the persistence or microchimerism of the donor splenocytes. The donor specificity of induced hyporesponsiveness was also demonstrated by the rapid rejection of third party allografts.

CTLA4-Ig treatment attenuates acute and chronic rejection (255), indicating that CTLA4-Ig is able to modulate both indirect and direct pathways of allorecognition. Blockade of the CD28-CD80/86 costimulatory pathway (using CTLA4-Ig) between DC and T cells also results in an increase in T cell apoptosis as measured by the level of DNA fragmentation in radiometric assays and by TUNEL assay (211). Moreover it was shown using FasL deficient DC that the increased apoptosis after costimulatory blockade was due to Fas/FasL independent pathways.

1.12.3. The Effects of CTLA4-Ig on the Th1/Th2 Pathway in Allotransplantation

In addition to reducing T cell proliferation, CTLA4-Ig blockade results in a significant shift in the polarisation of T cells towards a Th2 response. Guillot (257) demonstrated that CTLA4-Ig treatment lead to permanent cardiac allograft acceptance in rats, characterised by increased IL13 expression and decreased TNF-α expression. Similar results were found by Sayegh (258) in a murine renal transplant model. Although CTLA4-Ig treated mice still had mononuclear cell infiltration of the kidney this was associated with high levels of the Th2 cytokines IL-4 and IL-10 with no evidence of tissue damage. Kidneys of mice not treated with CTLA4-Ig had severe tissue damage and mononuclear infiltration, characterised by high levels of the Th1 cytokines IL-2 and IFNγ. It is however possible that the Th2 expression is not a direct effect of costimulatory blockade, but rather an outcome of inhibited T cell proliferation which may facilitate an increased effect of other signals.

1.12.4. IL-10 and Transplantation

While IL-10 has shown the ability to induce alloreactive T cell hypo-responsiveness *in vitro,* the matter is complicated *in vivo* by the broad range of IL-10 responsive cells. A number of different transplant models with different modes of IL-10 administration and timing regimes have been used with sharply contrasting results.

Intraperitoneal delivery of recombinant murine IL-10 at days 1, 0 and –1 modestly prolonged cardiac allograft acceptance at 25 μg/day (259). Higher or lower concentrations or administration at only days 0 and 6 post transplant resulted in precipitous rejection. A further study by Li (260) showed that an IL-10 regime given at days -3, -2, -1 pretransplant

prolonged allograft acceptance over the whole dose range of 0.2 to 200 μg/day. In contrast daily intraperitoneal administration of 100 μg/day of murine IL-10 at days 0-6 post-transplant resulted in exacerbated rejection characterised by increased circulating complement-dependent cytotoxic antibody titers and CTL splenic activity (261). Localised production of IL-10 however appears to have more success with intra-graft delivery prolonging allograft acceptance as it may circumvent the systemic activation of B cells and $CD8^+$ T cells (262-264). Thus it appears that limiting the systemic dose of IL-10 or careful control of the timing of delivery is crucial to the therapeutic outcome of IL-10 treatment. In contrast viral IL-10 has demonstrated prolongation of allograft survival in models for which mammalian IL-10 exacerbates rejection and may be a reflection of its less pleotropic nature (265, 266).

1.12.5. Limitations of Systemic CTLA4-Ig and IL-10 Treatments

The tolerogenic potential of CTLA4-Ig treatment has been demonstrated in a number of small animal and non-human primate models, however, systemic administration of CTLA4-Ig is likely to lack allo-specificity in attenuating T cell proliferation and therein may have similar limitations as current immunosuppressive drugs albeit over a shorter time span. Systemic treatment has been circumvented by recombinant gene expression of CTLA4-Ig within the transplanted graft and has prolonged the survival of transplanted islets (267) and hearts (257). Moreover an *ex vivo* approach to coat islets with CTLA4-Ig prior to transplantation in mice potentiated allograft survival and tolerance induction without systemic immunosuppression (268). As systemic administration of IL-10 can exacerbate allograft rejection (259, 261, 269), similar strategies have been used for IL-10. Notably *ex*

vivo adenoviral transfection of corneal allografts and intracoronary liposomal transfection of the IL-10 gene prolonged corneal and cardiac allograft survival, respectively (262, 263).

As transfection of whole organs can be difficult, genetic engineering of donor dendritic cells to produce CTLA4-Ig or IL-10 is viewed as an alternative approach, which would allow production of the proteins in a more localised fashion while providing allo-specificity.

1.13. Dendritic Cells as Gene Therapy Targets to Induce Transplantation Tolerance

1.13.1. The Role of Dendritic Cells in Transplantation

Dendritic cells (DC) are potent antigen presenting cells, expressing high levels of MHC Class I and II molecules and costimulatory molecules including CD80 and CD86 (95, 270). DC represent a significant portion of the "passenger leukocytes" responsible for direct allorecognition (189) and rapidly migrate to lymphoid tissue where they are able to augment the rejection process by activating allo-reactive T cells. The importance of DC in rejection was demonstrated by Lechler and Batchelor (271), by the induction of tolerance which was achieved by depleting rat kidney allografts of passenger leukocyte populations. Re-administration of donor derived DC resulted in reversal of tolerance. This demonstrates that DC are able to efficiently "educate" the recipient immune cells to donor antigens and play vital roles in transplant rejection. DC in the immature state (iDC) are found in the periphery and are characterised by high antigen uptake capabilities and low costimulatory

molecule and surface MHC expression, and thus are relatively weak stimulators of T cells. As DC migrate to secondary lymphoid tissues after antigen uptake, they mature with an increased T cell stimulatory capacity due to the upregulation of MHC and costimulatory molecule expression and reduced antigen capturing ability (272). The ability of DC to induce allostimulatory or tolerogenic responses has been shown to depend largely on the level of expression of costimulatory molecules including CD80 and CD86 (273). Indeed studies using immature DC (iDC) which lack sufficient CD80/86 costimulatory molecules have shown prolonged allograft survival in murine models of allograft transplantation (274). However rejection inevitably occurred which was attributed to *in vivo* DC maturation shifting the tolerogenic effect to an allostimulatory effect by the up-regulation of costimulatory molecules.

1.13.2. Genetic Modification of Dendritic Cells

A range of vectors is available for the transfer of genetic material into cells including viral and non-viral agents. Non-viral gene techniques include electroporation (275, 276), ballistic gene transfer (276), ultrasound (277), cationic liposomes and more recently use of nanoparticles (278) to facilitate gene transfer into target cells. However while non-viral technologies involve simple manufacture and minimal immunogenicity, gene transfer is often inefficient and transient (279-281). Viral vectors have been generated which typically offer higher levels of transfection efficiency. Advantages and disadvantages of the various vectors are shown in **table 1.2**.

Gene Therapy Vector	Advantages	Disadvantages	References
Non-Viral	Low production costs Low immunogenicity Good safety profile	Low transfection efficiency Transient gene expression Lack of clinical experience	(275-282)
Adenoviral	High transfection efficiency No insertional mutagenesis Infects dividing and non-dividing cells High titres may be generated Clinical experience	Strong immunogenicity (limits readministration) Moderate production costs Preferential targeting of the liver	(283-287)
Retroviral	Prolonged transgene expression Transgene expressed in progeny cells Clinical experience	Transfection of non-dividing cells is limited Potential of insertional mutagenesis Difficult manufacture	(288-293)
AAV	Long-term transgene expression Low toxicity	Potential for insertional mutagenesis Strong immunogenecity (limits readministration) Difficult manufacture Lack of clinical experience	(294-298)
Lentiviral*	High transfection efficiency Infects dividing and non-dividing cells	Potential for insertional mutagenesis Difficult manufacture Lack of clinical experience	(299, 300)

Table 1.2. Advantages and disadvantages of gene therapy techniques

A range of different viral and non-viral gene therapy agents have been developed to facilitate the incorporation of genetic material into target cells. Typically non-viral vectors have reduced costs associated with manufacture and a good safety profile although they are limited by poor transfection efficiency. Viral vectors, while demonstrating high transfection efficiency, are associated with immunological limitations and the potential for insertional mutagenesis. Viral vectors also have safety concerns related to the generation of replication-competent viruses during manufacture or *in vivo*.

*Lentiviral vectors have been developed from Retroviral vectors to overcome the requirement of cell division for transfection.

In the context of genetic manipulation of DC, viral vectors are typically used as they provide increased transfection efficiency compared to the non-viral alternatives. The terminal differentiation status of DC does however limit the effectiveness of retroviral vectors as the virus requires cells to undergo active division for infection. Adenoviral vectors may be readily grown to high titres and are able to infect non-dividing cells, making them ideal candidates for DC transfection. Importantly adenoviral transfection does not perturb DC function (301) although DC maturation has been reported (302, 303). Human monocyte-derived DC, particularly mDC, have been shown to lack coxsachie adenovirus receptors (304, 305), which are the primary cell attachment molecule for adenoviral serotype 5 vectors (306). However transfection of DC has been improved to levels greater than 90% by targeting the adenoviral vector to CD40 using bispecific antibodies (307) or adapter proteins (308) or by combining the adenoviral vector with cationic liposomes (309). More recently the modification of adenoviral vectors to express the fibre protein from group B adenoviruses has facilitated high levels of DC transfection by permitting binding to CD46 on the cell-surface (310, 311). Upon binding to DC, internalisation of adenoviral vectors is facilitated by $\alpha v\beta 3$ or $\alpha v\beta 5$ (312, 313).

The primary limitations of adenoviral vectors are the induction of strong anti-viral immune responses characterised by increased TNF, IL1 and IL6 secretion and CTL activation, which can result in the rapid clearance of adenoviral transfected cells and particles (283-285). However the immunogenicity of adenoviral transfected DC can be overcome by the incorporation of immunomodulatory genes as described in the next section.

1.13.3. Genetically Engineered Dendritic Cells in Tolerance Induction

The aim of DC treatment in a transplant setting is to increase the presentation of donor antigens to T cells in a tolerogenic setting without the requirement of systemic immunosuppression. Genetic modification of DC to produce immunomodulatory proteins has focussed on molecules that either block or reduce costimulatory molecule expression (IL-10, CTLA4-Ig, TGFβ), thereby negating the effects of DC maturation or molecules that promote apoptosis of allo-reactive T cells (FasL).

Treatment of DC with antisense oligonucleotides directed against CD40, CD80 and CD86 prevented autoimmune diabetes associated with an increase in regulatory T cells (314). In a further study, APC were transfected with a gene encoding a modified form of CTLA4, which was focussed to the endoplasmic reticulum preventing CD80/86 expression by intracellular binding and thereby inducing alloreactive T cell anergy (315).

Genetic modification of donor DC to produce TGFβ or FasL has prolonged heart allograft survival but has not addressed the issue of DC maturation (316-318). IL-10 treatment of DC is appealing as it can induce maturation arrest and downregulation of CD80/86 expression on DC, resulting in decreased allostimulatory capacity and inability to induce cytotoxic T cells (153, 165, 319, 320). *In vivo*, this form of treatment has reduced skin graft rejection in a humanised NOD-scid chimeric mouse model (264) and prolonged small intestine allo-transplantation from 7.3 days to 19.8 days (321). Furthermore daily administration of IL-10 transduced DC in an ovine model of renal transplantation demonstrated prolonged graft acceptance (322), however, the cessation of DC treatment resulted in rapid graft rejection indicating that the modified DCs were acting in an immunosuppressive rather that tolerogenic manner.

An alternate approach is to block existing CD80/86 ligands using CTLA4 fusion proteins. Transduction of DC would permit continuous production of fusion proteins capable of autocrine binding to the ligands and thereby is also likely to negate the effects of DC maturation. CTLA4-Ig modified DC induce allo-antigen T cell hyporesponsiveness as demonstrated by successful restimulation with third party but not donor-specific APC (323). *In vivo* DC engineered to produce CTLA4-Ig have demonstrated modest prolongation of islet allograft survival in murine models with survival increasing from 12 days to 20 days (253).

Adenoviral mediated gene transfer has been limited in many *in vivo* models by virtue of the rapid induction of T cell mediated immune responses against the adenovirus (324) although treatment with immunomodulatory proteins can attenuate this response. In particular systemic CTLA4-Ig treatment attenuates anti-viral immunity, thereby enhancing the persistence of adenoviral vectors *in vivo* (325). Moreover direct transfection of DC with CTLA4-Ig increases the survival of the cells in lymphoid tissues of MHC class II mismatched allogeneic recipients (323), providing evidence that CTLA4-Ig can act as a "stealth" gene to mask the immunogenicity of adenoviral vectors.

1.14. Targeting Multiple Dendritic Cell Pathways in Allotransplantation

While systemic administration of CTLA4-Ig or IL-10 has demonstrated prolonged allograft acceptance, indefinite allograft survival has not been achieved in large animal models. Furthermore, while genetic modification of DC to express CTLA4-Ig or IL-10 has demonstrated strong inhibitory responses *in vitro*, only marginal prolongation of allograft survival has been achieved. The redundancy of costimulatory pathways may account for the

failure of each agent to induce tolerance, as other positive costimulatory pathways such as ICOS may compensate for the loss of CD28 (326). Multiple pathways may therefore need to be targeted. Supporting the requirement of multiple agents Gorczynski (327) showed that portal vein infusion of dendritic cells transduced with adenoviral IL-10 and TGFβ prolonged murine renal allograft acceptance more than IL-10 alone. This was further prolonged by the infusion of CHO cells transfected with OX-2 (CD200) cDNA. Moreover the combination of CTLA4-Ig and OX40 (CD134) has also demonstrated additional benefits (328). Bonham (329) showed that long term allograft survival by DC was only accomplished when by transfection with adenoviral CTLA4-Ig was combined with blockade of NFκβ. Given that IL-10 is able to attenuate NFκβ, IL-10 may be a suitable agent to use in combination with adenoviral CTLA4 constructs to transfected DC. As well as operating through CD28 independent pathways, IL-10 is also able to downregulate CD80 and CD80 ligand expression, which may benefit CTLA4-Ig treatment by reducing the quantity required for complete sequestering of the ligands. Dendritic cell therapy with donor immature DC has demonstrated prolongation of allograft survival, however there is inferential evidence that the DC may mature *in vivo* (274). While IL-10 has been used to arrest DC maturation, the *in vivo* administration of IL-10 may be ineffective on pre-existing mature DC since those cells are IL-10 resistant. Thus dual gene transfer of CTLA4-Ig and IL-10 into DC potentially provides the advantage of safeguarding against costimulatory signal mediated activation of T cells upon DC maturation; that is as CD80/86 are upregulated, it is inferred that concomitant blockade by the autocrine and paracrine secretions of CTLA4-Ig occurs.

Genetic manipulation of donor DC to prolong allograft acceptance is an attractive strategy in that it can induce allo-antigen specific hyporesponsiveness, while sparing the non-donor reactive portion of the immune system. While promising results have been obtained in rodent models, there is a need to translate these findings into large animal models, which have more clinical relevance.

1.15. The Ovine Model of Renal Transplantation

The use of rodent models have been instrumental in the development of new therapies to prevent allograft rejection and acquire knowledge of immunological pathways, however direct extrapolation to clinical therapies is rare (330). The lack of correlation of clinical observations with rodent models has been attributed to a number of factors including the reduced prevalence and diversity of memory T cells (331-333) and the lack of expression of MHC Class II molecules on the vascular endothelium (334), a feature which has particular relevance to the rejection or acceptance of vascularised allografts (335). Moreover, significant differences in T_{reg} cell function have been highlighted between the murine and human species (336). Large animal models, although still not representing a perfect model of human immunity, address a number of these issues and are instrumental in the validation of therapies prior to clinical applications. Indeed while rodent models can provide important "proof of concept", large animal models represent a necessary step before clinical trials can proceed (337). The laboratory at The Queen Elizabeth Hospital (Adelaide, South Australia) has established an ovine model of renal transplantation based on the seminal work of Pedersen and Morris (338). The model involves the heterotropic

transplantation of the kidney to the neck region where it is anastomosed to the carotid artery and jugular vein. The transplanted organ is able to maintain renal function under immunosuppression and upon withdrawal exhibits rejection physiologically and histologically similar to human renal allograft rejection (339). While non-human primates do provide the closest matched models for human disease and therapy, use of such models is often limited by significant financial and social concerns (340). In comparison the sheep model represents reduced costs associated with purchase and husbandry. Moreover, the placid nature of sheep in addition to the well-characterised immune system makes the sheep model appealing for investigating pre-clinical therapies.

1.16. Project Aims:

Much progress has been made in murine transplant models with respect to novel immunomodulatory agents however, there is a requirement for reproducibility in large animal models. As the Transplantation Immunology Laboratory at The Queen Elizabeth Hospital has established an ovine model of renal transplantation, the focus of this thesis is related to the isolation and characterisation of the ovine CTLA4 molecule and its effects on the modulation of the ovine immune response both in vitro and in vivo. Since the effects of CTLA4-Ig on human cells have been extensively characterised, this study endeavors to compare both species and uses the human system to set *in vitro* baseline data.

The key aims of this study were

(i) To examine the baseline effect of CTLA4-Ig immunomodulation in human DC-MLR (**Chapter 3**) and due to the redundancy in CTLA4-Ig immunomodulation, also to investigate the combination with the immunosuppressive cytokine IL-10, based on the rationale described above in **section 1.15**.

(ii) To determine the immunomodulation of CTLA4 fusion proteins on ovine *in vitro* allogeneic immune responses by

   a) isolating and characterising ovine DC obtained by cannulation of sheep lymphatics (**Chapter 4**)

   b) generating adenoviral vectors incorporating a CTLA4-EGFP fusion construct and subsequently transducing DC to induce T cell hyporesponsiveness in the DC-MLR (**Chapter 5**)

(iii) To examine ovine DC cellular therapy strategies *in vivo* by specifically investigating the immunomodulation of ovine DC transduced with adenoviral CTLA4-EGFP in a chimeric NOD-*scid* mouse model of ovine skin rejection (**Chapter 6**).

Chapter 2

Materials and Methods

2.1. Materials

2.1.1. Antibodies

2.1.1.1. Anti-Human antibodies

CD80 (IgG1)	Immunotech, France
CD86 (IgG1)	Serotec, UK
MY-4 FITC-conjugated (IgG2b)	Coulter Corp., USA
CD4-PE conjugated (IgG1)	BD Biosciences, USA
CD56-FITC (IgG2b)	BD Biosciences, USA
CD14 (IgG2b)	Serotec, UK
CD83 (IgG2b)	Serotec, UK
CD83-PE (IgG2b)	Immunotech, France
CD1a (IgG2a)	Serotec, UK
MHC Class I (IgG2b)	Laboratory-derived supernatant
MHC Class II (IgG2a)	Laboratory-derived supernatant
CCR7 (IgG2a)	R&D Systems, USA
CD40 (IgG2a)	Serotec, UK
CMRF56 (IgG1)	Dr D. Hart, Mater Medical Institute
CD3 (IgG1)	BD Biosciences, USA

2.1.1.2. Anti-ovine antibodies

MHC Class I (SBU I, IgG1)	University of Melbourne*
MHC Class II DQ/DR (SBU II, IgG1)	University of Melbourne*
CD44 (clone 25.32, IgG1)	University of Melbourne*

CD1a (clone 20.27, IgG1)	University of Melbourne*
Anti bovine-CD21 (IgG1) – (ovine cross-reactive)	Serotec, UK
CD25 (IgG1)	Serotec, UK
CD31 (IgG2a)	Serotec, UK
CD4 (clone 44.38, IgG2a)	University of Melbourne*
CD14 (IgG1)	Serotec, UK
CD8 (clone 38.65, IgG2a)	University of Melbourne*

*University of Melbourne, School of Veterinary Science, Australia

2.1.1.3. Control antibodies

1D4.5 (IgG2a)	Dr P. Hart, Flinders University
X63 (IgG1)	ATCC, USA
PE conjugated mouse IgG2a	BD Biosciences, USA
FITC conjugated mouse IgG2b	BD Biosciences, USA

2.1.1.4. Secondary antibodies

FITC conjugated Sheep anti-mouse IgG	Chemicon, Australia
PE conjugated Sheep anti-mouse IgG	Chemicon, Australia

2.1.1.5. Other antibodies

GFP polyclonal (goat anti-GFP)	Rockland, USA
GFP monoclonal (mouse anti-GFP)	Roche, USA
Biotin conjugated horse anti-mouse IgG	Vector Laboratories, USA

2.1.2. Cell Lines

2.1.2.1. Bacterial

TG1α *E.coli*	IMVS, Adelaide
BJ5183 *E.coli*	Vogelstein, B.*
DH10β *E.coli*	IMVS, Adelaide
Staphylococcus aureus	IMVS, Adelaide

2.1.2.2. Cell culture

Ovine adult fibroblasts	Generated from ovine skin
HEK-293 cells	Vogelstein, B.*
CHO cells	IMVS, Adelaide

*The Howard Hughes Medical Institute, Baltimore, USA

2.1.3. Cytokines and recombinant proteins

Recombinant Enhanced Green Fluorescent Protein (EGFP)	Clontech, USA
Recombinant human Interleukin-10 (IL-10)	Bender Medsystems, Austria
Recombinant human Interleukin-4 (IL-4)	Peprotec, USA
Recombinant human Granulocyte-Macrophage Colony Stimulating Factor (GM-CSF)	Schering-Plough, Australia
Recombinant human Tumour Necrosis Factor α (TNFα)	Genzyme Corporation, USA
Recombinant human CTLA4-Ig	R&D Systems

2.1.4. Radiochemicals

[^{3}H]-labeled thymidine	Amersham, Australia
[^{35}S]-labeled methionine/cysteine	ICN, USA

2.1.5. Flow Cytometry Reagents

FACS Lysing^{TM} solution	Becton Dickinson, USA
Sodium azide	Ajax Chemicals, Australia

2.1.6. Tissue Culture Reagents

BetaPlate scintillation fluid	Wallac, Finland
Foetal Calf Serum (FCS)	CSL, Australia
L-Glutamine	Multicel, Australia
Lymphoprep^{TM}	Nycomed, Norway
Metrizamide	Nycomed, Norway
Minimal Essential Medium (MEM) (cat 61100-061)	Gibco BRL, USA
Mitomycin-C Kyowa	Bristol-Myers Squib, Australia
Non-Essential Amino Acids (10X)	ICN Biomedicals, USA
Penicillin/Streptomycin	Cytosystems, Australia
RPMI 1640 powdered media (cat: 1060120)	ICN, USA
RPMI 1640, methionine/cysteine deficient (cat 16464)	ICN, USA
Sodium pyruvate	ICN, USA
Trypsin	Sigma, USA

2.1.7. Histological Reagents

Avidin/Biotin blocking kit	Vector Laboratories, USA
Harris Hematoxylin Solution	Sigma, USA
Normal horse serum	ICN Biomedicals, Australia
Poly-L-lysine™	Sigma, USA
Streptavidin-Alkaline phosphate conjugate	Roche, Germany
SubX™ clearing solution	Surgipath Medical Industries, USA
SubX™ mounting media	Surgipath Medical Industries, USA
Vectastain ABC kit	Vector Laboratories, USA

2.1.8. Molecular Biology Reagents

Agarose (DNA grade)	Progen, Australia
Ampicillin	Roche, Germany
BglII	Roche, Germany
Calf Intestine Phosphatase (CIP)	Promega, USA
Custom oligonucleotides	Genset Pacific, Australia
EcoRI restriction endonuclease	New England Biolabs, USA
EcoRV restriction endonuclease	Roche, Germany
HindIII restriction endonuclease	Progen, Australia
KpnI restriction endonuclease	Fermentas, Lithuania
JETSTAR Midi Prep Plasmid kit	Genomed, USA
Kanamycin	Life Technologies, USA

LipofectAMINE™	Life Technologies, USA
$MgCl_2$ solution (25 mM)	Fisher Biotech, USA
Mineral Oil	Sigma, USA
MMLV Reverse Transcriptase	Life Technologies, USA
dNTPs	Promega, USA
NotI restriction endonuclease	New England Biolabs, USA
Oligo dT	Amersham, Australia
PacI restriction endonuclease	New England Biolab, USA
PmeI restriction endonuclease	New England Biolab, USA
Protease inhibitor cocktail kit	ICN Biomedicals, Australia
pUC19/HpaII Molecular Markers	Geneworks, Australia
RNase A	Sigma, USA
RNAsecure reagent	Ambion, USA
RNAsin	Promega, USA
RNA Storage Soln. (1mM Sodium Citrate pH 6.4)	Ambion, USA
SPP1/EcoRI Molecular Markers	Geneworks, Australia
T4 Ligase	Promega, USA
Tth1 Polymerase	Fisher Biotech, USA
Tth1 PCR buffer	Fisher Biotech, USA
Ultraclean DNA purification kit	Geneworks, Australia

2.1.9. Plasmid vectors

Living Colors® pEGFP-N1 Expression Vector	Clontech, USA
pAdEasy1	Stratagene, USA
pShuttleCMV	Stratagene, USA
pSecTagB	Invitrogen, USA

2.1.10. Immunoprecipitation Reagents

Acrylamide (40%) 39:1 acrylamide:bis-acrylamide	Bio-Rad, USA
Amplify™	Amersham, UK
β-mercaptoethanol	Sigma, USA
Bovine serum albumin	Sigma, USA
Bromophenol blue	Bio-Rad, USA
Coomassie brilliant blue R-250	ICN Biomedicals, USA
Glycerol	Ajax Chemicals, Australia
Low-range SDS-PAGE molecular weight standards	Bio-Rad, USA
Nitro-cellulose membrane	Bio-Rad, USA
Nonidet P-40 (NP-40)	Sigma, USA
Normal rabbit serum	ICN Biomedicals, Australia
Ovalbumin	Sigma, USA
Sodium dodecyl sulphate (SDS)	BDH, Australia
TEMED (N,N,N',N'-Tetramethylethylenediamine)	Bio-Rad, USA
Triton X-100	Bio-Rad, USA
Trizma base (Tris [hydroxymethyl] Aminomethane)	Sigma, USA

Trizma HCl (Aminomethane Hydrochloride)	Sigma, USA

2.1.11. Other Reagents

Bacto-Yeast extract	Oxoid, UK
Concanavalin A type IV (Con A)	Sigma, USA
Dimethyl sulphoxide (DMSO)	Ajax Chemicals, Australia
Diethanolamine	Ajax Chemicals, Australia
Ethylenediamine tetraacetic acid (EDTA)	Sigma, USA
Ethidium bromide	Sigma, USA
Patent Blue V Dye	Sigma, USA
Phenol	Progen, Australia
Sigma 104 Substrate	Sigma, USA
Trypan Blue	BDH, Australia
Tween-20	Bio-Rad, USA

2.2. Solutions and Buffers

2.2.1. Agarose Gel Electrophoresis Buffers and Solutions

50x TAE

Compound	Conc.	Amount
Trizma base	1.6 M	193.8 g
Sodium acetate	800 mM	65.6 g
EDTA	40.27 mM	14.9 g
H_2O		To 100ml
pH to 7.2. Diluted 1/10 in dH_2O for use		

6x Loading Buffer

Compound	Conc.	Amount
50X TAE	1X	50 µl
Glycerol	50%	1.25 ml
Bromophenol Blue	24%	600 µl
H_2O		To 2.5 ml

Ethidium Bromide (1.25 µg/ml)

Compound	Conc.	Amount
Ethidium Bromide (10 mg/ml stock)	1.25 µg/ml	50 µl
		To 400 ml

Agarose Gels

Compound	Conc.	Amount
Agarose (0.8% gel)	0.8%	0.48 g
Agarose (1% gel)	1%	0.6 g
Agarose (2% gel)	2%	1.2g
H_2O		To 60ml

2.2.2. RNA Extraction Buffers and Solutions

Chloroform/iso-amyl alcohol

Compound	Conc.	Amount
Chloroform	98%	196ml
Iso-amyl alcohol	2%	4ml

Solution D

Compound	Conc.	Amount
Guanidine Thiocyanate Salt	4 M	12.5 g
0.75 M Sodium Citrate (pH 7.0)	25 mM	0.88 ml
10% N-Lauroylsarcosine	0.5%	1.32 ml
H_2O		To 25 ml
Dissolved at 65°C. 180 µl (0.1 M) β-mercaptoethanol added.		

RNA Secure/Citrate Solution

Compound	Conc.	Amount
RNAsecure	4%	4 µl
RNA citrate storage solution	96%	96 µl

2.2.3. Cloning and Transfection Buffers and Solutions

Luria Broth (LB)

Compound	Conc.	Amount
Bacto-Yeast Extract		2.5 g
Bacto-Tryptone		5 g
Sodium Chloride		5 g
H_2O		To 500 ml
pH adjusted to 7.0 and autoclaved		

LB Agar

Compound	Conc.	Amount
Bacteriological Agar		15 g
LB		To 1 l
Kanamycin (30 mg/ml stock)	30 µg/ml	1 ml
LB was heated until agar was dissolved and cooled to 55°C before kanamycin was added. LB agar was poured into perti dishes and flamed to remove air bubbles.		

1M $CaCl_2$

Compound	Conc.	Amount
$CaCl_2$	1M	7.351 g
H_2O		To 50 ml
Solution autoclaved		

1M $MgCl_2$

Compound	Conc.	Amount
$MgCl_2.6H_2O$	1M	10.165 g
H_2O		To 50 ml
Solution autoclaved		

$CaCl_2/MgCl_2$ Transformation Solution

Compound	Conc.	Amount
1M $CaCl_2$	0.1M	2 ml
1M $MgCl_2.6H_2O$	20 mM	400 µl
H_2O		To 20 ml

Mini-Preparation Solution 1

Compound	Conc.	Amount
D-Glucose	50 mM	0.9 g
Tris-HCl	25 mM	0.934 g
0.5 M EDTA	10 mM	2 ml
H_2O		To 100 ml
pH adjusted to 8.0 and autoclaved		

Mini-Preparation Solution 2

Compound	Conc.	Amount
1 M sodium hydroxide	0.2 M	4 ml
20% SDS	1%	1ml
H_2O		To 20 ml
Solution autoclaved		

Mini-Preparation Solution 3

Compound	Conc.	Amount
Potassium acetate	3 M	29.4 g
Glacial acetic acid		11.5 ml
H_2O		To 100ml
pH adjusted to 4.8 and autoclaved		

Mini-Preparation Storage Solution (TE8/RNase)

Compound	Conc.	Amount
DNase inactivated RNaseA	200 ng	10 µl
TE8		5 ml

SOC Medium

Compound	Conc.	Amount
Bacto-Yeast Extract		5 g
Bacto-Tryptone		20 g
NaCl (5M)	10 mM	2 mL
KCl (1M)	2.5 mM	2.5 mL
H_2O		To 1 L
pH adjusted to 7.0 and autoclaved		

2.2.4. Tissue Culture Buffers and Solutions

Phosphate Buffered Saline (PBS)

Compound	Conc.	Amount
Sodium dihydrogen orthophosphate	40.1 mM	6.25 g
Sodium chloride,	1.2 M	70 g
Sodium hydrogen orthophosphate	161 mM	22.85 g
H_2O		To 1 L
Solution autoclaved and diluted 1/10 for use.		

RPMI 1640

Compound	Conc.	Amount
RPMI 1640 powdered media		1 sachet
Sodium pyruvate	1 mM	10 ml
Sodium bicarbonate	23.81 mM	2 g
HEPES	9.99 mM	2.38 g
Penicillin/Streptomycin	50 IU/ml	10 ml
Solution acidified to a pH of 7.3 by CO_2 bubbling and filter sterilised.		

S10g Tissue Culture Medium

Compound	Conc.	Amount
Fetal calf serum (FCS)	10%	10 ml
L-Glutamine	1%	1 ml
RPMI		To 100ml

Modified Essential Medium (MEM)

Compound	Conc.	Amount
MEM		1 sachet
Penicillin/streptomycin	1%	10 ml
$NaHCO_3$	26 mM	2.2 g
Solution prepared under endotoxin-free conditions		

Complete MEM (cMEM) Culture Medium

Compound	Conc.	Amount
FCS	10%	10 ml
L-Glutamine	1%	1 ml
Non-essential amino acids	1%	1 ml
MEM		To 100 ml

Citric Saline Solution

Compound	Conc.	Amount
KCl	1.35 M	10.06 g
Sodium citrate	150 µM	4.4 mg
H_2O		To 100 ml
Solution autoclaved		

Electroporation Media

Compound	Conc.	Amount
D-glucose	10 mM	100 µl
DTT	1mM	1 µl
RPMI 1640		To 10 ml

Mitomycin-C

Compound	Conc.	Amount
Mitomycin-C Kyowa	1 mg/ml	1 vial
S10g		10 ml
S10g added to vial using a sterile 21G needle to prevent contamination.		

2.2.5. Immunoprecipitation Buffers

RIPA buffer

Compound	Conc.	Amount
NaCl (1M)		15 ml
Sodium Dexoycholate	10%	5 ml
10% SDS	1%	1 ml
NP-40	1%	1 mL
Tris HCl		0.03 g
H_2O		To 100 mL

Laemmli buffer

Compound	Amount
Tris HCl (pH 6.8)	1.25 ml
10% SDS	2 ml
10% Glycerol	2 ml
10x Protease inhibitor	1 ml
Bromophenol blue (0.05% stock)	500 µl
H_2O	To 10 ml
10% (v/v) β-mercaptoethanol added for reducing gels	

Acrylamide 10% Resolving Gel

Compound	Amount
40% Acrylamide (36:1 Acrylamide:Bis Acrylamide)	1735 µl
H_2O	4135 µl
Solution A	1000 µl
10% SDS	70 µl
10% APS	45 µl
TEMED	10 µl
Gel poured immediately after TEMED and APS added	

Acrylamide 3% Stacking Gel

Compound	Amount
40% Acrylamide (36:1 Acrylamide:Bis Acrylamide)	200 µl
H_2O	1800 µl
Solution B	640 µl
10% SDS	21 µl
10% APS	15 µl
TEMED	5 µl
Gel poured immediately after TEMED and APS added	

SDS-PAGE Electrophoresis Buffer

Compound	Conc.	Amount
Trizma Base	0.05 mM	0.006 g
Glycine	0.37 mM	0.028 g
SDS	0.1% w/v	1 g
H_2O		To 1000 ml

Loading Buffer

Compound	Conc.	Amount
2X SDS Sample Buffer	50% v/v	500 µl
2X Lysis Buffer	50% v/v	500 µl
10% (v/v) β-Mercaptoethanol added for reduced gels		

2X Lysis Buffer (pH to 7.6)

Compound	Conc.	Amount
Trizma Base	10 mM	0.012 g
10% Triton X-100	1% v/v	1 ml
10% SDS	1% v/v	100 µl
NaCl	150 mM	0.088 g
H_2O		To 10 ml
pH adjusted to 7.6		

2X Sample Buffer (pH to 6.8)

Compound	Conc.	Amount
Trizma Base	12 mM	0.0726 g
SDS	6% w/v	3 g
Glycerol	20% v/v	10 ml
Bromophenol Blue	0.03% v/v	0.015 g
H_2O		To 50 ml
pH adjusted to 6.8		

10X Staining Solution

Compound	Conc.	Amount
Coomassie Brilliant Blue	2.5% v/v	12.5 g
Methanol	45% v/v	225 ml
Glacial Acetic Acid	10% v/v	50 ml
H_2O		To 500 ml
Diluted to 1X working conc. in Destain Solution		

Destain Solution

Compound	Conc.	Amount
Methanol	45% v/v	450 ml
Glacial Acetic Acid	10% v/v	100 ml
H_2O		To 1000 ml

2.2.6. Flow Cytometry Buffers and Solutions

FACS Washing Buffer

Compound	Conc.	Amount
FCS	2%	5 ml
Sodium azide	0.1%	100 µl
PBS		To 100 ml

FACS Lysing Buffer

Compound	Conc.	Amount
FACS Lysing solution	10%	10 ml
PBS		To 100 ml

2.2.7. Dephosphorylation Buffers and Solutions

STE buffer (10x)

Compound	Conc.	Amount
TrisHcl (pH 8)	100 mM	50 ng
NaCl	1 M	5 mg
EDTA	10 mM	0.5 ng
H_2O		To 1000 ml

2.2.8. ELISA Solutions

Coating buffer

Compound	Conc.	Amount
Na_2CO_3	150 mM	0.159 g
$NaHCO_3$	350 mM	0.293 g
H_2O		To 100 ml
pH adjusted to 9.6.		

PBS-Tween

Compound	Conc.	Amount
NaCl	0.14 M	8 g
KH_2PO_4	1.5 mM	0.2g
$Na_3HPO_4x12H_2O$	18.6 mM	2.9 g
KCl	2.7 mM	0.2 g
Tween-20		1 ml
H_2O		To 1000 ml
pH adjusted to 7.2-7.4.		

Diethanolamine buffer (per 500 ml)

Compound	Conc.	Amount
Diethanolamine	9.7%	48.5 ml
$MgCl_2x6H_2O$	0.5 mM	50 mg
NaN_3	3 mM	0.1 g
H_2O		To 500 ml

Phosphate Substrate

Compound	Conc.	Amount
Sigma 104 substrate		2 tablets
Diethanolamine buffer		10 ml
Sigma 104 substrate tablets dissolved in buffer at 37°C in the dark		

2.2.9. Immunohistology Solutions

Diaminobenzidine substrate solution

Compound	Conc.	Amount
Diaminobenzidine		1 mg
Tris buffer		1 ml
Solution diluted 50% with a 0.02% hydrogen peroxide solution and stored in the dark.		

Eosin

Compound	Conc.	Amount
1% aqueous eosin	10 mg/ml	50 ml
1% phloxine	10 mg/ml in H_2O	5 ml
Glacial acetic acid		2 ml
EtOH	95%	390 ml

Hydrogen peroxide solution

Compound	Conc.	Amount
Hydrogen peroxide	0.02%	2 µl
H_2O		To 10 ml

2.3. General Methods

2.3.1. Cell Culture

2.3.1.1. Ovine and Human Peripheral Blood Mononuclear Cell (PBMC) Extraction

Buffy coats were prepared from heparinised peripheral blood obtained from healthy donors (Red Cross Blood Service, Adelaide, Australia) and PBMC was isolated by differential centrifugation through a Lymphoprep density gradient.

Blood was aliquoted into 50 mL V-bottom tubes (10 mL per tube) with 25 mL PBS and underlayed with 10 mL of Lymphoprep. Tubes were centrifuged for 20 min at 770 g (540 g for human cells) with the brake turned off. The mononuclear cell layer was harvested and resuspended in PBS. Cells were centrifuged for a further 10 min at 770 g (540 g for human cells). Cells were washed in 45 mL PBS and centrifuged at 135 g (50 g for human) for 10 min to remove plasma followed by two more PBS washes at 340 g. Pellets were resuspended in 2 mL S10g and a cell count performed using a 1:2 Trypan Blue dilution on a haemocytometer.

2.3.1.2. Human Monocyte Derived Dendritic Cells

Monocytes were selected by adherence to plastic. Briefly, 5 x 10^7 PBMC were panned for 1 h at 37°C in 10 ml RPMI plus 1% FCS in 75 cm^2 plastic tissue culture flasks (Corning, USA). Non-adherent cells were removed and the remaining adherent cells were

cultured in complete medium supplemented with 400 U/ml IL-4 and 800 U/ml GM-CSF for 5 days to generate immature DC (iDC). The addition of 10 ng/ml TNF-α to the iDC for a further 2 days generated mature DC (mDC).

2.3.1.3. Nylon Wool Isolation of T Cells.

Following the removal of monocytes by adherence (**2.3.1.2**), nylon wool purified T cells (NWT) were obtained by applying the non-adherent cells to nylon wool columns equilibrated with RPMI. The non-adherent cells were incubated in the columns for 30 min at 37°C to adsorb B cells and the enriched NWT cells were obtained by elution with RPMI plus 10% FCS. Cells were washed twice in PBS prior to use.

2.3.1.4. Mixed Lymphocyte Reaction

PBMC were extracted from peripheral blood from two ovine or human individuals (**2.2.1.1**). PBMC were co-cultured in 96-well round-bottom plates (Corning, USA) with 1 x 10^5 cells from each individual in S10g media. The total volume for each well was 200 μL. In case of the DC-MLR, autologous or allogeneic DC were used in place of one PBMC population. Plates were incubated for 4 days in a 37°C, 5% CO_2 enriched and humidified incubator. Wells were individually pulsed with 1 μCi methyl [^{3}H] thymidine and incubated for a further 18 h. Cells were harvested using a Microtitre Tomtec Cell Harvester (Turku, Finland) onto Wallac gridded filter mats (Wallac, USA). Filter mats were treated with β-scintillant and cellular tritium incorporation measured using a Wallac MicroBeta® Scintillation Counter (USA). Results were expressed as the mean of triplicate wells +/- standard deviation. Paired two-tailed student t-tests were used for statistical analysis.

2.3.1.5. Cell Lines

Chinese hamster ovary (CHO) cells and fibroblasts were propagated in 75 cm^2 flasks in S10g. Upon confluence, CHO cells and fibroblasts were detached from the flasks with 2 mM EDTA, washed in PBS and used to reseed three 75 cm^2 flasks. Human embryonic kidney 293 (HEK-293) cells were grown in DMEM, until 70% confluence was achieved. At this time cells were detached using citric saline solution, washed in PBS containing 5% FCS and used to reseed three flasks. All cells were grown at 37°C, 5% CO_2.

2.3.2. Molecular Biology Methods

2.3.2.1. Total RNA Extraction

Total RNA was isolated using the Acid Guanidinium Thiocyanate-Phenol-Chloroform Extraction Method (341). Tissue or cells were vortexed with 500 µl Solution D to liberate intracellular components. Sequential addition of 50 µl sodium acetate (2M), 500 µl water-saturated RNA phenol and 100 µl chloroform:iso-amyl alcohol (49:1) was performed with vortexing of the mixture between each addition. The solution was incubated on ice for 15 min and centrifuged at 13 500 g for 20 min at 4°C. The upper aqueous layer was removed and added to an equal volume of isopropanol. The mixture was vortexed and RNA precipitated by overnight incubation at minus 70°C. RNA was pelleted by centrifugation at 13 500g for 10 min and washed twice with 75% ethanol. The purified pellet was air-dried, resuspended in 10 µl RNA secure citrate solution and heated at 65°C for 10 min. RNA concentration was determined by measuring the optical density (OD) of a

1:50 dilution in sH_2O at 260 nm in a Beckman (USA) spectrophotometer. One OD unit corresponded to 2 μg/μL total RNA.

2.3.2.2. Reverse Transcription (RT)

One microgram of RNA was then added to 4 μL Oligo dT, heated at 60°C for 5 min and snap cooled on ice. 33 μL RT-mastermix (**table 2.1**) was added giving a total volume of 40 μL.

Table 2.1. Reverse Transcription Master Mix

RT Component	Volume/reaction
Sterile H_2O	19 μl
5 x First Strand Buffer	8 μl
10mM dNTPs	4 μl
RNAsin	1 μl (40U)
MMLV reverse transcriptase	1 μl
	33 μl

Tubes were vortexed, pulsed and incubated at 37°C for 1 h. Reactions were heat inactivated at 70°C for 10 min, snap cooled and pulsed. Volume was made up to 100 μl with sterile milliQ H_2O and cDNA stored at -70°C.

2.3.2.3. Polymerase Chain Reaction (PCR)

Details of primers are set out in **appendix 1**. Tth Polymerase was used for all PCR reactions. PCR mastermix (**table 2.2**) was prepared in a DNA free room and 22.5 μl

aliquoted into PCR tubes. A drop of sterile mineral oil was added to prevent vapourisation and 2.5 µl cDNA added in the laboratory. PCR tubes were pulsed and reactions performed in a Perkin Elmer DNA Thermal Cycler (USA)

Table 2.2. PCR Mastermix	
PCR COMPONENT	**Vol/Reaction**
Sterile Water	16.4 µl
10x Tth Buffer	2.5 µl
25 mM $MgCl_2$	2.5 µl
dNTP (0.2 mM)	0.5 µl
Forward Primer (100 µM)	0.25 µl
Reverse Primer (100 µM)	0.25 µl
Tth Polymerase	0.1 µl
cDNA	2.5 µl
TOTAL VOLUME	25 µl

2.3.2.4. Agarose Gel Electrophoresis

PCR products (12.5 µl), premixed with 2.5 µl 6x loading buffer, were electrophoresed through 2% w/v agarose gels using a Bio-Rad Minigel apparatus. Restriction digest products (10 µl) were run with 2 µl 6x loading buffer on 1% w/v agarose gels. Adenoviral digest products were run on 0.8% w/v agarose gels due to the large size of the vectors. 2 µl of pUC19 (Bresatec, Australia) or SPP1/EcoRI (Geneworks, Adelaide) markers were premixed with 2.5 µl of 6x loading buffer (2.5 µl) and 10 µl TAE buffer. All samples were loaded onto the gel and electrophoresed at 90 V for approximately 1h. Gels were stained in ethidium bromide (1.25 µg/ml) for 20 min and photographed under UV illumination using Kodak 667 Instant Film (Kodak, Australia).

2.3.2.5. Endonuclease Restriction Digestion of DNA

Unless specified, 1 μg of DNA was digested in each reaction. DNA concentrations of PCR products were calculated based on band intensity comparison with molecular weight markers of known concentration, viewed on agarose gels under UV illumination (**2.2.5**). Digest reactions were setup as per **table 2.3** and were run overnight at 37°C.

Table 2.3: Restriction Digest Reactions

Single Digest Reaction	
DNA	1 μg
10 x Buffer	2 μl
10 x BSA	2 μl
Enzyme	1 μl (10 units)
H_2O	to 20 μl

Double Digest Reaction	
DNA	1 μg
10 x Buffer	2 μl
10 x BSA	2 μl
Enzyme 1	1 μl (10 units)
Enzyme 2	1 μl (10 units)
H_2O	To 20 μl

2.3.2.6. Agarose Gel Purification of Restriction Digest Products

Restriction digest products were loaded into multiple wells of a 1% w/v agarose gel and electrophoresed at 90 V for 1 h. Exterior lanes for each digest were excised, stained in ethidium bromide and illuminated under UV light. Bands were marked on the excised lanes and then used to identify the positions of the band regions on unstained lanes. Bands were excised from the unstained lanes, homogenised and transferred to pre-weighed eppendorf tubes for further purification (**2.3.2.7**). DNA recovery was estimated by

comparison against band intensities of molecular weight markers of known DNA concentration.

2.3.2.7. Ultraclean™ Purification of DNA

DNA in solution and isolated from gels was purified using the UltraClean™ DNA Purification Kit (Mo Bio Laboratories, USA). Purification was performed following manufacturer's guidelines, with an assumed 50% loss of DNA.

2.3.2.8. Ligation of DNA Fragments into Cloning Vectors

Ligation reactions were setup as per **table 2.4** and incubated overnight at 4°C in 0.5 mL tubes:

Table 2.4. Ligation Reaction	
DNA Inserts	X µl
10 x Ligase Buffer	1 µl
Plasmid DNA	1 µl (50 ng)
T4 Ligase enzyme	1 µl
Sterile H_2O	To 10 µl

2.3.2.9. Dephosphorylation of DNA Fragments

To 2 µg (10 µl) of digested DNA, 1 µl Calf Intestine Phosphatase (CIP), 5 µl CIP buffer (ProMega, USA) and 34 µL sH_2O was added. Dephosphorylation mixture was incubated at 37°C for 15 min and 56°C for 15 min. Another 1 µl CIP was added and incubated under the same cycle conditions. To inactivate the CIP 35 µl sH_2O, 10 µl STE

buffer (10x) and 5 µl SDS (10%) was added and incubated at 70°C for 15 min. DNA was purified as per **2.3.2.7**.

2.3.2.10. Preparation of Competent *E.coli* TG1α and DH10B Cells

Competent TG1α and DH10B *E.coli* cells were prepared following the same protocol. Cells from laboratory glycerol stocks were streaked onto LB plates (30 µg/ml). A single colony was resuspended in LB media and grown at 37°C, shaking at 200 rpm. 1ml of overnight culture was added to 25 ml LB and incubated (37°C, 200 rpm) until the culture reached OD_{600nm} of 0.42. Cells were chilled on ice for 15 min and centrifuged at 280 g for 10 min at 4°C. Pellets were resuspended in 2 ml ice cold 0.1 M $CaCl_2$/ 20 mM $MgCl_2$ solution and incubated on ice for 1 h.

2.3.2.11. Transformation of Competent *E.coli* Cells

5 µl ligation mix (**2.3.2.8**) was added to 200 µl competent *E.coli* cells (**2.3.2.10**) and incubated on ice for 30min. Cells were heat-shocked for exactly 90 s at 42°C and chilled on ice for 10 min. 500 µl LB medium was added and cells were incubated at 37°C, 200 rpm for 1 h. Cells were briefly pulsed in a centrifuge, 400 µl of supernatant was removed to concentrate the cells and the pellet was resuspended by flick-mixing. The resulting 300 µl of the cell suspension was spread evenly onto two LB kanamycin (30 µg/ml) plates and incubated overnight at 37°C. Uncut plasmid with no insert was used as a positive control for the efficiency of transformation and untransformed *E.coli* cells as a negative control.

2.3.2.12. Plasmid Mini-preparation (Mini-prep)

Single colonies from transformation spread plates were isolated, resuspended in 2 ml LB kanamycin (30 μg/ml) and incubated at 37°C, 200 rpm overnight. One and a half ml of the cell culture was used for mini-preparations. Culture was centrifuged on high setting (11, 600 g) for 1 min and the cell pellet was resuspended in 100 μl Mini-prep Solution-1 for 5 min. Cells were lysed by mixing with 200 μl Mini-prep Solution-2 and kept on ice for 5 min. The reaction was neutralised with 150 μl Mini-prep Solution-3 for 5 min on ice. Cell lysate was centrifuged for 10 min and the supernatant transferred to a new tube. DNA phenol (225μl) and chloroform (225μl) were added and the cells were centrifuged on high for 10 min. Plasmids were precipitated by the addition of 2 volumes (900 μl) of 100% ethanol and centrifuged on high for 10 min. Plasmid pellets were washed with 250 μl 70% ethanol, centrifuged for an additional 10 min and the pellet was air-dried. The pellet was resuspended in 45 ml TE8 and 5 μl DNase inactivated RNaseA (200 μg/ml).

2.3.2.13. Plasmid Midi-preparation (Midi-prep)

Single colonies were used to inoculate 2 ml of LB Kanamycin (30 μg/ml) and grown overnight at 37°C 200rpm. The overnight culture was used to seed 100 ml LB Kanamycin and incubated overnight at 37°C 200 rpm. Plasmid midi-prep was conducted using a JetStar 2.0 Plasmid Midi Kit (Genomed, Germany) as per the manufacturer's protocol. Column elution containing the plasmids was divided into 5 eppendorf tubes (1 ml into each) and plasmids were precipitated by addition of 700 μl cold isopropanol and centrifuged at 11,600g for 30 min at 4°C. Pellets were washed twice with 1.5 ml of 70% ethanol and centrifuged for 20 min after each wash. Pellets were air-dried, resuspended in

30 µl sterile milliQ water and pooled (total 150 µl). A 1 in 50 dilution was made in milliQ water and absorbance readings at 260 nm were performed with milliQ water as the blank. One OD unit corresponded to a DNA concentration of 2.5 µg/µl.

2.3.2.14 DNA Sequencing

DNA sequencing was performed by at the Sequencing Facility in the Department of Haematology at the Flinders Medical Centre. Complementary DNA (cDNA) of the gene of interest was cloned into an expression vector and sequenced in the forward and reverse directions using gene-specific primers (Table 2.1). Consensus sequences were constructed by alignment of forward and reverse primer sequences and verified against published data.

2.3.2.15. Transfection of CHO cells with purified plasmids

Plasmid DNA was quantified by spectrophotometry and 10 µg used to transfect Chinese Hamster Ovary (CHO) cells, which were grown to 70% confluence in 175 cm^2 tissue culture flasks. Cells were detached using 2 mM EDTA, resuspended in PBS and centrifuged at 345 g. The pellet was resuspended in electroporation media to a concentration of $1x10^7$ cells/mL. Plasmid DNA was mixed with 400 µL cells and transferred to a 4 mm gap electroporation curvette (Biorad, USA). The Biorad Gene Pulser II (USA) was set to 0.3 kV, 950 µF (high capacity) and infinity resistance. Cells were pulsed and transferred to 25 cm^2 flasks containing 5 mL S10g and incubated at 37°C 5% CO_2.

2.3.3. Adenoviral Methods

2.3.3.1. Preparation of Electrocompetent BJ5183 Cells

Ten milli-litres of LB streptomycin media (30 μg/mL) was inoculated with a single colony from a plate of BJ5183 *E.coli* cells and incubated overnight at 37°C, 200rpm. One milli-litre of the culture was used to seed 125 mL LB streptomycin media and incubated in a 1 L conical flask until the OD_{550nm} reached 0.8. The culture was divided into 4 Sorvall tubes and incubated on ice for 1 h. Cells were pelleted at 400 g for 10 min at 4°C, resuspended in ~30 mL sterile, ice cold 10% glycerol and repelleted. The 10% glycerol wash was repeated and all but 2.5 mL of supernatant removed. Cells were pooled into 1 tube and pelleted for 10 min. All but 625 μL supernatant was removed and cells resuspended. Aliquots (20μL) of electrocompetent BJ5183 cells were made in PCR tubes, snap frozen on dry ice and stored at -70°C.

2.3.3.2. Electrotransfection of BJ5183 cells

The pShuttleCMV vectors were linearised (**2.3.2.5**) with *Pme*I restriction enzyme. Dephosphorylation was performed (**2.3.2.9**) to prevent recircularisation of the vector. Electrocompetent BJ5183 cells (**2.3.3.1**) were co-electroporated with pAdEasy1 and linearised pShuttleCMV vectors using a Biorad Gene Pulser and 2 mm gap electroporation curvettes (Biorad, USA). The Gene Pulser was set to 2500 V/200 Ohms/25 μF and curvettes chilled on ice. pAdEasy (100 ng) was added to 40 μL of electro-competent cells with 5 μL (~1 μg) of linear pShuttleCMV plasmids and kept on ice for 1min. Cells were pipetted into the curvette and leveled by gentle tapping to reduce electric arcing. Cells were shocked for 5 msec and immediately resuspended in 1 mL SOC media, transferred to

a 2 mL eppendorf tube and incubated at 37°C, 200 rpm for 1 h. The culture was spread onto 6 LB kanamycin plates (50 μg/mL) and incubated overnight at 37°C.

2.3.3.3 Screening of Colonies for Homologous Recombination

As shown by the schematic diagrams of the adenoviral vectors (**Figure 5.1**), only pShuttleCMV confers kanamycin resistance. Cells only incorporating pAdEasy1 are therefore unable to form colonies on kanamycin plates. Linear forms of pShuttleCMV are not replicated and thus can not confer kanamycin resistance unless homologous recombination occurs with pAdEasy1 or upon recircularisation of the vector. The smallest colonies were selected for restriction digest screening as replication of the large recombinant vector would be expected to retard colony growth. Mini-preps of overnight cultures (**2.3.2.12**) were digested with *Pac*I in Buffer 1 (NEB, USA) to screen for homologous recombination. PShuttleCMV and pAdEasy1 contain two and one *Pac*I restriction sites respectively. Vectors positive for homologous recombination yield 33.5 kb and either 4.5 or 3 kb fragments after *Pac*I digestion depending on whether recombination occurs at the left arm homology region or the origin of replication.

2.3.3.4. Transformation of DH10β *E.coli* Cells

DH10β is a highly efficient plasmid propagation strain of E.*coli*. DH10β cells were made chemically competent (**2.3.2.10**) and transformed with undigested mini-prep samples from section **2.2.2.4**. Midi-preps (**2.3.2.13**) were performed and vectors were digested with *Pac*I to reconfirm the recombinant properties of the plasmid. PCR using CTLA4 and IL-10 primers was conducted on the plasmids to verify the presence of the inserts.

2.3.3.5. LipofectAMINE™ Transfection of Adenoviral Constructs into HEK-293 Cells

The Human Embryonic Kidney 293 (HEK-293) cell line is a genetically modified cell line containing the E1 gene, which allows for the packaging of adenoviral particles (342). The viral constructs (8 μg) were digested with *Pac*I (**2.3.2.5**) to linearise the vector. Digest products were ethanol precipitated by the addition of 10% NaAc (3 M) and two volumes of 100% ethanol and incubated overnight at -20°C. The ethanol/digest mix was centrifuged for 30 min at 11700 g 4°C and washed with 70% ethanol. DNA was centrifuged for a further 5 min and resuspended in 30 μL sH_2O. Each linearised vector (4 μg) was mixed with 10 μL sH_2O, 20 μL of the cationic liposome LipofectAMINE™ (GibcoBRL, USA) and 500 μL of MEM supplemented with glutamine. The mixture was incubated for 30 min at 37°C with gentle shaking. Near confluent flasks (25 cm^2) of HEK-293 cells were washed with plain MEM and then incubated with 2.5 mL MEM supplemented with glutamine at 37°C for 10 min. The DNA/LipofectAMINE™ mix was added to the flasks and incubated for a further 4 h. Media was removed and 6 mL complete MEM was added. Flasks were incubated for 10 days and viewed daily under a Nikon TM300 Inverted Fluorescent Microscope (Japan) for EGFP expression.

2.3.3.6. Preparation of Adenoviral HEK-293 cell lysates

Ten days post transfection, HEK-293 cells were scraped gently from the flasks using a rubber policeman and transferred to 50 mL tubes in sterile PBS. Cells were centrifuged at 1200 g for 10 min and resuspended in 2 mL sterile PBS. Cell suspensions were snap frozen in liquid nitrogen and thawed at 37°C. This cycle was repeated four times

with a 10 μL sample placed on a slide and viewed under the microscope to verify cell lysis. Cellular debris was removed by centrifugation at 1200 g.

2.3.3.7. Infection of HEK-293 Cells and Scale-up Viral Production

Media was decanted from confluent 25 cm^2 flasks of HEK-293 cells. Crude adenoviral extract (400 μL) was added to the flask and incubated for 1h at 37°C. Fresh cMEM media was added to bring the volume up to 6 mL and flasks were incubated at 37°C and 5% CO_2 until the cells had rounded up and detached due to cytoskeleton disruption as a result of viral production. Cells were washed out with PBS and cell lysates prepared (**2.2.2.7**). Viral production was scaled up by infection of fresh HEK-293 cells in 75 cm^2 flasks using 600 μL crude adenoviral extract.

2.3.3.8. Caesium Chloride (CsCl) Density Gradient Purification of Adenoviral Particles

Crude adenoviral lysates were prepared from twenty 75cm^2 flasks of 293 cells infected with virus at an MOI of 20 as described (**2.3.3.7**). Debris was removed by centrifugation at 10000 rpm in a Beckman centrifuge using gas-sterilised tubes to prevent endotoxin contamination. The supernatant was passed through a 21G needle 2-3 times to shear cellular DNA. The CsCl gradient was prepared using 4 M and 2.2 M solutions of CsCl in 10 mM HEPES (pH 7.4). Using a pasteur pipette, 2.5 ml 4 M CsCl was added to a Beckman Quickseal Ultracentrifuge tube and overlayed with 2.5 ml 2.2 M CsCl. Crude adenoviral lysate (8.5 ml) was overlayed on the CsCl gradient to fill the tube. In the case of insufficient lysate to fill the tube, PBS/10% glycerol was used to make up the volume.

Tubes were heat-sealed and balanced to within 100 mg and centrifuged in a Beckman Ultracentrifuge using a Ti80 fixed rotor for 2 h at 25000 rpm, 4°C with deceleration set to 6. After centrifugation, the tops of the tubes were punctured with 23 G needles and the viral layer was withdrawn by aspiration with a 21 G needle from the side of the tube. The volume of extracted virus was made up to 3.25 ml in PBS/10% glycerol and mixed with 3.25 ml saturated CsCl in 10 mM HEPES (pH 7.4). The mixture was transferred to fresh ultracentrifuge tubes and overlayed with 3 ml 4 M CsCl, with the remaining volume made up by overlaying with 2.2 M CsCl. Tubes were heat-sealed and centrifuged for a further 3 h at 35000 rpm, 4°C with a deceleration setting of 6. The viral band was collected as described above and dialysed to remove CsCl.

2.3.3.9. Dialysis of Caesium Chloride Purified Adenoviral Particles

Virus obtained from CsCl purification was dialysed using Slide-A-Lyzer® dialysis cassettes (Pierce, USA). Briefly, virus was added to the cassette using an 18G needle and all air was aspirated. The cassette was placed in a sterile 250 ml urine pot with endotoxin-free PBS with 10% glycerol at 4°C. Dialysis was performed at 4°C with constant agitation using magnetic stirrers. After overnight incubation, the PBS glycerol was replaced and incubated for an hour followed by four more changes of PBS glycerol. To remove the dialysed virus, 3 ml air was injected into the cassette and virus aspirated. The virus was stored in aliquots at -70°C until required.

2.3.3.10. Cytopathic Effect Assay (CPE) Quantification of Adenoviral Titres

293 cells were plated in 96 well flat-bottom plates with 1 x10^4 cells per well in 100 µl complete DMEM. Cells were incubated at 37°C 5% CO_2 overnight. Media was decanted from the confluent wells. Ten-fold viral dilutions were prepared in DMEM containing 10% normal horse serum, 0.05% yeast extract and 2 mM glutamine. Viral dilutions (50 µl) from 10^{-7} to 10^{-11} were added to wells with 10 wells prepared per dilution. Additional wells were prepared with 50 µl viral-free media were used as a control for monolayer durability. Plates were incubated for 6 days at 37°C and 50 µl additional media was added. Wells were examined by fluorescent and light microscopy for cytopathic effect from day 7. The viral titer was calculated by dividing the number of wells with cytopathic effect at the highest dilution by the total volume in all wells and multiplying by the dilution factor.

2.3.4. Flow Cytometry

2.3.4.1. Cell surface staining

Flow cytometric analysis was performed on cells using either phycoerythrin (PE) or fluorescein isothiocyanate (FITC) conjugated primary mAb or detection of primary murine antibodies using anti-mouse PE or FITC conjugated secondary mAb.

Cells were washed in FACS wash buffer and incubated for 30 min on ice with 50 µl of either saturated supernatant or 1–2 µg/ml purified primary antibody. In the case of unconjugated primary mAb, cells were washed in FACS wash buffer then incubated for 25 min on ice with isotype-specific, (FITC)- or (PE)- conjugated, anti-mouse antibodies. Cells

were incubated for a further 5 min at room temperature and fixed in 1 ml FACS lysing solution (BD Biosciences, USA). Isotype-control antibodies were used to determine background staining. Antibody staining was determined using a Becton Dickinson FACScan and analysed using WinMDI Version 2.8.

2.3.4.2. FITC-Dextran Assay

FITC-Dextran (Sigma, USA) was dissolved in S10g at 1 mg/ml, and maintained on ice until use. DC were resuspended in 1 ml FITC Dextran and incubated for 15 min either at 37°C (experimental DC) or on ice (control DC). Cells were washed three times with cold FACS-wash at 340 g, then fixed with 1 ml FACS lysing solution at room temperature for 20 min. After a final wash, cell were resuspended in 200 µl filtered saline and analysed by flow cytometry in the FL1 channel.

2.3.5. Histochemistry

2.3.5.1. Biopsy Preparation

Isolated tissues were embedded in Optimal Cutting Temperature (OCT) compound in cryostat moulds. Tissues were subsequently frozen in a bath of iso-pentane cooled by liquid nitrogen, then stored at -80°C until required. Sections were cut using a cryostat set to 6 µm onto slides and fixed in acetone for 5 min at 4°C. Slides were dried, wrapped in aluminum foil and stored at -80°C until required.

2.3.5.2. Hematoxylin and Eosin Staining

Slides were thawed, hydrated briefly in distilled H_2O and stained in hematoxylin for 5 min. Excess hematoxylin was removed by washing in running tap water for 2 min. Slides were dipped twice in acid alcohol and washed for a further 4 min in running tap water. After a brief dip in 70% EtOH, slides were stained for 30 s in eosin. Sequential dipping in two changes of 95% EtOH and then incubation in absolute EtOH for 5 min removed excess eosin. Slides were dehydrated and submerged in Sub X cleaning agent for 20 min, then Sub X mounting medium was used to mount the coverslips.

2.3.5.3. Immunohistochemistry

Slides were allowed to defrost to room temperature and rehydrated for 20 min with 3% horse serum in PBS. Endogenous avidin and biotin were blocked using an Avidin/Biotin blocking kit (Vector Laboratories, USA). After an initial wash in PBS, sections were covered with primary antibody and incubated overnight at 4°C in a humidified chamber. Sections were washed for 10 min in PBS followed by a 30 min incubation at room temperature with a biotinylated horse anti-mouse IgG mAb. After a further wash step, sections were incubated with a 1:1 preparation of Avidin DH and biotinylated horseradish peroxidase diluted in accordance with the manufacturers instructions (ABC kit, Vector Laboratories, USA) for 60 min. Sections were washed and incubated in the dark for 7 min with diaminobenzidine substrate solution, counterstained with Harris' haematoxylin and mounted under a cover slip. Positive staining was represented by brown colouration.

2.4. Centrifuges

-All tissue culture centrifugation was performed in a Beckman GP Centrifuge (USA).

-Centrifugation of all eppendorf, treff and PCR tubes was performed in an Orbital 100 Phoenix Centrifuge (USA).

-Centrifugation of all bacterial cultures was performed in a Sorvall RC-5B Refrigerated Superspeed Centrifuge (USA).

-CsCl density gradient separation was performed using a Beckman L8-70M Ultracentrifuge (USA).

Chapter 3

Immunomodulation of the Human DC-MLR by Combined IL-10 and CTLA4-Ig Treatment

Results from this chapter are also presented in the following publication

- Newland A.M., Russ G., Krishnan R. (2006). NK cells prime the responsiveness of autologous $CD4^+$ T cells to CTLA4-Ig and IL-10 mediated inhibition in an allogeneic dendritic cell-MLR. *Immunology (Accepted for publication 16/01/06).*

3.1 Introduction

DC are potent activators of naïve T cells and the specific blockade of costimulatory signals from these cellular interactions can result in T cell hyporesponsiveness or anergy. In the immature state, DC are less potent stimulators of T cell proliferation, due to the intrinsically lower expression of costimulatory molecules, CD80/86 and CD40 compared to mature DC (343). In addition, DC rendered deficient in costimulation (MHC Class II^{+}, $CD80^{dim}$, $CD86^{-}$) by culturing progenitor cells in GM-CSF alone are capable of inducing alloantigen specific T cell anergy (344) and prolonging the survival of cardiac and islet allografts in murine models (274, 345). However, in these studies transplant rejection eventually occurred as a consequence of *in vivo* maturation of the DC in secondary lymphoid tissues (274). In particular, DC progenitors treated with IL-10 prior to differentiation demonstrate downregulation of CD80/86 and CD40 expression, low IL-12 secretion and induce anergy in T cell allogeneic responders (164, 166, 167, 264, 346).

T cell hyporesponsiveness may also be induced with CTLA4-Ig which binds to CD80 and CD86 with higher affinity than CD28 and consequently blocks T cell activation mediated by these molecules (54, 74, 95). Furthermore, the observed *in vitro* immunomodulatory effect of CTLA4Ig was corroborated by the observation of prolongation of allograft survival when the agent was administered in experimental models (253, 255, 256). Importantly, long-term graft survival was not achieved unless treatment was combined with anti-CD40 mAb (347) or antisense NFκβ oligonucleotides (329). Since redundancy in costimulation is expected for CTLA4-Ig monotherapy, this chapter examines the effects of combining CTLA4-Ig with IL-10 in the DC MLR.

We hypothesized that the treatment of the DC-MLR with the combination of CTLA4-Ig and IL-10 will augment the inhibition of alloreactive T cell proliferation. To test this hypothesis, sub-optimal concentrations of IL-10 and CTLA4-Ig were added singly or in combination to the DC-MLR using nylon wool enriched T (NWT) cells or negatively selected $CD4^+$ T cells as the responder population.

The specific aims of this Chapter were-

(i) To provide base-line data identifying optimal and sub-optimal doses of CTLA4-Ig and IL-10 with respect to the inhibition of DC mediated T cell allostimulation.

(ii) To investigate the combined effects of sub-optimal doses of CTLA4-Ig and IL-10 in the allogeneic DC-MLR.

(iii) To investigate the effects of combined CTLA4-Ig and IL-10 treatment on isolated T cell subsets in the DC-MLR.

3.2 Materials and Methods

3.2.1. Preparation of cell populations

Buffy coats were prepared from heparinised peripheral blood obtained from healthy donors (Red Cross Blood Service, Adelaide, Australia) and PBMC was isolated by differential centrifugation through a Ficoll-Hypaque density gradient (**2.3.1.1**). Monocytes were selected by adherence to plastic and were cultured in complete medium supplemented with 400 U/ml IL-4 (Peprotech, USA) and 800 U/ml GM-CSF (Kenilworth, USA) for 5 days to generate immature DC (iDC) as detailed in **2.3.1.2**. The addition of 10 ng/ml TNF-α (Genzyme Corporation, USA) to the iDC for a further 2 days generated mature DC (mDC).

Following the removal of monocytes by adherence, nylon wool purified T cells (NWT) were obtained using nylon wool columns (**2.3.1.3**). $CD4^+$ T cells were negatively selected from NWT cells using a human T cell isolation kit (Miltenyi Biotech, Germany) by firstly staining NWT cells with a biotin-labeled antibody cocktail against other cellular populations, followed by incubation with anti-biotin microbeads and immunomagnetic separation with the AutoMACS (Miltenyi Biotech, Germany). To isolate $CD4^+CD25^+$ T_{reg} cells, the $CD4^+$ cells were further stained with anti-CD25-microbeads and positively selected. The negative fraction containing $CD4^+CD25^-$ cells was also retained.

NK cells were positively selected from NWT cells by staining with an anti-CD56-FITC conjugated antibody followed by incubation with anti-FITC microbeads and immunomagnetic selection.

3.2.2. Monoclonal antibodies and flow cytometry

Cell surface phenotype of DC, NK and T cells were determined by flow cytometry (**2.3.4.1**). Commercial monoclonal antibodies used included: anti-CD4-PE, anti-CD56-FITC, anti-CD80, anti-CD86 and anti-CD14, and anti-CD83-PE. Monoclonal antibody supernatants directed against CMRF56, CD1a, Class I, Class II, CCR7, and CD40 were also used. Isotype-matched control antibodies were used to determine background staining.

3.2.3. Proliferation Assays

The mixed lymphocyte reaction (MLR) was performed by co-culturing DC (1×10^3) with allogeneic T cells (1×10^5) which represents a stimulator:responder (S:R) ratio of 1:100. Cells were cultured in RPMI + 10% FCS for 96 h and then pulsed with 1 μCi of [^{3}H] thymidine (Amersham Biosciences, Sweden) for a further 20 h at 37°C. CTLA4-Ig (R&D Systems, USA) and human IL-10 (Bender MedSystems, Austria) were added to the cultured cells in the proliferation assays. The [^{3}H] thymidine-pulsed cells were harvested onto glassfibre filters and the incorporated radioactivity was determined by liquid scintillation counting in a Wallac MicroBeta Counter.

For T cell proliferation assays in the absence of DC, T cells were activated by addition to a round-bottom 96-well plate pre-coated with 10 μg/ml OKT3. NK cells were added to T cells in some wells at a concentration of 10% or 30% to assess the ability of NK cells to augment T cell proliferation. Triplicate determinations are expressed as mean counts per minute (cpm) +/- SD in all experiments.

3.2.4. Restimulation Assay

Primary MLR was set up as above using DC at a S/R of 1:100. After 5 days in culture the cells were pooled for each treatment. Three representative wells were pulsed with ^{3}H thymidine and harvested to confirm the initial response. T cells were isolated from the primary MLR by nylon wool purification and washed before being re-plated at 2 x 10^{6} cells/ml for a secondary MLR. Fresh DC from the same origin as those used in the primary MLR were added at a 1:100 ratio to the T cells. The volume of the wells was made up to 200 µl with S10g. Wells were pulsed with ^{3}H thymidine after 4 days in culture and harvested after a further 16 h incubation.

3.2.5. CFSE-MLR

Proliferation of T cell subsets was also investigated in a CFSE-MLR. In order to determine the specific proliferation of the T cell subset, NWT cells were labeled by incubation for 10 min at 37°C with CFSE (5-(and -6)-carboxyflourescein diacetate succinimidyl ester) diluted in PBS. Stained cells were washed three times with PBS and cultured with allogeneic DC at a S:R ratio of 1:100. After 5 days culture, cells were further labeled with either CD4-PE or CD8-PE and proliferation of each population determined by the dilution of the CFSE signal in the FL1 channel by flow cytometry.

3.3 Results

3.3.1 Phenotype of human monocyte-derived DC and associated function

Immature and mature monocyte-derived DC were analysed with respect to their cell-surface phenotype, FITC-Dextran uptake capacity and T cell stimulatory capacity. Immature DC demonstrated cell surface expression of the antigen presenting molecules MHC Class I and Class II, and the costimulatory molecules CD40, CD80, CD86. Notably the expression profiles of all these markers were dramatically increased upon DC maturation in addition to the maturation markers, CD83 and CMRF56 and the chemokine receptor CCR7 **(Figure 3.1.a)**. As shown in **Figure 3.1.b**, mature DC demonstrated only low levels of FITC-Dextran uptake compared with immature DC. The increased antigen presentation capacity and costimulatory molecule expression of mature DC was mirrored in the increased proliferation of T cells in the mature DC-MLR. While immature DC, used as the stimulator population in the MLR, yielded [^{3}H] incorporation counts of 27000, this was dramatically increased to 68000 ($p=0.00006$) when mature DC were used as the stimulators **(Figure 3.1.c)**.

3.3.2 Immunomodulatory properties of IL-10 and CTLA4-Ig

Dose response analyses of the inhibition of allogeneic T cell stimulation in the MLR by IL-10 and CTLA4Ig was undertaken to determine effective suboptimal doses of each agent to be used in the combination studies. The DC-MLR was assessed with both iDC and mDC as stimulators. Inhibition of NWT cell proliferation in the MLR was observed in a broad concentration range of >1 ng/ml to 100 ng/ml for human IL-10 and >5 ng/ml to 500 ng/ml for CTLA4-Ig **(Figure 3.2)**. The high concentrations of 100 ng/ml of IL-10 and 500

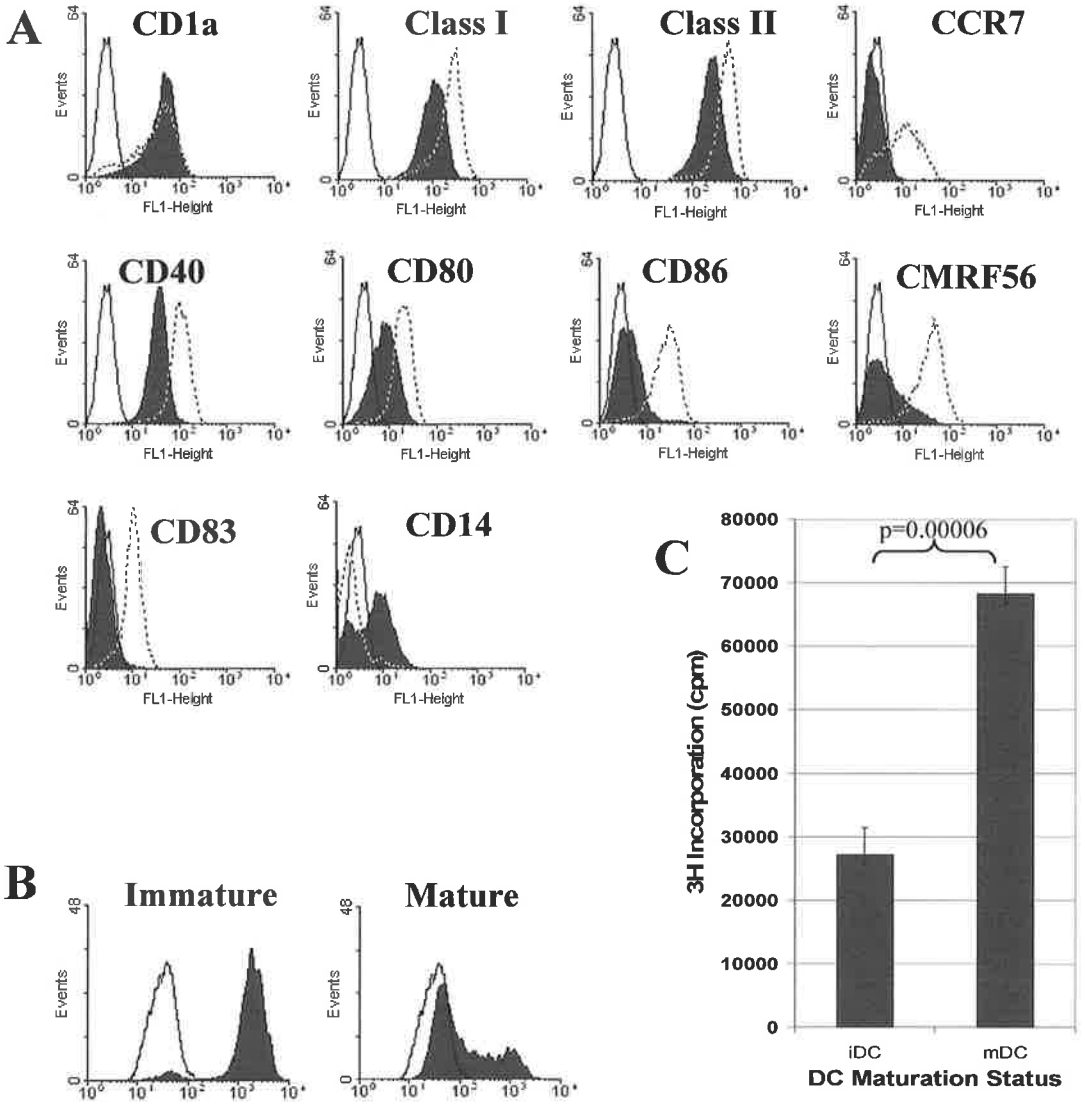

Figure 3.1. Characterisation of human monocyte-derived dendritic cells

A) Cell surface phenotype of immature (shaded) and mature (dotted) human monocyte-derived DC was determined by flow cytometric analysis. Unshaded solid line histogram represents staining with an isotype-matched control antibody.

B) Uptake of FITC-dextran by immature and mature human monocyte-derived DC was determined to compare antigen uptake capacity at the different levels of maturity. Shaded histograms represent FITC-dextran uptake at 37°C compared with 0°C (unshaded histogram) as determined by flow cytometric analysis.

C) The allostimulatory effect of immature and mature DC on allogeneic T cells was determined in the DC-MLR at an S/R of 1:100. The graph represents the typical differences in proliferation of T cells in response to iDC and mDC stimulators.

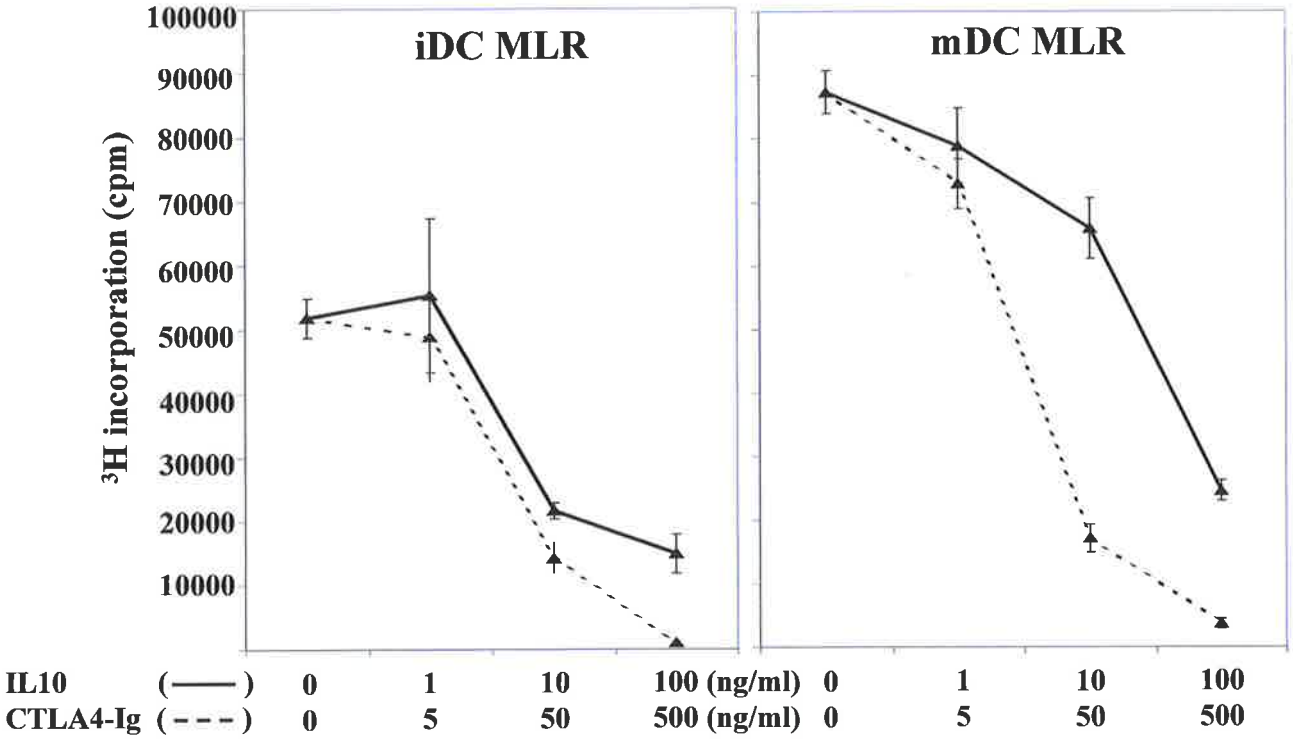

Figure 3.2. Titration of CTLA4-Ig and IL10
IL10 (solid line) and CTLA4-Ig (dashed line) were titrated with ten-fold dilutions in the DC-MLR. NWT cells were used as the responder population at a S:R ratio of 1:100. All samples were run in triplicate and proliferation measured by [^{3}H] thymidine incorporation with results represented as cpm +/- SD.

ng/ml of CTLA4 Ig demonstrated maximal inhibition of 70-95% of responder cell proliferation in the MLR for both iDC and mDC as stimulators. However, IL-10 at a concentration of 5 ng/ml and CTLA4-Ig at 20 ng/ml consistently yielded suboptimal inhibition of the MLR (data not shown) and thus these doses were deemed to be suitable to evaluate the effects of combined treatment in the proliferation assay.

The biological activity of CTLA4-Ig was blocked by the addition of anti-CTLA4 mAb to the DC-MLR. As shown in **Figure 3.3,** CTLA4-Ig at a concentration of 500 ng/ml resulted in an 80% inhibition of T cell proliferation. Addition of anti-CTLA4 mAb almost completely negated this inhibitory effect ($p=0.00001$). The normal rabbit serum control, however, had no effect on the inhibitory function of CTLA4-Ig.

At optimal concentrations, IL-10 has previously been reported to inhibit the maturation of DC. In this chapter the effects of sub-optimal concentrations of IL-10 on the differentiation and maturation of DC were investigated. When IL-10 was added to human monocytes at the time of IL-4/GMCSF treatment, minimal effects were observed on the level of expression of CD80 even after the induction of DC maturation. Interestingly the expression of CD86 was increased on mDC cultured in the presence of IL-10. The expression of CD83, however, was completely abrogated **(Figure 3.4)**. Conversely CTLA4-Ig treatment of monocytes promoted the expression of CD83 after differentiation to mature DC.

The influence of sub-optimal doses of IL-10 on the maturation of human monocyte-derived DC was also determined. IL-10 (5 ng/ml) or CTLA4-Ig (20 ng/ml) was added to iDC and incubated for 2 days in the presence or absence of TNFα. As shown in **Figure**

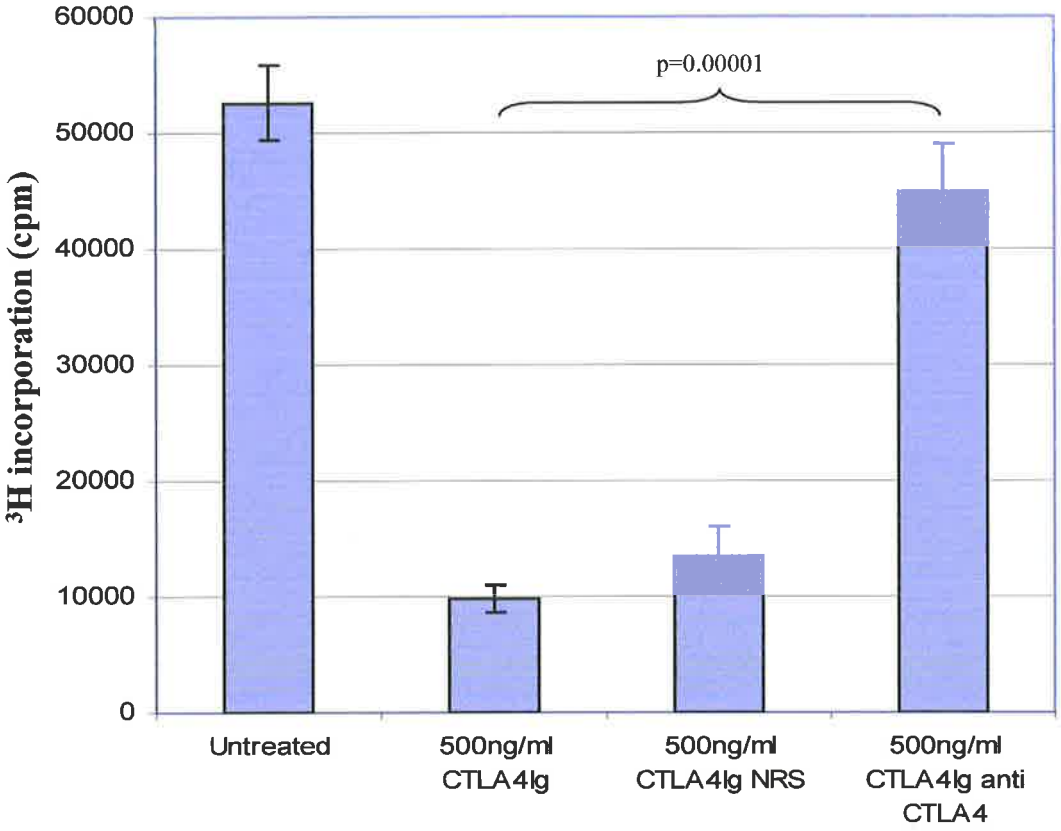

Figure 3.3. CTLA4-Ig blockade is reversed by treatment with anti-CTLA4 mAb
CTLA4-Ig was added to the mature DC-MLR at 500 ng/ml. Anti-CTLA4 mAb was added to determine whether the antibody could abrogate the binding of CTLA4-Ig to target DC. Normal rabbit serum (NRS) was added as a non-specific control. Data represents [^{3}H] incorporation of triplicate samples +/- SD.

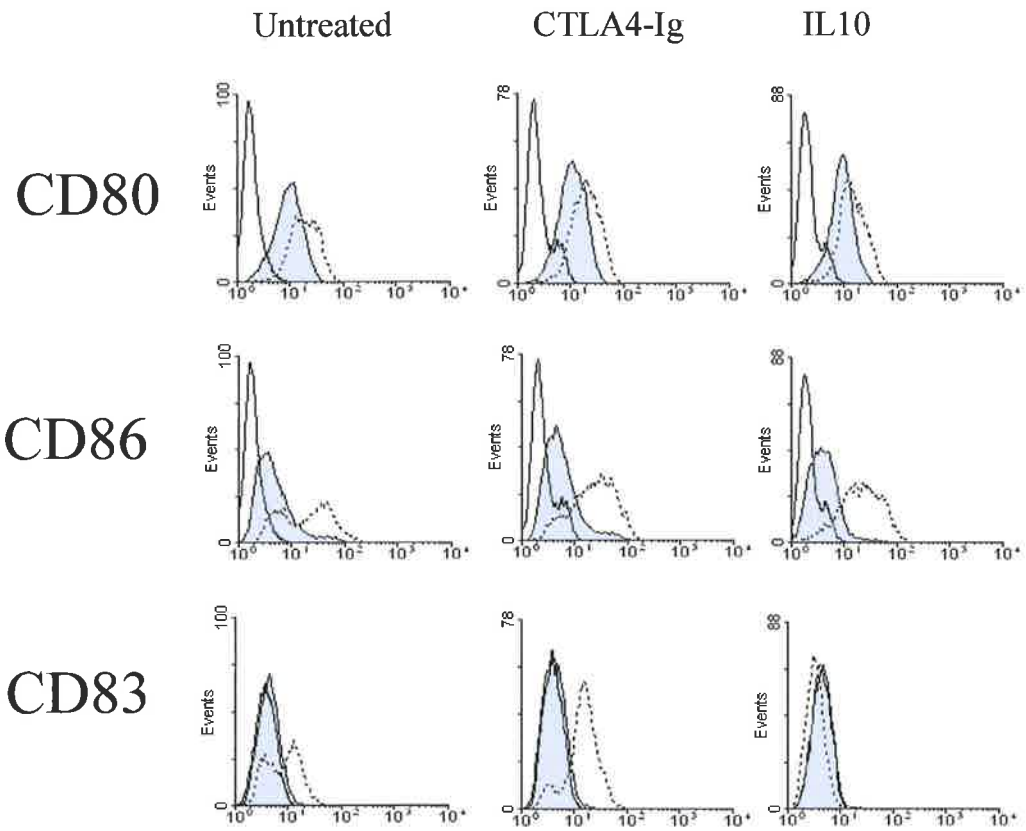

Figure 3.4 The effect of CTLA4-Ig and IL10 on the differentiation of DC from monocytes.

Human monocytes were cultured for 5 days with IL4 and GMCSF to induce differentiation into DC in the presence or absence of IL10 (5 ng/ml) or CTLA4-Ig (20 ng/ml). Cells were further cultured for 2 days in the presence of TNFα to induce DC maturation. Histograms represent cells cultured in the presence (dotted) or absence (shaded) of TNFα. The black unshaded histogram represents background staining with the isotype-matched control antibody. Histograms are representative of three independent experiments.

3.5, the addition of IL-10 at 5 ng/ml had no influence on the expression of CD40, CD80, CD86, CD83 or MHC Class II on DC irrespective of the addition of TNFα.

3.3.3 Combined treatment with IL-10 and CTLA4-Ig in the DC-MLR induces T cell hyporesponsiveness.

Sub-optimal doses of CTLA4-Ig (20 ng/ml) and IL-10 (5 ng/ml) were added to the DC-MLR at S:R of 1:100 with iDC or mDC as the stimulator populations. While CTLA4-Ig alone generated an inhibition of 8-10% of T cell proliferation, the combined treatment with IL-10 demonstrated a further increase in inhibition to 25% ($p=0.008$) and 38% ($p=0.0015$) in the MLR stimulated by iDC and mDC, respectively (**figure 3.6**). Significant differences in T cell proliferation were observed between IL-10 alone and in combination with CTLA4-Ig when mDC were used as stimulators ($p=0.006$).

3.3.4 $CD4^+$ and $CD8^+$ T cell stimulation by DC is inhibited by IL-10 and CTLA4-Ig in the CFSE-MLR.

In our analysis NWT cells typically had a composition of 65-80% $CD4^+$ T cells, 15-30% $CD8^+$ T cells and 5-15% $CD56^+$ NK cells in normal healthy individuals (N=4). CFSE was used to label NWT cells to determine the specific effects of IL-10 and CTLA4-Ig treatment on T cell subset proliferation in the MLR. After 5 days in culture the CFSE labeled cells were stained with either CD4-PE or CD8-PE to determine the proliferative capacity of each cell population depicted by CFSE dilution in FL-1 channel. Proliferating cells in the untreated CFSE-MLR represented 54% of the total $CD4^+$ T cell population with DC stimulators (**Figure 3.7**). Treatment with hIL-10 or CTLA4-Ig reduced the percentage of proliferating cells to 38% and 39% respectively, while the combined treatment reduced

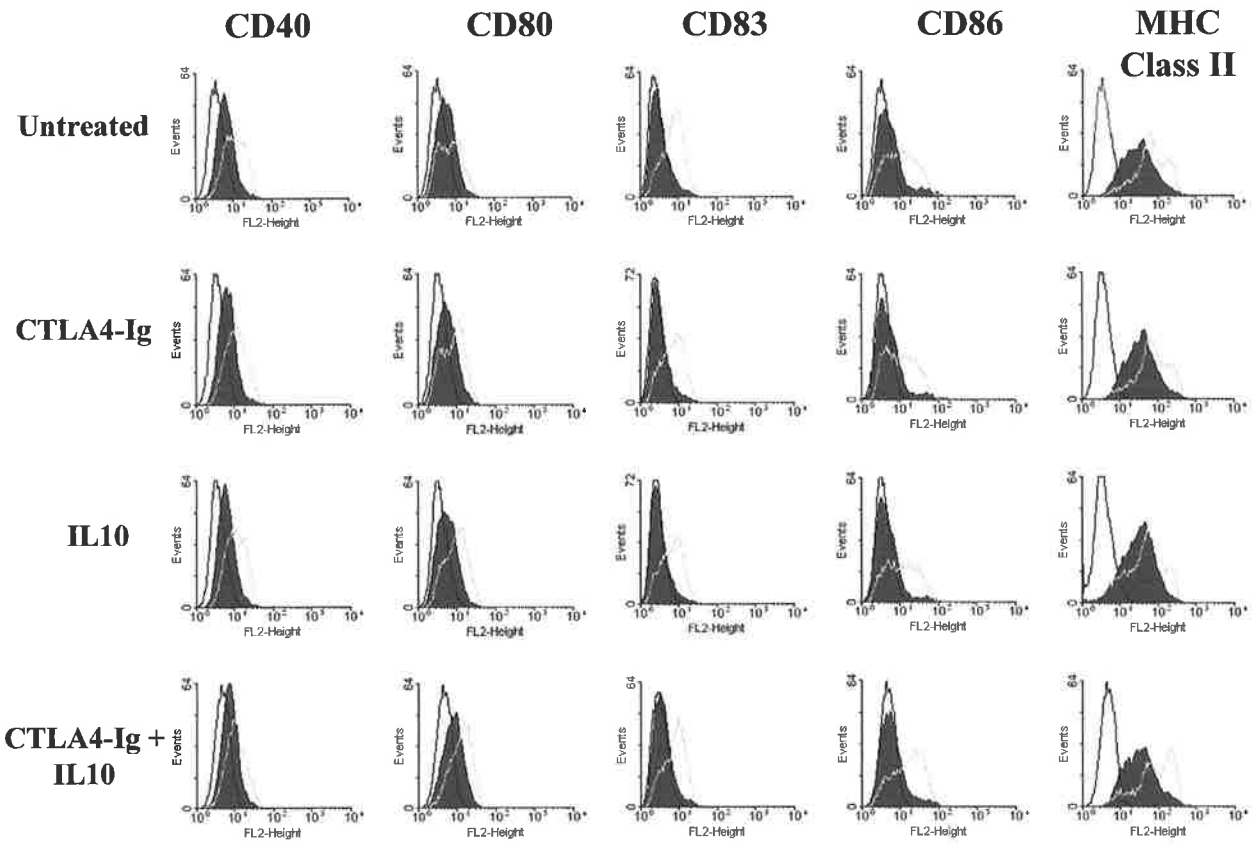

Figure 3.5 Effect of CTLA4 and IL10 on TNFα induced DC maturation.
Human DC were prepared by culturing monocytes for 5 days in the presence of IL4 and GMCSF. IL10 or CTLA4-Ig were then added and cells cultured for two more days in the presence or absence of TNFα to induce DC maturation. Flow cytometric analysis was then performed. Histograms represent DC cultured with TNFα (grey unshaded), without TNFα (shaded) or staining with an isotype-matched control antibody (black unshaded).

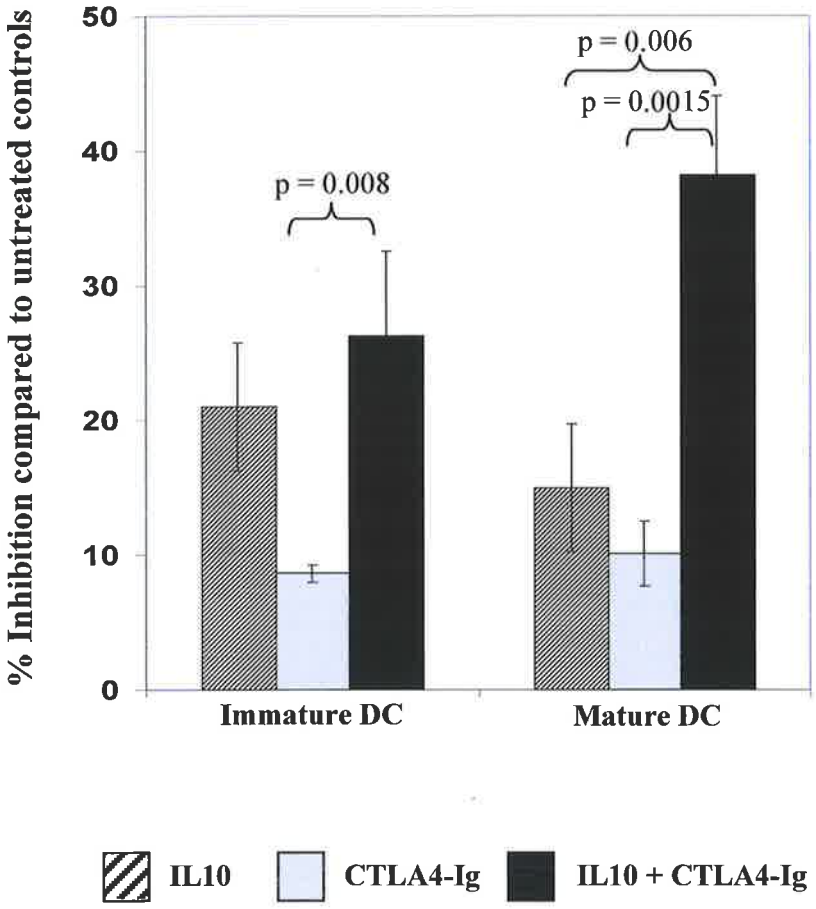

Figure 3.6 Combined treatment of the DC-MLR with IL10 and CTLA4-Ig. CTLA4-Ig (20 ng/ml) and IL10 (5 ng/ml) were added to the immature or mature DC-MLR alone or in combination. Graphs represent the percentage inhibition compared to untreated controls +/- SD. All samples were run in triplicate. Data presented is representative of 12 independent experiments.

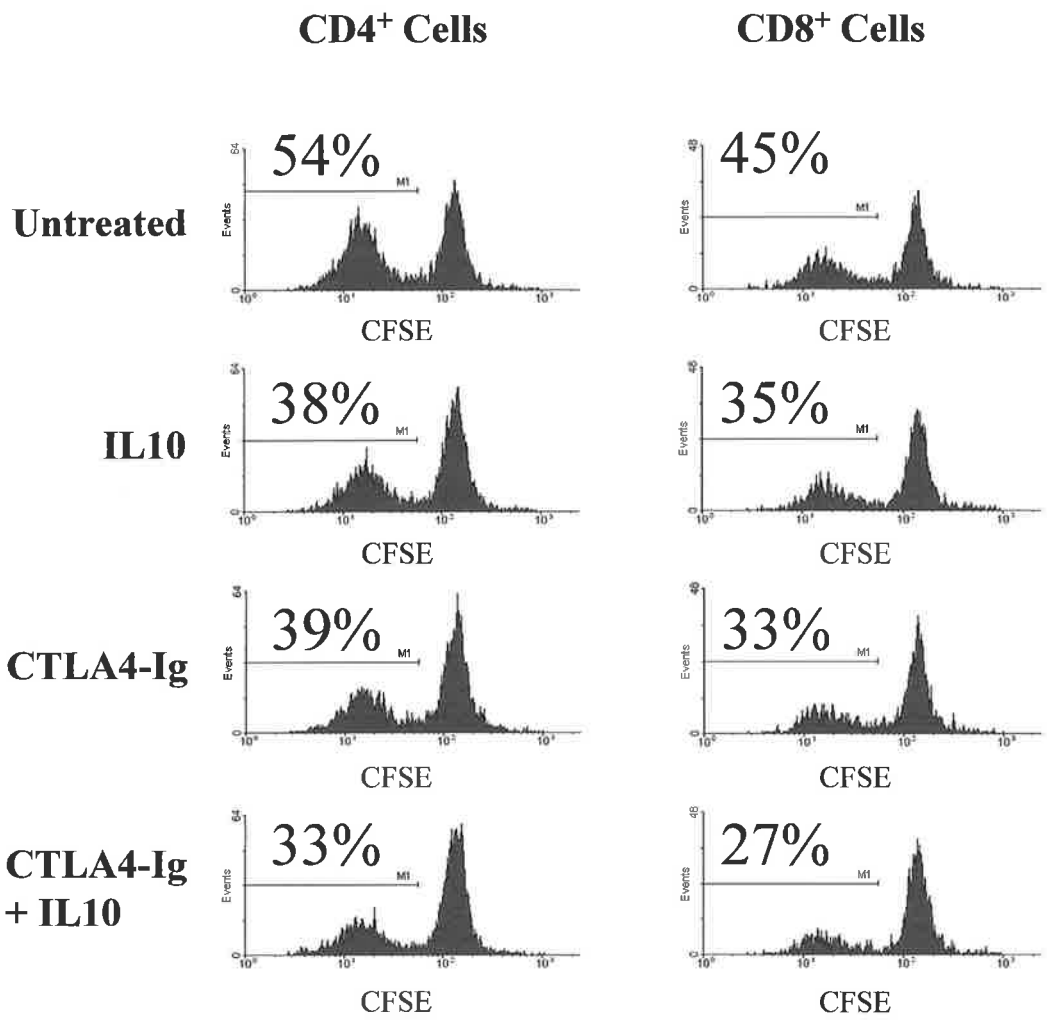

Figure 3.7 CTLA4 and IL10 inhibit proliferation of CFSE labeled T cells in the DC-MLR

Histograms represent the inhibition of $CD4^+$ and $CD8^+$ T cell proliferation by sub-optimal doses of IL10 and CTLA4-Ig in a CFSE-MLR. NWT cells were stained with CFSE and added to mature DC stimulators. After 5 days in culture, cells were stained with anti-CD4-PE or anti-CD8-PE and analysed by flow cytometric analysis to determine CFSE dilution in comparison to non-activated NWT cells. Histograms represent the percentage of proliferating $CD4^+$ and $CD8^+$ T cells based on CFSE dilution and are representative of four independent experiments.

proliferating cells to 33%. A similar trend was observed for $CD8^+$ T cells in the untreated CFSE-MLR with a proliferating population of 45% of the total $CD8^+$ cells that was reduced to 35% and 33% with IL-10 and CTLA4-Ig treatment alone, and 27% in combination.

3.3.5 T cells stimulated by DC in the presence of combined CTLA4-Ig and IL-10 treatment are hypo-responsive to restimulation.

T cells from the primary MLR treated with IL-10 and CTLA4-Ig were used for restimulation in a secondary MLR in the absence of both immunomodulatory agents. The data **(figure 3.8)** shows that T cell proliferation in the secondary MLR was 80% inhibited ($p=0.005$ compared with IL-10) for those T cells that were subject to prior treatments with the combination of agents compared to those cells that received CTLA4-Ig or IL-10 alone in the primary MLR (0% and 28% inhibition, respectively).

3.3.6 IL-10 and CTLA4-Ig mediated inhibition of the DC-MLR is not dependent on $CD4^+CD25^+$ regulatory T cells.

To investigate whether regulatory T (T_{reg}) cells play a role in the inhibitory function of CTLA4-Ig in combination with sub-optimal doses of IL-10, $CD4^+CD25^-$ T cells and $CD4^+CD25^+$ T_{reg} cells were isolated. The DC-MLR was set-up with NWT cells, $CD4^+CD25^-$ T cells and $CD4^+CD25^-$ T cells repleted with 10% $CD4^+CD25^+$ T_{reg} cells. As the data shown in **figure 3.9**, strong inhibition (52% - 94%) was observed for IL-10 (5 ng/ml) and CTLA4-Ig (20 ng/ml) alone and in combination when NWT cells were used as the responder population. In comparison, minimal inhibition (<15%) was observed from the $CD4^+CD25^-$ T cells irrespective of repletion with $CD4^+CD25^+$ T_{reg} cells.

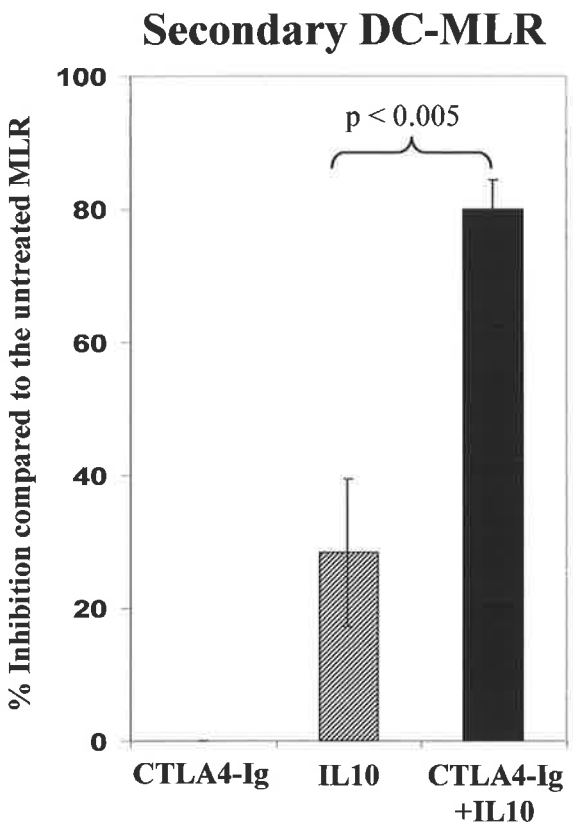

Figure 3.8 T cells cultured with IL10 and CTLA4-Ig in the primary mature DC-MLR are hypo-responsive to restimulation.
NWT cells were used in the primary DC-MLR at a S:R ratio of 1:100 with IL10 (5 ng/ml) and CTLA4 (20 ng/ml) alone or in combination. T cells were isolated from the MLR and restimulated in a secondary MLR in the absence of both immunomodulatory agents. Graphs represent the percentage inhibition compared to untreated controls. P values were determined by unpaired Student's *t*-test. All samples were run in triplicate and data is representative of 3 independent experiments.

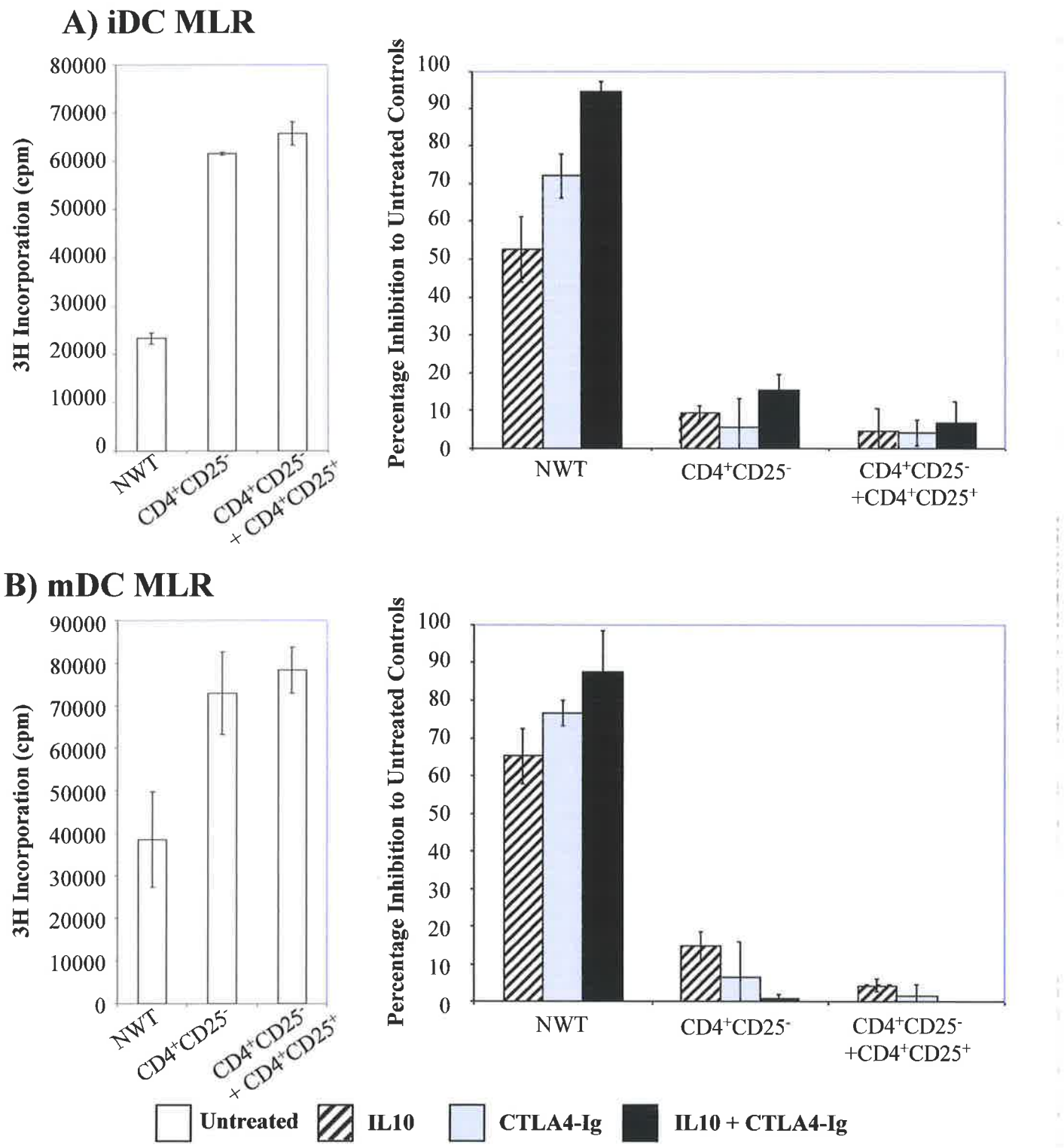

Figure 3.9 $CD4^+CD25^-$ T cells are unresponsive to sub-optimal IL10 and CTLA4-Ig treatment and are not influenced by repletion with $CD4^+CD25^+$ T_{reg} cells.

Immunomagnetic microbead separation was used to isolate $CD4^+CD25^-$ T cells and $CD4^+CD25^+$ T_{reg} cells. $CD4^+CD25^-$ T cells were used as the responder population in the immature and mature DC-MLR in the presence or absence of 10% $CD4^+CD25^+$ T_{reg} cells. IL10 (5 ng/ml) and CTLA4-Ig (20 ng/ml) were added alone or in combination to the MLR. Proliferation was measured by [^{3}H] thymidine incorporation and results expressed as the percentage inhibition of proliferation in comparison to untreated controls. P values were determined by unpaired Student's *t*-test. Data shown is representative of three independent experiments.

3.3.7 NK cells are required for the inhibition of T cell proliferation by sub-optimal doses of IL-10 and CTLA4-Ig.

Immunomagnetic separation was used to enrich the $CD4^+$ T cell population by negative selection from NWT cells resulting in greater than 98% purity **(figure 3.10)**. In comparison to NWT cells, purified $CD4^+$ T cells used as responders in the DC-MLR showed higher proliferative responses to both iDC and mDC stimulators in the MLR **(figure 3.11, experiment 1)**. The reconstitution of the purified $CD4^+$ T cells with 10% NK cells (87% purity as shown in **figure 3.10**) to match the NWT cell composition resulted in a reduction in T cell proliferation for both types of DC stimulators. Notably the purified NK cells were represented by an abundant $CD56^{dim}$ and a minor $CD56^{bright}$ population.

Consistent with the first set of experiments **(figure 3.6)** the NWT cells demonstrated strong hyporesponsiveness to CTLA4-Ig and IL-10 treatments. However, in contrast to NWT cells the combined doses of IL-10 (5 ng/ml) and CTLA4-Ig (20 ng/ml) on purified $CD4^+$ T cells in the DC-MLR were not as potent (16% for $CD4^+$ T cells vs 61% for NWT cells $p=0.0002$) for iDC and (12% for $CD4^+$ T cells vs 57% for NWT cells, $p=0.0005$) for mDC stimulators as shown in **figure 3.11 (experiment 1)**. Repletion of the purified $CD4^+$ T cells with 10% NK cells restored the inhibition of T cell proliferation mediated by the agents for both the iDC (52% +/- 4.8%) and mDC (51% +/- 2.7%) MLR. However, repletion of the $CD4^+$ T cells with $CD8^+$ cells did not restore the inhibitory effect of these agents (data not shown).

The lower proliferative response of untreated NWT cells or $CD4^+$ T cells repleted with NK cells compared with $CD4^+$ T cells observed in **experiment 1** is unlikely to account for the increased sensitivity to IL-10 and CTLA4-Ig as **experiment 2** revealed a similar

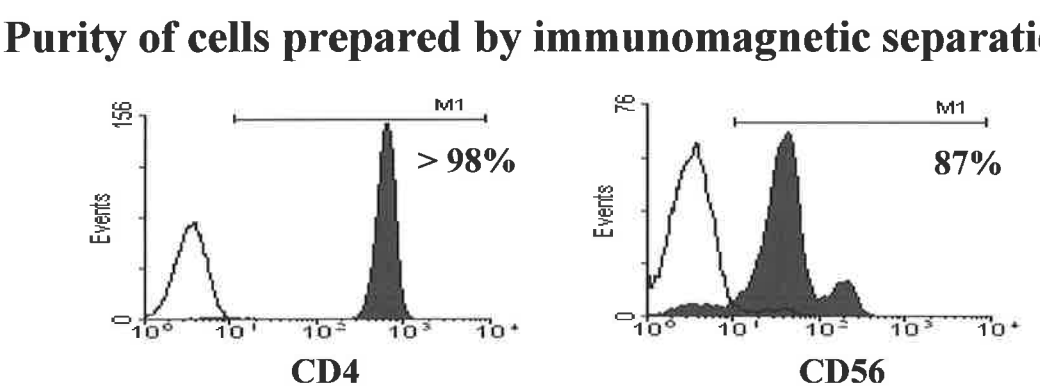

Figure 3.10 Isolation of CD4$^+$ T cells and CD56$^+$ NK cells
Immunomagnetic microbead separation was used to purify CD4$^+$ T cells and CD56$^+$ NK cells from NWT cells. CD4$^+$ T cells were isolated by negative selection and stained with anti-CD4-PE (shaded histogram) or negative control PE-conjugated mAb (unshaded histogram). NK cells were positively selected with anti-CD56-FITC conjugated mAb and captured using anti-FITC microbeads. The histogram shows the overlay of the positive fraction (shaded) against the negative fraction (unshaded).

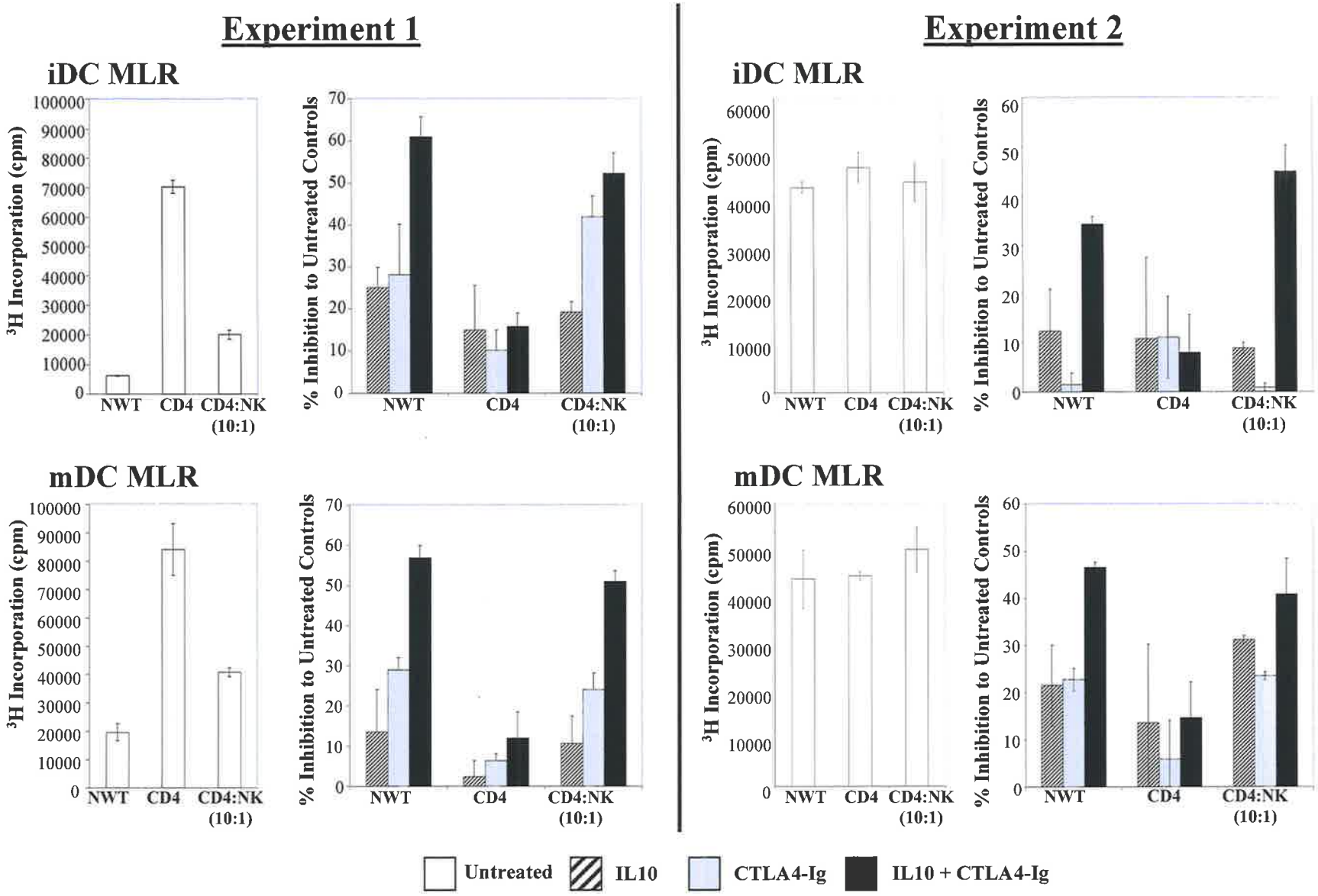

Figure 3.11 NK cells restore the capacity of sub-optimal doses of CTLA4-Ig and IL-10 to inhibit CD4$^+$ responder cells in the MLR
NWT cells, CD4$^+$ T cells or CD4$^+$ T cells + 10% CD56$^+$ NK cells as the responder populations were added to either allogeneic iDC or mDC stimulators. S:R ratios of 1:100 were used. IL10 (5 ng/ml) and CTLA4-Ig (20 ng/ml) were added alone or in combination to the MLR. Proliferation was measured by [^{3}H] thymidine incorporation and results expressed as the percentage inhibition of proliferation in comparison to untreated controls. Data shown represents two of three independent experiments.

inhibitory profile after treatment with the agents while untreated MLR counts remained comparable (**figure 3.11**).

3.3.8 NK cells Influence DC Function

The effect of NK cells on DC phenotype and function was examined by coculturing NK cells with allogeneic DC for 4 days at a NK:DC ratio of 1:5. Forward/ side-scatter density plots (**figure 3.12.a**) demonstrated a significant reduction in the numbers of gated iDC in cells cocultured with NK cells in comparison to untreated cells. In contrast the profile for mDC was unaffected by co-incubation with NK cells. While the expression of CD80 on gated DC showed upregulation on the iDC population only minor changes were noted in the mDC population (**figure 3.12.b**). The CD86 expression on either iDC or mDC showed no changes. NK cells were excluded from the analysis based on forward/side-scatter profiles and antibody staining patterns for CD56.

To investigate if NK cells pre-cultured with DC prime T cell responsiveness to IL-10/CTLA4-Ig, viable DC were separated from NK cells after a period of 3 days of coculture by Metrizamide density gradient separation, resulting in less than 1% residual NK cells (data not shown). Isolated NK primed-DC were then used as stimulators in the DC-T cell MLR with purified CD4 T cells. As shown in **figure 3.12.c**, iDC primed with NK cells produced a significant increase in T cell proliferation (35%) compared with unprimed iDC ($p=0.006$), however, primed mDC did not induce changes. Moreover, while IL-10/CTLA4-Ig demonstrated significant inhibition ($p < 0.01$) of the MLR for primed iDC (29%) and mDC (25%), both the unprimed iDC and mDC were not responsive to IL-10/CTLA4-Ig in the MLR.

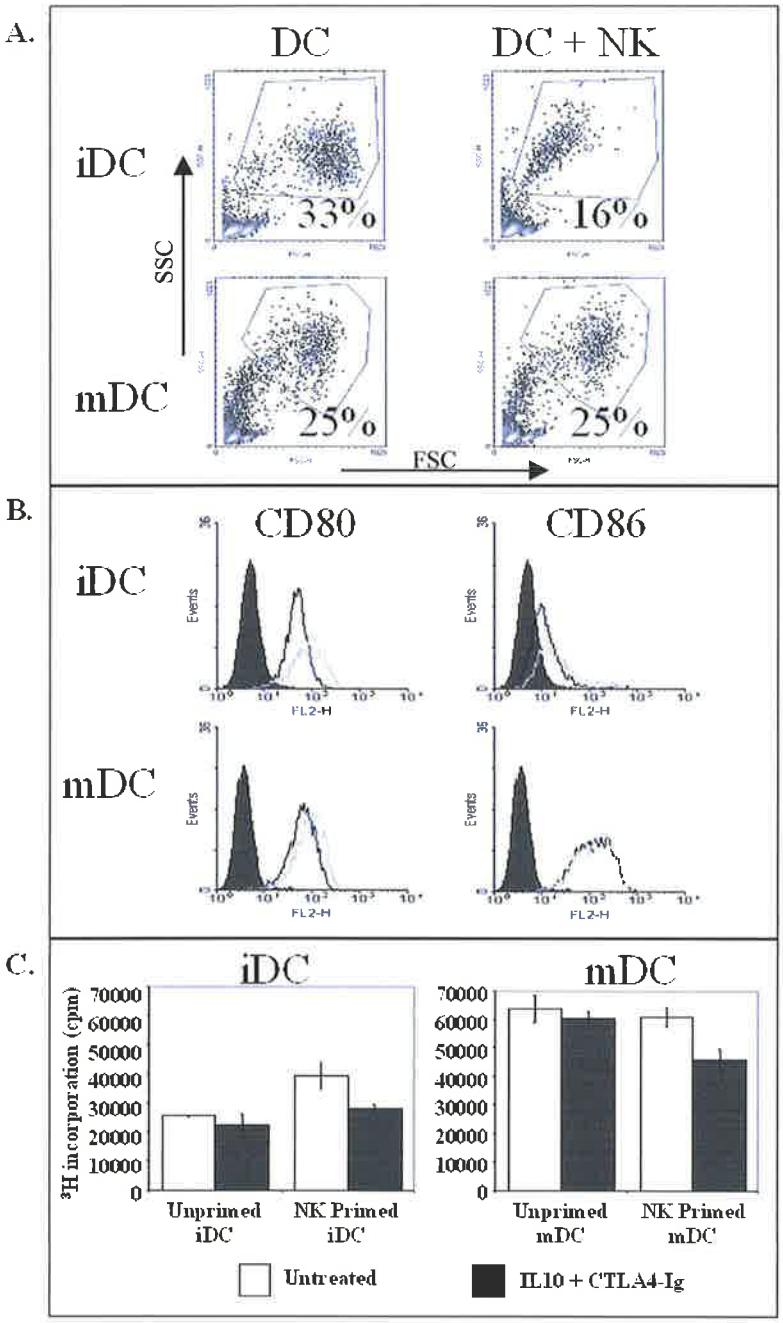

Figure 3.12: NK cells stimulate allogeneic DC lysis, activation and sensitivity to sub-optimal doses of CTLA4-Ig/IL10

Immature and mature DC were cocultured with allogeneic NK cells at a ratio of (5:1) for 3 days. **A)** Gated histograms represent the forward side-scatter profile of DC and reveal a significant decrease in iDC numbers after culture with NK cells. **B)** Flow cytometric analysis was performed on gated DC using mAb directed against CD80 and CD86. The expression of CD80 and CD86 on DC cultured alone (black line) or DC cocultured with NK cells (gray line) are shown in the histograms and demonstrate upregulation of CD80 on iDC. The shaded histogram represents isotype-matched control mAb staining. NK cells were distinguished from DC and excluded from analysis by gating based on their forward/side scatter profiles. Data shown is representative of three independent experiments. **C)** DC isolated from culture with NK cells were used as stimulators of allogeneic $CD4^+$ T cells. In the absence of NK cells, primed iDC revealed an increased stimulatory effect on T cells. Furthermore MLR stimulated by iDC or mDC primed by NK cells were sensitive to the inhibitory effects of sub-optimal CTLA4-Ig/IL10. Proliferation was measured by [^{3}H] thymidine incorporation and results expressed as the percentage inhibition of proliferation in comparison to untreated controls. P values were determined by unpaired Student's *t*-test.

3.3.9 NK cells prime $CD4^+$ T cell proliferation in a CTLA4-Ig sensitive manner

NK cells were cocultured for four days with OKT3 (anti-CD3 mAb) stimulated autologous $CD4^+$ T cells to investigate the effects of NK cells in the absence of DC stimulators. The data in **figure 3.13.a** show that the baseline $CD4^+$ T cell proliferation significantly increased ($p = 0.00006$) in a dose-dependent manner with the addition of NK cells at T cell:NK cell ratios of 10:1 and 10:3. The addition of CTLA4-Ig at a concentration of 20 ng/ml to the $CD4^+$ T cell: NK cell cocultures demonstrated inhibition of $CD4^+$ T cell proliferation ($p<0.01$) **(figure 3.13.a)**. NK cells cultured in OKT3 coated plates showed negligible counts (data not shown).

In order to determine the expression of CD80 or CD86 on NK cells, NK cells were cultured for four days in the presence or absence of 200 U/ml IL-2. Flow cytometric analysis showed moderate expression of CD86, which was upregulated by addition of IL-2 to the culture. There was no observed expression of CD80 compared to the negative mAb control irrespective of IL-2 addition in the culture **Figure 3.13.b**.

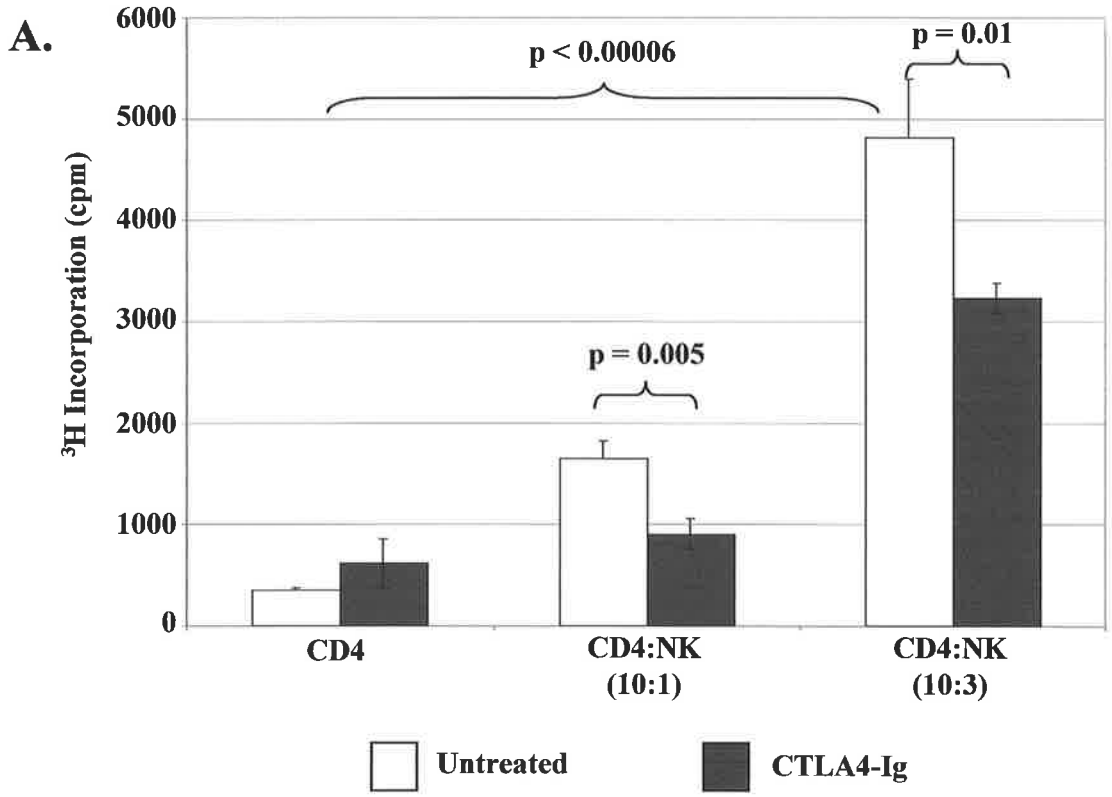

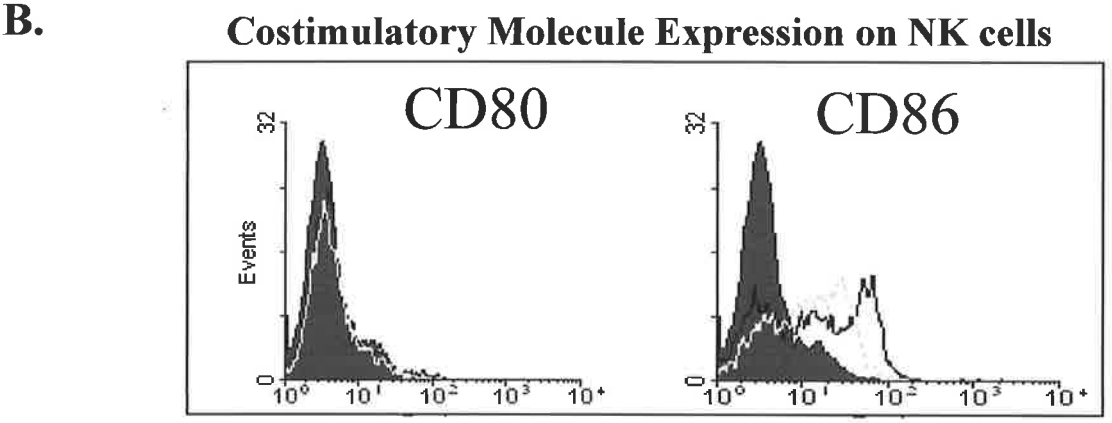

Figure 3.13 NK cells prime CD4$^+$ T cell proliferation.
A) CD4$^+$ T cells were cultured in anti-CD3-coated plates (10 μg/ml) in the presence or absence of CD56$^+$ NK cells. CTLA4-Ig was added to the co-cultures at 20 ng/ml (black bars). Samples were setup in triplicate, proliferation was measured by [^{3}H] thymidine incorporation and expressed as cpm +/- SD. P values were determined by unpaired Student's *t*-test. The data is representative of three independent experiments. **B)** The effect of IL2 on CD80 and CD86 expression by NK cells was also investigated. Histograms of CD80 or CD86 staining of NK cells cultured in the presence (black line), or absence (gray line) of 200 U/ml IL-2 were determined by flow cytomety. Shaded histograms represent isotype-matched control mAb staining. Data is representative of two independent experiments.

3.4 Discussion

As described in **chapter 1**, IL-10 and CTLA4-Ig are potent immunosuppressive agents. In this study the combined effects of sub-optimal doses of CTLA4-Ig and IL-10 in the human DC-MLR were investigated.

Human monocyte-derived DC were used in this study as opposed to primary DC as they are easy to grow in large numbers and the maturation status of the cells can be controlled. Consistent with previous reports (348-350) we were able to demonstrate TNFα induced maturation of DC based on cell surface phenotype, reduction in antigen uptake and increased allostimulatory capacity. Flow cytometric analysis demonstrated an upregulation of both MHC class I and MHC class II molecules which can increase antigen presentation, costimulatory molecule expression including CD40, CD80 and CD86 as well as the chemokine receptor CCR7, which is important for the migration of DC to secondary lymphoid tissue (351). Moreover we demonstrated the expression of CD83 and CMRF56 on mature DC, both of which are well characterised DC maturation markers (348, 352, 353).

While reported at optimal concentrations to influence DC maturation and costimulatory molecule expression (153, 166, 171, 354), we investigated the effects of sub-optimal doses of IL-10 firstly on the differentiation of human DC from monocytes and secondly on the inhibition of iDC maturation. Differentiation of DC from monocytes in the presence of a sub-optimal concentration of IL-10 led to the generation of cells morphologically resembling DC but lacking CD83 expression even after treatment with TNF-α. This peculiarity may be explained by previous studies which demonstrated that monocytes grown in GMCSF/IL13 in the presence of 20 ng/ml IL-10 differentiate into

macrophages as opposed to DC (355). A similar paper by Morel demonstrated that monocytes differentiated in the presence of IL-10 actually increased the level of costimulatory molecule expression despite being weaker stimulators of the MLR (356). This is similar to our findings in that CD86 was marginally increased upon differentiation in the presence of IL-10. Further staining with macrophage markers such as CD68 and CD16 would allow us to confirm differentiation to macrophages.

In contrast to previous reports using 20 ng/ml IL-10 (169), differentiated DC in our study appeared to be resistant to IL-10 at the sub-optimal concentrations used as no changes to costimulatory molecule expression were observed by flow cytometry. Moreover IL-10 at 5 ng/ml could not prevent the maturation of DC by TNFα treatment as evidenced by the expression of CD83. Thus in the DC-MLR, IL-10 at sub-optimal concentrations is unlikely to directly influence costimulatory molecule expression. IL-10 is also able to modify other APC functions such as IL-12 production (164, 200) and NFκβ blockade (183, 184) which were not investigated in this current study with sub-optimal IL-10 concentrations. Trans-well separation of DC and T cells has however revealed that IL-10 primarily inhibits T cell activation by down-regulation of costimulatory molecules and MHC expression rather than cytokine secretion (171).

The effect of IL-10 derived from Epstein Barr Virus (EBV) which shares 84% homology to human IL-10 (hIL-10) (129), was also investigated in this current study (data not shown). While viral IL-10 (vIL-10) has demonstrated greater prolongation of allograft acceptance compared to hIL-10 (180, 261), our experiments demonstrated almost identical function with respect to the differentiation and maturation of DC and inhibition of the DC-MLR. The similar functions observed between vIL-10 and hIL-10 within our experiments

were not surprising given that the primary reported differences between the two homologues is the type of cellular targets. While both hIL-10 and vIL-10 are able to inhibit DC, monocytes and $CD4^+$ T cells, hIL-10 is also capable of stimulating mast cells, B cells, thymocytes and $CD8^+$ T cells (130, 160, 357). Within our current study the range of cells was limited to DC, T cells and NK cells, thus restricting the differences between vIL-10 and hIL-10 function.

We further demonstrated that human IL-10 is able to augment CTLA4-Ig mediated inhibition of T cell proliferation in an allogeneic DC-MLR. In the first set of experiments, the DC-MLR was performed using NWT responder cells with either immature or mature DC as stimulators. As shown in **figure 3.2**, iDC were indeed poor stimulators of the MLR compared to mDC and the dose response studies identified optimal and suboptimal concentrations for CTLA4-Ig and IL-10 in these assays. At suboptimal concentrations, the combined dose of CTLA4-Ig and hIL-10 displayed two to three fold greater inhibition of NWT responder cell proliferation compared with either agent alone using mature DC as stimulators. Consistent with previous reports, human IL-10 alone appeared to be a more potent inhibitor in the iDC MLR (152, 153) which may account for the observation that CTLA4-Ig did not further augment the inhibition. While IL-10 has been reported to induce anergy (358), we demonstrate that much lower concentrations of IL-10 in combination with CTLA4-Ig can induce T cell hyporesponsiveness to restimulation in the secondary MLR (80% inhibition compared with 28% ($p=0.0045$) for IL-10 alone). Co-culturing CFSE labeled NWT cells with DC stimulators was also performed to determine the individual responsiveness of both $CD4^+$ and $CD8^+$ T cells in the NWT preparation. Flow analysis of CFSE labeled NWT cells, further stained with $CD4^+$ and $CD8^+$ T cell phenotypic markers, demonstrated that both populations were inhibited by IL-10 and CTLA4-Ig. The inhibition

of $CD8^+$ T cells was of particular note given that human IL-10 has been reported to stimulate $CD8^+$ T cells (162, 163). Our observation implies that IL-10 is primarily operating through the modulation of DC function, therein preventing $CD8^+$ T cell activation and is supported by previous findings, which indicate that IL-10 can act on DC to inhibit $CD8^+$ T cell activation (359).

In the studies reported here it could be assumed that the augmentation of T cell hyporesponsiveness is attributed to the combined effects of CTLA4-Ig blockade of CD28 costimulation (54) and the downregulation of CD80/86 expression on DC by IL-10 (264). However, given the wide-ranging effects of IL-10 and the demonstration that IL-10 at 5 ng/ml is unable to modify costimulatory molecule expression, the mechanisms are unlikely to be trivial.

The role of regulatory T cells (T_{reg}) in alloimmune responses is becoming increasingly important. Given our findings that sub-optimal doses of IL-10 are able to augment the inhibition induced by CTLA4-Ig while not influencing the level of costimulatory molecule expression, we sought to investigate whether T_{reg} cells were involved. Preliminary experiments were designed to determine whether depletion of T_{reg} cells could abrogate the inhibition induced by IL-10 and CTLA4-Ig. T_{reg} cells were isolated by immunomagnetic separation of both the $CD4^+CD25^+$ T_{reg} and $CD4^+CD25^-$ subsets. $CD4^+CD25^-$ T cells, when used as the responder population, did not show augmented inhibition with IL-10 and CTLA4-Ig and even appeared insensitive to each agent alone. As T_{reg} cells represent 5-10% of circulating T cells in humans (360), in our study $CD4^+CD25^-$ T cells were repleted with 10% $CD4^+CD25^+$ T_{reg} cells to determine whether T_{reg} cells could restore the sensitivity to IL-10 and CTLA4-Ig. The fact that inhibition was not restored after the repletion of T_{reg} cells indicated that these cells were not responsible for mediating

the sensitivity of the DC-MLR to suboptimal doses of IL-10 and CTLA4-Ig. The strong inhibition of NWT responder cells by IL-10 and CTLA4-Ig in the DC-MLR compared to purified $CD4^+CD25^-$ T cells, which demonstrated low suscepibility to the agents implied that another cell population within the NWT cells may mediate the activity of the agents. Flow cytometric analysis indicated three main populations within NWT cells; $CD4^+$ T cells (65-80%), $CD8^+$ T cells (15-30%), $CD56^+$ NK cells (5-15%).

While repletion of the purified $CD4^+$ T cells with $CD8^+$ T cells did not display any effect on the MLR (data not shown), the addition of NK cells at a concentration of 10% restored the high inhibitory capacity of CTLA4-Ig and IL-10 indicating that NK cells can potentially interact with either DC or T cells to modify the alloimmune response. Similarly, in another study reported by Akdis *et al.*, it was shown that anti-CD3 stimulated PBMC cultures were responsive to IL-10 mediated inhibition while purified CD45RO T cells were unaffected (175). This is suggestive that accessory populations such as NK cells or monocytes within PBMC potentially influenced the susceptibility of T cells to IL-10 mediated inhibition.

We cannot exclude the possibility of NK cell mediated lysis of the allogeneic DC in the DC-MLR reported in our studies as the stimulatory capacity of $CD4^+$ T cells repleted with NK cells was indeed reduced in **figure 3.11 (experiment 1)** although this was not a common feature between experiments **(experiment 2)**. Over the course of a number of experiments (n=12), NWT cells and $CD4^+$ T cells demonstrated significant inter-experiment variability with respect to proliferation counts in the DC-MLR with either no change or large reductions in NWT proliferation. Moreover repletion of $CD4^+$ T cells with NK cells resulted in reduced proliferation in 2 out of 3 experiments, although sensitisation to IL-10 and CTLA4-Ig was still induced in all three experiments. As shown in **figure 3.12**

iDC cultured in the presence of allogeneic NK cells exhibit evidence of lysis although this observation was not investigated with ^{51}chromium lysis assays. Whether NK cells lyse DC depends on a number of factors including the maturation status of the DC, the activation status of the NK cell, the ratio of NK cells to DC and recognition of MHC Class I molecules on the DC. While NK cells can lyse iDC at high NK:DC ratios, mDC are typically resistant to NK-mediated lysis (361, 362). This protection is primarily as a result of high level MHC Class I expression which can be recognised by inhibitory KIRs (killer-cell immunoglobulin-like receptors) (363, 364). Inter-experimental variation may thus be representative of divergent MHC Class I alleles which may or may not be recognised by inhibitory KIR on the allogeneic NK cells. These variations could be controlled by using various mouse stains with MHC class I matched or mismatched phenotypes, while allele typing would be required in the human situation, which was beyond the scope of these studies.

While NK cell mediated DC lysis may play a role in the sensitisation of T cells to sub-optimal concentrations of CTLA4-Ig and IL-10 by reducing the overall stimulation in the MLR, the demonstration of CTLA4-Ig/IL-10 inhibition in **figure 3.11 (experiment 2)** indicates that NK cells must also mediate other effects as NK cells themselves did not inhibit the untreated MLR. To ascertain these other mechanisms, DC were cultured for 3 days in the presence of allogeneic NK cells. Flow cytometric analysis revealed an upregulation of CD80 particularly on iDC which is consistent with previous reports in that autologous NK cells are able to activate DC in both cell-contact and cytokine dependent manners (365, 366). After three days in culture with allogeneic DC, NK cells were removed from culture and viable DC added to the MLR with allogeneic $CD4^+$ T cells. Consistent with the increased expression of CD80, iDC precultured with NK cells

demonstrated increased stimulatory capacity in the MLR. In addition both iDC and mDC precultured with NK cells showed sensitivity to suboptimal concentrations of IL-10 and CTLA4-Ig while DC not exposed to NK cells were non-responsive.

The influence of NK cells was not restricted to DC as interactions between autologous NK cells and T cells were also demonstrated. Confirming the specific interactions between NK and T cells with respect to CD28 costimulation (367, 368), our data demonstrated that NK cells cultured with IL-2, upregulated the expression of CD86 on autologous $CD4^+$ T cells. Furthermore, our study demonstrates that NK cells costimulate $CD4^+$ T cell proliferation and confirms the involvement of CD86 since CTLA4-Ig blockade was able to inhibit proliferation. Other costimulatory pathways apart from CD28 have also been implicated to drive NK cell mediated costimulation of T cells including OX40/OX40L (368) and 2B4/CD48 (369) interactions. Our observations (**figure 3.12**) in addition to these studies imply that the interactions between NK cells and T cells are sensitive and non-redundant since the blockade of either one of these pathways or CD28 costimulation abrogates the influence of the NK cells. While this study has provided some mechanisms by which NK cells influence the interactions between DC and T cells, the extent to which cell-contact or cytokines are involved has not been investigated.

Another point of interest within these studies was the observation of two populations of NK cells isolated by the immunomagnetic microbead separation. $CD56^{bright}$ (5-10%) and $CD56^{dim}$ (90-95%) populations were routinely purified. The relevance of these findings lies in the reports of a regulatory role played by $CD56^{bright}$ cells, which are cytokine producing, non-cytolytic cells in comparison with $CD56^{dim}$ cells (370, 371). The extent to which these regulatory $CD56^{bright}$ cells may have played in this current study was not investigated.

While the primary role of NK cells in the innate immune system is in the killing of autologous tumour and pathogen infected cells its consequential effects on the adaptive immune response may broaden the scope of these cells in directly activating the alloimmune response (372, 373). Recently, there has been accruing evidence for a fundamental role for NK cells in allograft rejection as these cells promote cardiac allograft vasculopathy (374) and cellular infiltration in the graft (375). In addition, studies have demonstrated a requirement for the depletion of NK cells to ensure robust allograft acceptance in association with tolerance inducing protocols (375, 376).

In summary we report that the combined treatment of the allogeneic DC MLR with suboptimal doses of IL-10 and CTLA4-Ig inhibits T cell activation. Notably, NK cells are potentially able to render autologous T cells and allogeneic DC susceptible to the inhibitory effects of IL-10 and CTLA4-Ig. Thus therapeutic strategies that involve the combination of CTLA4-Ig and IL-10 may be effective in promoting allograft tolerance by targeting NK cells associated with DC-T cell interactions. Moreover these data support investigation into the efficacy of DC genetically manipulated to express IL-10 and CTLA4 fusion proteins in the treatment of allograft rejection.

Chapter 4:

Isolation and Characterisation of Ovine Dendritic Cells Derived from Pseudo-afferent Lymph

Results from this chapter are also presented in the following publication

- Newland A.M., Kireta S., Russ G., Krishnan R. (2004). Ovine Dendritic Cells Transduced with an Adenoviral CTLA4$_e$EGFP Fusion Protein Construct Induce Hyporesponsiveness to Allostimulation. *Immunology*. **113**: 310-317.

4.1. Introduction

DC represent less than 2% of circulating blood mononuclear cells yet are present in blood and lymph and reside in almost all tissues (377-379). Depending on their tissue origin DC populations are phenotypically and functionally heterologous, expressing distinct characteristics. For instance in the absence of stimulus, DC which constitutively migrate from the lungs and intestines to lymph nodes display a tolerogenic phenotype, representing the need to prevent immunity against harmless antigens (380, 381). In contrast cutaneous DC isolated from lymph are typically more potent antigen presenting cells as migration is more dependent on inflammatory stimuli (382-384). Thus in this chapter it was proposed to obtain DC from the lymph vessels draining the skin.

4.1.1 Isolation of ovine dendritic cells from lymph nodes draining the skin

In comparison to the chained arrangement of human lymph nodes, sheep lymph nodes are generally characterised by a number of small afferent vessels draining into a large solitary lymph node with a single efferent lymphatic vessel allowing the study of immune reactions within individual lymph nodes (385-387). While the efferent lymphatic vessel is readily cannulated, DC are retained in the lymph node which accounts for the absence of DC in the single efferent lymphatic (388, 389). Afferent lymph contains 1-10% DC, however the small diameter of the vessels makes cannulation technically difficult and minimal lymph may be collected (390). Removal of the lymph node allows the multiple small afferent lymphatics to anastomose to the larger efferent lymphatic vessel, which may then be cannulated (391, 392). Due to the absence of the lymph node, pseudo-afferent lymph has a similar cellular composition of true afferent lymph. Dendritic cells may be purified from lymph by density gradient separation (379, 393).

4.1.2 In vivo properties of DC

To establish baseline *in vivo* function of isolated ovine DC it is important to establish that these cells are able to migrate to secondary lymph nodes and are also capable of eliciting an inflammatory response. In order to determine the in vivo inflammatory response of the isolated DC it was proposed to examine the normal lymphocyte transfer (NLT) reaction. The NLT reaction, originated in the 1960's as an *in vivo* histocompatibility test, was developed as a model for studying graft-versus-host (GVH) reactions as well as transplant immunity (394). The NLT reaction involves the transfer of allogeneic normal lymphocytes intradermally into a recipient, resulting in a biphasic skin response. The initial response occurs at around 48 h and is characterised by erythema and localised swelling, believed to be due to GVH reactions (390, 395). The secondary response is characterised as an indurated lesion with small areas of erythema (390, 396). At the immuno-histological level, this late response is associated with prominent infiltration of $CD4^+$ and $CD8^+$ lymphocytes and therein is thought to relate to host-versus-graft responses, akin to transplant rejection. During the late 1960s the NLT was shown to have a degree of predictive value in considering related individuals for transplantation (390, 397) before being replaced by the MLR for issues of ease and safety. This model does still however provide a technically easy model to test the ability of cells to induce an effective alloimmune response *in vivo*.

The NLT reaction has been characterised in murine (398), guinea pig (399), hamster (400) canine (401), bovine (402), ovine (403, 404) and human species (395, 405), however due to the unavailability of monoclonal antibodies at the time of these studies, the primary readouts from these experiments were based on physiological changes including

measurements of lesion induration and qualitative analysis of erythemal development. Only one recent study, using efferent lymph derived cells, has accurately quantified the intensity of erythemal development in the NLT reaction and utilised monoclonal antibodies to identify the involvement of CD4 and CD8 population of T cells (404). Of particular note in the NLT reaction, the origin of the injected cells can elicit profoundly different responses. In general efferent lymph cells provoke a more aggressive response with strong erythemal development and lesion induration. Afferent lymph cells in the NLT invoked a weaker response, which subside by day 7, compared with the stronger efferent derived NLT reaction which persisted until day 10 (406). Afferent cell populations did however induce a greater inflammatory response in the first 48 h. These differences are likely to reflect the cellular composition of the cells or their activation status. A particular difference is the absence of DC from efferent lymph while afferent lymph is composed of 1-10% (407). Moreover $CD4^+$ T cells isolated from afferent lymph typically display a memory T cell profile while efferent T cells are generally naïve (408, 409). Due to the lack of classification of these cells in the NLT reaction, the precise role of cell subsets remains elusive.

This current chapter details the isolation and characterisation of ovine DC derived by pseudo-afferent cannulation.

The specific aims of this chapter were to…

i. Obtain ovine DC by cannulating the afferent prefemoral lymphatic vesssel and to determine the *in vitro* characteristics of these DC with respect to their cell surface phenotype and ability to stimulate alloreactive T cells.

ii. Investigate the *in vivo* migratory and allostimulatory properties of ovine DC after intradermal administration, in particular the ability of these cells to elicit a NLT reaction.

4.2. Methods

4.2.1. Cannulation

Two-year old Merino sheep were obtained from the Institute of Medical and Veterinary Science (IMVS: Adelaide, Australia). Sheep were housed at the animal storage facility at The Queen Elizabeth Hospital and permitted free access to food and water. Animal ethics approval was obtained from the QEH and Adelaide University animal ethics committees (N16-2001). The prefemoral lymph nodes were identified and excised under general anaesthesia. To enable the site to be relocated, the lymphatics were tied off using non-degradable sutures. Animals were returned to the paddock for a 6-8 week agistment period to allow pseudoafferent vessels to develop. Sheep were returned to The Queen Elizabeth Hospital and 1 ml Patent Blue V® dye was subcutaneously injected under general anaesthesia into the hind leg draining towards the removed prefemoral lymph node. The region was re-opened and the non-degradable suture identified. Patent Blue V® dye is readily taken up into the lymphatics, enabling clear identification of enlarged lymphatic vessels. The lymphatic was cannulated using a 3Fr heparin-impregnated cannula (Carmeda, USA), externalised and sutured to the skin. Lymph was passively collected in emptied 100 ml sterile saline bags supplemented with 2500 IU heparin and 40 mg gentamicin sulphate. Bags were changed daily with an average yield of 100 ml.

4.2.2. Metrizamide Purification of ovine DC from lymph

Lymph was decanted into 50 ml tubes and centrifuged at 340 g for 7 min. Each pellet was resuspended in 7 ml PBS and transferred to 10 ml tubes. The cell suspension was underlayed with a pasteur pipette (~1.5 ml) of 14% Metrizamide^{TM} (Sigma, USA) in

RPMI. Cells were centrifuged at 800 g for 15 min with the brake off. The interface DC-rich layer was removed and washed twice in PBS at 340 g.

4.2.3. Flow Cytometry

The cell-surface phenotype of the Metrizamide enriched ovine lymphatic DC was analysed by flow cytometry (**2.3.4.1**). Monoclonal antibodies used were specific for ovine cell surface antigens or human antigens with demonstrated cross-reactivity to their respective ovine homologue. Isotype-control antibodies were used to determine background staining. Antibodies used were αCD1a (20.27), αCD4 (44.38), αCD8 (38.65), αCD25 (9.14), αCD44 (25.32), Class I (41.19), Class II DP (28.1) αCD14 (VPM65), αCD83 (HB15A17.11), αCD31 (CO.3E1D4), αCD21 (CC21), CMRF56, 1D4.5 and X63 (P3X63Ag8).

4.2.4. Dendritic Cell Mixed Lymphocyte Reaction

Ovine PBMC were isolated from peripheral blood as detailed in section **2.3.1.1.** The DC MLR was set up as per **2.3.1.4** with DC used as the stimulator population against allogeneic PBMC. DC were added at varying cell concentrations to titrate the proliferative effects. Stimulator to responder ratios used were 1:1, 1:10, 1:100 and 1:1000.

4.2.5. PKH26 Labeling

PKH26 was prepared at a concentration of 4 x 10^{-6} M solution by diluting the stock in Diluent C. Cells were pelleted at 400 g and the supernatant aspirated leaving approximately 25 µl. The pellet was gently resuspended in the residual supernatant and 1 ml Diluent C added. One millilitre of PKH26 was added and the cells were labeled at 25°C for 2-5 min with occasional inversion of the tube to ensure sufficient mixing. The addition of 2 ml FCS and incubation for 1 min stopped the labeling reaction. Cells were washed with complete media and centrifuged at 400 g for 10 min. Supernatant was aspirated and the pellet transferred to a fresh tube and washed again in complete media. Pellet transfer and washes were repeated a minimum of 3 times. PKH26 labeling efficiency was demonstrated by flow cytometric analysis in the FL2 channel in comparison to unlabeled cells.

4.2.6. Normal Lymphocyte Transfer Reaction

Isolated ovine DC (5 x 10^6) were mixed with autologous PBMC (5 x 10^7) and resuspended in 400 µl endotoxin-free PBS with 200 µl drawn up in 29G insulin syringes (BD, USA). Cells were injected intra-dermally in non-wool bearing skin of sheep. Injections were performed at duplicate sites using cells either autologous or allogeneic to the NLT recipient. Intradermal injections with endotoxin free PBS were used as controls. Injection sites were monitored daily for erythemal development and measurement of induration. The extent of induration was determined using venier calipers, with triplicate measurements for each injection site. Full skin thickness biopsies were excised under

general anesthesia at day 2 and day 7 post injection. Skin biopsies were embedded in OCT compound and frozen in liquid nitrogen for cryomicrotome sectioning.

4.2.7. Immunohistological analysis of Skin Biopsies

Using a cryomicrotome, 5 μm serial section were cut, dried overnight and fixed in acetone. Slides were either stained with H&E (**2.3.5.2**) to identify lymphocyte infiltrate or were used for immunohistochemical analysis (as described in **2.3.5.3**). Ovine antibodies used for staining included anti-CD4 (44.38), anti-CD8 (38.65) and anti-MHC Class II (28.1) with 1d4.5 used as the isotype-matched control antibody.

4.2.8. RNA Extraction from skin biopsies and PCR analysis of IL-2 mRNA expression

Ten 10 μm sections were cut and pooled for RNA extraction. RNA was extracted as per **2.3.2.1** and 1 μg total RNA reverse transcribed (**2.3.2.2**). PCR (**2.3.2.3**) was performed using ovine IL-2 primers and after an initial denaturing step at 95°C for 5 min, amplification was carried out for 26 cycles (94°C for 30 s, 55°C for 30 s, 72°C for 30 s) and a final extension at 72°C for 7 min. The β-Actin housekeeping gene was also amplified as an internal control. PCR products were analysed by electrophoresis on a 2% agarose gel, stained with ethidium bromide and illuminated with ultraviolet light.

4.2.9. Mitomycin C treatment of PBMC

PBMC (5×10^6) were resuspended in 8 ml S10g and 2ml Mitomycin C (1 mg/ml) added. Cells were incubated for 30 min at 37°C and 5% CO_2 and gently mixed every 10 min. Cells were washed twice in PBS and resuspended in S10g.

4.2.10. Sensitisation Assay

PBMC were isolated from NLT recipient sheep before and after the reaction and cryopreserved until required. The MLR was established using donor specific PBMC treated with Mitomycin C as stimulators against the pre- and post- NLT PBMC from the recipient sheep. Cell proliferation was measured by the level of [^{3}H] thymidine incorporation as described in **2.3.1.4**.

4.3. Results

4.3.1. Phenotype of ovine pseudo-afferent derived DC

Ovine lymph was collected from pseudo-afferent cannulated sheep. On average approximately 100 ml of lymph was collected each day, with patent cannulas maintained for up to five months. Lymphatic cells obtained from the cannulation of the pre-femoral lymph duct consisted of 60-80% of cells with typical dendritic cell morphology upon enrichment by Metrizamide density centrifugation (**figure 4.3.a**). The profiles of DC phenotypic markers were examined on cells that were obtained from the lymphatic drainage up to 14 days post cannulation. **Figure 4.1.a.** shows the typical cell surface profile of DC obtained 8 days post cannulation. Of particular note the cells demonstrated high level expression of the antigen presenting molecules MHC Class I and II, and the DC maturation markers CMRF56 and CD83. While this profile was reproduced between four sheep, one sheep (N16-09) consistently demonstrated an absence of CD83 expression (**figure 4.1.b**), despite maintaining strong allostimulatory properties (data not shown). Freshly isolated ovine DC demonstrated moderate uptake of FITC-Dextran (**figure 4.1.c.**).

4.3.2. Stimulatory capacity of ovine DC

Ovine DC were used in the DC-MLR at a 1:100 S/R ratio to stimulate autologous and allogeneic PBMC. As demonstrated in **figure 4.2.a.,** compared to the stimulation of autologous PBMC by DC (8300 +/- 260 cpm) and the two way allogeneic PBMC-MLR (4400 +/- 1700 cpm), DC elicited potent stimulation of allogeneic PBMC (40000 +/- 3200 cpm ($p=0.0026$)). The allostimulatory capacity of DC was titrated over a range of S/R ratios from 1:1 to 1:1000 (**figure 4.2.b**). While the 1:1 ratio was the most potent (128000

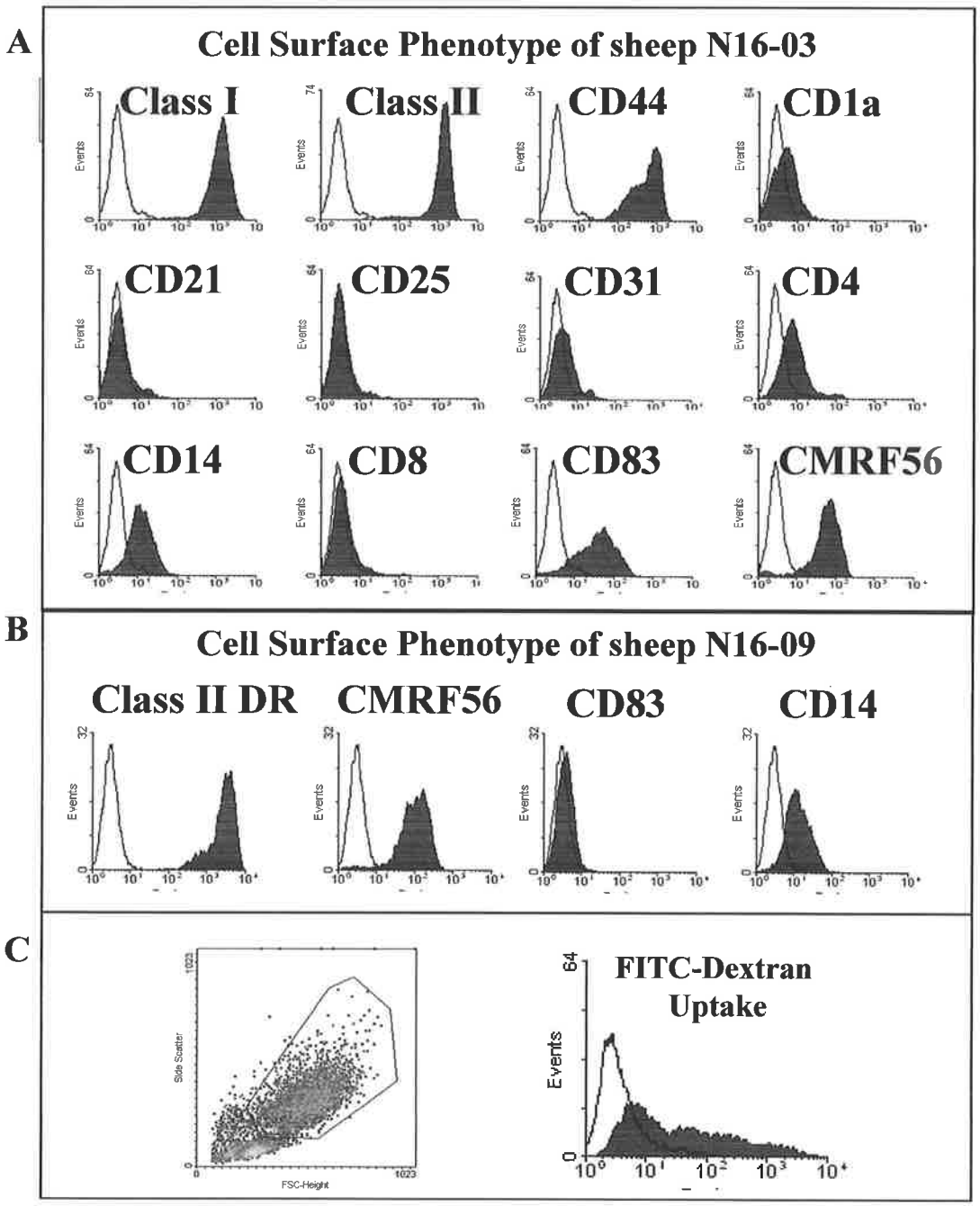

Figure 4.1. Characterisation of ovine DC obtained by pseudo-afferent cannulation
Lymph was collected from cannulated sheep and DC purified on a Metrizamide density gradient. Flow cytometric analysis was performed using antibodies directed against cell surface molecules. **Panel A** demonstrates the cell-surface phenotype of DC obtained from sheep N16-03, which was consistent with the profiles of 4 other sheep. **Panel B** shows some of the key DC markers expressed by sheep N16-09 which consistently demonstrated an absence of CD83 expression. Unshaded histograms represent staining by the isotype-matched control antobody. **Panel C** illustrates the forward-side scatter of the ovine DC and the gate used for analysis. The histogram demonstrates the capacity of ovine DC to take up FITC-Dextran at 37°C (shaded histogram) compared to the control temperature of 4°C (unshaded histogram).

A

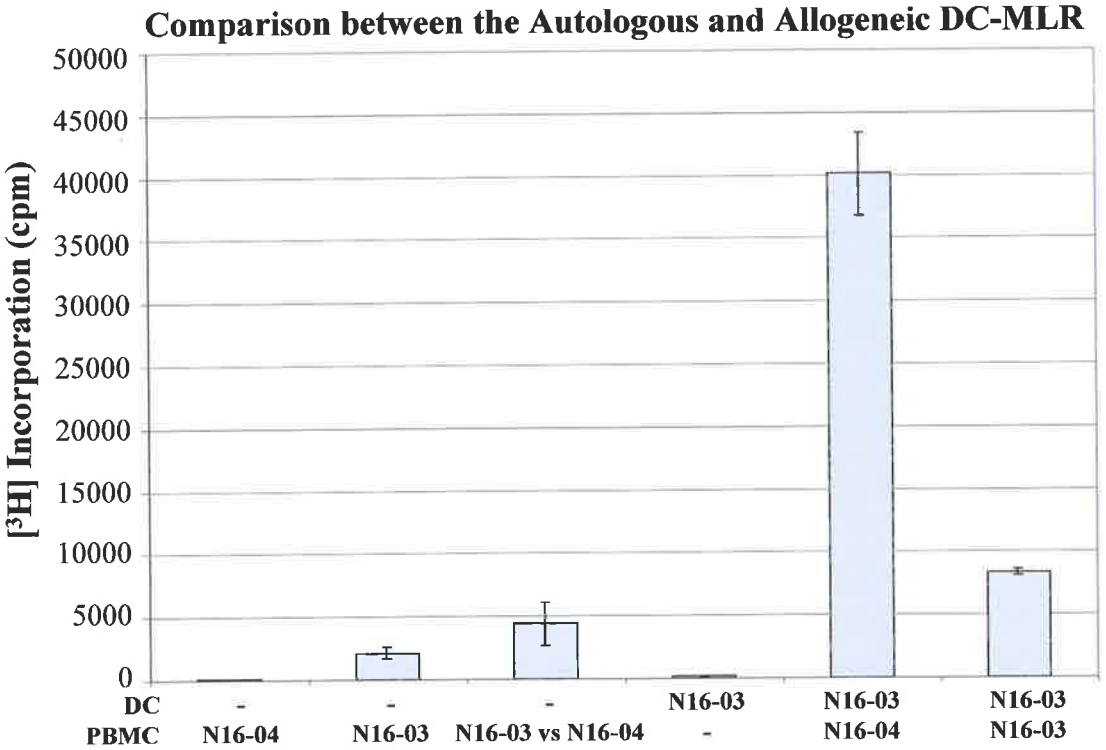

B

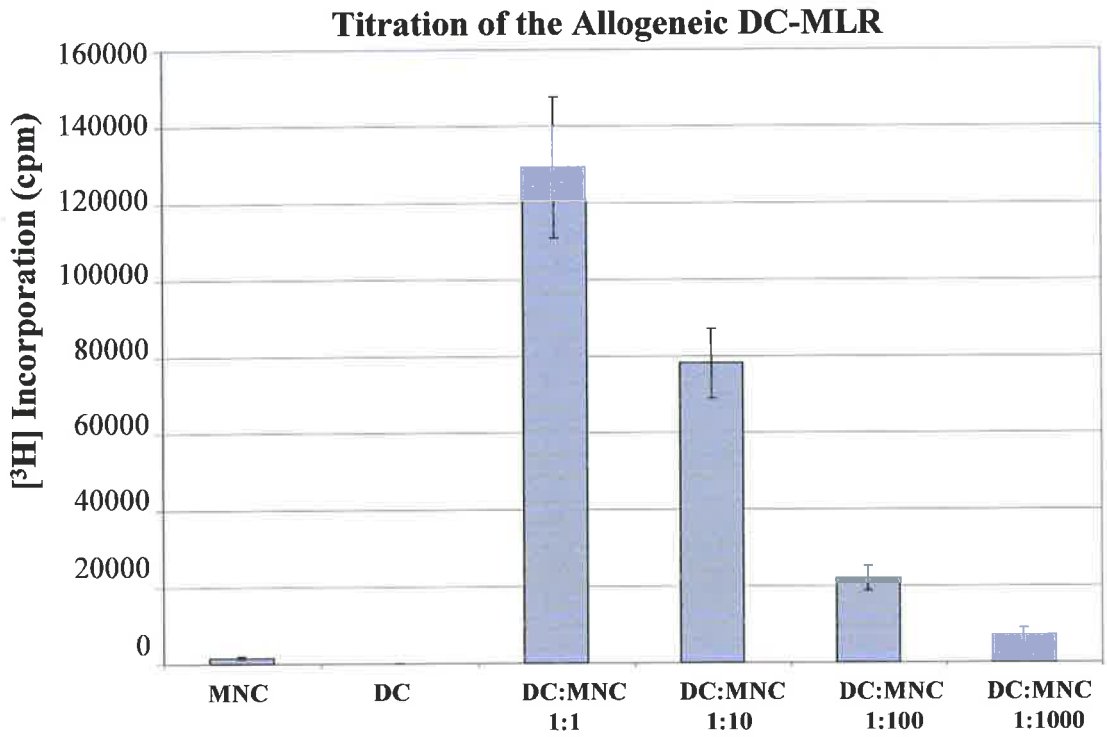

Figure 4.2. Ovine DC stimulate the proliferation of alloreactive PBMC
Ovine DC were used to stimulate PBMC in the DC-MLR. Each experimental point represents [^{3}H] incorporation of triplicate samples measured in cpm +/- SD.
A) At an S/R of 1:100, ovine DC were weak stimulators of autologous PBMC. In comparison profound stimulation of allogeneic PBMC occurred at the same ratio.
B) The stimulatory capacity of ovine DC on allogeneic PBMC was titrated over S/R ratios from 1:1 to 1:1000.

+/- 18400 cpm), even at the 1:1000 ratio, DC were still able to produce synergistic proliferation (7100 +/- 1900 cpm) compared with MNC cultured alone (1500 +/- 290 cpm (p=0.008)).

4.3.3. Dendritic cells rapidly migrate to the draining lymph node

Ovine DC were stained with the fluorescent dye PKH26 with greater than 90% efficiency (**figure 4.3.b.**). Labeled DC (5 x 10^6) were intradermally injected into the hind leg region of a sheep with cannulated pre-femoral lymphatics. Lymph was collected at intervals over a 40 h period and lymph cells analysed by flow cytometry for the presence of PKH26 labeled cells. Compared with cells isolated prior to the injection, a shift in fluorescence was observed within 4 h, peaking at 24 h (**figure 4.3.c.**). The presence of PKH26 labeled cells began to dissipate after 40 h.

4.3.4. Intradermal injection of allogeneic DC and PBMC elicits a strong NLT response

PBMC supplemented with 10% DC were intradermally injected into autologous (n=2) or allogeneic sheep (n=3). The reactions were monitored over the course of 14 days with daily double-skin thickness measurements conducted and skin biopsies taken at days 2 and 7 for immunohistological analysis. The allogeneic NLT reaction was characterised by an indurated lesion and faint erythema (**figure 4.4**). As shown in **figure 4.5** within 24 h there was a dramatic increase in the thickness of the skin of the allogeneic and autologous NLT reactions at the site of injection. This was not attributed to the injected innoculum volume as the injected fluid rapidly diffused within a period of 5 minutes. The increase in skin thickness observed at 24 h rapidly decreased in the autologous NLT reaction with levels returning to baseline measurements within a few days (**figure 4.5**). In comparison

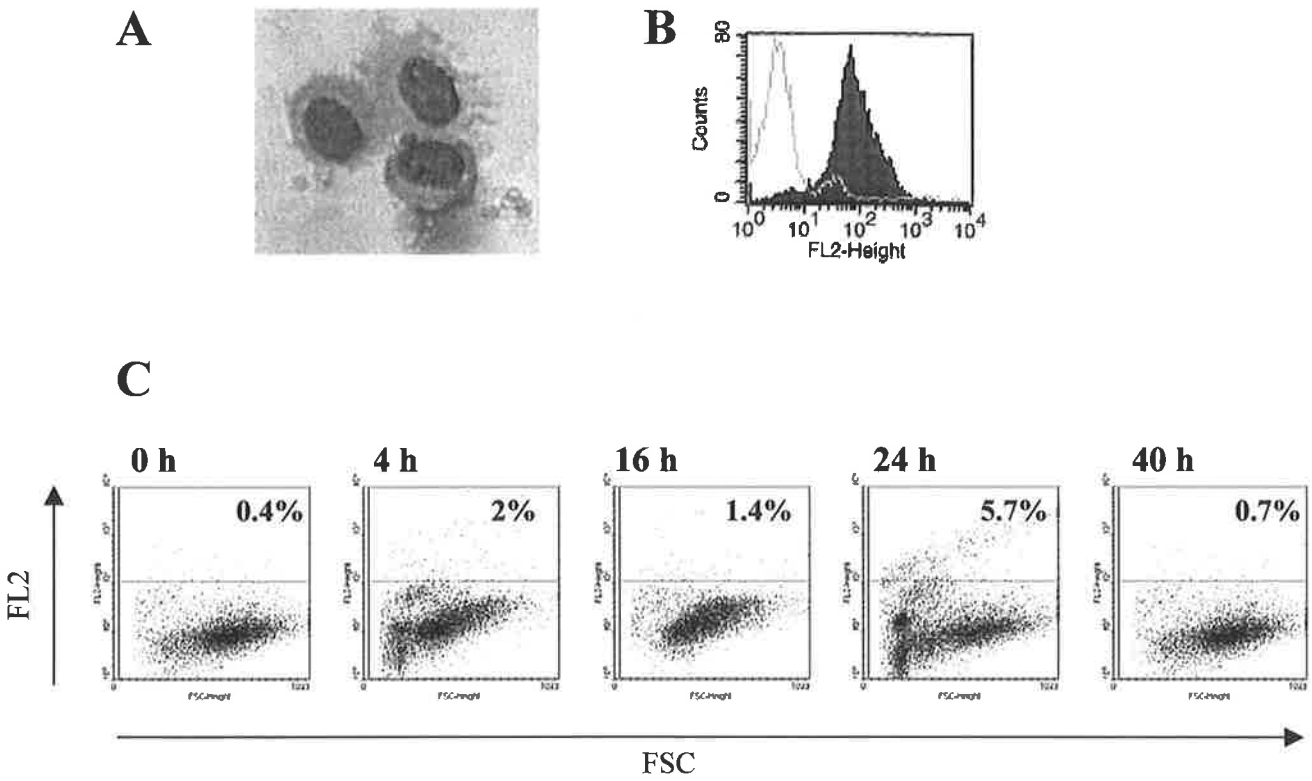

Figure 4.3. Intradermally injected DC rapidly migrate to the draining lymph node
A) Light microscope image of freshly isolated ovine DC treated with giemsa stain, demonstrating characteristic dendrites.
B) Flow cytometric analysis demonstrating the efficacy of PKH26 staining of DC (shaded histogram). Unshaded histogram represents unstained DC.
C) Autologous DC labeled *ex vivo* with PKH26 were intradermally injected into the hind leg region of a previously cannulated sheep. Lymph was collected at different time points and cells were analysed for fluorescence in the FL2 channel by flow cytometry. The percentages shown represent the percentage of PKH26 positive cells in the lymph at each time point.

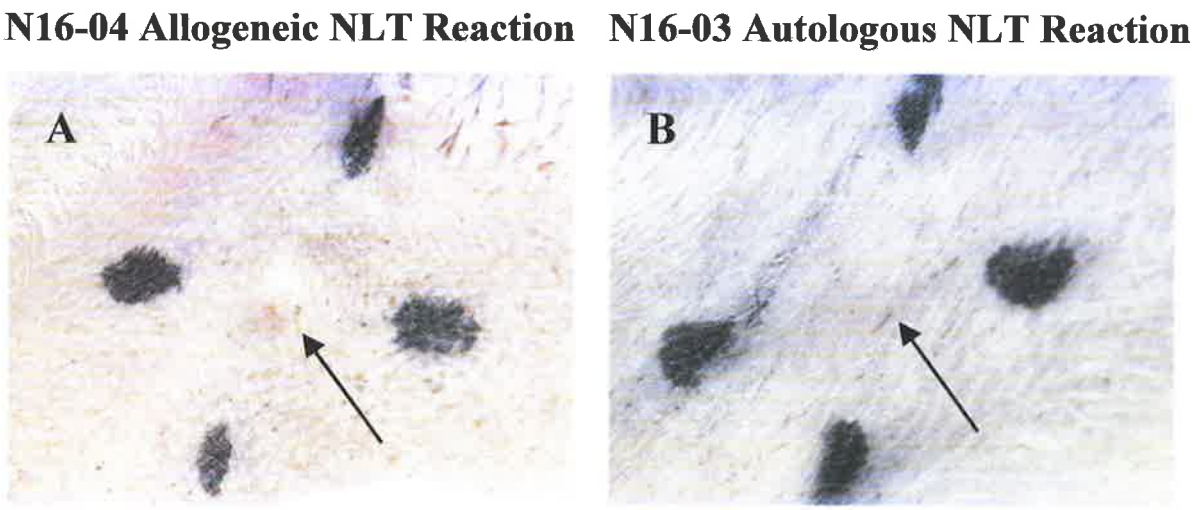

Figure 4.4. The Allogeneic NLT reaction induces an indurated lesion at the site of injection Autologous and allogeneic normal lymphocyte transfer (NLT) reactions were established by the intradermal injection of PBMC and 10% DC isolated from N16-03 into non-wool bearing sheep skin. Panel A and panel B respectively represent the allogeneic and autologous NLT reactions 96 h post-injection. The original injection sites are shown by the arrows.

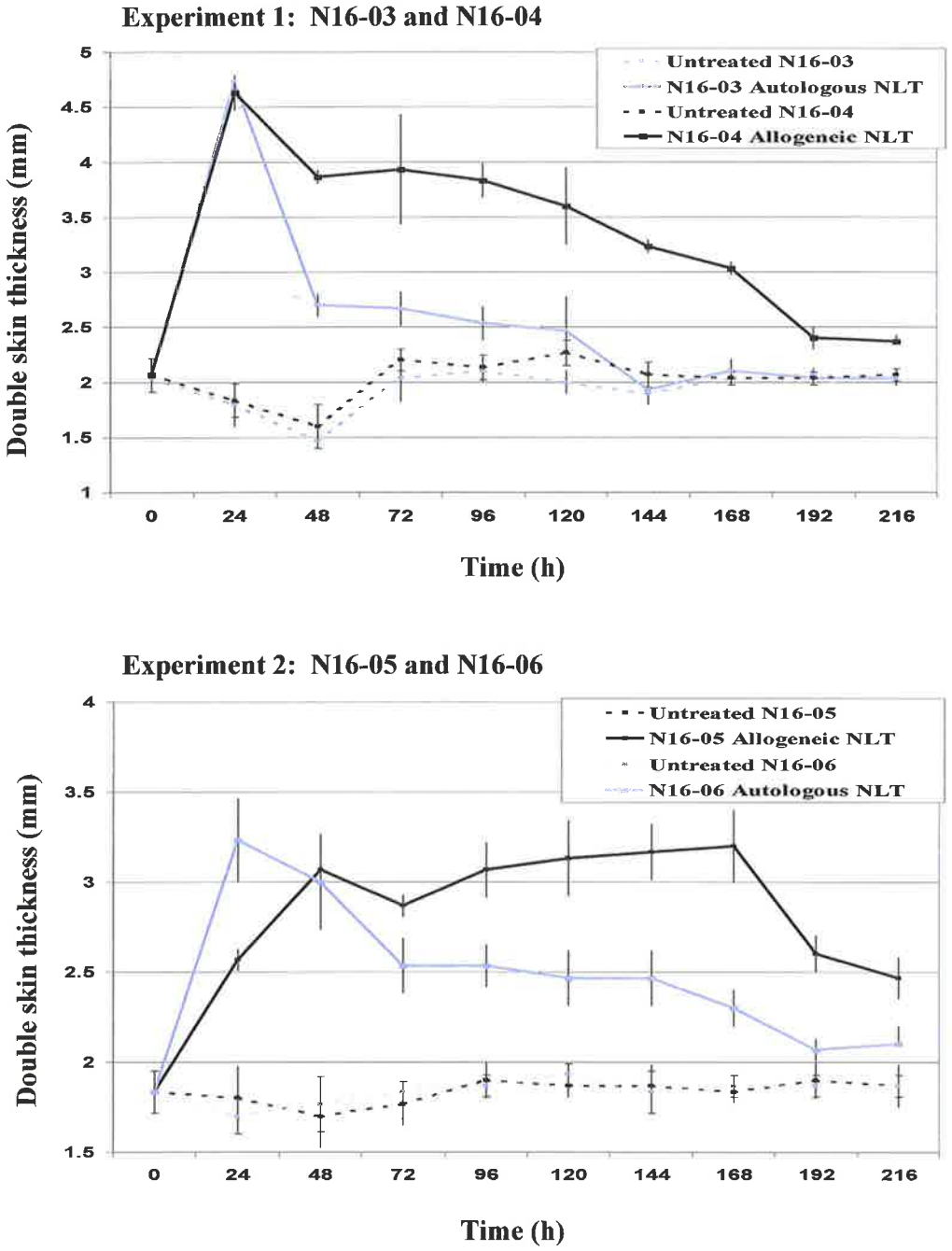

Figure 4.5. Quantification of lesion induration in the NLT reaction.
Double skin thickness measurements using venier calipers were taken at 24 h intervals after injection of cells autologous or allogeneic to the recipient sheep. NLT reactions were performed in duplicate and triplicate measurements made by two independent assessors. Measurements were taken of the NLT injection sites and untreated skin regions as controls. Graphs represent the measurements in mm +/- SD.

skin thickness levels of the allogeneic NLT reactions remained significantly thicker than untreated skin throughout the duration of the experiment ($p < 0.05$, paired student T test), with close to baseline levels observed only after 9 days. H&E staining of skin biopsies taken 2 and 7 days post NLT revealed massive lymphocyte infiltrates in the allogeneic NLT reaction while the autologous NLT reaction had a sparse distribution of lymphocytes (**figure 4.6.A**). Untreated skin biopsies were devoid of lymphocyte infiltrate. RT-PCR of skin biopsy sections revealed a significant upregulation of IL-2 mRNA expression in the allogeneic NLT reaction at both 2 and 7 days post injection (**Figure 4.6.B**). Low levels of IL-2 mRNA were detected in the autologous NLT reactions. PCR amplification of the β-Actin housekeeping gene was performed as an internal control. Immunohistological staining of allogeneic biopsies revealed that the infiltrate was comprised of both $CD4^+$ and $CD8^+$ T cells with a high level of MHC Class II expression (**Figure 4.7**). To investigate the systemic sensitisation to donor antigen from the NLT reaction, host PBMC were isolated before and after the NLT reaction and cryopreserved until required. In response to mitomycin C treated donor cells, host cells isolated after the NLT reaction demonstrated a three-fold increase in proliferation ($p < 0.0007$) compared to cells isolated prior to the NLT reaction (**figure 4.8**).

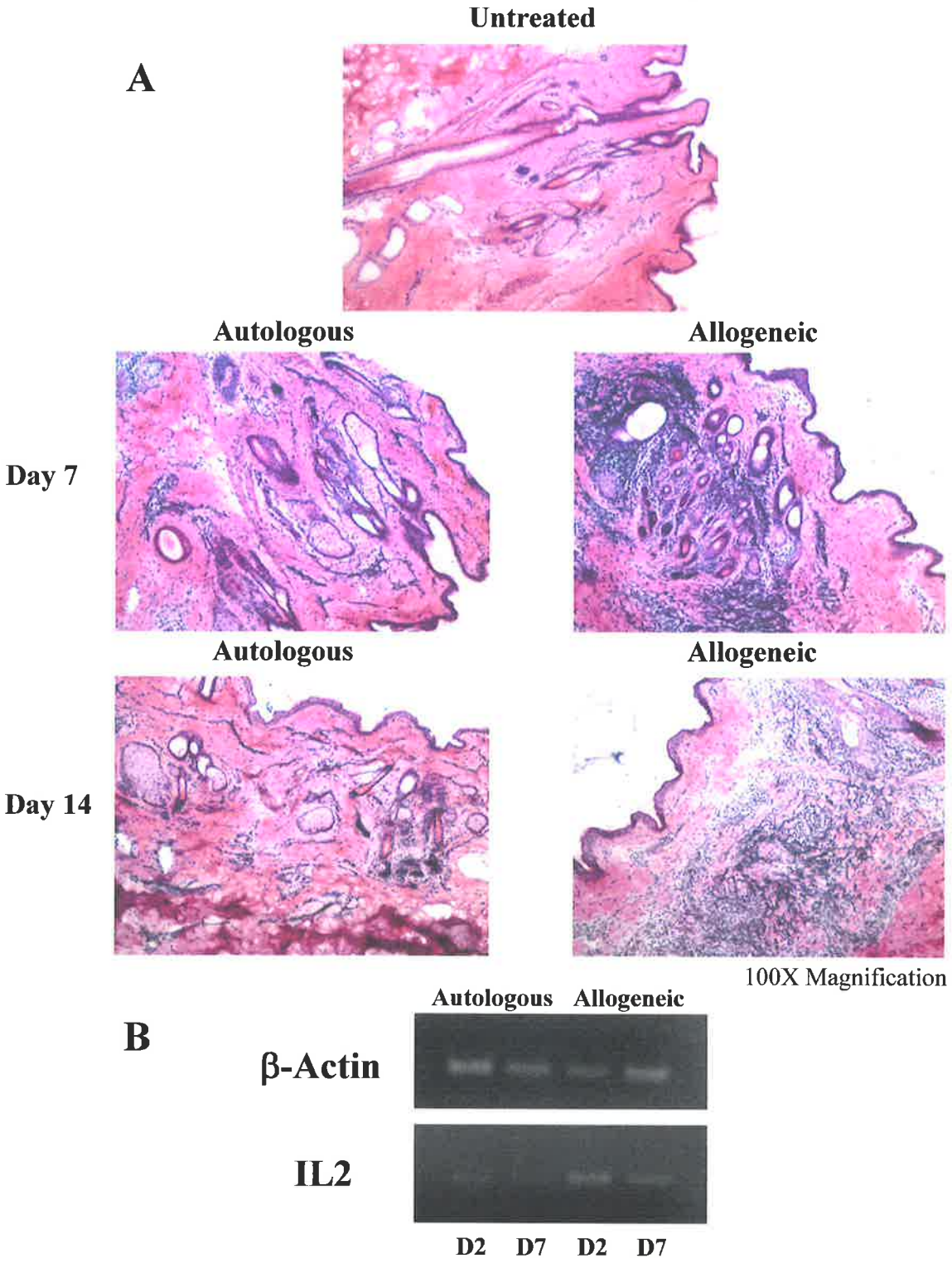

Figure 4.6. The allogeneic NLT reaction is characterised by extensive lymphocyte infiltration
A) Full-skin thickness biopsies were taken from the injection sites of the NLT reactions and sections stained with H&E. Sections represent untreated skin biopsies and skin biopsies taken from autologous or allogeneic NLT reactions at days 2 or 7. Histology is representative of two autologous and three allogeneic NLT reactions. Sections from the allogeneic NLT reaction demonstrated aggressive staining of lymphocytes, compared to the sparse staining of cells in the autologous reaction.
B) PCR using ovine IL2 primers was conducted on cDNA reverse transcribed from RNA extracted from the sections. Allogeneic NLT sections demonstrated higher production of IL2 per μg total RNA. β-Actin PCR was used as a control house-keeping gene.

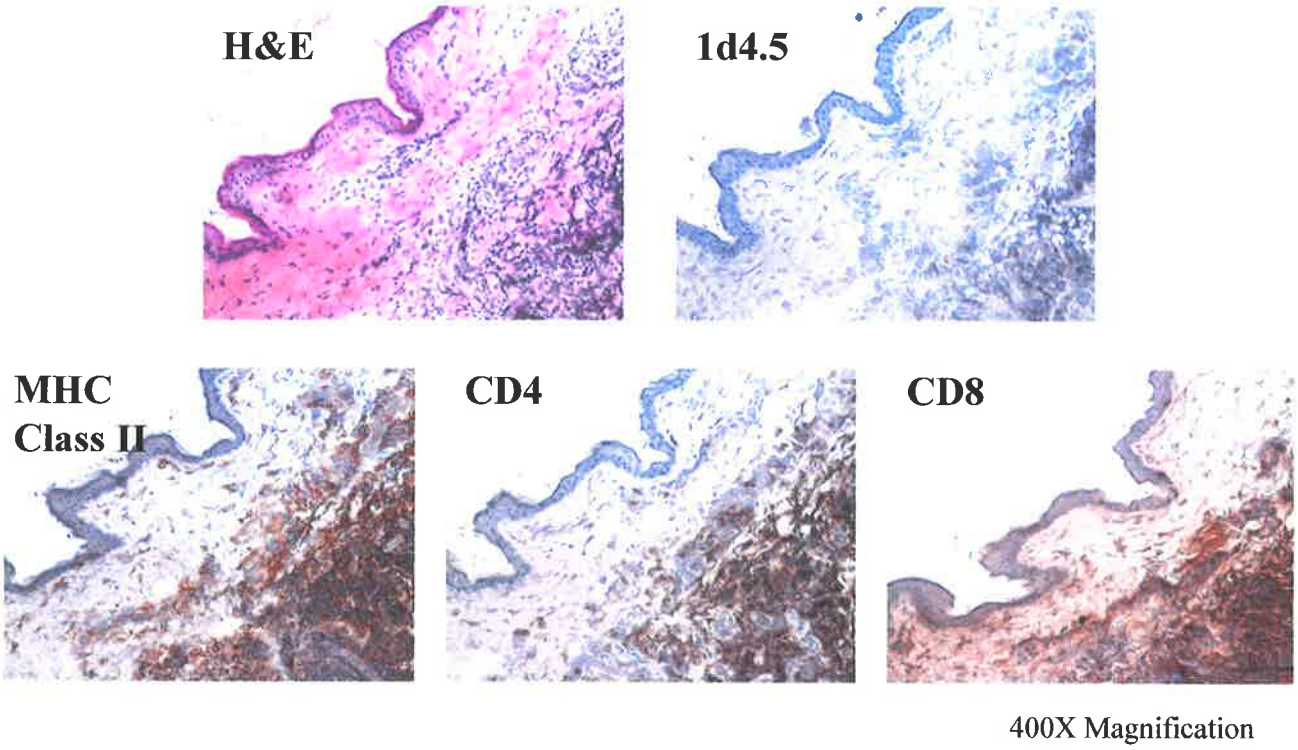

Figure 4.7. Infiltrates of the allogeneic NLT reaction consist of both $CD4^+$ and $CD8^+$ cells. Serial allogeneic NLT sections were either stained with H&E (panel A) or primary antibodies. Immunohistological sections were developed with DAB stain. 1d4.5 was used as an isotype-matched irrelevant control antibody. Staining revealed the presence of both $CD4^+$ and $CD8^+$ cells as well as a high level of staining for MHC Class II.

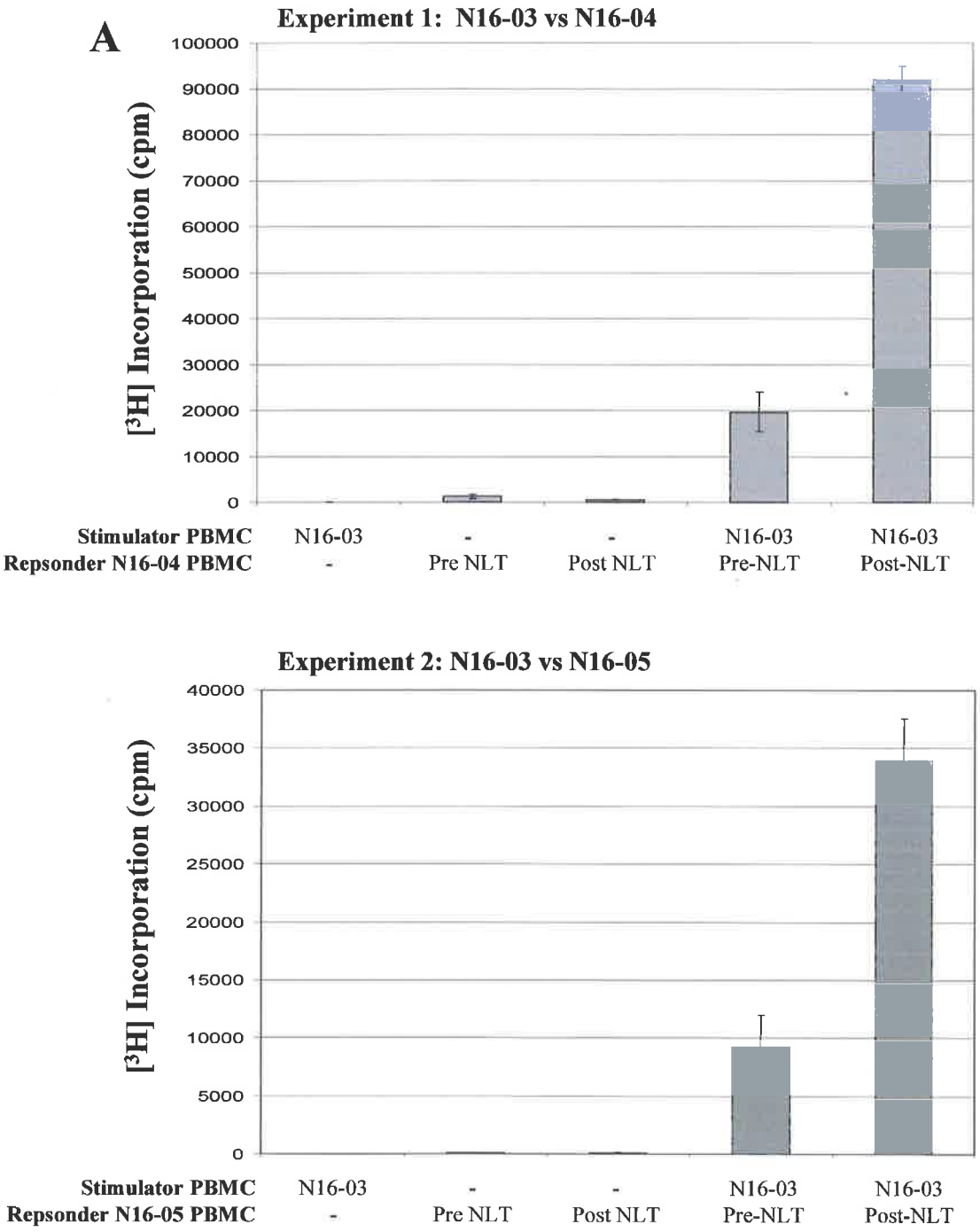

Figure 4.8. The NLT reaction results in a systemic sensitisation to NLT donor antigen PBMC isolated before and after the NLT reaction were used in a one-way MLR against mitomycin C treated donor PBMC. Close to a 3 fold increase in the proliferative response against donor-specific stimulator cells was observed using post-NLT purified PBMC, indicating a systemic sensitisation to donor antigens in the NLT reaction.

4.4. Discussion

In this study ovine dendritic cells were obtained by the cannulation of the afferent pre-femoral lymphatics of sheep. In contrast to the human or murine situation the feasibility of generating ovine DC from peripheral blood monocyte precursors was restricted by the availability of ovine specific GMCSF and IL-4. The generation of ovine DC from monocytes has been reported however the efficiency of obtaining large numbers for an experimental therapeutic strategy is potentially limited by poor yields (410). Based on our experience with lymphatic cannulation, approximately 5 million DC/day was obtained routinely with a purity of 60-80% following metrizamide gradient enrichment with cannulas remaining patent for up to 5 months. The daily collection of DC and cryo-preservation of cells provides a means for building up a cache for subsequent cellular therapy in a transplant setting. In addition to the earlier studies on ovine DC phenotype (393) our study provides a more definitive characterisation of these cells by the cross-reactivity of mAb to the human DC markers, CMRF-56 (352) and CD83 (411). Indeed these isolated DC demonstrated other typical features, which included high MHC class II expression and the morphological presence of dendrites. Freshly isolated ovine DC also demonstrated a modest ability to take up antigens based on a FITC-Dextran assay. FITC-Dextran is endocytosed by DC mediated by the mannose receptor and is a feature lost upon full maturation (350, 412, 413). Taken with the fact that CD83 and CMRF56 are maturation markers of human DC, ovine DC represent either a population of partially matured DC or a heterologous population. Moreover the presence of DC in afferent lymph draining from the skin indicates a degree of maturation (383). Immature and mature DC respond to different chemokines, which direct their migration (351, 414) and while immature DC are recruited to sites of inflammation, mature DC respond to distinct

chemokines facilitating their migration to secondary lymphoid tissue (415, 416). Irrespective of the maturation status, the ovine DC isolated in this study were able to provoke a strong proliferative stimulus when challenged with allogeneic lymphocytes. DC invoked five-fold greater stimulation of allogeneic PBMC over autologous PBMC. This would be accounted for by the absence of antigenic stimuli in the autologous DC-MLR, while the high proportion of T cells reactive to allo-MHC peptides facilitates the stimulation in the allogeneic MLR (188). Accordingly pulsing the DC with antigens would potently stimulate the autologous DC-MLR (417). The titration of the allogeneic DC in the MLR has demonstrated the potency of DC as antigen-presenting cells. Consistent with previous observations (343), while maximal counts were observed using a S/R ratio of 1:1, a stimulatory effect was still observed at the lower ratio of 1:1000.

Intriguingly DC obtained from the sheep designated "N16-09", lacked expression of CD83 throughout the three-month patency of the cannula. Moreover CD83 could not be induced by the treatment with TNFα or LPS (data not shown). However despite this abnormality the cells maintained the morphological characteristics and functionality of DC. In particular these cells were still potent stimulators of the allogeneic mixed lymphocyte reaction and maintained a strong expression of the CMRF56 maturation marker (352).

For DC to stimulate T cells *in vivo* they must be capable of migration to secondary lymphoid tissues. Thus we utilised the pseudo-afferent cannulation model to study the migratory kinetics of DC intradermally injected into the draining region. DC stained with the highly efficient fluorescent PKH26 dye demonstrated rapid migratory properties after intradermal injection, with stained cells identified by flow cytometry within the draining lymphatics in a matter of hours. PKH26 was selected as it binds irreversibly to the cell membrane and has been well characterised as a non-radioactive agent to investigate cell

migration (418-420). The rapid migration into the draining lymphatics indicates that the DC will be appropriate for stimulating alloreactivity *in vivo* by allowing interactions with allogeneic T cells in secondary lymphoid tissues. Similar migratory kinetics have been shown after the intradermal injection of a plasmid encoding a fluorescent EGFP gene which permitted the detection of skin-derived DC in draining lymph within 4 hours (421).

As ovine DC obtained by pseudo-afferent cannulation were capable of migration to secondary lymphoid tissues, we next investigated the influence of DC in conjunction with PBMC in the context of autologous and allogeneic NLT reactions. The NLT reaction is essentially the *in vivo* equivalent of the two-way MLR with cellular populations from each cell donor able to interact with and against cells from the other donor. The importance of the donor cells is demonstrated by the failure of irradiated lymphocytes to induce an NLT response in the sheep model (422). In the NLT reaction, both host and recipient immune cells are likely to account for the resulting lesion with a role played by donor DC and host DC similar to that of allograft rejection models (423). Lymphocyte infiltrate may be a result of donor lymphocytes reacting against recipient antigens presented by DC via the direct or indirect pathways and also recipient inflammatory responses to clear the donor cells. Moreover the magnitude of the primary donor vs. host cell reaction will increase the response of the host vs donor cells due to an increase in the antigenic load. Clearance of donor cells by host immune responses in our study is supported by the cessation of the NLT reaction by day nine. Moreover re-injection of allogeneic lymphocytes 6 days later did not invoke an NLT response which may be due to the sensitisation of the host immune system clearing the cells before a graft vs. host reaction could be elicited (422).

In this present study PBMC were isolated and supplemented with 10% DC, thus providing a cellular population similar to that of afferent lymph. The alloreactivity between

sheep was confirmed in the MLR prior to the NLT reaction (data not shown). Intradermal injection of allogeneic lymphocytes and DC, elicited a strong NLT reaction characterised by a maintained indurated lesion and a mild erythemal development over the first 48 h. The autologous NLT reaction, aside from an initial non-specific response, did not elicit a skin response, which is consistent with previous reports (401). Furthermore biopsies taken at days two and seven revealed massive infiltration of $CD4^+$ and $CD8^+$ T cells in the allogeneic NLT reaction, characterised by increased IL-2 mRNA expression, indicating lymphocyte activation. Autologous NLT and control skin biopsies were almost devoid of lymphocyte infiltrate as evidenced by H&E staining. While the NLT reaction was evidenced by a localised inflammatory reaction, we were also able to demonstrate a systemic sensitisation to donor antigens by comparing the proliferative response of PBMC isolated and cryo-preserved before and after the NLT reaction upon challenge with donor PBMC. Two independent experiments from different allogeneic NLT reactions demonstrated more than a three-fold increase in proliferative response post NLT (**figure 4.8**). The systemic nature of the NLT reaction is supported by Su *et al.,* (404) who demonstrated the activation of lymphocytes in both the NLT-stimulated and the contralateral control efferent lymphatics.

In summary this chapter provides a definitive characterisation of ovine pseudo-afferent derived DC. Moreover, while the precise nature of the NLT reaction remains obscure, we demonstrate that PBMC reconstituted with DC are able to elicit both a localised and systemic allogeneic immune reaction *in vivo*. The ability of ovine DC to migrate from the skin to draining lymph nodes and interact with the host immune system supports the use of these cells as vehicles for the delivery of immunomodulatory proteins.

Chapter 5:

Generation of an Adenoviral Ovine CTLA4-EGFP Construct and the Immunomodulatory Effects of Transduced DC

Results from this chapter are also presented in the following publication

- Newland A.M., Kireta S., Russ G., Krishnan R. (2004). Ovine Dendritic Cells Transduced with an Adenoviral CTLA4$_e$EGFP Fusion Protein Construct Induce Hyporesponsiveness to Allostimulation. *Immunology*. **113:** 310-317.

5.1. Introduction

Data from **chapter 4** provides evidence for the suitability of ovine pseudo-afferent derived DC as vehicles for gene therapy to prolong allograft acceptance in that they express high levels of MHC Class II molecules, rapidly migrate to secondary lymphoid tissues and are able to interact with alloreactive lymphocytes. Attenuation of costimulation on these cells has the potential to induce donor-specific tolerance via the direct pathway of allorecognition (253).

As outlined in **chapter 1**, interruption of the CD28 costimulatory pathway has been shown to inhibit alloreactivity. While antibodies directed against CD80 and CD86 have been used to block CD28 costimulation, CTLA4-Ig is favored due to its duel-specificity to CD80 and CD86 ligands. Blockade of the CD28 costimulatory pathway with CTLA4-Ig is able to induce alloreactive T cell hyporesponsiveness *in vitro* (54) and abrogate acute rejection in vascularised transplant models, with a key role played by the addition of donor splenocytes at the time of transplantation (250, 255, 256, 424). Donor splenocytes increase the exposure of the host to donor antigens under the influence of immunomodulation by CTLA4-Ig thus it is likely that treatment with donor DC would facilitate a similar effect. While administration of CTLA4-Ig can block CD28 costimulation, thereby inhibiting alloreactive immune responses, the systemic nature of the treatment is also likely to inhibit immune responses against pathogens and tumor antigens. As an alternative, donor DC may be genetically modified *ex vivo* to express CTLA4-Ig, therein minimising systemic exposure to CTLA4-Ig and attributed non-specific immunosuppression while still permitting blockade of CD80/86 ligands on the DC.

Current literature on the effects of DC engineered to express CTLA4 fusion proteins is limited to murine models. Notably murine DC transfected with adenoviral CTLA4-Ig have produced alloreactive T cell hyporesponsiveness *in vitro* and maintain migratory properties to secondary lymphoid tissues *in vivo* (425). Moreover transfection of a murine DC cell-line demonstrated modestly prolonged islet allograft acceptance (253) while combined treatment of bone marrow derived DC with AdCTLA4-Ig in conjunction with NF-κβ oligodeoxyribonucleotide decoys permitted long-term allograft acceptance (329).

This chapter reports the generation of an adenoviral construct encoding the extracellular domain of the ovine CTLA4 sequence fused with an EGFP tag and the investigation of the immunomodulatory effects of transduced ovine and human DC *in vitro*. Fusion partners are used to generate constructs with the extracellular domain of CTLA4 in order to confer strong protein stability. The most commonly used fusion partner for CTLA4 consists of the hinge and CH2/CH3 domains of IgG1. However in this study Enhanced Green Fluorescent Protein (EGFP), a variant of GFP characterised by increased fluorescence (426, 427), was selected as it allows direct measurement of transfection efficiency by flow cytometry or fluorescent microscopy by virtue of its inherent fluorescence and may allow the enrichment of transfected cells by flow sorting (319). Moreover, the EGFP tag provides a surrogate antigenic target for the immunoprecipitation and ELISA quantification of the CTLA4-EGFP fusion protein. Furthermore, the selection of EGFP as a fusion partner has demonstrated increased protein stability and protection from intracellular degradation (428) while also allowing normal localisation of the target protein (429). Of important relevance to this study is that EGFP introduced into mammalian cells has minimal adverse effects (428-431).

While there are a number of protocols for the genetic modification of cells including various viral and non-viral techniques, as outlined in **section 1.13**, adenoviral vectors were selected for this study due to their high transfection efficiency and the relative ease by which high viral titers may be generated. Adenoviral vectors in this current study were generated with a pAdEasy1 adenoviral vector system kindly provided by Bert Volgelstein (The Howard Hughes Medical Institute). The pAdEasy1 system utilises an E1/E3 deleted replication deficient human serotype 5 adenovirus (432). Due to the large size of the viral vector, incorporation of the gene of interest requires cloning into a shuttle vector and subsequent homologous recombination with the pAdEasy1 vector, which contains the viral genome. Characteristics of the shuttle and pAdEasy1 vectors and homologous recombination are shown in **Appendix 2** and **figure 5.1**. The primary limitation of adenoviral vectors is host immune reactions against the viral particles and infected cells. This issue has been overcome in a number of models in which so called "stealth genes" have been used to prevent immune reactivity (433, 434). Interestingly these approaches often engineer CTLA4-Ig into the adenoviral construct, attenuating anti-viral immune reactivity and permitting re-administration (435-437). Thus in addition to inducing alloreactive T cell hyporesponsiveness, DC transfected with AdCTLA-EGFP are also likely limit anti-viral immunoreactivity, which could otherwise limit the life-span of the DC and the effectiveness of the treatment. The second limitation of adenoviral transfection of DC is the associated maturation of DC resulting in an upregulation of MHC Class I and II molecules and costimulatory molecules (302), although autocrine production of CTLA4-EGFP may sequester the upregulated CD80/86 ligands thereby limit the effect of DC maturation.

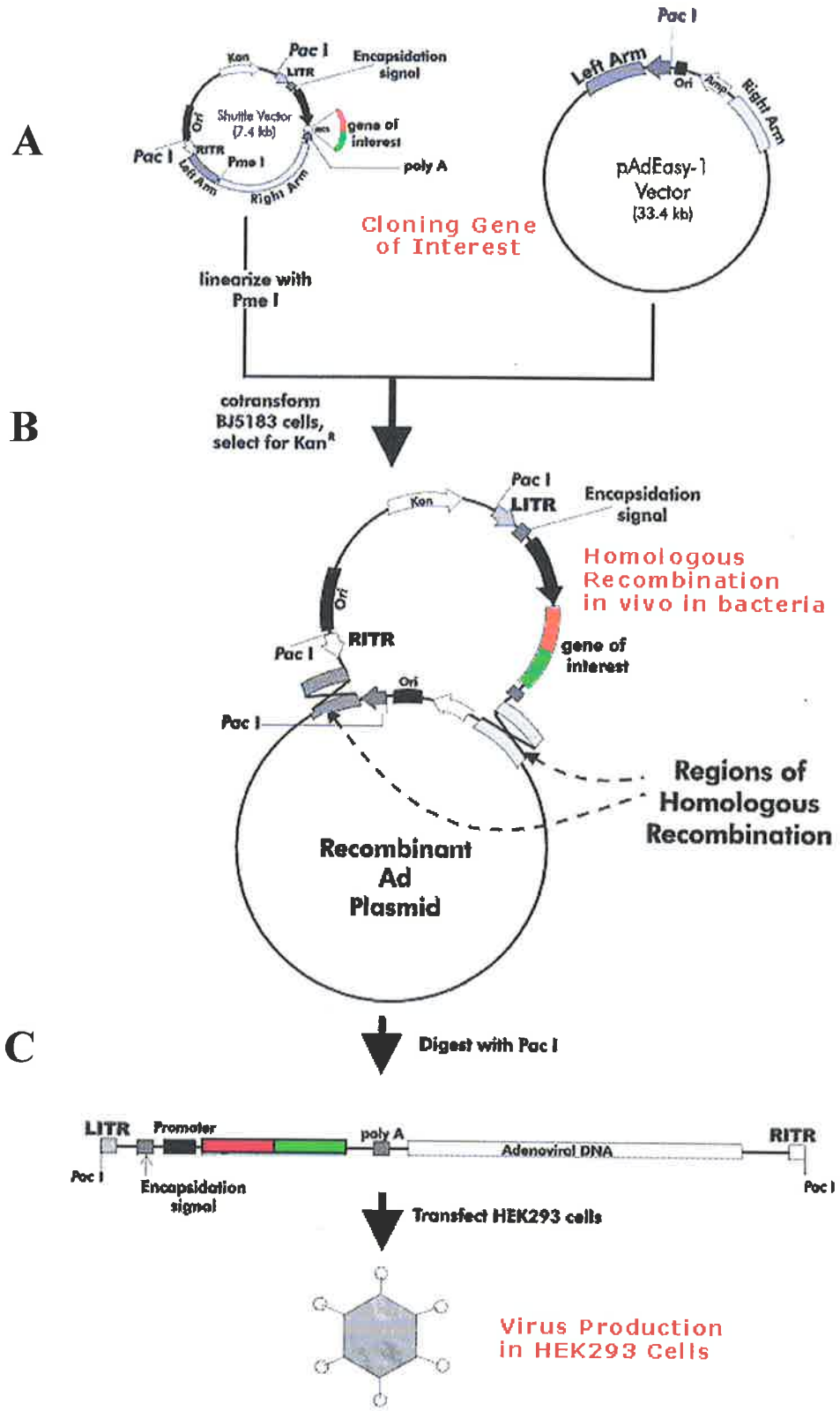

Figure 5.1. Schematic representation of adenoviral CTLA4-EGFP construction
A) Cloning of CTLA4-EGFP into pShuttleCMV
B) Co-transformation and homologous recombination of linear pShuttleCMV with pAdEasy1
C) Production of the adenovirus in HEK-293 cells
CTLA4-EGFP is represented by

Diagram modified from Stratagene website (www.stratagene.com/vectors)

This chapter focuses on the generation and characterisation of an adenoviral construct encoding a unique ovine CTLA4-EGFP fusion. Moreover this chapter expands on the characterisation of ovine DC reported in **chapter 4** by investigating the effect of genetic modification with AdCTLA4-EGFP constructs in order to induce alloreactive T cell hyporesponsiveness. Importantly the biological effects of AdCTLA4-EGFP transduced ovine DC are also compared with human monocyte-derived DC. It was hypothesised that adenoviral CTLA4-EGFP transduced DC would induce alloreactive T cell hyporesponsiveness *in vitro* by blockade of CD28 costimulation as a result of autocrine/paracrine binding of secreted CTLA4-EGFP to CD80/86 ligands on the DC. Moreover that the EGFP tag would provide the additional benefits of enabling direct assessment of AdCTLA4-EGFP transfection efficiency in addition to a surrogate antigenic target for immunological detection.

The specific aims of this chapter were to-

(i) Clone the extracellular domain of ovine CTLA4 and generate fusion constructs with EGFP and ovine IgG fusion partners.

(ii) Verify the immunomodulatory function of the CTLA4-EGFP and CTLA4-Ig fusion proteins in the DC-MLR.

(iii) Incorporate the CTLA4-EGFP and EGFP vector blank sequences into adenoviral vectors by homologous recombination

(iv) Investigate the immunomodulatory effects of DC transduced with the adenoviral vectors.

5.2. Materials and Methods

5.2.1. Cloning of the extracellular domain of ovine CTLA4

PBMC were isolated from ovine peripheral blood by density gradient separation using Lymphoprep™ (**2.3.1.1**) and resuspended in complete medium at $1x10^6$ cells/ml. Total RNA was extracted from PBMC stimulated with 1 μg/ml Con A for 48 h and reverse transcription performed on 1 μg of total RNA (**2.3.2.2**). PCR was performed to amplify CTLA4 and IgG (**2.3.2.3**) using primers detailed in **Appendix 1**. Primers designed to amplify the extracellular domain of ovine CTLA4 were based on published sequence (57) (Genbank Accession: AF092740) and incorporated respective *BglII* and *KpnI* restriction sites in the forward and reverse primers for cloning into pEGFP or *HindIII* and *EcoRI* for cloning into pSecTagB. Primers to amplify the hinge and CH2/CH3 domains of ovine IgG were designed based on the published sequence (438) (Genbank Accession: X70983) and incorporated *EcoRV* and *NotI* restriction sites into the forward and reverse primers, respectively. Primers were designed such that CTLA4 was cloned "in frame" with the EGFP and IgG sequences.

PCR products were digested with the appropriate restriction enzymes and cloned into pEGFP-N1 or pSecTagB expression vectors (**figure 5.2/5.3**). The CTLA4 and IgG inserts in the resulting plasmid vector constructs, namely CTLA4-EGFP and CTLA4-Ig, were confirmed to be authentic by sequencing and Genbank database analysis.

5.2.2. Generation of adenoviral constructs

Adenoviral constructs containing ovine CTLA4-EGFP and the EGFP-vector blank were generated using protocols established by He (432). Ovine CTLA4-EGFP was excised

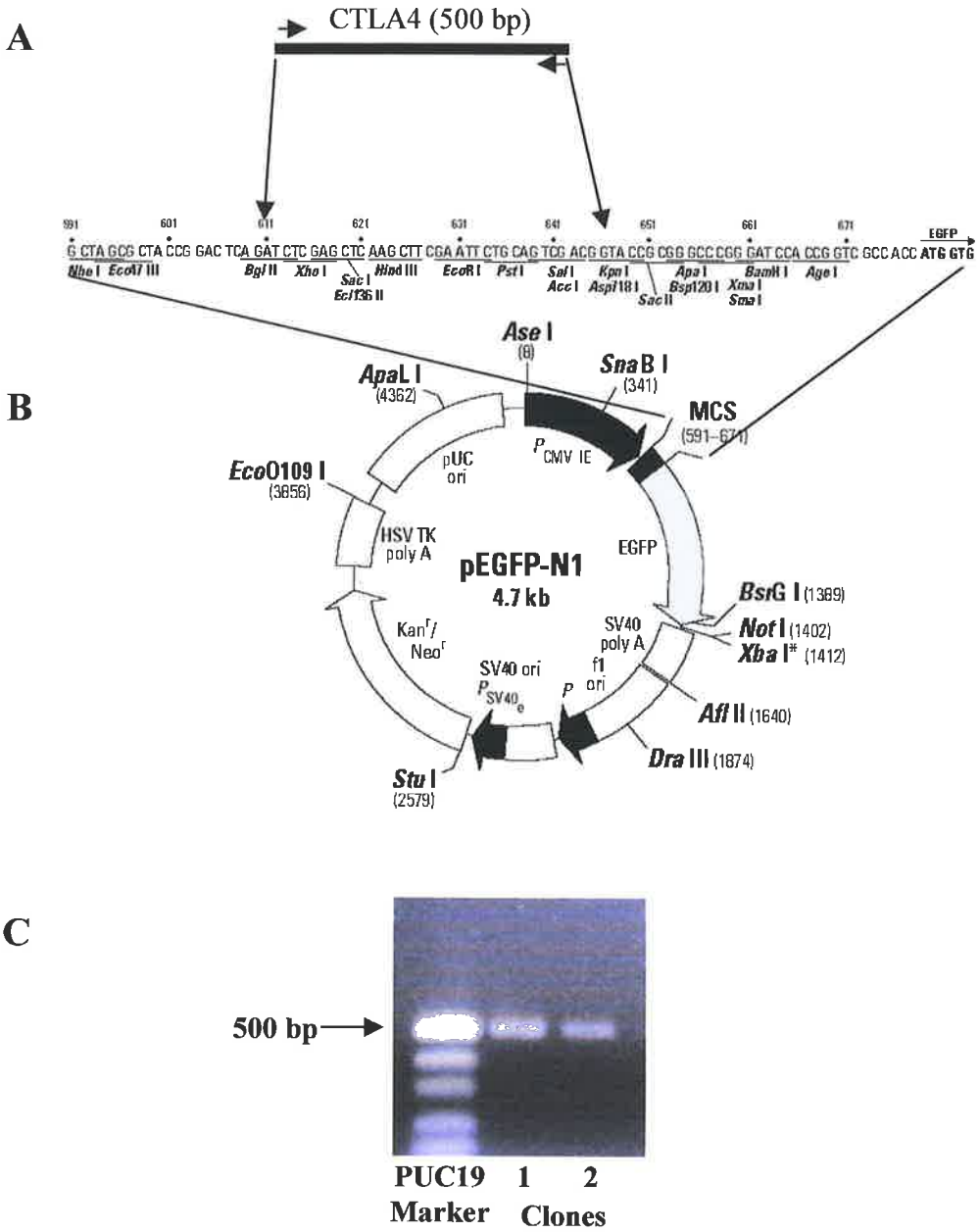

Figure 5.2. Cloning of ovine CTLA4-EGFP

A) The extracellular domain of ovine CTLA4 was amplified from cDNA of ConA stimulated PBMC using forward and reverse primers incorporating restriction enzyme sites for *BglII* and *Kpn1* respectively.

B) PCR products and the pEGFP-N1 vector were digested with *BglII* and *Kpn1*, ligated and used to transform TG1α *E.coli*.

C) Recombinant plasmids were purified and insertion of CTLA4-EGFP confirmed by restriction digest analysis (data not shown) and PCR with the presence of the predicted 500bp product demonstrated. Cloned CTLA4 was also sequenced and the identity confirmed by sequence analysis performed against published data.

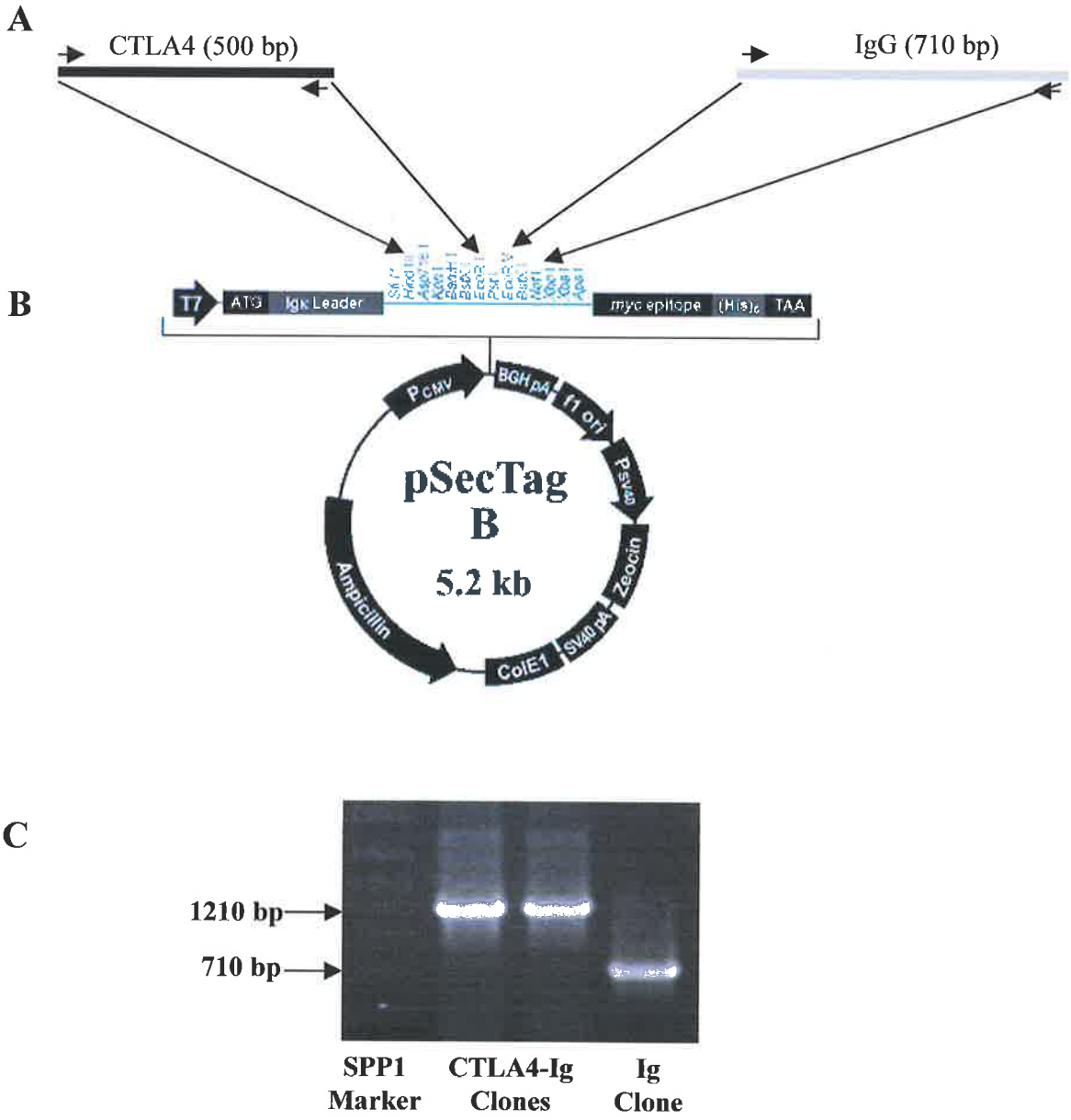

Figure 5.3. Cloning of ovine CTLA4-Ig

A) The extracellular domain of ovine CTLA4 was amplified from cDNA of ConA stimulated PBMC using forward and reverse primers incorporating restriction enzyme sites for *HindIII* and *EcoR1* respectively. Ovine IgG was amplified using primers incorporating *EcoRV* and *Not1* sites. **B)** IgG PCR products and the pSecTagB plasmid were initially digested with *EcoRV* and *Not1* and ligation performed. Plasmids were propogated, screened for insertion and purified. IgGpSecTagB plasmids were then digested with *HindIII* and *EcoR1* and ligation performed with digested CTLA4 PCR products.

C) Recombinant plasmids were purified and insertion of CTLA4-Ig and Ig confirmed by restriction digest analysis (data not shown) and PCR using a forward CTLA4 primer and reverse Ig primer. Both CTLA4-Ig clones demonstrated the predicted 1210 bp product size and the Ig clone 710 bp (using a forward Ig primer). Cloned CTLA4-Ig was also sequenced and the identity confirmed by sequence analysis performed against published data.

from pCTLA4-EGFP by *BglII/NotI* digestion and ligated into the pShuttleCMV vector. Homologous recombination was facilitated by co-electroporation of *PmeI* linearised recombinant pShuttleCMV vector with the pAdEasy1 vector into electrocompetent BJ5183 cells (**2.3.3.2**). In order to generate recombinant adenoviral particles, the adenoviral constructs, AdCTLA4-EGFP, AdEGFP were linearised with *PacI* and used to transfect the HEK-293 packaging cell line with LipofectAMINE^{TM} (**2.3.3.5**). Infectious adenoviral particles were obtained by freeze-thaw-lysis (**2.3.3.6**) of the transfected HEK-293 cells and purified by CsCl density gradient ultra-centrifugation (**2.3.3.8**) as previously described (439) and dialysed (**2.3.3.9**). Quantification of adenoviral titres was performed by the cytopathic effect assay (440) and values expressed as plaque forming units (pfu) (**2.3.3.10**).

5.2.3 Preparation of CTLA4-EGFP fusion proteins

Ovine adult skin fibroblasts were infected with adenoviral particles at a multiplicity of infection (MOI) of 50. Adenoviral constructs consisted of AdCTLA4-EGFP or the AdEGFP vector blank control. Cells were incubated with the appropriate recombinant adenoviral vector for 1 h to permit viral adsorption followed by the addition of fresh medium and incubation for a further 48 h to allow for gene transduction. Conditioned medium was obtained by centrifugation of the cultures.

5.2.4. Immunoprecipitation from infected fibroblasts

Gene transfer was conducted by infection of fibroblasts with recombinant adenovirus. After overnight incubation, cells were cultured in methionine/cysteine free RPMI supplemented with glutamine and 1% FCS and incubated at 37°C for 1 h. Media

were replaced with 1.5ml methionine/cysteine free media containing 100 μCi/ml Tran^{35}S-Label™ (ICN Biomedicals, California) and incubated overnight. Conditioned media were treated with 10% (v/v) protease inhibitor and blocked with 5% (v/v) normal rabbit serum. Media were pre-cleared with *Staphylococcus aureus* in RIPA buffer (1 M NaCl, 10% sodium deoxycholate, 10% SDS, 1%NP40, 1 M Tris-HCl) at 11, 600 g for 5 min at 4°C. Supernatants were treated with 5 μg mouse anti-GFP mAb (Roche, USA) and incubated at 4°C rotating overnight. S.*aureus* supplemented with 1 mg/ml ovalbumin (100μl) was added for 1 h, and washed twice with RIPA buffer at 3870 g. Pellets were resuspended in Laemmli's buffer with an aliquot reduced with β-mercaptoethanol and after incubation at 100°C for 15 min samples were run on 12.5% SDS-PAGE gels. Gels were stained with commassie blue and impregnated with Amplify™ for 30 min prior to autoradiography on Kodak XAR5 film.

5.2.5. Quantification of EGFP and CTLA4-EGFP fusion protein by ELISA

An ELISA was established to quantify CTLA4-EGFP secreted from adenoviral infected ovine fibroblasts. Due to the unavailability of ovine CTLA4 specific antibodies, capture and detection antibodies were directed against the EGFP fusion protein. Titertek Immuno Assay Plates were coated with polyclonal goat anti-GFP antibody at 2 μg/ml in bicarbonate buffer (pH 9.6) for 2 h at room temperature and then incubated overnight at 4°C. Standard curves were generated by titrating recombinant EGFP (Clontech, USA) in the antibody-coated plates at a concentration range of 0.001 to 10 ng/ml. Serial dilutions of the unknown concentrations of EGFP and CTLA4-EGFP in conditioned medium were also added to the antibody-coated plates. After overnight incubations, and following washes

with PBS Tween-20, 1 μg/ml of mouse anti-green fluorescent protein (GFP) mAb was used to detect the captured fusion protein and native EGFP for 2 h at room temperature. A 1/1000 dilution of the secondary biotinylated horse anti-mouse IgG conjugate in 10% FCS was then added to the plates and was detected with a 1/1000 dilution of Streptavidin-Alkaline-Phosphatase in PBS/Tween-20. The colorimetric reaction was produced by the addition of Sigma 104 Phosphatase Substrate in diethanolamine buffer and absorbance at A_{405} was determined after terminating the reaction with 0.5 M EDTA. Since the standard curve was derived with native EGFP the values obtained for CTLA4-EGFP depict equivalent molar concentrations.

5.2.6. CTLA4-EGFP Binding Assay

Ovine and human DC were used as target cells to establish the binding activity of CTLA4-EGFP. Primary mAb directed against the CD80 (Immunotech, France) and CD86 (Serotech, UK) ligands were used to confirm the expression of these molecules on the human DC. The CTLA4-EGFP binding assay involved three steps. DC were firstly incubated with 200 μl of CTLA4-EGFP at a concentration of 20 μg/ml. Secondly, cells were washed and incubated with a primary anti-GFP mAb. X63 was used as an isotype-matched negative control mAb. Finally, a polyclonal anti-mouse Ig Fab2 FITC-conjugated antibody (Silenus, Australia) was added to the cells to detect the primary antibody. Human CTLA4Ig (4 μg, R&D Systems, USA) was added as a competitor in the binding assay to establish the specificity of binding of CTLA4-EGFP to CD80/86 expressed on both human and ovine DC. Flow cytometric analysis was performed as described in section **2.3.4.1**.

5.2.7. Two-way Mixed Lymphocyte Reaction

Conditioned media from recombinant adenoviral infected fibroblasts were quantified by ELISA and tested for inhibitory activity in a two-way MLR as described below. Either sheep or human PBMC from two unrelated donors were co-cultured in 96-well round-bottom plates to a final cell concentration of $2x10^5$ cells per well. The MLR was performed in complete medium in a volume of 200 µl. The mixed cultures were incubated at 37°C for 4 days and then pulsed for 20 h with 1 µCi of [^{3}H] thymidine. The cells were harvested onto filters and the incorporated radioactivity was determined by liquid scintillation counting in a Wallac Microbeta Counter. All determinations were expressed as counts per minute (cpm) and performed in triplicate.

5.2.8. Genetically modified DC as stimulators in the MLR

Unlike gene transfer by infection of fibroblasts, ovine and human DC were genetically modified by combining the cells with the specific recombinant adenovirus (1 x 10^9 pfu) and 2 µg of LipofectAMINE™ in 100 µl RPMI. Briefly, after 15 min of incubation at room temperature, DC (1 x 10^6 cells) were mixed with the adenoviral-LipofectAMINE™ complex to a final MOI of 1000 and incubated for a further 2 h to allow viral adsorption. The transfected DC were incubated for a further 48 h to establish gene transduction prior to use in the MLR as stimulators at 1:10 and 1:100 S/R ratios against responder T cells.

5.3. Results

5.3.1 Generation and Characterisation of fusion protein constructs

Plasmids encoding CTLA4-EGFP and CTLA4-Ig fusion constructs (pCTLA4-EGFP and pCTLA4-Ig) were generated by cloning the extracellular domain of ovine CTLA4 in frame with the EGFP gene in the pEGFP-N1 expression vector or an ovine IgG gene which had been cloned into the expression vector pSecTagB. Unmodified pEGFP-N1 was used as the vector blank control for pCTLA4-EGFP while pSecTagB with only an Ig insert was used as the control for pCTLA4-Ig. Correct insertion of the genes was confirmed by PCR analysis using gene specific primers (**figures 5.2 and 5.3**). This was further confirmed by restriction digest analysis (data not shown) and by sequence analysis (**appendices 3 and 4**). CHO cells were electroporated with pCTLA4-EGFP, pCTLA4-Ig or the appropriate vector blank control and conditioned media (CM) used in the two-way ovine MLR. As demonstrated in **figure 5.4**, both CTLA4-EGFP (15167 +/- 1270 cpm) and CTLA4-Ig (23182 +/- 3310 cpm) were able to significantly ($p < 0.005$) inhibit the MLR compared to their respective controls, EGFP (55504 +/- 1270 cpm) or Ig (40148 +/- 1700 cpm) or sham transfected cell CM (35572 +/- 1851 cpm). Notably both vector blank control CM and CM from sham transfectants also inhibited the MLR with counts significantly ($p < 0.0011$) lower than the untreated control (83143 +/- 1734 cpm).

5.3.2. Generation and characterisation of adenoviral constructs

CTLA4-EGFP and CTLA4-Ig were able to inhibit the MLR and hence were both candidates for incorporation into adenoviral constructs. CTLA4-EGFP was selected as the EGFP fusion tag offers the additional benefits of direct monitoring of cell transfection.

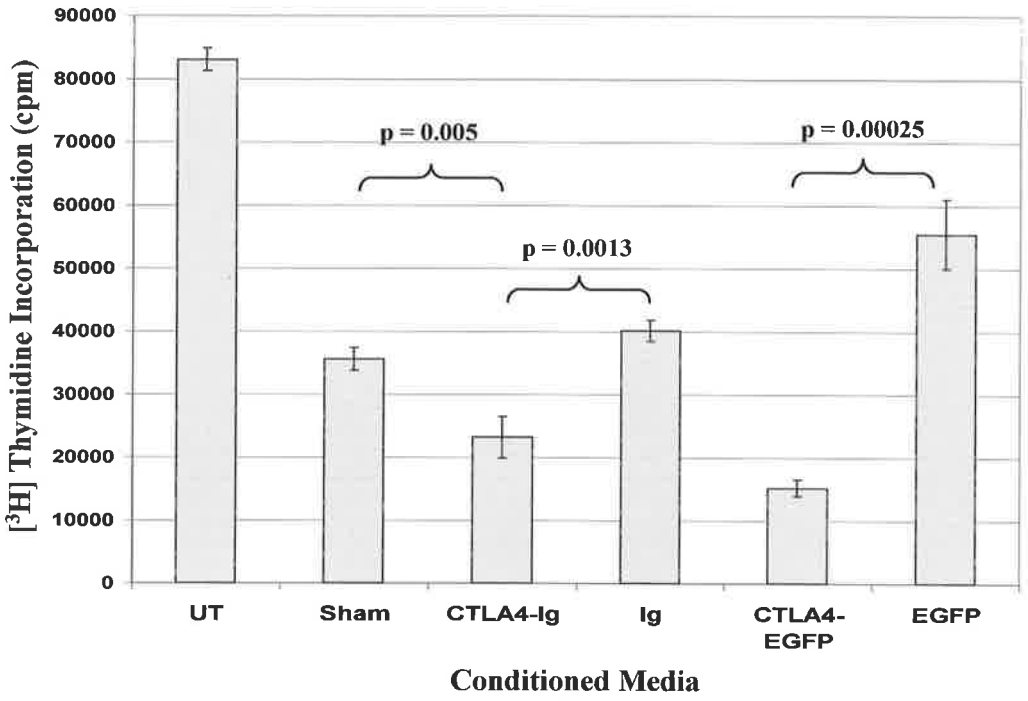

Figure 5.4. Conditioned media from CTLA4-EGFP and CTLA4-Ig electroporated cells inhibit the ovine two-way MLR

CHO cells were electroporated with 10 μg of CTLA4-EGFP, CTLA4-Ig or the appropriated vector blank control plasmid. Conditioned media was collected after 48 h of culture and 100 μl (50% of the well volume) added to the ovine two-way MLR. Graph represents [^{3}H] incorporation +/- SD. Sham transfectant CM was derived by electroporation of CHO cells in the absence of plasmid DNA.

CTLA4-EGFP and EGFP were excised from their respective plasmids and cloned into the multiple cloning site (MCS) of the pShuttleCMV vector. The genes were subsequently incorporated into the adenoviral genome by homologous recombination with the pAdEasy1 vector as outline in **figure 5.1**. **Figure 5.5** represents the screening of CTLA4-EGFP clones, with 50% positive for homologous recombination. Similar screening was performed for clones incorporating the other genes. Positive clones were then used to generate infectious adenoviral particles with adenoviral titers up to 5 x 10^{11} PFU/ml achieved after CsCl purification as assessed by CPE assay.

5.3.3. Adenoviral transfection of ovine fibroblasts

Figure 5.6 shows the fluorescence of fibroblasts under the UV microscope infected with AdCTLA4-EGFP or AdEGFP. Of particular note was that AdEGFP transduced fibroblasts demonstrated stronger nuclear and cytoplasmic localisation of the EGFP in contrast to the diffuse cytoplasmic staining observed with those cells genetically modified with AdCTLA4-EGFP. The high levels of cell transfection evident by the fluorescent microscopy pictures were confirmed by flow cytometric analysis of AdCTLA4-EGFP and AdEGFP infected fibroblasts with respective transfection efficiency of 97% and 99%. AdEGFP infected fibroblasts (MFI = 144) demonstrated a higher mean fluorescence intensity (MFI) than AdCTLA4-EGFP infected fibroblasts (MFI = 88). Negligible autofluorescence was observed in transfected fibroblasts (MFI = 3.4).

A

Figure 5.5. *PacI* restriction digest screening of clones for homologous recombination between CTLA4-EGFPpShuttleCMV and pAdEasy1 vectors.
Mini-prep vectors from transfected BJ5183 clones were screened for homologous recombination between CTLA4-EGFPpShuttleCMV and pAdEasy1 vectors by digestion with *Pac*I. Clones are labeled 1 to 8. Clones positive for homologous recombination demonstrate a digest profile characterised by a high molecular weight band (~33 kb) and either a 3 kb or 4.5 kb band depending on the site of homologous recombination.

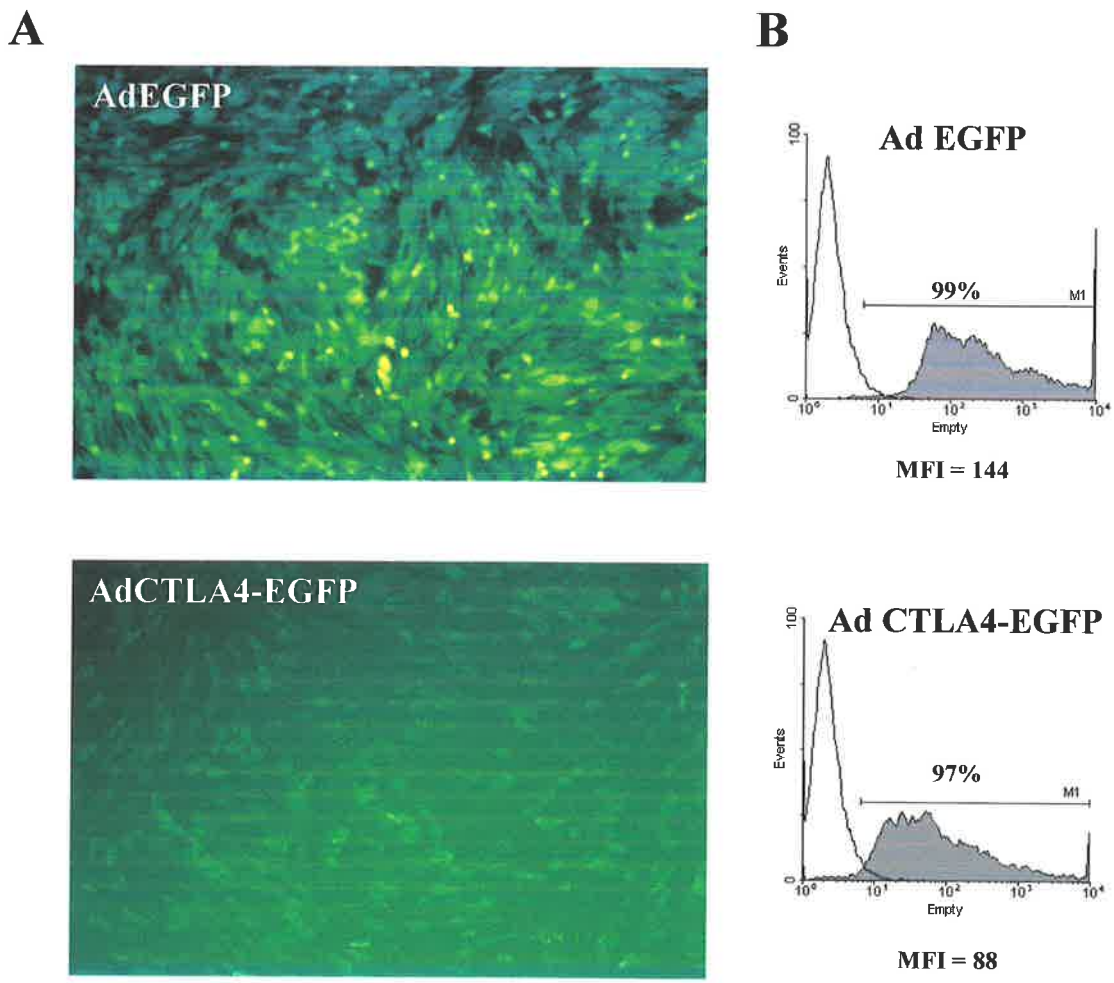

Figure 5.6. Assessment of the fluorescence of AdCTLA4-EGFP and AdEGFP transduced ovine fibroblasts.

Ovine dermal fibroblasts were infected with adenoviral constructs at a MOI of 50. **Panel A** represents transfected fibroblasts viewed using UV-microscopy (200X magnification) after 48 h in culture. **Panel B** demonstrates the percentage of fluorescent cells after adenoviral transduction of fibroblasts with AdCTLA4-EGFP or AdEGFP as determined by flow cytometric analysis. Autofluorescence of untransfected cells was negligible (data not shown).

5.3.4. Secretion and function of ovine CTLA4-EGFP from adenoviral infected fibroblasts.

Fibroblasts infected with AdCTLA4-EGFP were shown to secrete CTLA4-EGFP proteins by immunoprecipitation of the CM with anti-GFP mAb. CM from AdEGFP infected fibroblasts was used as controls for EGFP synthesis. As shown in **figure 5.7** autoradiographs of immunoprecipitates demonstrated a distinct 30 kDa band corresponding to EGFP, while immunoprecipitates of AdCTLA4-EGFP CM revealed an intense 62 kDa band, confirming secretion of the proteins. A less intense band of 120 kDa was also observed in the CTLA4-EGFP immunoprecipitate indicating that some dimerisation does occur, although the monomeric form of the protein is most prominent. The 120 kDa band was not observed when the immunoprecipitates were run under reducing conditions.

ELISA, using anti-GFP antibodies, was used to quantify the secretion of CTLA4-EGFP and EGFP from infected fibroblasts with up to 20 μg/ml CTLA4-EGFP and 10 μg/ml EGFP obtained over 48 h. CTLA4-EGFP was titrated for immunomodulatory function in the two-way MLR in a concentration range of 0.625-10 μg/ml. Optimal inhibition (80-90%) compared to the untreated MLR was demonstrated in the concentration range of 5-10 μg/ml (**figure 5.8**).

5.3.5. Binding of CTLA4-EGFP to ovine and human DC

The CTLA4-EGFP fusion protein obtained from fibroblast infected with AdCTLA4-EGFP was quantified by ELISA and used at a concentration equivalent to 20 μg/ml of EGFP to assess the binding activity to both human and ovine DC. While human monocyte-derived DC were confirmed by flow cytometry to express the CTLA4 receptors

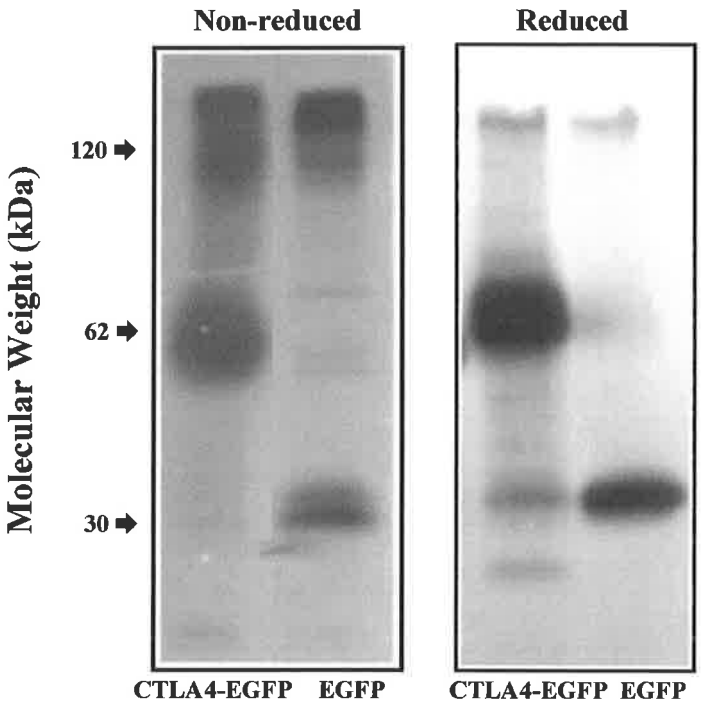

Figure 5.7. Immunoprecipitation of CTLA4-EGFP from infected fibroblasts
The autoradiographs show the immunoprecipitation of ^{35}S methionine/cysteine-labeled proteins from fibroblasts transfected with AdCTLA4-EGFP or AdEGFP using anti-EGFP mAb. Immunoprecipitates were subject to electrophoresis in 12.5% SDS-PAGE gels under reducing or non-reducing conditions.

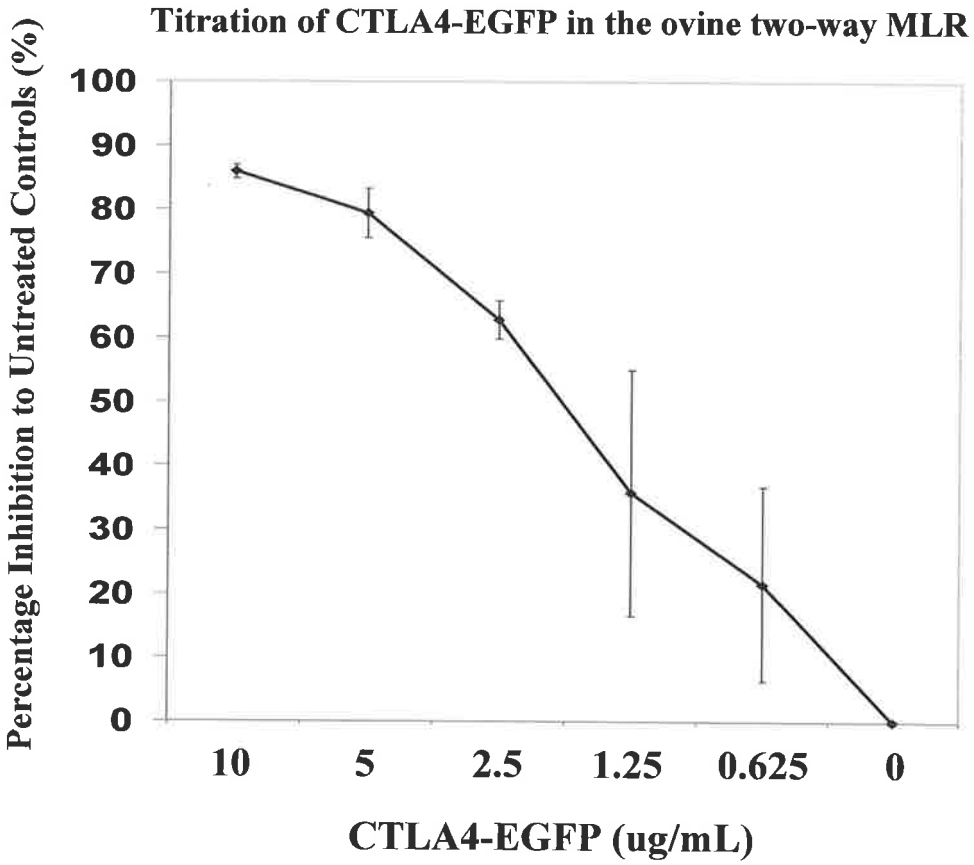

Figure 5.8. Dose-response inhibition of an ovine two-way MLR by CTLA4-EGFP
Conditioned media was obtained from fibroblasts transduced with AdCTLA4-EGFP and the concentration of CTLA4-EGFP determined by ELISA. CTLA4-EGFP was added to the MLR at two-fold dilutions ranging from 10 μg/ml to 625 ng/ml. MLR responses are expressed as the percentage of inhibition relative to the untreated MLR +/- SD.

CD80/86 (**figure 5.9**) this was not established for the ovine cells due to the unavailability of ovine specific mAb. Anti-GFP mAb staining demonstrated binding of CTLA4-EGFP to both ovine and human DC as shown by increased shifts in fluorescence compared to the isotype-matched X63 control (**figure 5.9**). In contrast the EGFP native protein, as a negative control, showed no reactivity (data not shown). Furthermore, the specificity of CTLA4-EGFP binding to CD80/86 on both human and ovine DC was confirmed by blockade with recombinant human CTLA4-Ig.

5.3.6. Adenoviral CTLA4-EGFP transfected DC have reduced allostimulatory capacity.

Given the ability of CTLA4-EGFP to bind to CD80/86 ligands on ovine and human DC and inhibit the MLR, ovine and human DC were transfected with AdCTLA4-EGFP or AdEGFP in association with LipofectAMINE^{TM} and assessed for their ability to inhibit the alloreactive T cell proliferation. Fluorescence resulting from the EGFP tag in transfected DC was evaluated for both the native and fusion protein by flow cytometry to determine transfection efficiency. Transfection efficiency for both adenoviral constructs was between 73-75% for ovine DC and 91-95% for immature human monocyte-derived DC (**figure 5.10**). Notably AdEGFP transfected DC demonstrated significantly higher MFI than AdCTLA4-EGFP transfected DC (105 vs. 48 for ovine DC and 331 vs. 124 for human DC).

In the ovine DC-MLR at respective stimulator:responder ratios of 1:10 and 1:100, AdCTLA4-EGFP transfected DC demonstrated an inhibition of 41% ($p=0.003$) and 64% ($p=0.003$) compared to unmodified DC (**figure 5.10**). Surprisingly, in contrast to the two-way MLR, AdEGFP transfected DC also inhibited the MLR but to a lesser extent than AdCTLA4-EGFP transfected DC. Similar results were obtained with human DC with

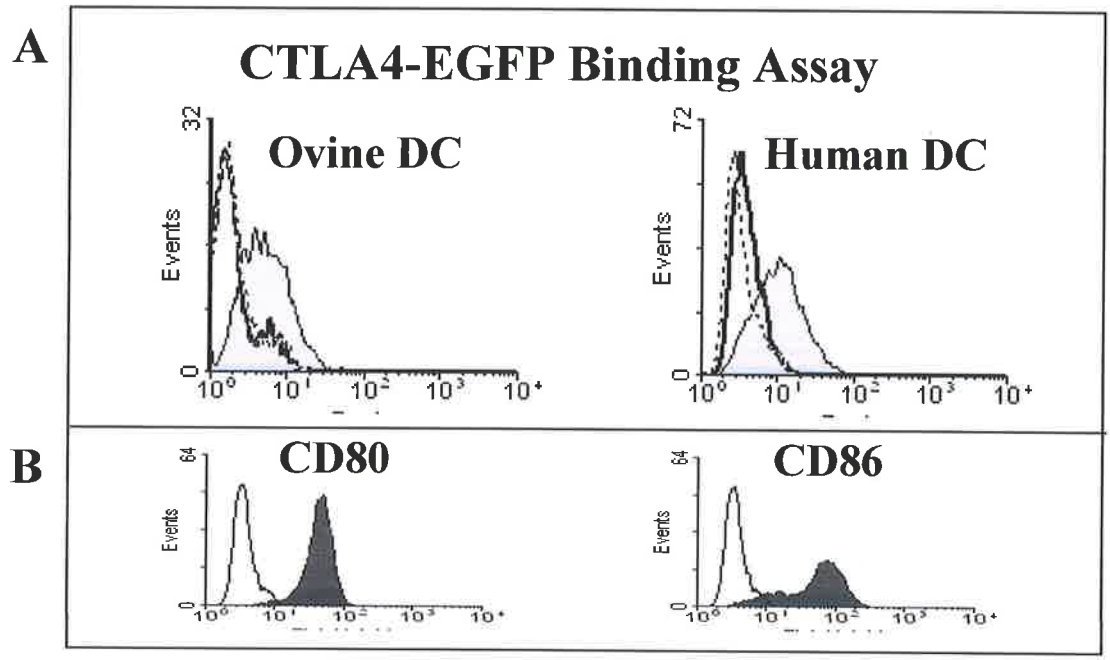

Figure 5.9. Binding of ovine CTLA4-EGFP to ovine and human DC
A) Human or ovine DC were incubated with CTLA4-EGFP derived from recombinant adenovirus modified fibroblasts. Bound CTLA4-EGFP was detected with an anti-GFP mAb as shown by the shaded histogram. The negative-isotype matched mAb (X63) is represented by the solid line. The dotted line represents blockade of CTLA4-EGFP binding by pre-incubation with commercial human recombinant CTLA4-Ig.
B) Expression of CD80 and CD86 ligands on human monocyte-derived DC was confirmed by flow cytometry.

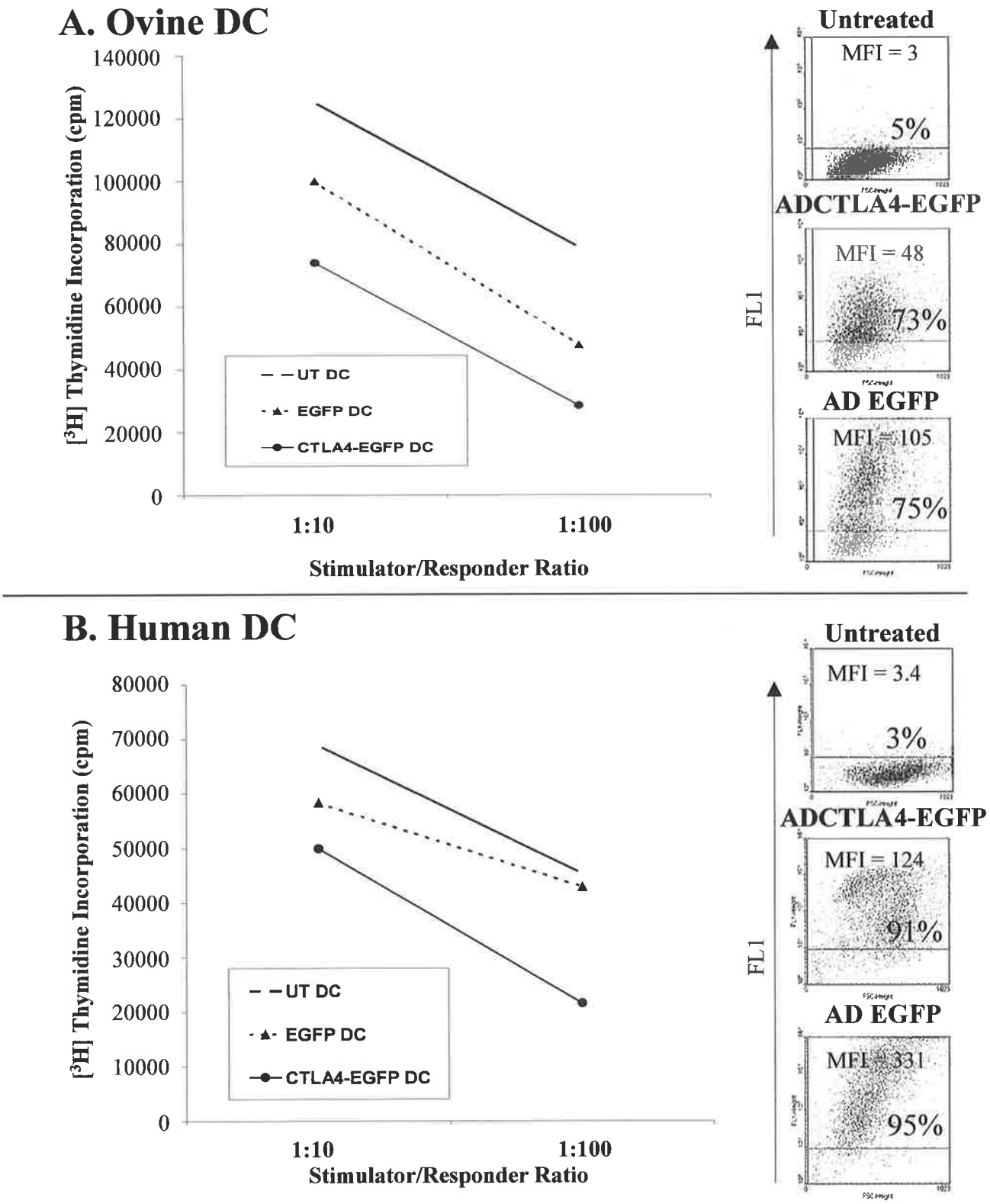

Figure 5.10. AdCTLA4-EGFP Transduced ovine and human DC inhibit the MLR
Ovine (graph A) and human (graph B) DC were transfected with either AdCTLA4-EGFP or AdEGFP and used as stimulators in the allogeneic DC-MLR at stimulator/responder ratios of 1:10 and 1:100. Unmodified DC were used as controls. Each graph is representative of three independent experiments. Transfection efficiency was determined by flow cytometric analysis prior to use in the MLR and data is represented as a dot-plot (FL-1 vs forward scatter).

AdCTLA4-EGFP transfected DC inhibiting the MLR by 28% ($p = 0.016$) and 52% ($p = 0.00003$) compared to untreated DC at 1:10 and 1:100 S/R ratios respectively (**figure 5.10**). Also consistent with ovine DC, AdEGFP transfected human DC demonstrated 15% inhibition of the MLR at the 1:10 ratio ($p = 0.013$). To clarify the observed immunomodulation by AdCTLA4-EGFP and AdEGFP, phenotypic analysis was performed on transfected human DC. The phenotypic investigation was confined to human DC due to the lack of availability of ovine reactive mAb. These analyses revealed that AdCTLA4-EGFP transfection showed a modest upregulation of CD40 expression on DC whereas AdEGFP transfection resulted in a 15-20% downregulation (**figure 5.11**). However, both constructs produced only modest increases in the expression of MHC class II, CD86 and CD83 which is consistent with previously reported effects mediated by adenoviral transfection (441).

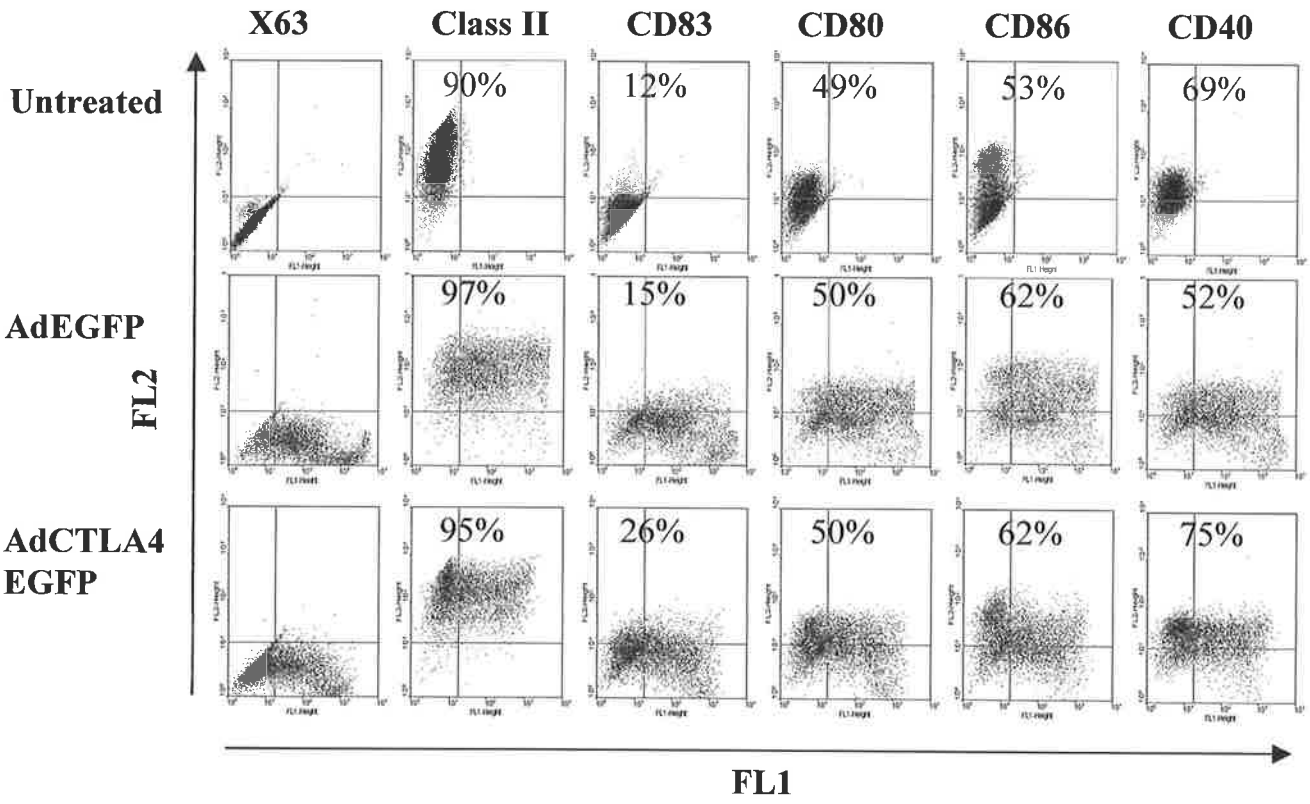

Figure 5.11. Effect of adenoviral transfection on human DC cell-surface marker expression
To assess the influence of AdCTLA4-EGFP and AdEGFP on costimulatory molecule and maturation marker expression, human monocyte-derived DC were transfected with the adenoviral constructs and stained with marker-specific primary antibodies. Binding was detected by secondary labeling with PE-conjugated anti-mouse antibodies and cells analysed by dual-colour flow cytometric analysis. Histograms represent FL1 staining (transfection efficiency) vs FL2 staining (antibody staining). Percentages represent the proportion of cells expressing the particular cell-surface markers. Histograms are representative of two independent experiments.

5.4. Discussion

This chapter reports the cloning of the extracellular domain of ovine CTLA4 fused to EGFP, and subsequent incorporation into an adenoviral vector to generate potentially tolerogenic DC.

The extracellular domain of CTLA4 was cloned "in frame" with the EGFP gene, originally cloned from the jellyfish *Aequorea victoria*, and an ovine IgG gene. Cytoplasmic and trans-membrane domains of CTLA4 were omitted to prevent binding to the cell surface, as is the case for native CTLA4. Moreover the omission of the cytoplasmic region removes the stop codon permitting read-though to the fusion partner. The EGFP-N1 plasmid was selected as it permits insertion of CTLA4 into the vector such that the carboxy terminal end of the gene is fused to the N-terminal end of EGFP. Primers to ovine IgG were designed so as to amplify the hinge region of IgG in association with the CH2 and CH3 domains, consistent with the generation of human and murine homologues (54). Sequencing was performed on the CTLA4-EGFP and CTLA4-Ig plasmids to confirm the authenticity of the gene fusions (**appendices 3 and 4**). Conditioned media was generated for preliminary investigations into the functions of the proteins by electroporation of CHO cells. Despite only 20-40% transfection efficiency achieved, as determined by EGFP fluorescence, CTLA4-EGFP and CTLA4-Ig CM demonstrated 82% and 72% inhibition of the MLR compared to untreated controls and 38% and 58% compared to sham transfected cells (**figure 5.4**). The inhibition evident in the sham transfected CM indicates the presence of inhibitory factors as a result of electroporation procedure. Conditioned media from EGFP transfected cells were stimulatory compared to sham transfectant CM which may be due to reactivity against the native EGFP proteins.

Cloning of CTLA4-Ig into the pSecTagB vector inadvertently led to the incorporation of two signal peptides. However, based on the ability of CTLA4-Ig in the CM to inhibit the MLR (**figure 5.4**), it is suggested that the second signal peptide has not affected the secretion of the protein. Subsequent cloning of CTLA4-Ig from pSecTagB into an adenoviral construct will exclude the Igκ leader sequence. The concentrations of CTLA4-EGFP and CTLA4-Ig in the conditioned media were not quantified in this set of experiments; thus we were unable to conclude whether either fusion partner offered better assistance to the function of CTLA4. In a clinical setting a species specific Ig partner would be more beneficial as it would reduce the neutralisation of the fusion protein. However for the purpose of these current studies, the EGFP partner offers the distinct advantage of permitting direct analysis of transfection efficiency and antibodies directed against EGFP are commercially available permitting characterisation of the protein. For these reasons the CTLA4-EGFP gene fusion was further cloned into an adenoviral construct.

The incorporation of CTLA4-EGFP into an adenoviral construct permitted high levels of gene transfection into fibroblasts with almost 100% transfection efficiency (**figure 5.6**). Interestingly AdCTLA4-EGFP and AdEGFP transfected fibroblasts revealed significantly different fluorescent staining patterns. The intense and uniform fluorescent staining of AdEGFP transfected fibroblasts indicates a high level of protein expression and/or the lack of signals directing the secretion of EGFP, leading to an accumulation of intracellular protein. In contrast AdCTLA4-EGFP transfectants demonstrated more diffuse peri-nuclear staining with focal punctate staining, likely to be the packaging of proteins within the cellular machinery in preparation for secretion. Indeed quantification of the recombinant proteins in the conditioned media of adenoviral infected fibroblasts revealed

significantly higher secretion of CTLA4-EGFP (up to 20 μg/ml) compared to EGFP (up to 10 μg/ml) within 48 h.

Secretion of CTLA4-EGFP was also confirmed by immunoprecipitation of conditioned media from transfected cells (**figure 5.7**). Immunoprecipitates indicated that CTLA4-EGFP is secreted primarily in monomeric form, although there was a minor proportion of a high molecular species only identified in non-reducing SDS-PAGE, which is indicative of sulphydryl protein interaction and dimer formation. The importance of CTLA4-Ig dimer formation remains unresolved. While the native membrane-bound CTLA4 exists predominantly in dimeric form, potentially facilitating intracellular signaling and disruption of the immunological synapse (60, 61), binding to CD80/86 is not dependent on dimerisation as the binding interface is identical in monomeric and dimeric forms (58). Recent data using a mutant form of CTLA4 demonstrated that the monomeric form is capable of localisation to the immunological synapse and inhibition of T cell proliferation (442). However as dimerisation of CTLA4 places the binding domains distal to the dimer interface, dimeric forms of CTLA4 may permit stronger association with target cells as each dimer is able to bind to two distinct CD80/86 ligands (58). In accordance with these observations we demonstrated the ability of ovine CTLA4-EGFP to bind to both ovine and human DC (**figure 5.9**). The specificity of binding was illustrated by the pre-incubation of DC with recombinant human CTLA4-Ig, which effectively blocked the binding of CTLA4-EGFP. The ability of both ovine CTLA4-EGFP and the commercial human CTLA4-Ig proteins to bind to ovine and human DC indicates cross-species reactivity. This observation is not surprising giving the conservation of the MYPPPY motif between the species which facilitates the strong binding capacity to CD80/86 (59). Binding of CTLA4-

EGFP was also shown to mediate strong alloreactive T cell hyporesponsiveness at concentrations between 1-10 μg/ml, comparable with previous reports characterising the inhibitory function of CTLA4-Ig (328).

While adenoviral vectors are able to infect fibroblast with high efficiency using a low multiplicity of infection, DC are typically more difficult to transfect. Adenoviral entry into cells is facilitated by the binding of the viral particles to the coxsackievirus and adenovirus receptors (CAR) on the cell surface which facilitates interactions with αvβ3 and αvβ5 integrins and subsequent internalisation (443). Combining adenoviral transfection with cationic liposomes can increase the transfection efficiency of difficult to transfect cells. Consistent with previous reports using combined adenoviral/LipofectAMINE^{TM} transfection (309) we were able to transfect human DC with greater than 90% efficiency (**figure 5.10**). In contrast however, ovine DC were only transfected at an efficiency of 73-75%, which may reflect the purity or heterogenicity of the cells. Regardless, both ovine and human AdCTLA4-EGFP transfected DC induced alloreactive T cell hyporesponsiveness with greater than 50% inhibition of T cell proliferation at a 1:100 S/R ration compared to untransfected DC. Surprisingly and in contrast to AdEGFP conditioned media, which produced a moderate stimulatory function in the MLR, AdEGFP transfected DC also inhibited the DC-MLR although to a lesser extent than AdCTLA4-EGFP transfected DC. This was a consistent observation between the ovine and human DC-MLR. Due to the restricted availability of mAb directed against ovine costimulatory molecules, the phenotypic analysis of transfected DC was confined to human DC. In accordance with the previously reported effects of adenoviral transfection on DC (302, 303), transfection with AdCTLA4-EGFP and AdEGFP resulted in modest upregulation of MHC Class II, CD86

and CD83 molecules (**figure 5.11**). Interestingly, while AdCTLA4-EGFP transfected DC also showed a slight increase in CD40 expression, AdEGFP transfectants revealed a 15-20% downregulation of CD40, potentially explaining their mild inhibitory effect on alloreactive T cells. The mechanism for CD40 down-regulation upon AdEGFP transfection is unknown but it may be reflective of the disruption to cell function due to the accumulation of intracellular EGFP. Conversely the inhibition may be related to adenoviral-mediated upregulation of IDO expression which has been recently reported in transfected DC (444).

As outlined in **section 1.14** blockade of multiple costimulatory pathways may be required to induce long-term allograft acceptance. In particular systemic treatment of non-human primates with CTLA4-Ig only induces long-term renal allograft acceptance when used in combination with anti-CD154 mAb (347). Moreover in the context of DC therapy, DC transfected with AdCTLA4-Ig only modestly prolong islet allograft survival (253), while the combination of AdCTLA4-Ig with NFκβ oligodeoxyribonucleotide decoys induced long-term acceptance (329). In **chapter 3** the combination of sub-optimal doses of CTLA4-Ig and IL-10 provides evidence supporting the use of both agents to modify DC. An adenoviral construct encoding ovine IL-10 fused to DsRED, a fluorescent gene cloned from coral of the Discosoma genus (445), was generated in order to test the benefits of DC cotransfected with AdCTLA4-EGFP and AdIL-10-DsRED. The DsRED fusion partner was selected to permit quantification of the transfection efficiencies of both AdIL-10-RED and AdCTLA4-EGFP within single cells as the emission spectra of EGFP and DsRED are distinguishable by flow cytometry (446). While cells transfected with AdIL-10-DsRED exhibited significant fluorescence and the IL-10 sequence was confirmed (**appendix 5**), the immunomodulatory activity of conditioned media from transfected fibroblasts or

transfected DC was unable to be established (data not shown). Recent studies have indicated that while initially generated as a monomer, DsRED only demonstrates fluorescence as a tetrameric structure (447). Thus the large tetrameric structure of DsRED may have interfered with the conformational arrangement or binding domains of IL-10. Use of a newly generated DsRED-monomer by Clontech is likely to overcome this limitation and permit dual transfection studies of DC in conjunction with AdCTLA4-EGFP.

In summary in this chapter a biologically active form of ovine CTLA4 fused with an EGFP fusion partner was generated and subsequently incorporated into an adenoviral vector, allowing transfection of DC with high efficiency. The EGFP tag proved advantageous over typical CTLA4-Ig fusion constructs in that it allowed direct analysis of gene transduction. Ovine DC transfected with AdCTLA4-EGFP induced alloreactive T cell hyporesponsiveness in the MLR associated with the blockade of CD28 costimulation as a consequence of CTLA4-EGFP binding to the CD80/86 ligands expressed on the DC, thereby raising the threshold required for T cell activation. Concurrent studies investigating the immunomodulatory effects of AdCTLA4-EGFP on human monocyte-derived DC demonstrated cross-species reactivity of ovine CTLA4-EGFP and permitted a detailed analysis of the biological activity.

Taken in conjunction with the ability of ovine DC to migrate to secondary lymphoid tissues and interact with alloreactive lymphocytes (**chapter 4**), the induction of alloreactive T cell hyporesponsiveness by ovine DC transduced with AdCTLA4-EGFP reported in this chapter warrants the investigation of AdCTLA4-EGFP transfected DC in an *in vivo* model of alloreactivity.

Chapter 6

Immunomodulatory function of ovine DC transfected with adenoviral CTLA4-EGFP in a NOD-scid model of ovine skin allograft rejection

6.1. Introduction

In **chapter 5** adenoviral constructs encoding ovine CTLA4-EGFP were generated. Both human and ovine DC, transduced with AdCTLA4-EGFP, induced alloreactive T cell hyporesponsiveness *in vitro* associated with the autocrine/paracrine binding of secreted CTLA4-EGFP to CD80/86 ligands expressed on the DC. With the ability of AdCTLA4-EGFP transduced DC to induce T cell hyporesponsiveness *in vitro* demonstrated, the aim of this current chapter was to provide *in vivo* proof of principle that AdCTLA4-EGFP transduced ovine DC can inhibit alloreactivity *in vivo*.

Immunodeficient mice have been used to construct models of human vascularised skin allograft rejection, referred to as human PBL-*scid* models (448). The lack of functional immunity in these mice facilitates the transfer of human skin and allogeneic lymphocytes providing a murine model of human allograft rejection. Similar models have also been used to study a number of human diseases including graft Vs. host disease, HIV pathogenicity and cancer treatment (449).

While a number of different strains of immunodeficient strains have been generated (450), the NOD-*scid* mouse provides a good model for immune reconstitution (451, 452). NOD/*scid* mice were developed by backcrossing the *scid* mutation over ten generations onto the NOD/Lt strain (452). The SCID (severe combined immunodeficient) mutation in mice is characterised by defective DNA-repair mechanisms and an inability to rearrange the variable, diversity and joining (VDJ) segments of TCR and immunoglobulins which results in a lack of functional T and B lymphocytes (453-455). While initial human lymphocyte reconstitution was possible in SCID mice, long-term persistence was limited by innate immune responses (454). Furthermore the mutation of VDJ recombination in SCID mice is

incomplete and leads to "leakiness" in which residual T and B cell activity can expand, a phenomenon which increases with age. The NOD/Lt mutation results in defective differentiation and function of antigen presenting cells (456), a lack of circulating complement (457) and functionally inept natural killer (NK) cells (458). Crossing the NOD and SCID mutation resulted in a strain (NOD-*scid*) lacking functional T and B cells, reduced NK cell activity, lack circulating complement and are diabetes and insulitis free throughout life (451) and furthermore have demonstrated more reliable and efficient immune reconstitution compared with SCID mice (459).

A NOD-*scid* model of ovine skin allograft rejection was established in this study based on the human equivalent models detailed above. The NOD-*scid* model represents a short-term model of *in vivo* alloreactivity and does not test for long-term tolerance as the immune reconstitution does not facilitate *de novo* lymphocyte generation (450). The model has however demonstrated a predictive value of the efficacy of immunosuppressive strategies on human lymphocytes *in vivo* including cyclosporin treatment and CD2/LFA blockade (448, 460-462). Administration of AdCTLA4-EGFP transduced DC autologous to the skin donor specifically investigates the influence of CTLA4-EGFP on the direct pathway of allorecognition which, as described in **section 1.9.1**, plays an important role in acute rejection.

As described in previous chapters, current *in vivo* data on the use of DC modified to produce CTLA4 fusion proteins is limited to two studies. While Lu *et al.* (211) demonstrated the efficacy of AdCTLA4-Ig transduced DC *in vitro* and showed that the cells were able to migrate to secondary lymphoid tissues, no functional data was reported with respect to *in vivo* immunomodulation. In the second study O'Rourke *et al.* (253) showed that a DC-cell line transduced with AdCTLA4-Ig significantly prolonged allograft

acceptance in mice. In this chapter we provide data demonstrating the ability of primary ovine DC modified with AdCTLA4-EGFP to inhibit alloreactivity *in vivo*.

The specific aims of this chapter were

(i) To determine baseline conditions for vascularised ovine skin allograft rejection in a NOD-*scid* mouse model.

(ii) To assess the ability of ovine DC genetically modified with adenoviral ovCTLA4-EGFP to inhibit skin allograft rejection in this model.

6.2. Materials and Methods

6.2.1. NOD-*scid* mice

NOD-*scid* mice were purchased from the IMVS (Adelaide, SA) at four weeks of age. Animals were housed in a pathogen-free environment at the Adelaide University Central Storage Facility and allowed free access to food and water throughout the duration of the experiments. Animal ethics approval for the experiments were obtained from Adelaide University and The Queen Elizabeth Hospital animal ethics boards (animal ethics number N16-2001).

6.2.2. Harvesting of ovine skin

Sheep were fasted for 12 h and anaesthetised with 0.4 ml/kg intravenous Nembutol, intubated and anaesthesia maintained with an inhaled Flurothane/O_2 mixture. Full skin thickness biopsies were taken from the non-wool bearing region of the upper thigh of sheep using an 8 mm disposable biopsy punch (Stiefel Laboratories, Australia). Sheep were administered a single intramuscular dose of penicillin/streptomycin as a post-operative prophylaxis against infection. To facilitate effective engraftment, excess sub-cutaneous tissue was removed from the skin biopsies to yield a thickness of approximately 0.5 mm.

6.2.3. Grafting of ovine skin

NOD-*scid* mice were anaesthetized with a mixture of oxygen and halothane. Mouse skin was excised from the dorsal aspect of the mouse thorax and replaced with sheep skin, which was maintained in sterile RPMI at 4°C prior to transplantation. Wounds were covered with RPMI soaked Sorbsan Calcium Alginate dressing (Steriseal, England) and

wrapped with two coats of Tegaderm bandages (3M, Australia). Dressings were removed after seven days, with a further week uncovered healing permitted prior to challenge with PBMC allogeneic to the donated skin. The protocol for the engraftment of ovine skin in the NOD-*scid* experiments is illustrated in **figure 6.1**.

6.2.4. Intra-peritoneal challenge with allogeneic ovine PBMC and DC

PBMC and DC were isolated from sheep as described (**2.3.1.1 and 4.2.1**) and alloreactivity against the skin donor verified by MLR (**2.3.1.4**). For the appropriate experiments ovine DC were transfected with AdCTLA4-EGFP or AdEGFP. PBMC (1-2 x 10^8 cells) and DC (1-2 x 10^6) were mixed and immediately injected into the peritoneal cavity of the mice using 29G insulin needles. Treatment groups and animal numbers are detailed in the **table 6.1**.

Table 6.1. NOD-*scid* treatment groups

DC Treatment	Lymphocytes	n =
Untreated	Allogeneic	8
Untreated	Autologous	4
AdCTLA4-EGFP	Allogeneic	4
AdEGFP	Allogeneic	4

In all treatment groups DC autologous to the skin donor were used.

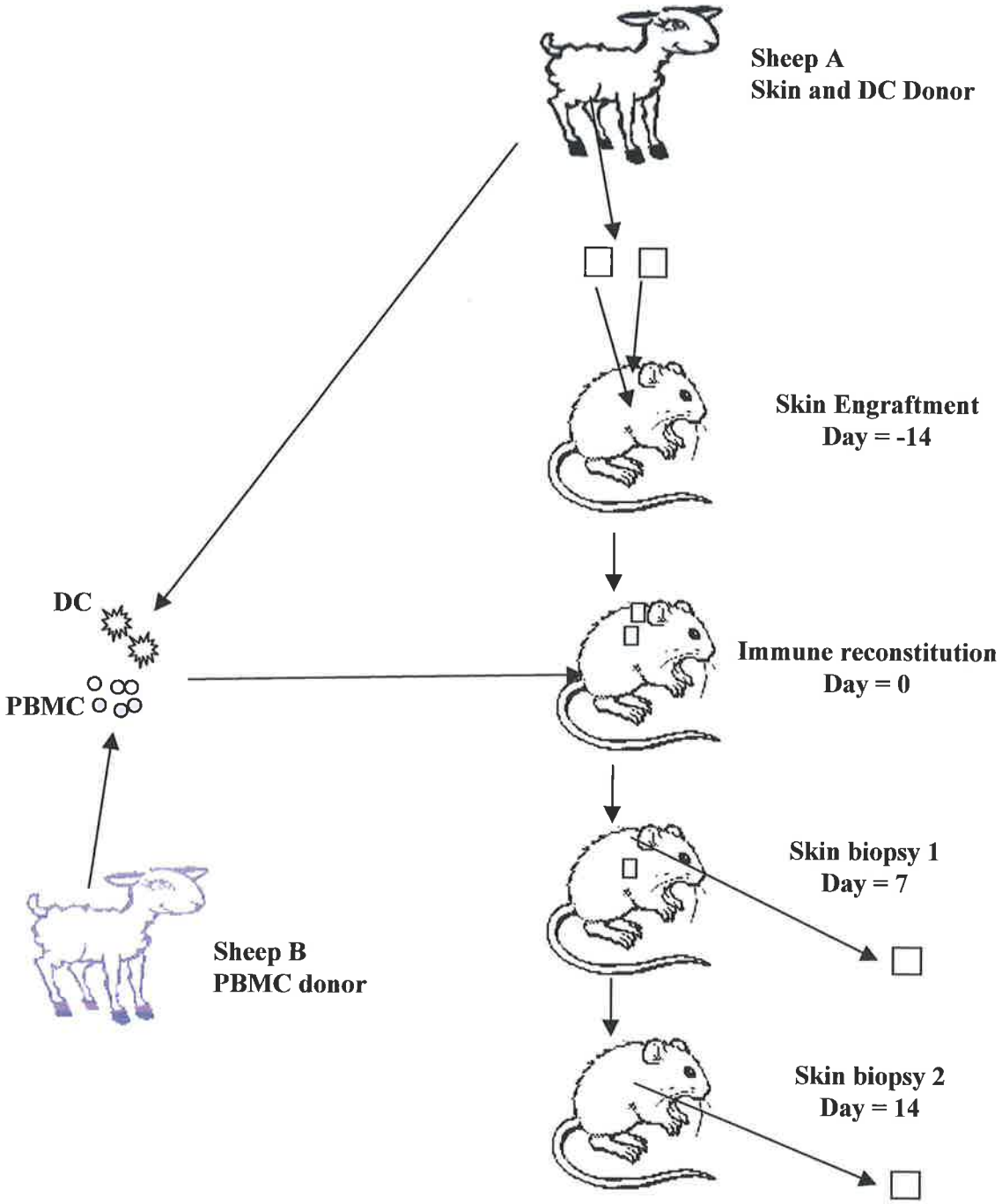

Figure 6.1. Schematic representation of skin grafting and immune reconstitution of NOD-*scid* mice.
Ovine skin biopsies were taken from sheep which had been cannulated to provide a source of DC autologous to the skin transplants. Two skin biopsies were grafted onto NOD-*scid* mice with healing permitted for 14 days. At the experimental time, day = 0, ovine DC (1-2 x 10^6) autologous to the skin donor were co-injected with allogeneic ovine PBMC (1-2 x 10^8). Skin grafts were removed for analysis at days 7 and 14. In the case of DC genetically modified with AdCTLA4-EGFP or AdEGFP, DC were transfected 48 h prior to injection to facilitate gene transduction.

6.2.5. Adenoviral transduction of ovine DC

Ovine pseudo-afferent derived DC were transfected with AdCTLA4-EGFP or the AdEGFP vector blank in conjunction with LipofectAMINE^{TM} as described (**5.2.8**). Transfected DC were cultured for two days in complete media to facilitate gene transduction prior to injection into recipient mice.

6.2.6. ELISA Quantification of CTLA4-EGFP and EGFP

An ELISA was set-up to quantify the level of CTLA4-EGFP and EGFP production from transfected DC and in the serum of mice treated with transfected DC. DC were transfected with either AdCTLA4-EGFP or AdEGFP and after 2 days in culture, conditioned media was cleared of cells by centrifugation and used in the ELISA. To quantify CTLA4-EGFP and EGFP in circulation after treatment of NOD-*scid* mice with transfected DC, blood was drawn from the tail vein. Blood was allowed to settle by overnight incubation at 4°C and serum isolated from cells by centrifugation. The ELISA was performed as described in **5.2.5** using antibodies directed against EGFP.

6.2.7. Histological Analysis of Skin Biopsies

Grafted skin was excised from mice seven and fourteen days post immune reconstitution and wounds sutured with 4.0 silk ties. Skin biopsies were embedded in OCT and 6 μm sections performed using a cryomicrotome. H&E (**2.3.5.2**) and immunohistochemical staining (**2.3.5.3**) using sheep specific anti-CD4 and anti-CD8 were performed to assess the level of lymphocyte infiltrate and characterise the infiltrating cells.

6.2.8. Rejection Scores

Rejection scores for H&E, CD4 and CD8 staining were based on the definitions in **table 6.2**. Scoring was performed by two assessors blinded to the treatments. Statistical comparisons were made using the Mann-Whitney U test.

Table 6.2 Scoring for ovine skin allograft rejection

H&E Scoring	
Score	**Definition**
1	<25% scattered leukocytes
2	<25% focal infiltration
3	25-50% moderate diffuse infiltration
4	>50% infiltration
CD4/CD8 Scoring	
Score	**Definition**
1	No staining
2	Scattered discretely stained cells
3	Marked focal staining
4	Marked diffuse staining

6.3. Results

6.3.1. Ovine skin engraftment in NOD-scid mice

Ovine skin allografts on NOD-*scid* mice were well tolerated and free of scabbing or necrosis (**figure 6.2.a**). Vascularisation of the graft was demonstrated by H&E staining with patent vessels observed in the within the dermis of unchallenged and reconstituted mice (**figure 6.2.b**). While vessels in unchallenged mice remained free of peri-vascular infiltrate, mice reconstituted with allogeneic ovine lymphocytes often revealed intense peri-vascular staining (**figure 6.3.b**). Distinct ovine-murine epidermal junctions were observed in all skin grafts and transplanted ovine skin demonstrated significant hyperkeratosis compared with freshly isolated ovine skin (**figure 6.2.c-6.2.f**).

6.3.2. Injection of allogeneic DC and PBMC provokes rejection of ovine skin allografts

While injection of autologous DC and PBMC resulted in diffuse lymphocyte infiltrate in skin sections taken at days 7 and 14, injection of allogeneic cells was characterised by extensive lymphocyte infiltration (**figure 6.3.a**). Focal localisation of lymphocytes at the dermal-epidermal junction and peri-vascular staining were particular features of the allogeneic response (**figure 6.3.b**). Typically greater levels of infiltration were observed at day 7 compared to day 14. As shown in **figure 6.4**, lymphocyte infiltrates were comprised of both $CD4^+$ and $CD8^+$ T cells. Compared to the allogeneic response, histological scoring of skin biopsies revealed significantly less infiltrate in autologous challenged samples (**figure 6.5**). While significant differences were observed by histology, no discolouration or necrosis of the skin was observed. The mean rejection score for allogeneic treated animals at day 7 was significantly higher (3.4 +/- 0.45) than animals

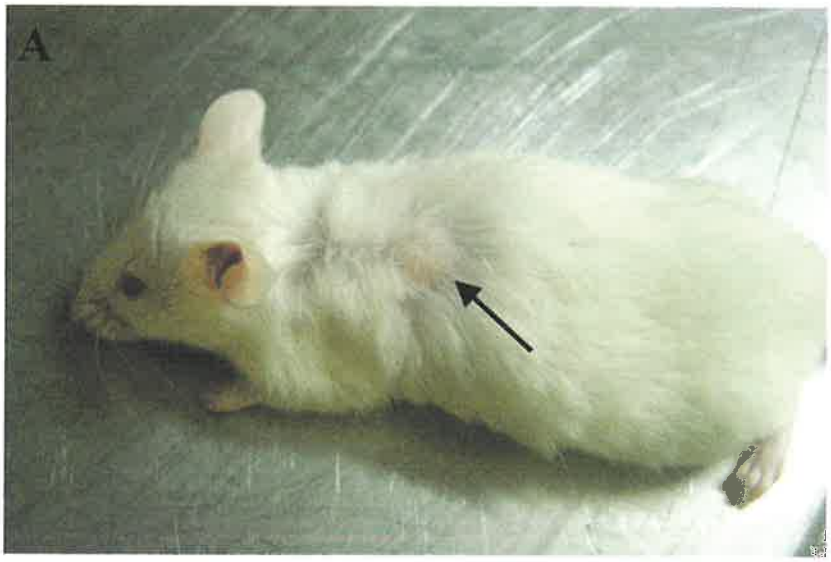

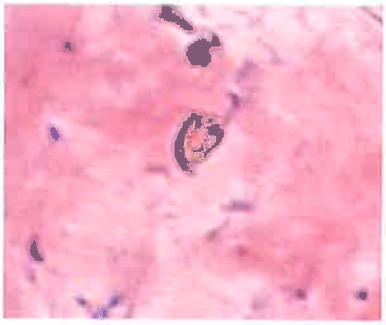

400X Magnification

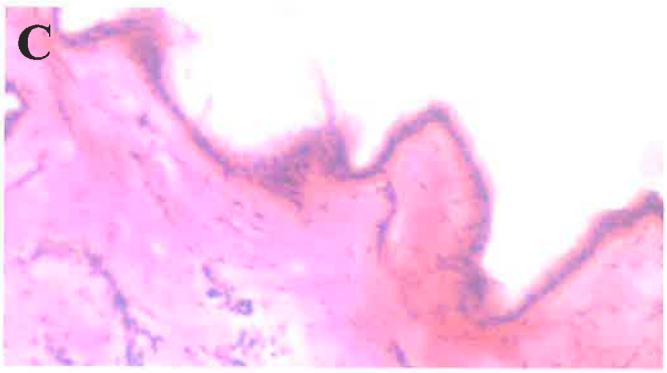

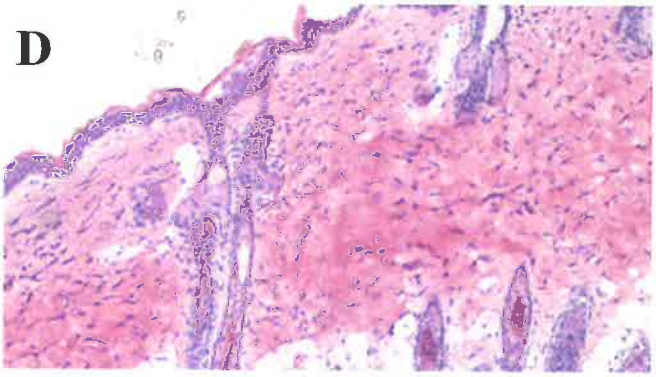

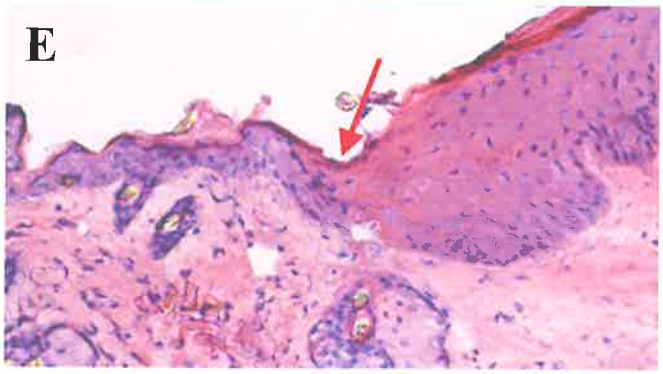

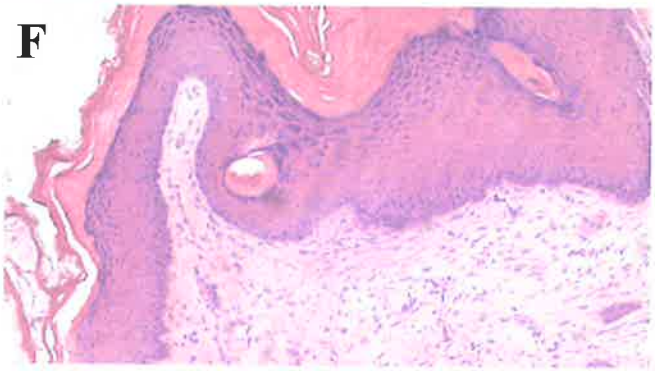

100X Magnification

Figure 6.2. Ovine Skin Engraftment onto NOD-*scid* Mice

A) Ovine skin grafted onto a NOD-*scid* mouse 21 days post-transplantation displayed a normal macroscopic appearance with no necrosis.

B) Patent vessels were observed in ovine skin biopsies from unchallenged mice.

C) Freshly isolated ovine skin pre-transplantation, stained with H&E, demonstrated normal ovine skin architecture.

D) Normal architecture of untreated NOD-*scid* mouse skin.

E) Grafted skin removed 21 days post-transplantation from a non-challenged NOD-*scid* mouse showed significant hyperkeratosis and a clearly defined murine-ovine epidermal junction.

F) Unchallenged skin removed 21 days post-transplantation from a non-challenged NOD-*scid* mouse remained free of infiltrating lymphocytes

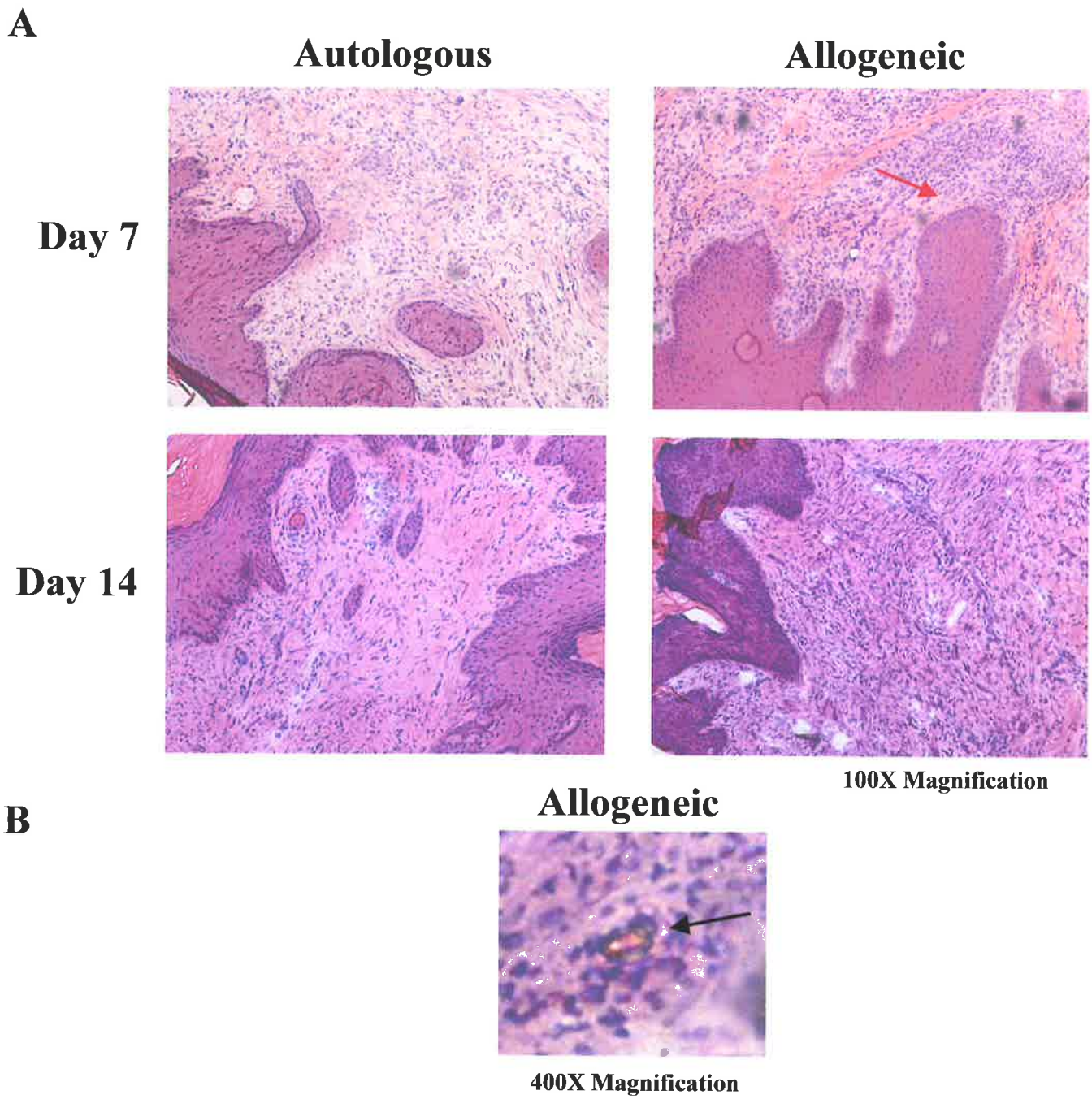

Figure 6.3. Lymphocyte Infiltrate after Autologous and Allogeneic Immune Reconstitution.
A) H&E staining was performed on ovine skin sections from autologous or allogeneic challenged NOD-*scid* mice. Compared to NOD-*scid* mice reconstituted with PBMC and DC autologous to the skin donor which demonstrated diffuse lymphocyte infiltrate, injection of allogeneic PBMC and autologous DC resulted in massive lymphocyte infiltration.
B) Lymphocyte infiltrates were predominant at the dermal-epidermal junction (red arrow) and around vessels (black arrow).

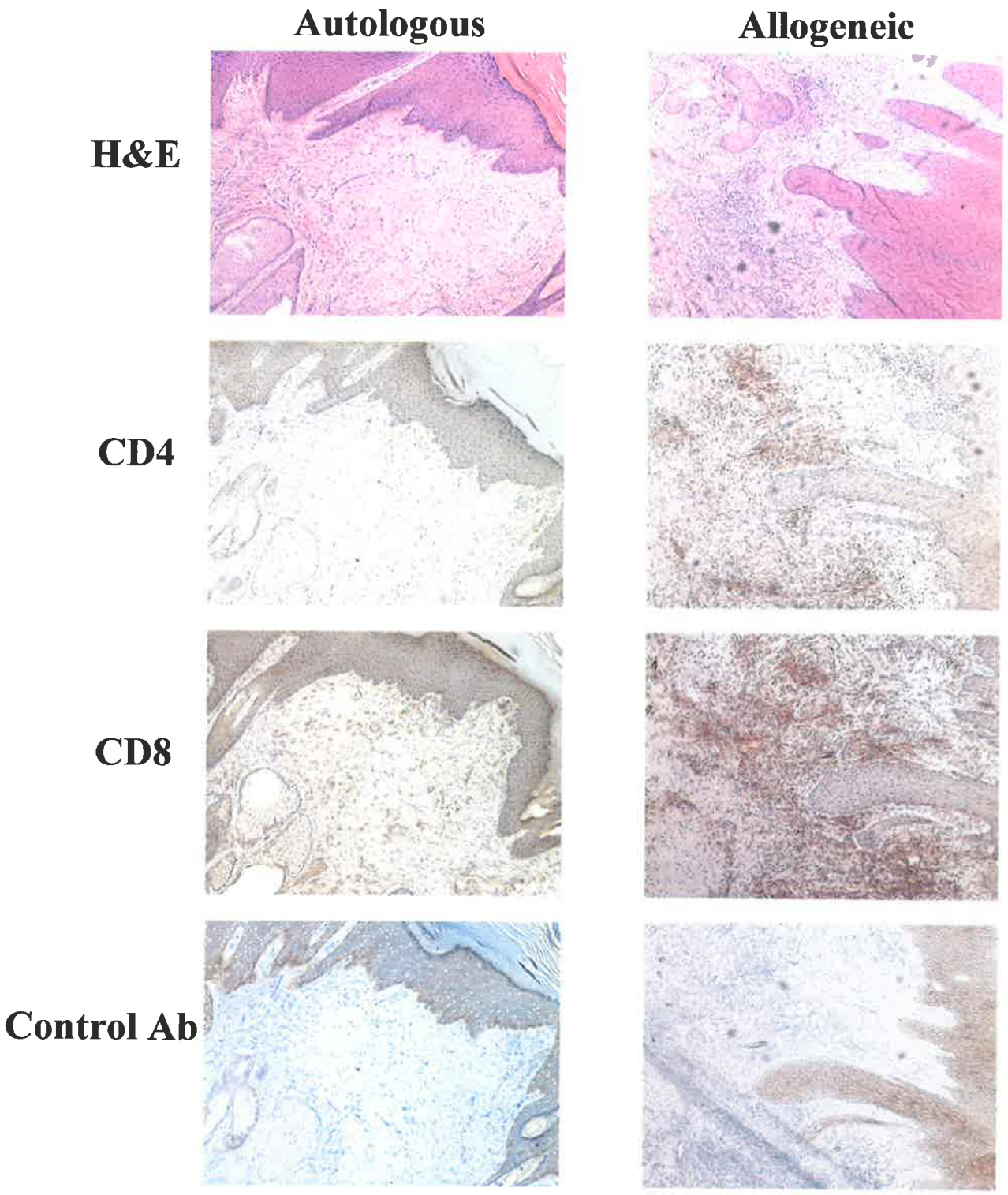

Figure 6.4. Lymphocyte infiltrates of ovine skin after autologous and allogeneic challenge of NOD-*scid* mice consist of CD4$^+$ and CD8$^+$ T cells.
Serial sections from day 7 autologous and allogeneic NOD-*scid* mice were stained with H&E or primary antibodies. Reactions were developed with DAB stain and reveal the presence of both CD4+ and CD8+ cells within the infiltrate.

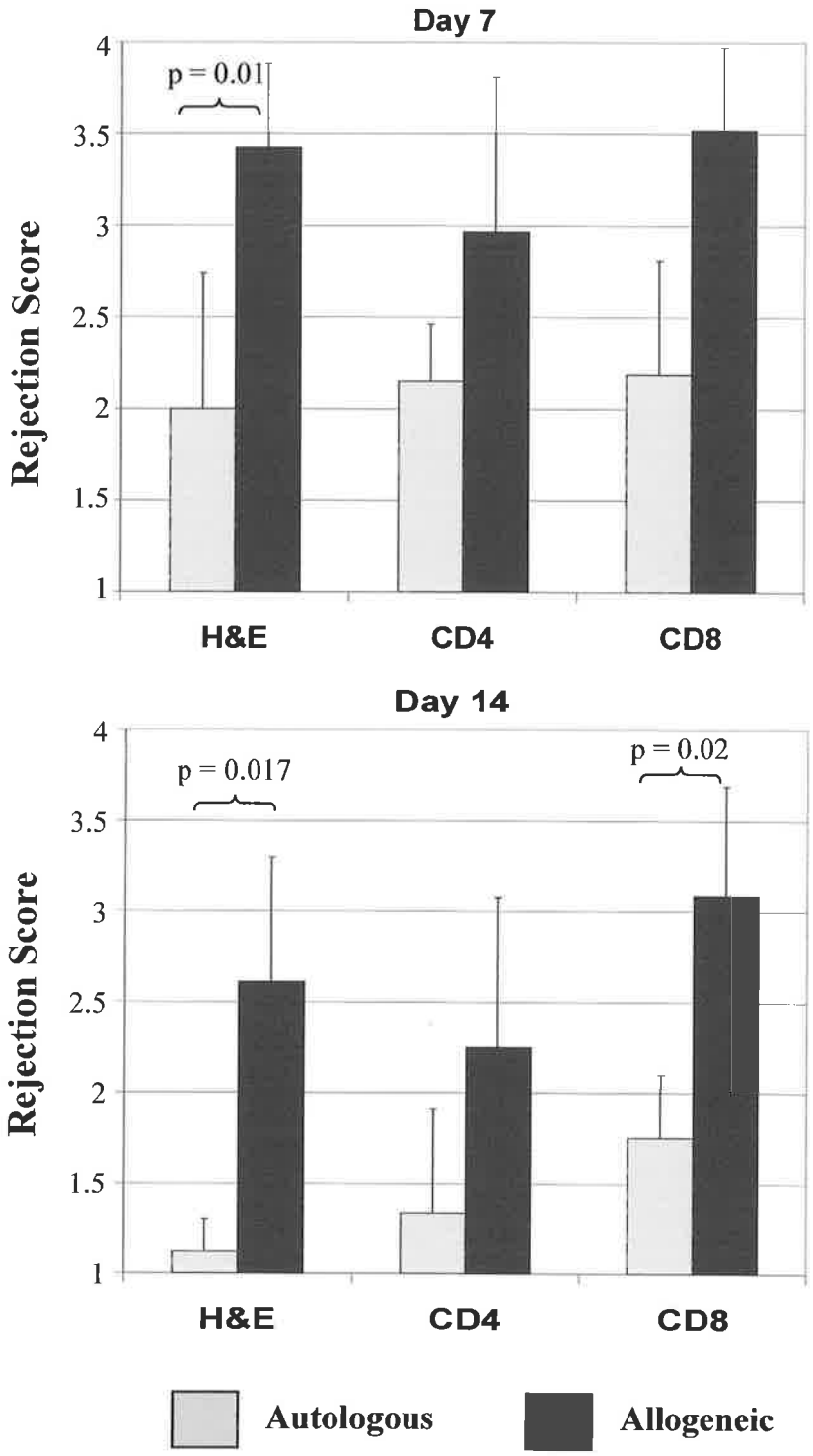

Figure 6.5. Quantitative analysis of lymphocyte infiltrates in ovine skin exposed *in vivo* to autologous or allogeneic challenge

Serial sections from day 7 and day 14 autologous (n=4) and allogeneic (n=8) treated NOD-*scid* mice were stained with H&E or primary antibodies. Sections were scored by two assessors blinded to the treatment groups. Rejection scores for H&E staining were calculated using the following scale: grade 1 <25% scattered leucocytes, grade 2 <25% focal leucocytes, grade 3 25-50% moderate diffuse leucocytes, grade 4 >50% leucocytes. Scoring for CD4 and CD8 staining were based on following scale: grade 1 no staining, grade 2 scattered discretely stained cells, grade 3 marked focal staining, grade 4 marked diffuse staining. Statistical analysis was performed using Mann Whitney U tests.

treated with autologous lymphocytes with a mean rejection score of 2 +/- 0.74 ($p = 0.01$) (**figure 6.5**). Higher mean rejection scores ($p=0.017$) for animals treated with allogeneic lymphocytes (2.6 +/- 0.69) at day 14 were also observed compared to autologous lymphocyte treated animals (1.125 +/- 0.18).

6.3.3. Dendritic cells transfected with adenoviral vectors migrate to the skin graft after intraperitoneal injection.

Ovine DC were transfected with either AdCTLA4-EGFP or AdEGFP, with transgene expression confirmed by fluorescent microscopy (data not shown) and secretion quantified by ELISA with a daily production of approximately 10 ng of CTLA4-EGFP per 1 $x10^6$ cells (**figure 6.6**). In order to assess the migration of ovine DC injected into NOD-*scid* mice transplanted with ovine skin, DC were transfected with the adenoviral constructs and injected into the peritoneum of NOD-*scid* mice. Skin grafts were removed 7 days post injection and examined by fluorescent microscopy. AdCTLA4-EGFP transfected DC were detected in the dermis of the skin transplants of treated animals (**figure 6.7**) but not in the spleen (data not shown). Migration of AdCTLA4-EGFP transfected DC to the skin was confirmed by RT-PCR demonstrating mRNA expression of CTLA4-EGFP in skin sections (**figure 6.7**).

6.3.4. Injection of donor-specific ovine DC transfected with adenoviral CTLA4-EGFP protects ovine skin grafts from rejection.

Ovine DC of the same origin as the donated skin were transfected with AdCTLA4-EGFP, mixed with allogeneic PBMC and immediately injected into the peritoneal cavity of the mice. AdEGFP transfected DC were used as the control treatment. Aggressive

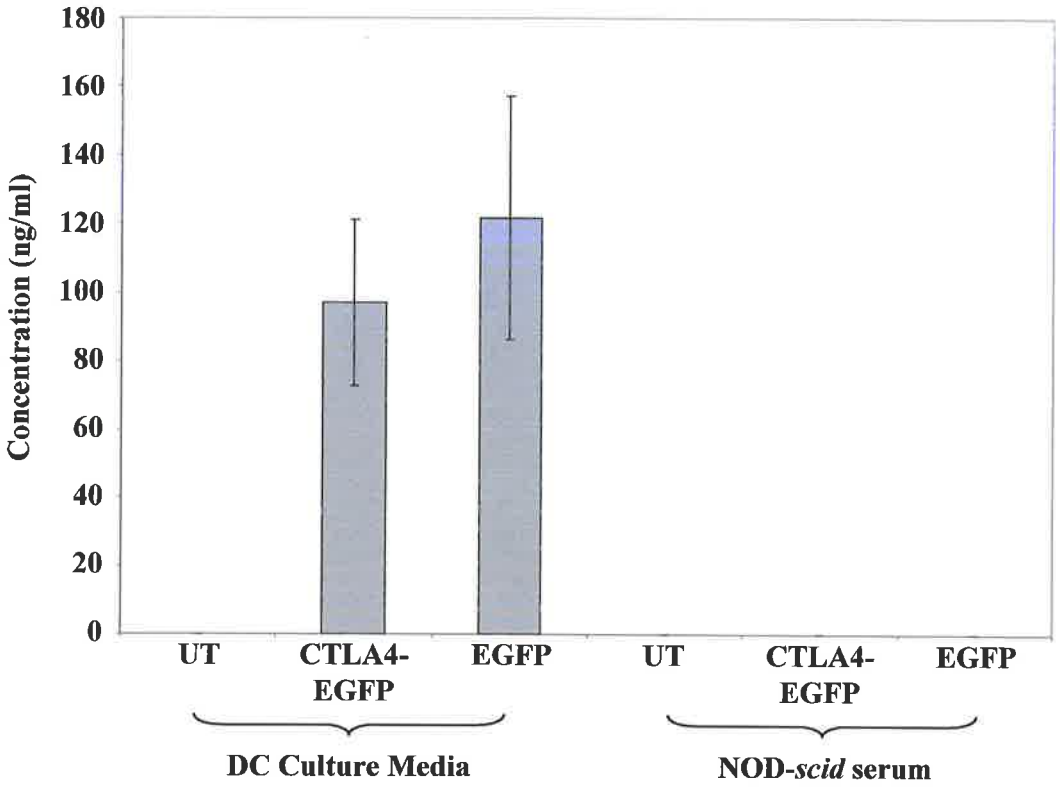

Figure 6.6. ELISA quantification of CTLA4-EGFP and EGFP from transfected DC and serum from NOD-*scid* mice treated with transfected DC

ELISA quantification was performed on 2-day conditioned media of DC (1 x 10^6) transfected with either AdCTLA4-EGFP or AdEGFP and cultured in 200 µl of media. ELISA was also performed on the serum derived from NOD-*scid* mice treated with AdCTLA4-EGFP or AdEGFP transfected DC.

A. Fluorescent microscopy of skin sections

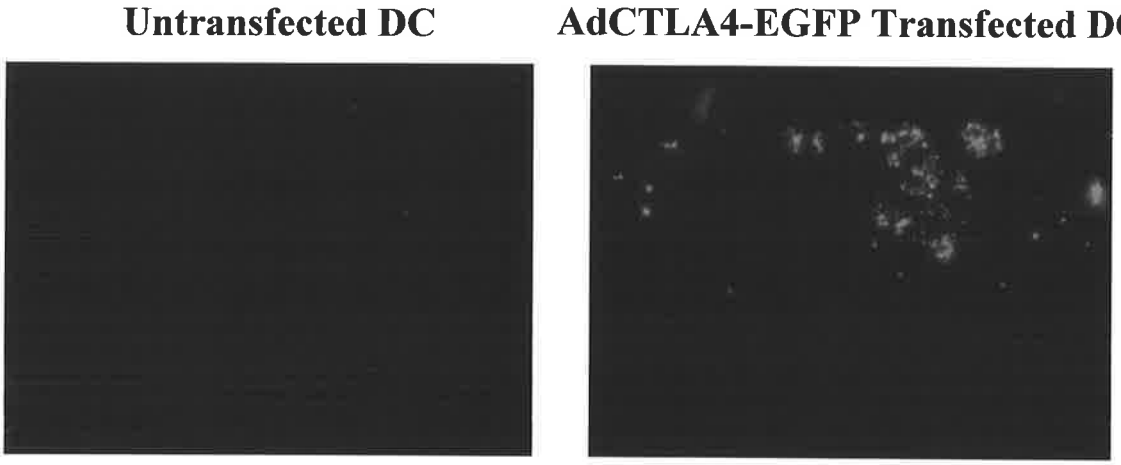

B. PCR analysis of skin and spleen sections

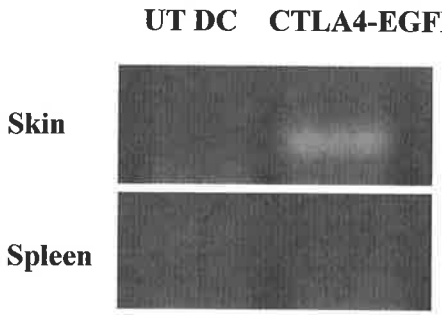

Figure 6.7. Adenoviral CTLA4-EGFP transfected ovine DC migrate to the ovine skin allograft in NOD-scid mice

A) Skin sections were assessed by fluorescent microscopy to determine whether adenoviral transfected DC were capable of migration to the transplanted ovine skin after intraperitoneal injection. Pictures above represent skin sections from NOD-*scid* mice injected with AdCTLA4-EGFP or untransfected DC. Fluorescence was detected in 50% of skin biopsies from AdCTLA4-EGFP DC treated animals.

B) Total RNA was extracted from skin and spleen biopsies of NOD-*scid* mice after intraperitoneal injection of AdCTLA4-EGFP transfected DC and reverse transcribed. PCR amplification of cDNA using forward CTLA4 and reverse EGFP primers confirmed CTLA4-EGFP mRNA expression in ovine skin but not the spleen. PCR amplification with β-Actin housekeeping primers confirmed the equivalent amount of cDNA in each sample (data not shown).

rejection was observed in AdEGFP treated animals (3.83 +/- 0.289), characterised by massive $CD4^+$ and $CD8^+$ T cell infiltration. In contrast animals receiving AdCTLA4-EGFP transfected DC demonstrated significantly reduced (p=0.029) lymphocyte infiltration (1.625 +/- 0.595) **(figures 6.8/6.9)**. The inhibition was not due to systemic immunosuppression, as CTLA4-EGFP was not detected in the serum of mice by ELISA **(figure 6.6)**. The aggressive response in AdEGFP treated animals was transient with a reduction in lymphocyte infiltration evident by day 14. In order to quantify the differences in rejection by AdCTLA4-EGFP and AdEGFP treatment, rejection scores were calculated based on the examination by two observers blinded to the treatment groups. As shown in **figure 6.9** the mean rejection score for animals treated with AdCTLA4-EGFP transfected DC at day 7 was 1.625 +/- 0.59 compared to animals treated with AdEGFP transfected DC with a mean rejection score of 3.83 +/- 0.28 ($p = 0.029$).

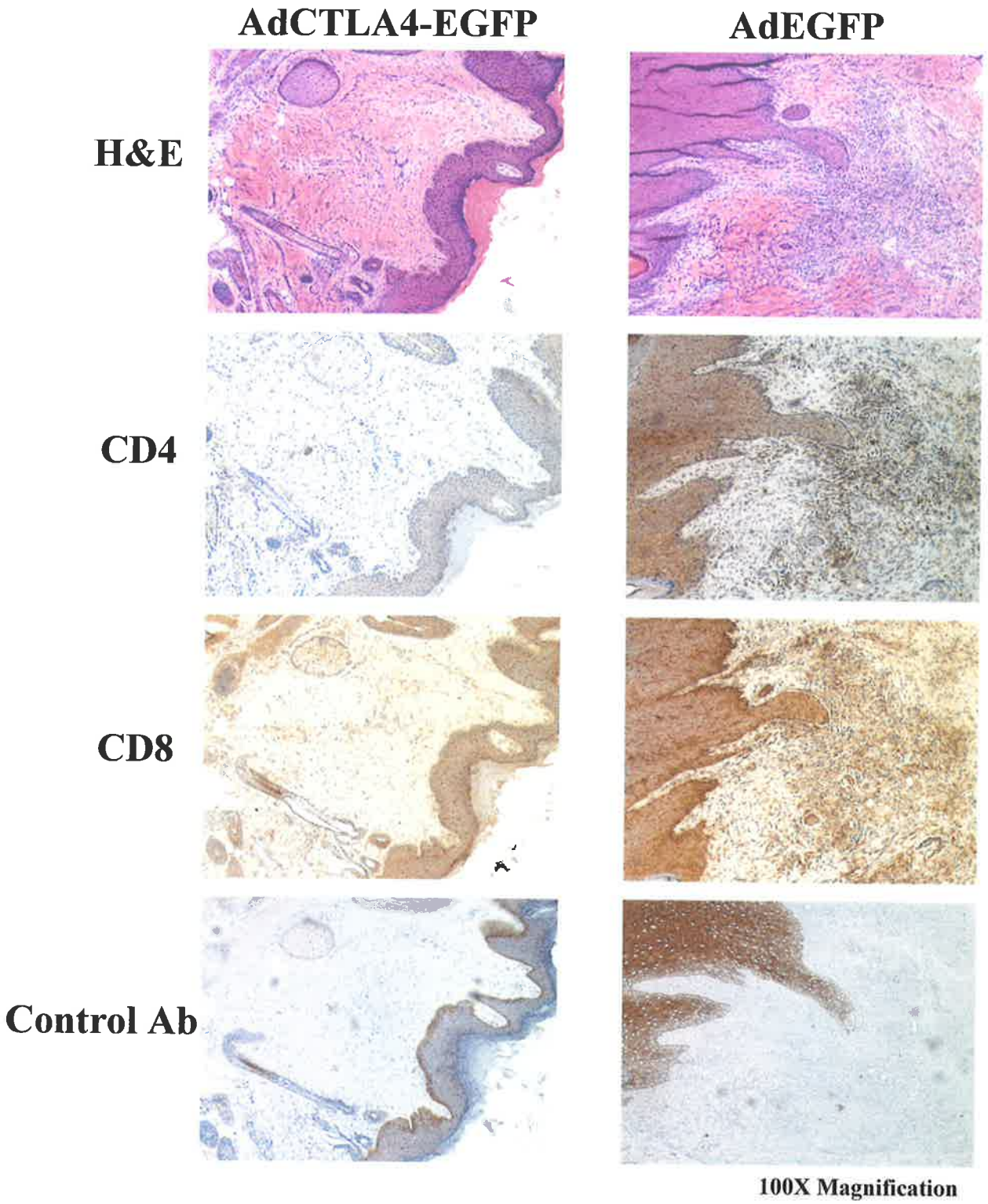

Figure 6.8. Ovine skin from NOD-*scid* mice treated with AdCTLA4-EGFP transfected ovine DC demonstrate reduced lymphocyte infiltration compared with AdEGFP transfected control DC. Serial sections of ovine skin biopsies from day 7 allogeneic NOD-*scid* mice treated with AdCTLA4-EGFP or AdEGFP transfected ovine DC were stained with H&E or primary antibodies. Immuno-histochemical reactions were developed with DAB. Treatment with AdCTLA4-EGFP transfected DC resulted in a marked reduction of lymphocyte infiltration

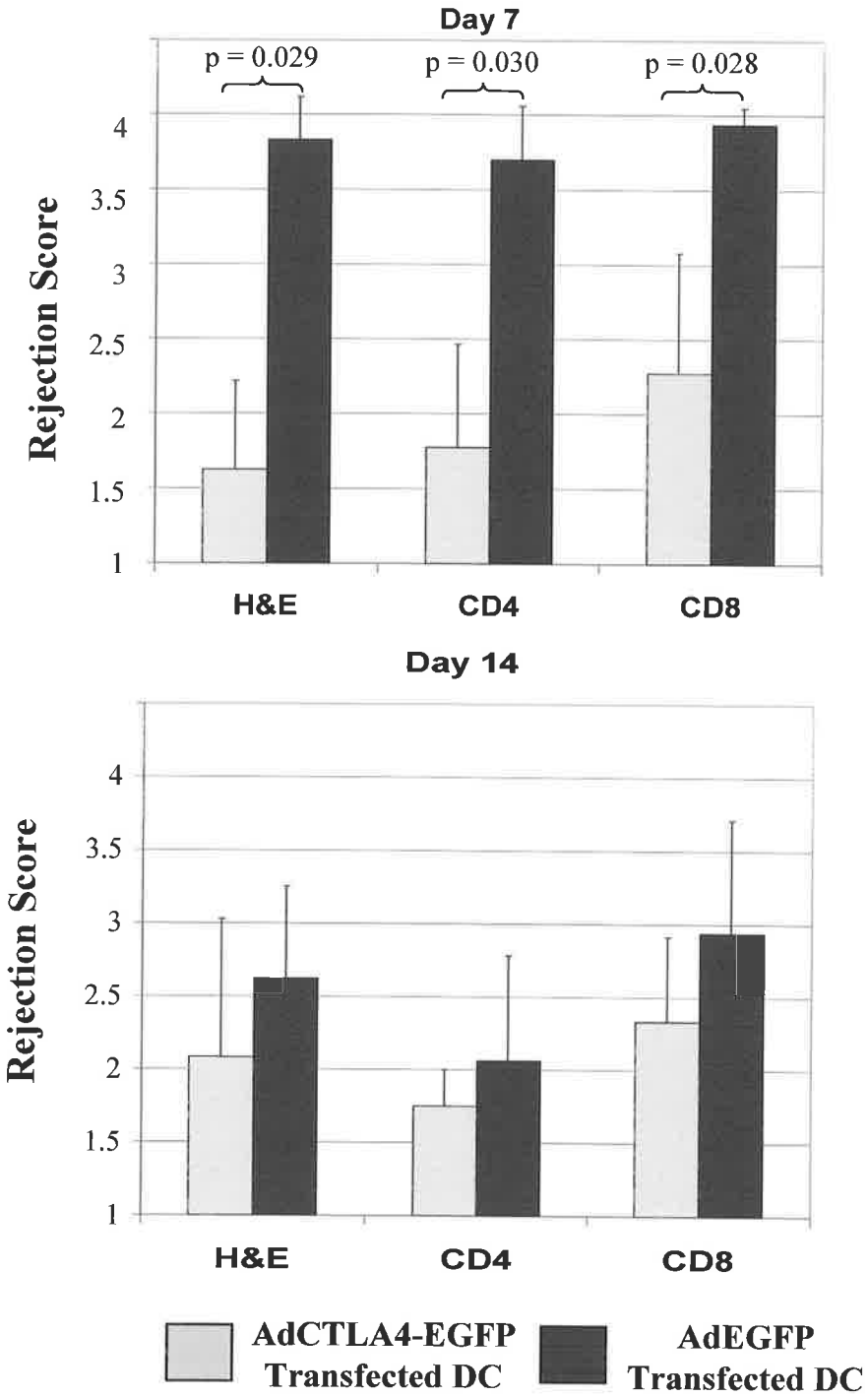

Figure 6.9. Quantitative analysis of lymphocyte infiltration in ovine skin exposed *in vivo* to allogeneic challenge and treated with AdCTLA4-EGFP or AdEGFP transfected ovine DC. Serial sections from sheep skin isolated at day 7 and day 14 from AdCTLA4-EGFP (n=4) and AdEGFP (n=4) DC treated NOD-*scid* mice were stained with H&E or primary antibodies. Sections were scored by two assessors blinded to the treatment groups. Rejection scores for H&E staining were calculated using the following scale: grade 1 <25% scattered leucocytes, grade 2 <25% focal leucocytes, grade 3 25-50% moderate diffuse leucocytes, grade 4 >50% leucocytes. Scoring for CD4 and CD8 staining were based on following scale: grade 1 no staining, grade 2 scattered discretely stained cells, grade 3 marked focal staining, grade 4 marked diffuse staining. Statistical analysis was performed using Mann Whitney U tests.

6.4. Discussion

This chapter reports the generation and characterisation of a murine model of ovine skin rejection and examines the ability of ovine DC transfected with adenoviral CTLA4-EGFP to induce T cell hyporesponsiveness *in vivo* in this model. NOD-*scid* mice were used as transplant recipients as their lack of functional T and B lymphocytes facilitates the successful engraftment of most tissues without rejection (463). In the context of skin allografts, this model permits the vascularisation of the graft prior to allogeneic challenge, preventing necrosis typically observed in skin allograft rejection (461, 464, 465). Indeed we found that skin grafts were accepted well and persisted indefinitely without signs of rejection and vascularisation of the graft was observed within 14 days of transplantation.

Intraperitoneal injection of 1-2 x 10^8 allogeneic lymphocytes and 1-2 x 10^6 DC autologous to the skin allograft donor, resulted in extensive lymphocyte infiltration of the dermis of the transplanted ovine skin. The number of lymphocytes and route of administration were based on previous humanized *scid* models (264, 466), with intraperitoneal injection demonstrating more consistent reconstitution than intravenous delivery and resulting in the detection of T and B cells in the peripheral blood, peritoneal cavity, lymph nodes and spleen (466, 467). After injection of lymphocytes, the peritoneal cavity provides a similar function to that of a lymph node in which lymphocyte interaction and activation can occur (466, 468-470). Coinjection of allogeneic lymphocytes and DC autologous to the skin, permits direct allorecognition to occur, leading to rapid lymphocyte activation and proliferation. Lymphocytes primed by the DC are then able to recognise allopeptides on the skin allografts leading to lymphocyte infiltration of the graft. Histological rejection of ovine skin allografts treated with allogeneic lymphocytes was

demonstrated by extensive infiltration of both $CD4^+$ and $CD8^+$ T cells, with focal clustering at the dermal-epidermal junction and peri-vascular infiltration also noted. In contrast with the human PBL-*scid* model, in which maximal rejection is observed between 16 and 21 days (448, 471), the level of infiltration in this study was more profound at day 7 with more diffuse lymphocyte staining observed at day 14. In most human PBL-*scid* models, human PBMC are administered in the absence of DC. Thus for alloactivation to occur, DC (which represent <1% of PBMC) or monocytes within the cell inoculum must migrate to the skin allograft, process the alloantigens and then prime the alloreactive T cells via the indirect pathway of allorecognition. Alternatively DC resident in the skin allograft (i.e. Langerhans cells) may migrate from the skin facilitating the direct presentation to alloreactive lymphocytes. These two processes are likely to account for the delayed onset of rejection. Consistent with our findings, intraperitoneal injection of DC mixed with allogeneic PBMC resulted in strong skin rejection at day 7 in humanised NOD-*scid* chimeric mice (264).

The apparent attenuation of rejection by day 14 in the current study may be explained by examining some of the limitations of the model. The immunodeficient mouse models are not long-term allograft models in which tolerance can be examined as lymphocyte engraftment is transient as *de novo* generation of donor lymphocytes is not evident (450). Thus the attenuation of lymphocyte function by anergy or viability as a result of AICD (450) can limit the duration of graft rejection. Although not as much an issue with NOD-*scid* mice, the presence of functional murine NK cells can result in donor lymphocyte elimination, as evidenced in *scid* mouse models (451, 472, 473). Attenuation of donor lymphocyte reactivity may also occur as a result of T cell anergy due to chronic stimulation by murine antigens, although this is more prevalent upon prolonged engraftment (474, 475). Importantly for a period of 2-3 weeks after adoptive transfer,

human lymphocytes injected into NOD-*scid* mice demonstrate functional activity (476), which is within the time-frame of this study.

The observed lymphocyte infiltration in skin grafts treated with autologous lymphocytes, albeit at lower levels than the allogeneic response may be reflective of passive migration or activation of the autologous T cells by presentation of murine antigens processed by skin DC. Indeed human lymphocytes injected into SCID mice have demonstrated modest upregulation of IL-2R indicating partial activation (466) with evidence of human anti-mouse reactivity (477). In this study, while priming the anti-ovine response, coinjected ovine DC by virtue of their ability to endocytose antigens as reported in **chapter 4**, may also process murine antigens provoking anti-mouse reactivity and therein an increase in proliferating lymphocytes.

As reported in **Chapter 5**, transfection of ovine DC with AdCTLA4-EGFP resulted in alloreactive T cell hyporesponsiveness *in vitro* by blockade of the CD28 costimulatory pathway. Thus in the second part of this chapter the attenuation of graft rejection by genetic modification of donor specific ovine DC was investigated. Ovine DC (1-2 x 10^6) were transfected with AdCTLA4-EGFP or the vector blank AdEGFP and maintained in culture media for 2 days to permit viral transduction prior to injection into NOD-*scid* mice engrafted with ovine skin. Consistent with the findings in **chapter 5**, adenoviral transfection resulted in >70% gene transduction as determined by the detection of the inherent fluorescence of the EGFP protein (data not shown). Moreover secretion of CTLA4-EGFP by DC was confirmed by ELISA, with a daily production of 10 ng per 1 x10^6 cells.

Intraperitoneal injection of allogeneic lymphocytes and donor specific DC transfected with AdCTLA4-EGFP resulted in a profound reduction in skin allograft

rejection compared with AdEGFP transfected DC controls. Transfected DC were identified in the skin of animals treated with AdCTLA4-EGFP as indicated by fluorescence and mRNA expression, indicating that AdCTLA4-EGFP transfected DC may mediate their inhibitory effects on alloreactive lymphocytes both within the peritoneal cavity and additionally at the site of the allograft. While not conducted in this study, washing of the lymphocytes from the peritoneal cavity may confirm the persistence of transfected DC in addition to permitting the activational status of the lymphocytes to be determined.

In transplantation, the purpose of DC based therapies is to directly attenuate alloreactive cells while preserving normal immune function. That CTLA4-EGFP was not detected in the serum of non-graft-rejecting mice supports the restricted production of CTLA4-EGFP to local microenvironments in which DC may interact with allogeneic lymphocytes, thereby negating the potentially detrimental effects of systemic immunosuppression.

AdCTLA4-EGFP transfected DC, in contrast to control transfectants, produced significantly lower lymphocyte infiltration in the ovine skin grafts 7 days post-challenge with allogeneic PBMNC. Peculiar to this model is the observation that the infiltration response subsides with time, which is indicated by the reduction in rejection scores at 14 days post-challenge in comparison to day 7 even in the presence of control DC transfectants. This may reflect either transient immunomodulation by AdCTLA4-EGFP transfected DC or the attenuation of the immune response in AdEGFP transfected DC as a result of lymphocyte exhaustion.

A limitation of this current study was the numbers of animals in each treatment group. For effective statistical analysis there should be at least 6 animals in each group. This study does nevertheless provide strong preliminary data as to the efficacy of

AdCTLA4-EGFP transduced ovine DC in attenuating ovine skin allograft rejection in an immunologically reconstituted NOD-*scid* mouse model. In addition to increasing the experimental numbers, transplantation of skin from two different sheep onto the dorsal flank of single mice, followed by challenge with allogeneic lymphocytes and AdCTLA4-EGFP transduced DC autologous to one skin donor could be performed to assess the allo-specificity of the treatment.

In summary, this chapter reports the characterisation of a short-term murine model of vascularised ovine skin allograft rejection. The model provides an effective means to screen novel immuno-therapies *in vivo* prior to the application in the ovine renal transplant model. Furthermore, consistent with the findings of O'Rourke (253), we demonstrate that DC transfected with AdCTLA4-EGFP inhibit alloreactivity *in vivo* without the requirement for systemic immunosuppression.

Chapter 7

Concluding Remarks

7.1. Concluding Remarks and Future Directions

Due to the limitations of current immunosuppressive drugs, development of novel immunotherapies and drugs is required. Increasingly the focus of transplant research is swaying away from immunosuppressive regimes towards the induction of tolerance, which holds promise for permanent allograft survival in the absence of immunosuppressive drugs. The antigen presenting properties of DC are being harnessed for gene therapy applications due to their potential to induce alloreactive T cell hyporesponsiveness by 1) allowing allopresentation in the absence of sufficient costimulation, 2) providing signals to induce alloreactive T cell apoptosis or 3) engagement of negative signaling pathways including PD-1 (115, 316, 318, 425, 478). The primary benefit of genetic modification of DC is the ability of these cells to migrate to secondary lymphoid tissues and interact with naïve T cells, thereby overcoming the requirement for systemic immunosuppression.

While the use of immature DC or genetically modified DC has prolonged allograft survival in murine models, data in large animal transplant models is limited. Thus this thesis focussed on the development and characterisation of ovine DC genetically modified to produce CTLA4 fusion proteins in order to provide *in vivo* proof of function for use in an ovine model of renal transplantation.

In **chapter 4** DC were isolated by pseudoafferent cannulation of the prefemoral lymphatics of sheep. The DC were characterised for their suitability as vehicles for gene therapy to induce alloreactive T cell hyporesponsiveness. The DC fulfilled the primary requirements in that they express high levels of MHC Class II complex, were able to migrate to sites of antigen presentation *in vivo* and interact with alloreactive T cells. While clinical applications of DC therapies will certainly utilise monocyte-derived DC as these

cells represent a homologous DC population with a controlled maturation status, the generation of DC from ovine monocytes is still in its infancy (410) although further progression of this research will have profound benefits to the sheep model.

In **chapter 5** an adenoviral construct incorporating the fusion of the extracellular domain of ovine CTLA4 with an EGFP tag was generated and characterised. The CTLA4-EGFP fusion protein proved to be functional in that it was capable of binding to CD80/86 on ovine and human DC thereby inhibiting alloreactive T cell proliferation *in vitro*. In addition to providing a target for immunological detection, the EGFP fusion tag also facilitated the direct monitoring of transfection efficiency due to its inherent fluorescence. The EGFP protein did not appear to affect the functional activity of CTLA4 as binding to CD80/86 on DC and inhibition of alloreactive T cell proliferation was demonstrated consistent with ovine CTLA4-Ig, which was also generated in this study. Consistent with the modification of murine DC with AdCTLA4-Ig (425), ovine and human DC transduced with AdCTLA4-EGFP demonstrated autocrine/paracrine binding of secreted CTLA4-EGFP resulting in the induction of alloreactive T cell hyporesponsiveness. Upregulation of IDO expression as a result of both adenoviral transfection (444) and CTLA4-EGFP engagement of CD80/86 (106) may also play a role, although this was not investigated in this study.

As the maximal transfection efficiency of ovine DC was 75%, flow sorting could be conducted in future studies to achieve close to 100% purity of CTLA4-EGFP DC transfectants, which may further improve the inhibitory effects demonstrated in the DC-MLR. Higher levels of transfected DC may also enhance their therapeutic potential in transplantation.

Chapter 6 provided proof of function that ovine DC transfected with AdCTLA4-EGFP are capable of inhibiting alloreactivity *in vivo*. The model used was a short-term chimeric NOD-*scid* mouse model. The unchallenged immunodeficient mice permitted indefinite engraftment of ovine skin allografts. Subsequent immune challenge with allogeneic ovine PBMC and DC autologous to the skin donor resulted in histological rejection characterised by high levels of $CD4^+$ and $CD8^+$ lymphocyte infiltrates within the skin allograft. AdCTLA4-EGFP transfected DC inhibited skin allograft rejection and were identified in the skin grafts by fluorescence and PCR detection. Soluble CTLA4-EGFP was not detected in the serum of NOD-*scid* mice, which supports the role of autocrine/paracrine secretion of the fusion protein by the DC to induce *in vivo* hyporesponsiveness. Although this model does not investigate tolerance induction, attenuation of the direct pathway of allorecognition which is a key mechanism in acute allograft rejection (188) was clearly demonstrated. Hence the results obtained in this study support further testing of AdCTLA4-EGFP transfected DC in the ovine model of renal transplantation.

The ovine transplant model (**1.15**) provides a good representation of human renal transplantation and will allow further elucidation of the mechanisms of action of AdCTLA4-EGFP transduced DC such as the induction of tolerance, the influence of the indirect pathway of allorecognition and the generation of T_{reg} cells. The utility of the ovine model is supported by the growing immunological "toolbox" which includes numerous ovine-specific antibodies and reagents, in addition to genomic sequencing data and the ability to generate twin sheep. Such a support nextwork has and will continue to aid the development and utility of this large animal model. Proteonomic and microarray analysis of rejecting/tolerised allografts and draining lymph can further be used to generate a

diagnostic profile of rejection and tolerance in sheep, which then can be applied to human transplantation.

The indication from other DC therapies is that multiple pathways may need to be targeted to induce long-term allograft acceptance. Notably DC transfected with adenoviral vectors encoding IL-10 and TGFβ provided increased efficacy compared to either agent alone and allograft survival was further enhanced by concomitant infusion of CHO cells transfected with cDNA for murine OX-2 (479). Moreover while DC transfected with AdCTLA4-Ig prolonged islet allograft survival (253), in another model AdCTLA4-Ig transfected DC had no significant effect on cardiac survival unless the DC were also treated with NFκβ decoy oligonucleotides (329). Therefore it is likely that AdCTLA4-EGFP transfected DC will require further modifications. IL-10 may be suitable for combination therapy due to the diversity in its mode of action. In addition to the inhibition of NF-κβ, which has been shown to synergise with CTLA4-Ig treatment of DC, IL-10 is also able to attenuate CD80, CD86 and CD40 costimulatory molecules expression and inhibit Th1 cytokine production including IL-12. Indeed in **chapter 3** the combined treatment of the human DC-MLR with sub-optimal doses of CTLA4-Ig and IL-10 provided greater inhibition than either agent alone with inhibition of both $CD4^+$ and $CD8^+$ T cells. The combined effect of CTLA4-Ig and IL-10 was most evident upon restimulation of T cells with 80% inhibition of the secondary MLR in the absence of both agents, indicating the induction of T cell anergy. Sub-optimal doses of each agent were investigated in this study to determine the contributions of each agent without either one overwhelming the response. For therapeutic use, DC would be transfected with adenoviral vectors encoding the two proteins with maximal expression of both desired. Transfection of DC with AdIL-10

induces maturation arrest characterised by low levels of CD80/86 and CD40 expression (171, 319, 320). Moreover IL-10 is able to inhibit NFκβ and IL-12 production by DC (164, 183, 184). AdIL-10 treatment of DC is therein likely to augment the effects of AdCTLA4-EGFP treatment by limiting CD80/86 expression, subsequently reducing the amount of CTLA4-EGFP required to sequester these ligands. Down-regulation of CD40 and NFκβ by IL-10 further targets pathways reported to synergise with CTLA4 fusion proteins (329, 347). Cotransfection of DC with AdCTLA4-EGFP may also benefit AdIL-10 treatment by acting as a safeguard against DC maturation in that CTLA4-EGFP can block CD80/86 ligands as they are upregulated.

In **chapter 3** we also reported that NK cells are potentially able to render autologous T cells and allogeneic DC susceptible to the inhibitory effects of sub-optimal doses of IL-10 and CTLA4-Ig, providing evidence for the potential interaction between innate and adaptive immunity. Indeed the role of NK cells in allograft rejection is becoming more evident with the induction of tolerance not evident in some studies unless NK cells are depleted (375, 376). Thus therapeutic strategies that involve the combination of CTLA4-Ig and IL-10 may be effective in promoting allograft tolerance by targeting NK cells associated with DC-T cell interactions.

An attempt was made to generate an adenoviral construct incorporating a fusion between ovine IL-10 and DsRED2. DsRED2 was selected so as to provide a fluorescent contrast against CTLA4-EGFP, which would permit quantification of the efficiency of transfection of each agent. While DsRED2 as a fusion partner demonstrated fluorescence, the protein masked the functional activity of IL-10 as a result of tetrameric formation. Newer DsRED mutants which do not form tetrameric structures may be more suitable

fusion partners and would allow further investigation into the combined effects of DC transfected with adenoviral CTLA4-EGFP and adenoviral IL-10-RED *in vitro* and *in vivo*.

While adenoviral vectors provide an invaluable research tool for the genetic modification of cells and tissues, there are currently no adenoviral therapies approved for clinical application. Indeed the recent death of a patient during an adenoviral gene therapy pilot (safety) clinical trial to treat partial ornithine transcarbamylase (OTC) deficiency is likely to limit the translation of adenoviral therapies to the clinic (287). While *ex vivo* manipulation of DC is likely to limit the exposure of adenoviral particles to the host, as non-viral transfection techniques improve, they are likely to be the vectors of choice. Nevertheless while adenoviral therapies are unlikely to make the clinic, they still provide the highest levels of transfection efficiency and allow vital proof of concept for novel therapies in animal models.

In conclusion this study has identified IL-10 as a potential adjunct agent to improve CTLA4 fusion protein therapy. Moreover this study has also provided useful proof of concept for the gene transfection of ovine DC with an adenoviral construct encoding a CTLA4-EGFP fusion construct to inhibit alloreactivity. AdCTLA4-EGFP transfected DC inhibited alloreactive T cell activation *in vitro* attributed to the blockade of the CD28 costimulatory pathway by autocrine/paracrine production of CTLA4-EGFP. Moreover when applied to a NOD-*scid* mouse model of ovine skin allograft rejection, AdCTLA4-EGFP transduced DC prevented rejection while negating the requirement for systemic immunosuppressive treatment. Moreover the inherent fluorescence of the CTLA4-EGFP fusion provided advantages over the classical CTLA4-Ig constructs in that cell migration and transfection efficiencies were readily determined. These results support the application of AdCTLA4-EGFP transfected DC in the preclinical ovine model of renal transplantation.

Appendices

PCR Target	Product size	Primer	Primer Sequence	RE Site
Ovine CTLA4 for EGFP cloning	507bp	Forward	5' GGG*AGATC*T***ATG**GCTTGCTCTGGATTCCAGAGTC 3'	BglII
		Reverse	5' GA*GGTAC*C*GAATCCGGGCATGGTTCTGGA 3'	*Kpn1*
Ovine CTLA4 for IgG cloning	507 bp	Forward	5' GGG*A*AGCTT***ATG**GCTTGCTCTGGATTCCAGAGTC 3'	*HindIII*
		Reverse	5' GA*G*AATTC*GAATCCGGGCATGGTTCTGGA 3'	*EcoR1*
Ovine IgG	687bp	Forward	5' GGG*GCGGCC*GC*TCATTTACCCGGAGGCTTAGA 3'	*EcoRV*
		Reverse	5' GA*GAT*ATC*GAATCCGGGCATGGTTCTGGA 3'	*Not1*
Ovine IL-10	530bp	Forward	5' GG*AGATC*T***ATG**CCCAGCAGCTCAGCCG 3'	*BglII*
		Reverse	5' CA*A*AGCTT*CATCTTCGTTGTCATGTA 3'	*HindIII*
β-Actin	850bp	Forward	5' ATCATGTTTGAGACCTTCAA 3'	
		Reverse	5' CATCTCTTGCTCGAAGTCCA 3'	
Ovine IL-2	409bp	Forward	5' AACTCTTGTCTTGCATT 3'	
		Reverse	5' GATGCTTTGACAAAAGGT 3'	

Appendix 1: Primers.
Primers for CTLA4, IgG and IL-10 were used for cloning and screening of plasmids for correct insertion. Forward and reverse primers incorporated restriction endonuclease sites identified by blue italics font with the cut site indicated by *. **ATG** start codons for the CTLA4 and IL-10 genes are shown in bold.

A

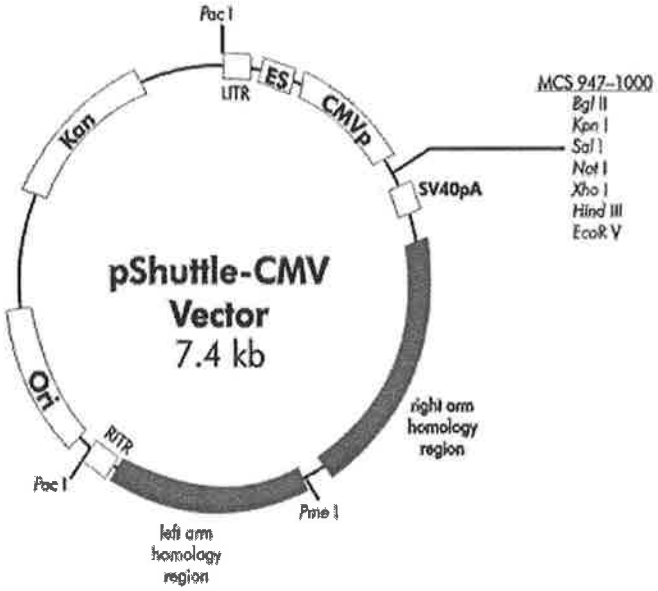

B

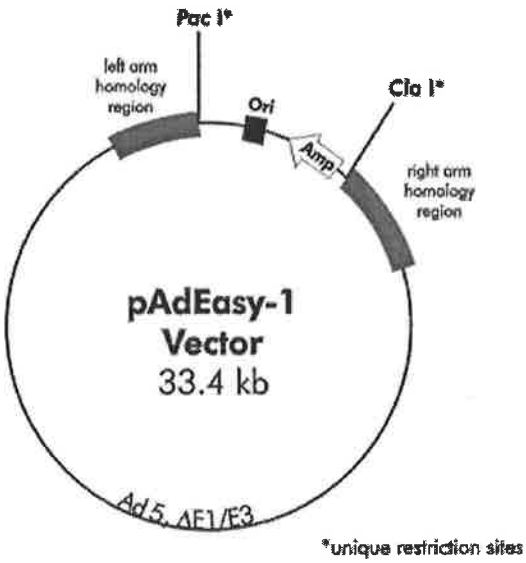

Appendix 2. Adenoviral Vectors

A) Features of the pShuttleCMV vector include the presence of a multiple cloning site (MCS), left arm and right arm homology regions and a kanamycin resistance gene.
B) pAdEasy-1 vector contains the genomic material of a human serotype 5 adenovirus. The deletion of the E1 gene renders the adenovirus replication deficient by preventing the assembly of infectious viral particles. The pAdEasy-1 vector also contains left arm and right arm homology regions as well as an ampicillin resistance gene.

Appendix 3: Ovine CTLA4 Sequence from CTLA4-EGFP

Amino acid and nucleotide sequences represent consensus sequences of the extracellular domain of ovine CTLA4 obtained from forward and reverse CTLA4 primer sequencing of the ovine CTLA4-EGFP plasmid.

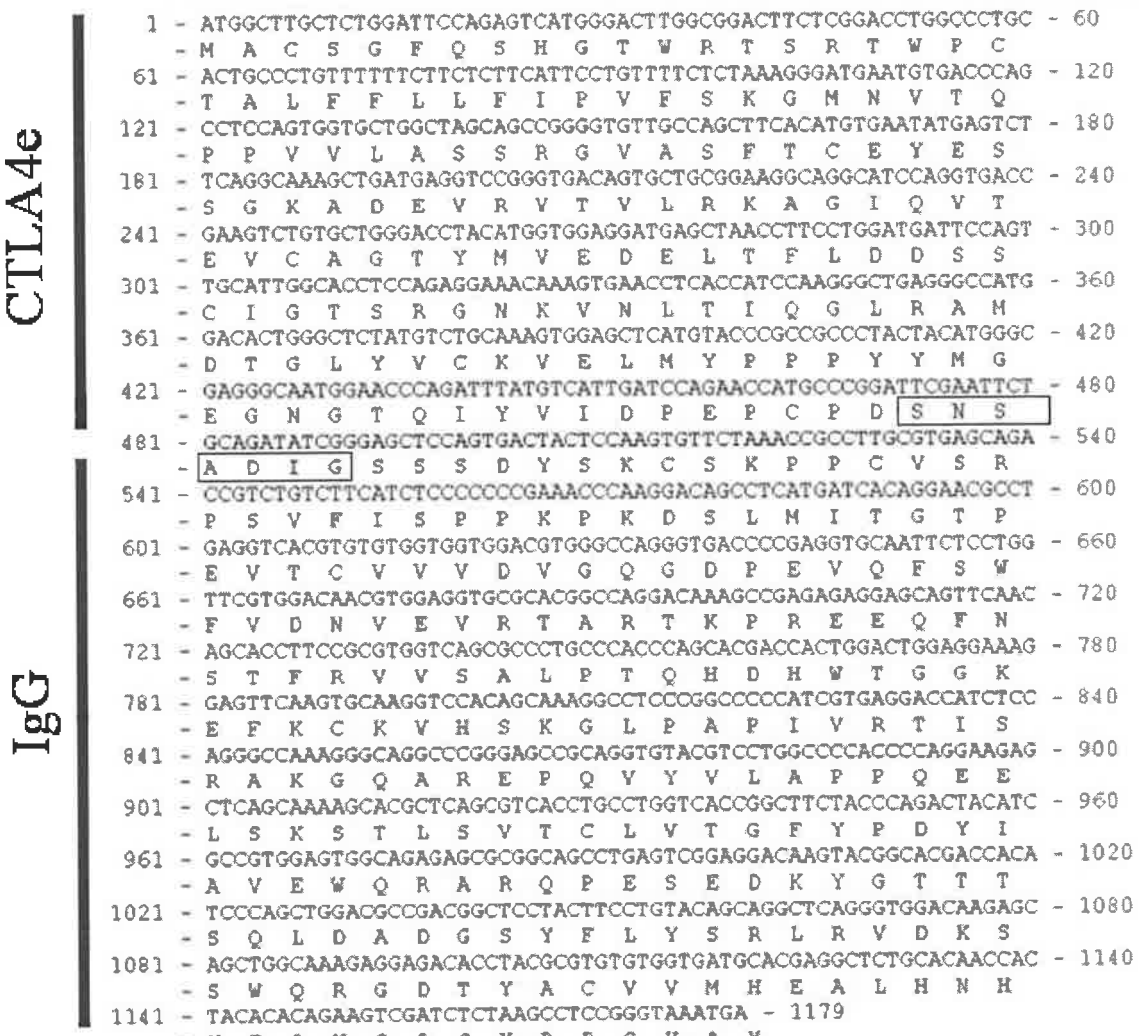

Appendix 4: Ovine CTLA4-Ig Sequence

Amino acid and nucleotide sequences represent consensus sequences obtained from forward CTLA4 and reverse IgG primer sequencing of the ovine CTLA4-IgG plasmid. The extracellular domain of CTLA4 and hinge-CH2/CH3 domains of IgG are marked by the green and blue regions respectively. Boxed amino acids account for the plasmid coding region between the two genes.

IL10

Appendix 5: Ovine IL-10 Sequence from IL-10-DsRED2

Amino acid and nucleotide sequences represent consensus sequences obtained from forward and reverse IL-10 primer sequencing of the ovine IL-10-DsRED2 plasmid.

Rererence List

References

1. Lafferty J, Woolnough, J. 1977. The origin and mechanism of the allograft rejection. *Immunol. Rev.* 35: 231-49

2. Viola A, Lanzavecchia A. 1996. T cell activation determined by T cell receptor number and tunable thresholds. *Science* 273: 104-6

3. Schwartz RH. 1996. Models of T cell anergy: is there a common molecular mechanism? *J Exp Med* 184: 1-8

4. Schwartz RH. 1990. A cell culture model for T lymphocyte clonal anergy. *Science* 4961: 1349-56

5. Matsui K, Boniface JJ, Steffner P, Reay PA, Davis MM. 1994. Kinetics of T-cell receptor binding to peptide/I-Ek complexes: correlation of the dissociation rate with T-cell responsiveness. *Proc Natl Acad Sci U S A* 91: 12862-6

6. Iezzi G, Karjalainen K, Lanzavecchia A. 1998. The duration of antigenic stimulation determines the fate of naive and effector T cells. *Immunity* 8: 89-95

7. Monks CR, Freiberg BA, Kupfer H, Sciaky N, Kupfer A. 1998. Three-dimensional segregation of supramolecular activation clusters in T cells. *Nature* 395: 82-6

8. Grakoui A, et al.,. 1999. The immunological synapse: a molecular machine controlling T cell activation. *Science* 285: 221-7

9. Huppa J, Davis, M. 2003. T-cell-antigen recognition and the immunological synapse. *Nat. Rev. Immunol.* 3: 973-

10. Bunnell SC, Hong DI, Kardon JR, Yamazaki T, McGlade CJ, Barr VA, Samelson LE. 2002. T cell receptor ligation induces the formation of dynamically regulated signaling assemblies. *J Cell Biol* 158: 1263-75

11. Wetzel SA, McKeithan TW, Parker DC. 2002. Live-cell dynamics and the role of costimulation in immunological synapse formation. *J Immunol* 169: 6092-101

12. Wild MK, Cambiaggi A, Brown MH, Davies EA, Ohno H, Saito T, van der Merwe PA. 1999. Dependence of T cell antigen recognition on the dimensions of an accessory receptor-ligand complex. *J Exp Med* 190: 31-41

13. Green JM, Karpitskiy V, Kimzey SL, Shaw AS. 2000. Coordinate regulation of T cell activation by CD2 and CD28. *J Immunol* 164: 3591-5

14. Lucas PJ, Negishi, I., Nakayama, K., Fields, L.E., Loh, D.Y. 1997. Naive CD28-deficient T cells can initiate but not sustain an in vitro antigen-specific immune response. *J. Immunol.* 154: 5757-68

15. Shahinian A, Pfeffer K, Lee KP, Kundig TM, Kishihara K, Wakeham A, Kawai K, Ohashi PS, Thompson CB, Mak TW. 1993. Differential T cell costimulatory requirements in CD28-deficient mice. *Science* 261: 609-12

16. Lucas PJ, Negishi I, Nakayama K, Fields LE, Loh DY. 1995. Naive CD28-deficient T cells can initiate but not sustain an in vitro antigen-specific immune response. *J Immunol* 154: 5757-68

17. Girvin AM, Dal Canto MC, Rhee L, Salomon B, Sharpe A, Bluestone JA, Miller SD. 2000. A critical role for B7/CD28 costimulation in experimental autoimmune encephalomyelitis: a comparative study using costimulatory molecule-deficient mice and monoclonal antibody blockade. *J Immunol* 164: 136-43

18. Tada Y, Nagasawa K, Ho A, Morito F, Ushiyama O, Suzuki N, Ohta H, Mak TW. 1999. CD28-deficient mice are highly resistant to collagen-induced arthritis. *J Immunol* 162: 203-8

19. June CH, Bluestone JA, Nadler LM, Thompson CB. 1994. The B7 and CD28 receptor families. *Immunol Today* 15: 321-31

20. Gross JA, Callas E, Allison JP. 1992. Identification and distribution of the costimulatory receptor CD28 in the mouse. *J Immunol* 149: 380-8

21. Azuma M, Ito D, Yagita H, Okumura K, Phillips JH, Lanier LL, Somoza C. 1993. B70 antigen is a second ligand for CTLA-4 and CD28. *Nature* 366: 76-9

22. Andres PG, Howland KC, Dresnek D, Edmondson S, Abbas AK, Krummel MF. 2004. CD28 signals in the immature immunological synapse. *J Immunol* 172: 5880-6

23. Shaw AS, Dustin, M.L. 1997. Making the T cell receptor go the distance: a topological view of T cell activation. *Immunity* 6: 361-9.

24. Bromley SK, Laboni, A., Davis, S.J., Whitty, A., Green, J.M., Shaw, A.S., Weiss, A., Dustin, M.L. 2001. The immunological synapse and CD28-CD80 interactions. *Nat. Immunol.* 2: 1159-66

25. Thompson CB, Lindsten T, Ledbetter JA, Kunkel SL, Young HA, Emerson SG, Leiden JM, June CH. 1989. CD28 activation pathway regulates the production of multiple T-cell-derived lymphokines/cytokines. *Proc Natl Acad Sci U S A* 86: 1333-7

26. Bluestone JA. 1997. Is CTLA-4 a master switch for peripheral T cell tolerance? *J Immunol* 158: 1989-93

27. Burr JS, Savage ND, Messah GE, Kimzey SL, Shaw AS, Arch RH, Green JM. 2001. Cutting edge: distinct motifs within CD28 regulate T cell proliferation and induction of Bcl-XL. *J Immunol* 166: 5331-5

28. Parra E, Mustelin T, Dohlsten M, Mercola D. 2001. Identification of a CD28 response element in the CD40 ligand promoter. *J Immunol* 166: 2437-43

29. McAdam AJ, Chang, T.T., Lumelsky, A.E. 2000. Mouse inducible costimulatory molecule (ICOS) expression is enhanced by CD28 costimulation and regulates differentiation of CD4+ T cells. *J Immunol* 165: 5035

30. Su B, Jacinto, E., Hibi, M., Kallunki, T., Karin, M., Ben-Neriah, Y. 1994. JNK is involved in signal integration during costimulation of T lymphocytes. *Cell* 77: 727-36

31. Pages F, Ragueneau M, Rottapel R, Truneh A, Nunes J, Imbert J, Olive D. 1994. Binding of phosphatidylinositol-3-OH kinase to CD28 is required for T-cell signalling. *Nature* 369: 327-9

32. August A, Gibson S, Kawakami Y, Kawakami T, Mills GB, Dupont B. 1994. CD28 is associated with and induces the immediate tyrosine phosphorylation and activation of the Tec family kinase ITK/EMT in the human Jurkat leukemic T-cell line. *Proc Natl Acad Sci U S A* 91: 9347-51

33. Holdorf AD, Green JM, Levin SD, Denny MF, Straus DB, Link V, Changelian PS, Allen PM, Shaw AS. 1999. Proline residues in CD28 and the Src homology (SH)3 domain of Lck are required for T cell costimulation. *J Exp Med* 190: 375-84

34. Sanchez-Lockhart M, Marin E, Graf B, Abe R, Harada Y, Sedwick CE, Miller J. 2004. Cutting edge: CD28-mediated transcriptional and posttranscriptional regulation of IL-2 expression are controlled through different signaling pathways. *J Immunol* 173: 7120-4

35. Rao N, Dodge I, Band H. 2002. The Cbl family of ubiquitin ligases: critical negative regulators of tyrosine kinase signaling in the immune system. *J Leukoc Biol* 71: 753-63

36. Smit L, Borst J. 1997. The Cbl family of signal transduction molecules. *Crit Rev Oncog* 8: 359-79

37. Li D, Gal I, Vermes C, Alegre ML, Chong AS, Chen L, Shao Q, Adarichev V, Xu X, Koreny T, Mikecz K, Finnegan A, Glant TT, Zhang J. 2004. Cutting edge: Cbl-b: one of the key molecules tuning CD28- and CTLA-4-mediated T cell costimulation. *J Immunol* 173: 7135-9

38. Chambers CA, Sullivan TJ, Allison JP. 1997. Lymphoproliferation in CTLA-4-deficient mice is mediated by costimulation-dependent activation of CD4+ T cells. *Immunity* 7: 885-95

39. Brunet JF, Denizot F, Luciani MF, Roux-Dosseto M, Suzan M, Mattei MG, Golstein P. 1987. A new member of the immunoglobulin superfamily--CTLA-4. *Nature* 328: 267-70

40. Perkins D, Wang Z, Donovan C, He H, Mark D, Guan G, Wang Y, Walunas T, Bluestone J, Listman J, Finn PW. 1996. Regulation of CTLA-4 expression during T cell activation. *J Immunol* 156: 4154-9

41. Alegre ML, Noel PJ, Eisfelder BJ, Chuang E, Clark MR, Reiner SL, Thompson CB. 1996. Regulation of surface and intracellular expression of CTLA4 on mouse T cells. *J Immunol* 157: 4762-70

42. Lindsten T, Lee KP, Harris ES, Petryniak B, Craighead N, Reynolds PJ, Lombard DB, Freeman GJ, Nadler LM, Gray GS, et al. 1993. Characterization of CTLA-4 structure and expression on human T cells. *J Immunol* 151: 3489-99

43. Walunas TL, Lenschow DJ, Bakker CY, Linsley PS, Freeman GJ, Green JM, Thompson CB, Bluestone JA. 1994. CTLA-4 can function as a negative regulator of T cell activation. *Immunity* 1: 405-13

44. Dariavach P, Mattei MG, Golstein P, Lefranc MP. 1988. Human Ig superfamily CTLA-4 gene: chromosomal localization and identity of protein sequence between murine and human CTLA-4 cytoplasmic domains. *Eur J Immunol* 18: 1901-5

45. Linsley PS, Bradshaw J, Greene J, Peach R, Bennett KL, Mittler RS. 1996. Intracellular trafficking of CTLA-4 and focal localization towards sites of TCR engagement. *Immunity* 4: 535-43

46. Kupfer A, Swain SL, Singer SJ. 1987. The specific direct interaction of helper T cells and antigen-presenting B cells. II. Reorientation of the microtubule organizing center and reorganization of the membrane-associated cytoskeleton inside the bound helper T cells. *J Exp Med* 165: 1565-80

47. Shiratori T, Miyatake S, Ohno H, Nakaseko C, Isono K, Bonifacino JS, Saito T. 1997. Tyrosine phosphorylation controls internalization of CTLA-4 by regulating its interaction with clathrin-associated adaptor complex AP-2. *Immunity* 6: 583-9

48. Leung HT, Bradshaw J, Cleaveland JS, Linsley PS. 1995. Cytotoxic T lymphocyte-associated molecule-4, a high-avidity receptor for CD80 and CD86, contains an intracellular localization motif in its cytoplasmic tail. *J Biol Chem* 270: 25107-14

49. Masteller EL, Chuang E, Mullen AC, Reiner SL, Thompson CB. 2000. Structural analysis of CTLA-4 function in vivo. *J Immunol* 164: 5319-27

50. Chuang E, Alegre ML, Duckett CS, Noel PJ, Vander Heiden MG, Thompson CB. 1997. Interaction of CTLA-4 with the clathrin-associated protein AP50 results in ligand-independent endocytosis that limits cell surface expression. *J Immunol* 159: 144-51

51. Linsley PS, Greene JL, Tan P, Bradshaw J, Ledbetter JA, Anasetti C, Damle NK. 1992. Coexpression and functional cooperation of CTLA-4 and CD28 on activated T lymphocytes. *J Exp Med* 176: 1595-604

52. Jago CB, Yates, J., Camara, N.O., Lechler, R.I., Lombardi, G. 2004. Differential expression of CTLA-4 among T cell subsets. *Clin Exp Immunol* 136: 463-71

53. Halloran PF, Broski AP, Batiuk TD, Madrenas J. 1993. The molecular immunology of acute rejection: an overview. *Transpl Immunol* 1: 3-27

54. Linsley PS, Brady W, Urnes M, Grosmaire LS, Damle NK, Ledbetter JA. 1991. CTLA-4 is a second receptor for the B cell activation antigen B7. *J Exp Med* 174: 561-9

55. Parsons KR, Young JR, Collins BA, Howard CJ. 1996. Cattle CTLA-4, CD28 and chicken CD28 bind CD86: MYPPPY is not conserved in cattle CD28. *Immunogenetics* 43: 388-91

56. Metzler WJ, Bajorath, J., Fenderson, W., Shaw, S.Y., Constantine, K.L., et al.,. 1997. Solution structure of human CTLA-4 and delineation of a CD80/CD86 binding site conserved in CD28. *Nat. Struct. Biol.* 4: 527-31

57. Chaplin PJ, Pietrala LN, Scheerlinck JP. 1999. Cloning and sequence comparison of sheep CD28 and CTLA-4. *Immunogenetics* 49: 583-4

58. Schwartz JC, Zhang X, Fedorov AA, Nathenson SG, Almo SC. 2001. Structural basis for co-stimulation by the human CTLA-4/B7-2 complex. *Nature* 410: 604-8

59. Peach RJ, Bajorath J, Brady W, Leytze G, Greene J, Naemura J, Linsley PS. 1994. Complementarity determining region 1 (CDR1)- and CDR3-analogous regions in CTLA-4 and CD28 determine the binding to B7-1. *J Exp Med* 180: 2049-58

60. Ostrov DA, Shi, W., Schwartz, J.C.D, Almo, S.C., Nathenson, S.G. 2000. Structure of murine CTLA-4: a novel dimer modulating T cell responsiveness. *Science* 290: 816-9

61. Ikemizu S, Gilbert, R.J., Fennelly, J.A., Collins, A.V., Harlos, K., et al.,. 2000. Structure and dimerization of a soluble form of B7-1. *Immunity* 12: 51-60

62. Martin M, Schneider H, Azouz A, Rudd CE. 2001. Cytotoxic T lymphocyte antigen 4 and CD28 modulate cell surface raft expression in their regulation of T cell function. *J Exp Med* 194: 1675-81

63. Tivol EA, Borriello F, Schweitzer AN, Lynch WP, Bluestone JA, Sharpe AH. 1995. Loss of CTLA-4 leads to massive lymphoproliferation and fatal multiorgan tissue destruction, revealing a critical negative regulatory role of CTLA-4. *Immunity* 3: 541-7

64. Chambers CA, Cado D, Truong T, Allison JP. 1997. Thymocyte development is normal in CTLA-4-deficient mice. *Proc Natl Acad Sci U S A* 94: 9296-301

65. Khattri R, Auger JA, Griffin MD, Sharpe AH, Bluestone JA. 1999. Lymphoproliferative disorder in CTLA-4 knockout mice is characterized by CD28-regulated activation of Th2 responses. *J Immunol* 162: 5784-91

66. Tivol EA, Boyd SD, McKeon S, Borriello F, Nickerson P, Strom TB, Sharpe AH. 1997. CTLA4Ig prevents lymphoproliferation and fatal multiorgan tissue destruction in CTLA-4-deficient mice. *J Immunol* 158: 5091-4

67. Krummel MF, Allison JP. 1996. CTLA-4 engagement inhibits IL-2 accumulation and cell cycle progression upon activation of resting T cells. *J Exp Med* 183: 2533-40

68. Chen W, Jin W, Wahl SM. 1998. Engagement of cytotoxic T lymphocyte-associated antigen 4 (CTLA-4) induces transforming growth factor beta (TGF-beta) production by murine CD4(+) T cells. *J Exp Med* 188: 1849-57

69. Leach DR, Krummel MF, Allison JP. 1996. Enhancement of antitumor immunity by CTLA-4 blockade. *Science* 271: 1734-6

70. Luhder F, Hoglund P, Allison JP, Benoist C, Mathis D. 1998. Cytotoxic T lymphocyte-associated antigen 4 (CTLA-4) regulates the unfolding of autoimmune diabetes. *J Exp Med* 187: 427-32

71. Scheipers P, Reiser H. 1998. Fas-independent death of activated CD4(+) T lymphocytes induced by CTLA-4 crosslinking. *Proc Natl Acad Sci U S A* 95: 10083-8

72. Blair PJ, Riley JL, Levine BL, Lee KP, Craighead N, Francomano T, Perfetto SJ, Gray GS, Carreno BM, June CH. 1998. CTLA-4 ligation delivers a unique signal to resting human CD4 T cells that inhibits interleukin-2 secretion but allows Bcl-X(L) induction. *J Immunol* 160: 12-5

73. Chambers CA, Kuhns, M.S., Egan, J.G., Allison, J.P. 2001. CTLA-4-mediated inhibition in regulation of T cell responses; mechanisms and manipulation in tumor immunotherapy. *Annu. Rev. Immunol.* 19: 565-94

74. van der Merwe PA, Bodian DL, Daenke S, Linsley P, Davis SJ. 1997. CD80 (B7-1) binds both CD28 and CTLA-4 with a low affinity and very fast kinetics. *J Exp Med* 185: 393-403

75. Carreno BM, Bennett F, Chau TA, Ling V, Luxenberg D, Jussif J, Baroja ML, Madrenas J. 2000. CTLA-4 (CD152) can inhibit T cell activation by two different mechanisms depending on its level of cell surface expression. *J Immunol* 165: 1352-6

76. Nakaseko C, Miyatake S, Iida T, Hara S, Abe R, Ohno H, Saito Y, Saito T. 1999. Cytotoxic T lymphocyte antigen 4 (CTLA-4) engagement delivers an inhibitory signal through the membrane-proximal region in the absence of the tyrosine motif in the cytoplasmic tail. *J Exp Med* 190: 765-74

77. Baroja ML, Luxenberg D, Chau T, Ling V, Strathdee CA, Carreno BM, Madrenas J. 2000. The inhibitory function of CTLA-4 does not require its tyrosine phosphorylation. *J Immunol* 164: 49-55

78. Krummel MF, Allison JP. 1995. CD28 and CTLA-4 have opposing effects on the response of T cells to stimulation. *J Exp Med* 182: 459-65

79. Lin H, Rathmell, J.C., Gray, G.S. 1998. Cytotoxic T lymphocyte antigen 4 (CTLA4) blockade accelerates the acute rejection of cardiac allografts in CD28-deficient mice: CTLA4 can function independently of CD28. *J Exp Med* 188: 199

80. Chikuma S, Abbas AK, Bluestone JA. 2005. B7-independent inhibition of T cells by CTLA-4. *J Immunol* 175: 177-81

81. Egen JG, Allison JP. 2002. Cytotoxic T lymphocyte antigen-4 accumulation in the immunological synapse is regulated by TCR signal strength. *Immunity* 16: 23-35

82. Kuhns MS, Epshteyn, V., Sobel, R.A., Allison, J.P. 2000. CTLA-4 regulates the size, function, and reactivity of a primed pool of T cells. *Proc Natl Acad Sci U S A* 97

83. Lee KM, Chuang E, Griffin M, Khattri R, Hong DK, Zhang W, Straus D, Samelson LE, Thompson CB, Bluestone JA. 1998. Molecular basis of T cell inactivation by CTLA-4. *Science* 282: 2263-6

84. Bachmann MF, Gallimore A, Linkert S, Cerundolo V, Lanzavecchia A, Kopf M, Viola A. 1999. Developmental regulation of Lck targeting to the CD8 coreceptor controls signaling in naive and memory T cells. *J Exp Med* 189: 1521-30

85. Stein PH, Fraser, J.D., Weiss, A. 1994. The cytoplasmic domain of CD28 is both necessary and sufficient for costimulation of interleukin-2 secretion and association with phosphatidylinositol 3'-kinase. *Mol Cell Biol* 14: 3392-402

86. Fraser JH, Rincon M, McCoy KD, Le Gros G. 1999. CTLA4 ligation attenuates AP-1, NFAT and NF-kappaB activity in activated T cells. *Eur J Immunol* 29: 838-44

87. Pioli C, Gatta L, Frasca D, Doria G. 1999. Cytotoxic T lymphocyte antigen 4 (CTLA-4) inhibits CD28-induced IkappaBalpha degradation and RelA activation. *Eur J Immunol* 29: 856-63

88. Alegre ML, Shiels H, Thompson CB, Gajewski TF. 1998. Expression and function of CTLA-4 in Th1 and Th2 cells. *J Immunol* 161: 3347-56

89. Yokochi T, Holly RD, Clark EA. 1982. B lymphoblast antigen (BB-1) expressed on Epstein-Barr virus-activated B cell blasts, B lymphoblastoid cell lines, and Burkitt's lymphomas. *J Immunol* 128: 823-7

90. Freedman AS, Freeman G, Horowitz JC, Daley J, Nadler LM. 1987. B7, a B-cell-restricted antigen that identifies preactivated B cells. *J Immunol* 139: 3260-7

91. Freeman GJ, Borriello F, Hodes RJ, Reiser H, Hathcock KS, Laszlo G, McKnight AJ, Kim J, Du L, Lombard DB, et al. 1993. Uncovering of functional alternative CTLA-4 counter-receptor in B7-deficient mice. *Science* 262: 907-9

92. Freeman GJ, Gribben JG, Boussiotis VA, Ng JW, Restivo VA, Jr., Lombard LA, Gray GS, Nadler LM. 1993. Cloning of B7-2: a CTLA-4 counter-receptor that costimulates human T cell proliferation. *Science* 262: 909-11

93. Collins AV, Brodie, D.W., Gilbert, R.J.C., Iaboni, A., Manso-Sancho, R., et al.,. 2002. The interaction properties of costimulatory molecules revisited. *Immunity* 17: 201-10

94. Zhang X, Schwartz, J.C., Almo, S.C., Nathenson, S.G. 2002. Expression, refolding, purification, molecular characterization, crystallization, and preliminary X-ray analysis of the receptor binding domain of human B7-2. *Protein Expr. Purif.* 25: 105-13

95. Hathcock KS, Laszlo G, Pucillo C, Linsley P, Hodes RJ. 1994. Comparative analysis of B7-1 and B7-2 costimulatory ligands: expression and function. *J Exp Med* 180: 631-40

96. Ranheim EA, Kipps TJ. 1993. Activated T cells induce expression of B7/BB1 on normal or leukemic B cells through a CD40-dependent signal. *J Exp Med* 177: 925-35

97. Yang Y, Wilson JM. 1996. CD40 ligand-dependent T cell activation: requirement of B7-CD28 signaling through CD40. *Science* 273: 1862-4

98. Pentcheva-Hoang T, Egan, J.G., Wojnoonski, K., Allison, J.P. 2004. B7-1 and B7-2 selectively recruit CTLA4 and CD28 to the immunological synapse. *Immunity* 21: 401-13

99. Olsson C, Michaelsson, E., Parra, E., Pettersson, U., Lando, P.A., Dohlsten, M. 1998. Biased dependency of CD80 versus CD86 in the induction of transcription factors regulating the human IL-2 promoter. *International Immunology* 10: 499-506

100. Lenschow DJ, Zeng, Y., Hathcock, K.S. 1995. Inhibition of transplant rejection following treatment with anti-B7-2 and anti-B7-1 antibodies. *Transplantation* 60: 1171

101. Judge TA, Wu, Z., Zheng, X.G. 1999. The role of CD80, CD86 and CTLA4 in alloimmune responses and the induction of long-term allograft survival. *J Immunol* 162: 1947

102. Yamada A, Kishimoto, K., Dong, V.M. 2001. CD28-independent costimulation of T cells in alloimmune responses. *J Immunol* 167: 140

103. Salomon B, Lenschow DJ, Rhee L, Ashourian N, Singh B, Sharpe A, Bluestone JA. 2000. B7/CD28 costimulation is essential for the homeostasis of the CD4+CD25+ immunoregulatory T cells that control autoimmune diabetes. *Immunity* 12: 431-40

104. Tang Q, Henriksen KJ, Boden EK, Tooley AJ, Ye J, Subudhi SK, Zheng XX, Strom TB, Bluestone JA. 2003. Cutting edge: CD28 controls peripheral homeostasis of CD4+CD25+ regulatory T cells. *J Immunol* 171: 3348-52

105. Taylor PA, Lees CJ, Fournier S, Allison JP, Sharpe AH, Blazar BR. 2004. B7 expression on T cells down-regulates immune responses through CTLA-4 ligation via T-T interactions [corrections]. *J Immunol* 172: 34-9

106. Grohmann U, Orabona C, Fallarino F, Vacca C, Calcinaro F, Falorni A, Candeloro P, Belladonna ML, Bianchi R, Fioretti MC, Puccetti P. 2002. CTLA-4-Ig regulates tryptophan catabolism in vivo. *Nat Immunol* 3: 1097-101

107. Fallarino F, Grohmann U, Hwang KW, Orabona C, Vacca C, Bianchi R, Belladonna ML, Fioretti MC, Alegre ML, Puccetti P. 2003. Modulation of tryptophan catabolism by regulatory T cells. *Nat Immunol* 4: 1206-12

108. Munn DH, Sharma MD, Mellor AL. 2004. Ligation of B7-1/B7-2 by human CD4+ T cells triggers indoleamine 2,3-dioxygenase activity in dendritic cells. *J Immunol* 172: 4100-10

109. Orabona C, Grohmann U, Belladonna ML, Fallarino F, Vacca C, Bianchi R, Bozza S, Volpi C, Salomon BL, Fioretti MC, Romani L, Puccetti P. 2004. CD28 induces immunostimulatory signals in dendritic cells via CD80 and CD86. *Nat Immunol* 5: 1134-42

110. Podojil JR, Sanders VM. 2003. Selective regulation of mature IgG1 transcription by CD86 and beta 2-adrenergic receptor stimulation. *J Immunol* 170: 5143-51

111. Podojil JR, Kin NW, Sanders VM. 2004. CD86 and beta2-adrenergic receptor signaling pathways, respectively, increase Oct-2 and OCA-B Expression and binding to the 3'-IgH enhancer in B cells. *J Biol Chem* 279: 23394-404

112. Agata Y, Kawasaki A, Nishimura H, Ishida Y, Tsubata T, Yagita H, Honjo T. 1996. Expression of the PD-1 antigen on the surface of stimulated mouse T and B lymphocytes. *Int Immunol* 8: 765-72

113. Liang SC, Latchman YE, Buhlmann JE, Tomczak MF, Horwitz BH, Freeman GJ, Sharpe AH. 2003. Regulation of PD-1, PD-L1, and PD-L2 expression during normal and autoimmune responses. *Eur J Immunol* 33: 2706-16

114. Parry RV, Chemnitz JM, Frauwirth KA, Lanfranco AR, Braunstein I, Kobayashi SV, Linsley PS, Thompson CB, Riley JL. 2005. CTLA-4 and PD-1 Receptors Inhibit T-Cell Activation by Distinct Mechanisms. *Mol Cell Biol* 25: 9543-53

115. Gao W, Demirci G, Strom TB, Li XC. 2003. Stimulating PD-1-negative signals concurrent with blocking CD154 co-stimulation induces long-term islet allograft survival. *Transplantation* 76: 994-9

116. Greenwald RJ, Freeman GJ, Sharpe AH. 2005. The B7 family revisited. *Annu Rev Immunol* 23: 515-48

117. Watanabe N, Gavrieli, M., Sedy, J.R., Yang, J., Fallarino, F., Loftin, S.K., Hurchla, M.A., Zimmerman, N., Sim, J., Zang, X., Murphy, T.L., Russell, J.H., Allison, J.P., Murphy, K.M. 2003. BTLA is a lymphocyte inhibitor receptor with similarities to CTLA-4 and PD-1. *Nat Immunol* 4: 647-8

118. Vallejo AN, Bryl E, Klarskov K, Naylor S, Weyand CM, Goronzy JJ. 2002. Molecular basis for the loss of CD28 expression in senescent T cells. *J Biol Chem* 277: 46940-9

119. Dennett NS, Barcia RN, McLeod JD. 2002. Age associated decline in CD25 and CD28 expression correlate with an increased susceptibility to CD95 mediated apoptosis in T cells. *Exp Gerontol* 37: 271-83

120. Bryl E, Vallejo AN, Weyand CM, Goronzy JJ. 2001. Down-regulation of CD28 expression by TNF-alpha. *J Immunol* 167: 3231-8

121. Walker LS, McLeod JD, Boulougouris G, Patel YI, Hall ND, Sansom DM. 1998. Down-regulation of CD28 via Fas (CD95): influence of CD28 on T-cell apoptosis. *Immunology* 94: 41-7

122. Ma S, Ochi H, Cui L, He W. 2003. FasL-induced downregulation of CD28 expression on jurkat cells in vitro is associated with activation of caspases. *Cell Biol Int* 27: 959-64

123. Swigut T, Shohdy N, Skowronski J. 2001. Mechanism for down-regulation of CD28 by Nef. *Embo J* 20: 1593-604

124. Gamberg J, Pardoe I, Bowmer MI, Howley C, Grant M. 2004. Lack of CD28 expression on HIV-specific cytotoxic T lymphocytes is associated with disease progression. *Immunol Cell Biol* 82: 38-46

125. Fessler BJ, Paliogianni F, Hama N, Balow JE, Boumpas DT. 1996. Glucocorticoids modulate CD28 mediated pathways for interleukin 2 production in human T cells: evidence for posttranscriptional regulation. *Transplantation* 62: 1113-8

126. Butler JJ, Cochran J, Ward N, Hoskin DW. 2002. Activation-induced expression of cell surface CD28 on mouse T lymphocytes is inhibited by cyclosporine A. *Am J Transplant* 2: 215-22

127. Fiorentino DF, Bond MW, Mosmann TR. 1989. Two types of mouse T helper cell. IV. Th2 clones secrete a factor that inhibits cytokine production by Th1 clones. *J Exp Med* 170: 2081-95

128. Mosmann TR, Moore KW. 1991. The role of IL-10 in crossregulation of TH1 and TH2 responses. *Immunol Today* 12: A49-53

129. Moore KW, Vieira P, Fiorentino DF, Trounstine ML, Khan TA, Mosmann TR. 1990. Homology of cytokine synthesis inhibitory factor (IL-10) to the Epstein-Barr virus gene BCRFI. *Science* 248: 1230-4

130. Vieira P, de Waal-Malefyt, R., Dand, M.N., Johnson, K.E., Kastelein, R., Fiorentino, D.F., deVries, J.E., Roncarolo, M.G., Mosmann, T.R., Moore, K.W. 1991. Isolation and expression of human cytokine synthesis inhibitory factor (CFIF/IL10) cDNA clones: homology to Epstein-Barr virus open reading frame BCRFI. *Proc Natl Acad Sci U S A* 88: 1172-6

131. Moore K.W. OGA, de Waale Malefyt R., Vieira P., Mosmann T.R. 1993. Interleukin-10. *Annu Rev Immunol* 11: 165-90

132. Howard M, O'Garra A, Ishida H, de Waal Malefyt R, de Vries J. 1992. Biological properties of interleukin 10. *J Clin Immunol* 12: 239-47

133. Kang KH, Im SH. 2005. Differential regulation of the IL-10 gene in Th1 and th2 T cells. *Ann N Y Acad Sci* 1050: 97-107

134. Fiorentino DF, Zlotnik A, Vieira P, Mosmann TR, Howard M, Moore KW, O'Garra A. 1991. IL-10 acts on the antigen-presenting cell to inhibit cytokine production by Th1 cells. *J Immunol* 146: 3444-51

135. Witsch EJ, Peiser M, Hutloff A, Buchner K, Dorner BG, Jonuleit H, Mages HW, Kroczek RA. 2002. ICOS and CD28 reversely regulate IL-10 on re-activation of human effector T cells with mature dendritic cells. *Eur J Immunol* 32: 2680-6

136. Kube D, Platzer C, von Knethen A, Straub H, Bohlen H, Hafner M, Tesch H. 1995. Isolation of the human interleukin 10 promoter. Characterization of the promoter activity in Burkitt's lymphoma cell lines. *Cytokine* 7: 1-7

137. Spits H, De Waal Malefyt, R. 1992. Functional characterization of human IL-10. *Int. Arch. Allergy Appl. Immunol.* 99: 8–15.

138. Platzer C, Volk, H.D., and Platzer, M. 1994. 5' noncoding sequence of human IL-10 gene obtained by oligo-cassete PCR walking. *DNA Seq.* 4: 399–401

139. Tone M, Powell MJ, Tone Y, Thompson SA, Waldmann H. 2000. IL-10 gene expression is controlled by the transcription factors Sp1 and Sp3. *J Immunol* 165: 286-91

140. Powell MJ, Thompson SA, Tone Y, Waldmann H, Tone M. 2000. Posttranscriptional regulation of IL-10 gene expression through sequences in the 3'-untranslated region. *J Immunol* 165: 292-6

141. Moore K.W. dWM, Coffman R.L., O'Garra A. 2001. Interleukin-10 and the Interleukin-10 Receptor. *Annu Rev Immunol* 19: 683-765

142. Zdanov A, Schalk-Hihi C, Wlodawer A. 1996. Crystal structure of human interleukin-10 at 1.6 A resolution and a model of a complex with its soluble receptor. *Protein Sci* 5: 1955-62

143. Zdanov A, Schalk-Hihi C, Menon S, Moore KW, Wlodawer A. 1997. Crystal structure of Epstein-Barr virus protein BCRF1, a homolog of cellular interleukin-10. *J Mol Biol* 268: 460-7

144. Shanafelt AB, Miyajima, A., Kitamura, T., Kastelein, R.A. 1991. The amino-terminal helix of GM-CSF and IL-5 governs high-affinity binding to their receptors. *Embo J* 10: 4105-12

145. Kim JM, Brannan, C.I., Copeland, N.G., Jenkins, N.A., Khan, T.A., Moore, K.W. 1992. Structure of the mouse interleukin-10 gene and chromosomal localisation of the mouse and human genes. *J. Immunol.* 148: 3618-23

146. Baer R, Bankier, A.T., Biggin, M.D., Deininger, P.L., Farrell, P.J., Gibson, T.J., Hatfull, G., Hudson, G.S., Satchwell, S.C., Seguin, C., Tuffnell, P.T., Barrell, B.G. 1984. DNA sequence and expression of the B95-8 Epstein-Barr virus genome. *Nature* 310: 207-11

147. Liu Y, Wei SH, Ho AS, de Waal Malefyt R, Moore KW. 1994. Expression cloning and characterization of a human IL-10 receptor. *J Immunol* 152: 1821-9

148. Gibbs VC, Pennica D. 1997. CRF2-4: isolation of cDNA clones encoding the human and mouse proteins. *Gene* 186: 97-101

149. Kotenko SV, Krause CD, Izotova LS, Pollack BP, Wu W, Pestka S. 1997. Identification and functional characterization of a second chain of the interleukin-10 receptor complex. *Embo J* 16: 5894-903

150. Spencer SD, Di Marco F, Hooley J, Pitts-Meek S, Bauer M, Ryan AM, Sordat B, Gibbs VC, Aguet M. 1998. The orphan receptor CRF2-4 is an essential subunit of the interleukin 10 receptor. *J Exp Med* 187: 571-8

151. Lutfalla G, Gardiner K, Uze G. 1993. A new member of the cytokine receptor gene family maps on chromosome 21 at less than 35 kb from IFNAR. *Genomics* 16: 366-73

152. Corinti S, Albanesi C, la Sala A, Pastore S, Girolomoni G. 2001. Regulatory activity of autocrine IL-10 on dendritic cell functions. *J Immunol* 166: 4312-8

153. Steinbrink K, Wolfl M, Jonuleit H, Knop J, Enk AH. 1997. Induction of tolerance by IL-10-treated dendritic cells. *J Immunol* 159: 4772-80

154. Kuhn R, Lohler J, Rennick D, Rajewsky K, Muller W. 1993. Interleukin-10-deficient mice develop chronic enterocolitis. *Cell* 75: 263-74

155. Yang X, Gartner J, Zhu L, Wang S, Brunham RC. 1999. IL-10 gene knockout mice show enhanced Th1-like protective immunity and absent granuloma formation following Chlamydia trachomatis lung infection. *J Immunol* 162: 1010-7

156. Murray PJ, Young RA. 1999. Increased antimycobacterial immunity in interleukin-10-deficient mice. *Infect Immun* 67: 3087-95

157. Tournoy KG, Kips JC, Pauwels RA. 2000. Endogenous interleukin-10 suppresses allergen-induced airway inflammation and nonspecific airway responsiveness. *Clin Exp Allergy* 30: 775-83

158. Grunig G, Corry DB, Leach MW, Seymour BW, Kurup VP, Rennick DM. 1997. Interleukin-10 is a natural suppressor of cytokine production and inflammation in a murine model of allergic bronchopulmonary aspergillosis. *J Exp Med* 185: 1089-99

159. Go NF, Castle BE, Barrett R, Kastelein R, Dang W, Mosmann TR, Moore KW, Howard M. 1990. Interleukin 10, a novel B cell stimulatory factor: unresponsiveness of X chromosome-linked immunodeficiency B cells. *J Exp Med* 172: 1625-31

160. Thompson-Snipes L, Dhar V, Bond MW, Mosmann TR, Moore KW, Rennick DM. 1991. Interleukin 10: a novel stimulatory factor for mast cells and their progenitors. *J Exp Med* 173: 507-10

161. O'Garra A, Howard M. 1992. Cytokines and Ly-1 (B1) B cells. *Int Rev Immunol* 8: 219-34

162. Hurme M, Henttinen T, Karppelin M, Varkila K, Matikainen S. 1994. Effect of interleukin-10 on NF-kB and AP-1 activities in interleukin-2 dependent CD8 T lymphoblasts. *Immunol Lett* 42: 129-33

163. Groux H, Bigler M, de Vries JE, Roncarolo MG. 1998. Inhibitory and stimulatory effects of IL-10 on human CD8+ T cells. *J Immunol* 160: 3188-93

164. De Smedt T, Van Mechelen M, De Becker G, Urbain J, Leo O, Moser M. 1997. Effect of interleukin-10 on dendritic cell maturation and function. *Eur J Immunol* 27: 1229-35

165. Willems F, Marchant A, Delville JP, Gerard C, Delvaux A, Velu T, de Boer M, Goldman M. 1994. Interleukin-10 inhibits B7 and intercellular adhesion molecule-1 expression on human monocytes. *Eur J Immunol* 24: 1007-9

166. Buelens C, Willems F, Delvaux A, Pierard G, Delville JP, Velu T, Goldman M. 1995. Interleukin-10 differentially regulates B7-1 (CD80) and B7-2 (CD86) expression on human peripheral blood dendritic cells. *Eur J Immunol* 25: 2668-72

167. Shurin MR, Yurkovetsky ZR, Tourkova IL, Balkir L, Shurin GV. 2002. Inhibition of CD40 expression and CD40-mediated dendritic cell function by tumor-derived IL-10. *Int J Cancer* 101: 61-8

168. Liu G, Ng H, Akasaki Y, Yuan X, Ehtesham M, Yin D, Black KL, Yu JS. 2004. Small interference RNA modulation of IL-10 in human monocyte-derived dendritic cells enhances the Th1 response. *Eur J Immunol* 34: 1680-7

169. Faulkner L, Buchan, G., Baird, M. 2000. Interleukin-10 does not affect phagocytosis of particulate antigen by bone marrow-derived dendritic cells but does impair antigen presentation. *Immunology* 99: 523-31

170. Haase C, Jorgensen TN, Michelsen BK. 2002. Both exogenous and endogenous interleukin-10 affects the maturation of bone-marrow-derived dendritic cells in vitro and strongly influences T-cell priming in vivo. *Immunology* 107: 489-99

171. McBride JM, Jung T, de Vries JE, Aversa G. 2002. IL-10 alters DC function via modulation of cell surface molecules resulting in impaired T-cell responses. *Cell Immunol* 215: 162-72

172. Beinhauer BG, McBride JM, Graf P, Pursch E, Bongers M, Rogy M, Korthauer U, de Vries JE, Aversa G, Jung T. 2004. Interleukin 10 regulates cell surface and soluble LIR-2 (CD85d) expression on dendritic cells resulting in T cell hyporesponsiveness in vitro. *Eur J Immunol* 34: 74-80

173. de Waal Malefyt R, Yssel H, de Vries JE. 1993. Direct effects of IL-10 on subsets of human CD4+ T cell clones and resting T cells. Specific inhibition of IL-2 production and proliferation. *J Immunol* 150: 4754-65

174. Taga K, Mostowski H, Tosato G. 1993. Human interleukin-10 can directly inhibit T-cell growth. *Blood* 81: 2964-71

175. Akdis CA, Joss A, Akdis M, Faith A, Blaser K. 2000. A molecular basis for T cell suppression by IL-10: CD28-associated IL-10 receptor inhibits CD28 tyrosine phosphorylation and phosphatidylinositol 3-kinase binding. *Faseb J* 14: 1666-8

176. Cottrez F, Groux H. 2001. Regulation of TGF-beta response during T cell activation is modulated by IL-10. *J Immunol* 167: 773-8

177. Groux H, Cottrez F, Rouleau M, Mauze S, Antonenko S, Hurst S, McNeil T, Bigler M, Roncarolo MG, Coffman RL. 1999. A transgenic model to analyze the immunoregulatory role of IL-10 secreted by antigen-presenting cells. *J Immunol* 162: 1723-9

178. Stewart JP, Behm FG, Arrand JR, Rooney CM. 1994. Differential expression of viral and human interleukin-10 (IL-10) by primary B cell tumors and B cell lines. *Virology* 200: 724-32

179. Kotenko SV, Saccani S, Izotova LS, Mirochnitchenko OV, Pestka S. 2000. Human cytomegalovirus harbors its own unique IL-10 homolog (cmvIL-10). *Proc Natl Acad Sci U S A* 97: 1695-700

180. Ding Y, Qin L, Kotenko SV, Pestka S, Bromberg JS. 2000. A single amino acid determines the immunostimulatory activity of interleukin 10. *J Exp Med* 191: 213-24

181. D'Andrea A, Aste-Amezaga M, Valiante NM, Ma X, Kubin M, Trinchieri G. 1993. Interleukin 10 (IL-10) inhibits human lymphocyte interferon gamma-production by suppressing natural killer cell stimulatory factor/IL-12 synthesis in accessory cells. *J Exp Med* 178: 1041-8

182. Akdis CA, Joss A, Akdis M, Blaser K. 2001. Mechanism of IL-10-induced T cell inactivation in allergic inflammation and normal response to allergens. *Int Arch Allergy Immunol* 124: 180-2

183. Wang P, Wu, P., Siegel, M.I., Egan, R.W., Billah, M.M. 1995. Interleukin (IL)-10 inhibits nuclear factor kappa B (NF kappa B) activation in human monocytes. IL-10 and IL-4 suppress cytokine synthesis by different mechanisms. *J. Biol. Chem.* 270: 9558–63

184. Schottelius AJ, Mayo MW, Sartor RB, Baldwin AS, Jr. 1999. Interleukin-10 signaling blocks inhibitor of kappaB kinase activity and nuclear factor kappaB DNA binding. *J Biol Chem* 274: 31868-74

185. Laderach D, Compagno, D., Danos, O., Vainchenker, W., Galy, A. 2003. RNA interference shows critical requirement for NF-kappa-beta p50 in the production of IL-12 by human dendritic cells. *J Immunol* 171: 1750-7

186. Baldwin AS. 1996. The NK-kappa-beta and I-kappa-beta proteins: New dicoveries and insights. *Annu Rev Immunol* 14: 649-81

187. Krensky AM, Weiss A, Crabtree G, Davis MM, Parham P. 1990. T-lymphocyte-antigen interactions in transplant rejection. *N Engl J Med* 322: 510-7

188. Liu Z, Sun YK, Xi YP, Maffei A, Reed E, Harris P, Suciu-Foca N. 1993. Contribution of direct and indirect recognition pathways to T cell alloreactivity. *J Exp Med* 177: 1643-50

189. Larsen CP, Morris PJ, Austyn JM. 1990. Migration of dendritic leukocytes from cardiac allografts into host spleens. A novel pathway for initiation of rejection. *J Exp Med* 171: 307-14

190. Austyn JM, Larsen CP. 1990. Migration patterns of dendritic leukocytes. Implications for transplantation. *Transplantation* 49: 1-7

191. Benichou G, Valujskikh A, Heeger PS. 1999. Contributions of direct and indirect T cell alloreactivity during allograft rejection in mice. *J Immunol* 162: 352-8

192. Mosmann TR, Coffman RL. 1989. TH1 and TH2 cells: different patterns of lymphokine secretion lead to different functional properties. *Annu Rev Immunol* 7: 145-73

193. Waaga AM, Gasser M, Kist-van Holthe JE, Najafian N, Muller A, Vella JP, Womer KL, Chandraker A, Khoury SJ, Sayegh MH. 2001. Regulatory functions of self-

restricted MHC class II allopeptide-specific Th2 clones in vivo. *J Clin Invest* 107: 909-16

194. Andres PG, Howland KC, Nirula A, Kane LP, Barron L, Dresnek D, Sadra A, Imboden J, Weiss A, Abbas AK. 2004. Distinct regions in the CD28 cytoplasmic domain are required for T helper type 2 differentiation. *Nat Immunol* 5: 435-42

195. Yamane H, Igarashi O, Kato T, Nariuchi H. 2000. Positive and negative regulation of IL-12 receptor expression of naive CD4(+) T cells by CD28/CD152 co-stimulation. *Eur J Immunol* 30: 3171-80

196. Pandiyan P, Gartner D, Soezeri O, Radbruch A, Schulze-Osthoff K, Brunner-Weinzierl MC. 2004. CD152 (CTLA-4) determines the unequal resistance of Th1 and Th2 cells against activation-induced cell death by a mechanism requiring PI3 kinase function. *J Exp Med* 199: 831-42

197. Asadullah K, Sterry, W., Volk, H.D. 2003. Interleukin-10 therapy - review of a new approach. *Pharmacol Rev* 55: 241-69

198. Asadullah K, Sterry, W., Stephanek, K., Jasulaitis, D., Leupold, M., Audring, H., Volk, H.D., Do¨cke, W.D. 1998. IL-10 is a key cytokine in psoriasis: proof of principle by IL-10 therapy—a new therapeutic approach. *J. Clin. Investig.* 101: 783–94

199. Adikari SB, Pettersson A, Soderstrom M, Huang YM, Link H. 2004. Interleukin-10-modulated immature dendritic cells control the proinflammatory environment in multiple sclerosis. *Scand J Immunol* 59: 600-6

200. Koch F, Stanzl U, Jennewein P, Janke K, Heufler C, Kampgen E, Romani N, Schuler G. 1996. High level IL-12 production by murine dendritic cells: upregulation via MHC class II and CD40 molecules and downregulation by IL-4 and IL-10. *J Exp Med* 184: 741-6

201. Macatonia SE, Doherty TM, Knight SC, O'Garra A. 1993. Differential effect of IL-10 on dendritic cell-induced T cell proliferation and IFN-gamma production. *J Immunol* 150: 3755-65

202. Jung M, Sabat, R., Kratzschmar, J., Seidel, H., Wolk, K., Schonbein, C., Schutt, S., Friedrich, M., Docke, W.D., Asadullah, K., Volk, H.D., Grutz, G. 2004. Expression profiling of IL-10-regulated genes in human monocytes and peripheral blood mononuclear cells from psoriatic patients during IL-10 therapy. *Eur J Immunol* 34: 481-93

203. Schwartz RH. 2003. T cell anergy. *Annu Rev Immunol* 21: 305-34

204. Gimmi CD, Freeman GJ, Gribben JG, Gray G, Nadler LM. 1993. Human T-cell clonal anergy is induced by antigen presentation in the absence of B7 costimulation. *Proc Natl Acad Sci U S A* 90: 6586-90

205. Becker JC, Brabletz T, Kirchner T, Conrad CT, Brocker EB, Reisfeld RA. 1995. Negative transcriptional regulation in anergic T cells. *Proc Natl Acad Sci U S A* 92: 2375-8

206. Jenkins MK. 1992. The role of cell division in the induction of clonal anergy. *Immunol Today* 13: 69-73

207. Wells AD, Walsh MC, Bluestone JA, Turka LA. 2001. Signaling through CD28 and CTLA-4 controls two distinct forms of T cell anergy. *J Clin Invest* 108: 895-903

208. Essery G, Feldmann M, Lamb JR. 1988. Interleukin-2 can prevent and reverse antigen-induced unresponsiveness in cloned human T lymphocytes. *Immunology* 64: 413-7

209. Roncarolo MG, Bacchetta R, Bordignon C, Narula S, Levings MK. 2001. Type 1 T regulatory cells. *Immunol Rev* 182: 68-79

210. Cohen JJ, Duke, R.C. 1992. Apoptosis and programmed cell death in immunity. *Annu. Rev. Immunol.* 10: 267-93

211. Lu L, Qian S, Hershberger PA, Rudert WA, Lynch DH, Thomson AW. 1997. Fas ligand (CD95L) and B7 expression on dendritic cells provide counter-regulatory signals for T cell survival and proliferation. *J Immunol* 158: 5676-84

212. Green DR, Droin N, Pinkoski M. 2003. Activation-induced cell death in T cells. *Immunol Rev* 193: 70-81

213. Gershon RK, Kondo K. 1970. Cell interactions in the induction of tolerance: the role of thymic lymphocytes. *Immunology* 18: 723-37

214. Sakaguchi S, Sakaguchi N, Asano M, Itoh M, Toda M. 1995. Immunologic self-tolerance maintained by activated T cells expressing IL-2 receptor alpha-chains (CD25). Breakdown of a single mechanism of self-tolerance causes various autoimmune diseases. *J Immunol* 155: 1151-64

215. Shevach EM. 2004. Regulatory T cells. Introduction. *Semin Immunol* 16: 69-71

216. Hori S, Nomura T, Sakaguchi S. 2003. Control of regulatory T cell development by the transcription factor Foxp3. *Science* 299: 1057-61

217. Takahashi T, Tagami T, Yamazaki S, Uede T, Shimizu J, Sakaguchi N, Mak TW, Sakaguchi S. 2000. Immunologic self-tolerance maintained by CD25(+)CD4(+) regulatory T cells constitutively expressing cytotoxic T lymphocyte-associated antigen 4. *J Exp Med* 192: 303-10

218. Qin S, Cobbold SP, Pope H, Elliott J, Kioussis D, Davies J, Waldmann H. 1993. "Infectious" transplantation tolerance. *Science* 259: 974-7

219. Cobbold SP, Graca L, Lin CY, Adams E, Waldmann H. 2003. Regulatory T cells in the induction and maintenance of peripheral transplantation tolerance. *Transpl Int* 16: 66-75

220. Zheng SG, Wang JH, Gray JD, Soucier H, Horwitz DA. 2004. Natural and induced CD4+CD25+ cells educate CD4+CD25- cells to develop suppressive activity: the role of IL-2, TGF-beta, and IL-10. *J Immunol* 172: 5213-21

221. Dieckmann D, Bruett CH, Ploettner H, Lutz MB, Schuler G. 2002. Human CD4(+)CD25(+) regulatory, contact-dependent T cells induce interleukin 10-producing, contact-independent type 1-like regulatory T cells [corrected]. *J Exp Med* 196: 247-53

222. Jonuleit H, Schmitt E, Kakirman H, Stassen M, Knop J, Enk AH. 2002. Infectious tolerance: human CD25(+) regulatory T cells convey suppressor activity to conventional CD4(+) T helper cells. *J Exp Med* 196: 255-60

223. Groux H, O'Garra A, Bigler M, Rouleau M, Antonenko S, de Vries JE, Roncarolo MG. 1997. A CD4+ T-cell subset inhibits antigen-specific T-cell responses and prevents colitis. *Nature* 389: 737-42

224. Inobe J, Slavin AJ, Komagata Y, Chen Y, Liu L, Weiner HL. 1998. IL-4 is a differentiation factor for transforming growth factor-beta secreting Th3 cells and oral administration of IL-4 enhances oral tolerance in experimental allergic encephalomyelitis. *Eur J Immunol* 28: 2780-90

225. Chen Y, Kuchroo VK, Inobe J, Hafler DA, Weiner HL. 1994. Regulatory T cell clones induced by oral tolerance: suppression of autoimmune encephalomyelitis. *Science* 265: 1237-40

226. Denton MD, Magee CC, Sayegh MH. 1999. Immunosuppressive strategies in transplantation. *Lancet* 353: 1083-91

227. Vats A. 2004. BK virus-associated transplant nephropathy: need for increased awareness in children. *Pediatr Transplant* 8: 421-5

228. Dharnidharka VR, Harmon WE. 2001. Management of pediatric postrenal transplantation infections. *Semin Nephrol* 21: 521-31

229. Ondrus D, Pribylincova V, Breza J, Bujdak P, Miklosi M, Reznicek J, Zvara V. 1999. The incidence of tumours in renal transplant recipients with long-term immunosuppressive therapy. *Int Urol Nephrol* 31: 417-22

230. Hojo M, Morimoto T, Maluccio M, Asano T, Morimoto K, Lagman M, Shimbo T, Suthanthiran M. 1999. Cyclosporine induces cancer progression by a cell-autonomous mechanism. *Nature* 397: 530-4

231. Nagano H, Tilney NL. 1997. Chronic allograft failure: the clinical problem. *Am J Med Sci* 313: 305-9

232. Monaco AP, Burke JF, Jr., Ferguson RM, Halloran PF, Kahan BD, Light JA, Matas AJ, Solez K. 1999. Current thinking on chronic renal allograft rejection: issues, concerns, and recommendations from a 1997 roundtable discussion. *Am J Kidney Dis* 33: 150-60

233. Meier-Kriesche HU, Schold, J.D., Srinivas, T.R., Kaplan, B. 2004. Lack of improvement in renal allograft survival despite a marked decrease in acute rejection rates over the most recent era. *Am J Transplant* 4: 378

234. Wood KJ. 1991. Transplantation tolerance. *Curr Opin Immunol* 3: 710-4

235. Davis GF. 1986. Adverse effects of corticosteroids: II. Systemic. *Clin Dermatol* 4: 161-9

236. Crabtree GR, Clipstone NA. 1994. Signal transmission between the plasma membrane and nucleus of T lymphocytes. *Annu Rev Biochem* 63: 1045-83

237. Lu CY, Sicher SC, Vazquez MA. 1993. Prevention and treatment of renal allograft rejection: new therapeutic approaches and new insights into established therapies. *J Am Soc Nephrol* 4: 1239-56

238. Masri MA, Shakuntala V, Dhawan IK, Zahir M, Shanwaz M, Hayes K, Pingle A. 1993. Cyclosporine monotherapy versus conventional therapy in the living-related renal transplant: a one center retrospective study. *Transplant Proc* 25: 2248-9

239. Masri MA. 2003. The mosaic of immunosuppressive drugs. *Mol Immunol* 39: 1073-7

240. Smith DF, Toft DO. 1993. Steroid receptors and their associated proteins. *Mol Endocrinol* 7: 4-11

241. Natsumeda Y, Ohno S, Kawasaki H, Konno Y, Weber G, Suzuki K. 1990. Two distinct cDNAs for human IMP dehydrogenase. *J Biol Chem* 265: 5292-5

242. Sollinger HW. 1995. Mycophenolate mofetil for the prevention of acute rejection in primary cadaveric renal allograft recipients. U.S. Renal Transplant Mycophenolate Mofetil Study Group. *Transplantation* 60: 225-32

243. Sehgal SN, Camardo JS, Scarola JA, Maida BT. 1995. Rapamycin (sirolimus, rapamune). *Curr Opin Nephrol Hypertens* 4: 482-7

244. Brown EJ, Albers MW, Shin TB, Ichikawa K, Keith CT, Lane WS, Schreiber SL. 1994. A mammalian protein targeted by G1-arresting rapamycin-receptor complex. *Nature* 369: 756-8

245. Vincenti F. 2003. New monoclonal antibodies in renal transplantation. *Minerva Urol Nefrol* 55: 57

246. Liang X, Lu L, Chen Z, Vickers T, Zhang H, Fung JJ, Qian S. 2003. Administration of dendritic cells transduced with antisense oligodeoxyribonucleotides targeting CD80 or CD86 prolongs allograft survival. *Transplantation* 76: 721-9

247. Van Gool SW, Vermeiren J, Rafiq K, Lorr K, de Boer M, Ceuppens JL. 1999. Blocking CD40 - CD154 and CD80/CD86 - CD28 interactions during primary allogeneic stimulation results in T cell anergy and high IL-10 production. *Eur J Immunol* 29: 2367-75

248. Judge TA, Wu Z, Zheng XG, Sharpe AH, Sayegh MH, Turka LA. 1999. The role of CD80, CD86, and CTLA4 in alloimmune responses and the induction of long-term allograft survival. *J Immunol* 162: 1947-51

249. Pearson TC, Alexander DZ, Hendrix R, Elwood ET, Linsley PS, Winn KJ, Larsen CP. 1996. CTLA4-Ig plus bone marrow induces long-term allograft survival and donor specific unresponsiveness in the murine model. Evidence for hematopoietic chimerism. *Transplantation* 61: 997-1004

250. Turka LA, Linsley PS, Lin H, Brady W, Leiden JM, Wei RQ, Gibson ML, Zheng XG, Myrdal S, Gordon D, et al. 1992. T-cell activation by the CD28 ligand B7 is required for cardiac allograft rejection in vivo. *Proc Natl Acad Sci U S A* 89: 11102-5

251. Shi WY, Xie LX. 2004. [CTLA4-Ig prevents corneal allograft rejection in mice]. *Zhonghua Yan Ke Za Zhi* 40: 696-700

252. Azuma H, Chandraker A, Nadeau K, Hancock WW, Carpenter CB, Tilney NL, Sayegh MH. 1996. Blockade of T-cell costimulation prevents development of experimental chronic renal allograft rejection. *Proc Natl Acad Sci U S A* 93: 12439-44

253. O'Rourke RW, Kang SM, Lower JA, Feng S, Ascher NL, Baekkeskov S, Stock PG. 2000. A dendritic cell line genetically modified to express CTLA4-IG as a means to prolong islet allograft survival. *Transplantation* 69: 1440-6

254. Larsen CP, Elwood ET, Alexander DZ, Ritchie SC, Hendrix R, Tucker-Burden C, Cho HR, Aruffo A, Hollenbaugh D, Linsley PS, Winn KJ, Pearson TC. 1996. Long-term acceptance of skin and cardiac allografts after blocking CD40 and CD28 pathways. *Nature* 381: 434-8

255. Sayegh MH, Zheng XG, Magee C, Hancock WW, Turka LA. 1997. Donor antigen is necessary for the prevention of chronic rejection in CTLA4Ig-treated murine cardiac allograft recipients. *Transplantation* 64: 1646-50

256. Lin H, Bolling SF, Linsley PS, Wei RQ, Gordon D, Thompson CB, Turka LA. 1993. Long-term acceptance of major histocompatibility complex mismatched cardiac allografts induced by CTLA4Ig plus donor-specific transfusion. *J Exp Med* 178: 1801-6

257. Guillot C, Mathieu P, Coathalem H, Le Mauff B, Castro MG, Tesson L, Usal C, Laumonier T, Brouard S, Soulillou JP, Lowenstein PR, Cuturi MC, Anegon I. 2000.

Tolerance to cardiac allografts via local and systemic mechanisms after adenovirus-mediated CTLA4Ig expression. *J Immunol* 164: 5258-68

258. Sayegh MH, Akalin E, Hancock WW, Russell ME, Carpenter CB, Linsley PS, Turka LA. 1995. CD28-B7 blockade after alloantigenic challenge in vivo inhibits Th1 cytokines but spares Th2. *J Exp Med* 181: 1869-74

259. Li W, Lu L, Li Y, Fu F, Fung JJ, Thomson AW, Qian S. 1997. High-dose cellular IL-10 exacerbates rejection and reverses effects of cyclosporine and tacrolimus in Mouse cardiac transplantation. *Transplant Proc* 29: 1081-2

260. Li W, Fu F, Lu L, Narula SK, Fung JJ, Thomson AW, Qian S. 1999. Recipient pretreatment with mammalian IL-10 prolongs mouse cardiac allograft survival by inhibition of anti-donor T cell responses. *Transplant Proc* 31: 115

261. Qian S, Li W, Li Y, Fu F, Lu L, Fung JJ, Thomson AW. 1996. Systemic administration of cellular interleukin-10 can exacerbate cardiac allograft rejection in mice. *Transplantation* 62: 1709-14

262. Oshima K, Sen L, Cui G, Tung T, Sacks BM, Arellano-Kruse A, Laks H. 2002. Localized interleukin-10 gene transfer induces apoptosis of alloreactive T cells via FAS/FASL pathway, improves function, and prolongs survival of cardiac allograft. *Transplantation* 73: 1019-26

263. Klebe S, Sykes PJ, Coster DJ, Krishnan R, Williams KA. 2001. Prolongation of sheep corneal allograft survival by ex vivo transfer of the gene encoding interleukin-10. *Transplantation* 71: 1214-20

264. Coates PT, Krishnan R, Kireta S, Johnston J, Russ GR. 2001. Human myeloid dendritic cells transduced with an adenoviral interleukin-10 gene construct inhibit human skin graft rejection in humanized NOD-scid chimeric mice. *Gene Ther* 8: 1224-33

265. Qin L, Chavin KD, Ding Y, Tahara H, Favaro JP, Woodward JE, Suzuki T, Robbins PD, Lotze MT, Bromberg JS. 1996. Retrovirus-mediated transfer of viral IL-10 gene prolongs murine cardiac allograft survival. *J Immunol* 156: 2316-23

266. Zuo Z, Wang C, Carpenter D, Okada Y, Nicolaidou E, Toyoda M, Trento A, Jordan SC. 2001. Prolongation of allograft survival with viral IL-10 transfection in a highly histoincompatible model of rat heart allograft rejection. *Transplantation* 71: 686-91

267. Feng S, Quickel RR, Hollister-Lock J, McLeod M, Bonner-Weir S, Mulligan RC, Weir GC. 1999. Prolonged xenograft survival of islets infected with small doses of adenovirus expressing CTLA4Ig. *Transplantation* 67: 1607-13

268. Steurer W, Nickerson PW, Steele AW, Steiger J, Zheng XX, Strom TB. 1995. Ex vivo coating of islet cell allografts with murine CTLA4/Fc promotes graft tolerance. *J Immunol* 155: 1165-74

269. Li W, Fu F, Lu L, Narula SK, Fung JJ, Thomson AW, Qian S. 1999. Differential effects of exogenous interleukin-10 on cardiac allograft survival: inhibition of rejection by recipient pretreatment reflects impaired host accessory cell function. *Transplantation* 68: 1402-9

270. Larsen CP, Ritchie SC, Pearson TC, Linsley PS, Lowry RP. 1992. Functional expression of the costimulatory molecule, B7/BB1, on murine dendritic cell populations. *J Exp Med* 176: 1215-20

271. Lechler RI, Batchelor JR. 1982. Restoration of immunogenicity to passenger cell-depleted kidney allografts by the addition of donor strain dendritic cells. *J Exp Med* 155: 31-41

272. Banchereau J, Briere, F., Caux, C., Davoust, J., Lebecque, S., Liu, Y., Pulendran, B., Palucka, K. 2000. Immunobiology of Dendritic Cells. *Annu Rev Biochem* 18: 767-811

273. Finkelman FD, Lees A, Birnbaum R, Gause WC, Morris SC. 1996. Dendritic cells can present antigen in vivo in a tolerogenic or immunogenic fashion. *J Immunol* 157: 1406-14

274. Fu F, Li Y, Qian S, Lu L, Chambers F, Starzl TE, Fung JJ, Thomson AW. 1996. Costimulatory molecule-deficient dendritic cell progenitors (MHC class II+, CD80dim, CD86-) prolong cardiac allograft survival in nonimmunosuppressed recipients. *Transplantation* 62: 659-65

275. Canatella PJ, Prausnitz MR. 2001. Prediction and optimization of gene transfection and drug delivery by electroporation. *Gene Ther* 8: 1464-9

276. Satkauskas S, Bureau MF, Puc M, Mahfoudi A, Scherman D, Miklavcic D, Mir LM. 2002. Mechanisms of in vivo DNA electrotransfer: respective contributions of cell electropermeabilization and DNA electrophoresis. *Mol Ther* 5: 133-40

277. Taniyama Y, Tachibana K, Hiraoka K, Aoki M, Yamamoto S, Matsumoto K, Nakamura T, Ogihara T, Kaneda Y, Morishita R. 2002. Development of safe and efficient novel nonviral gene transfer using ultrasound: enhancement of transfection efficiency of naked plasmid DNA in skeletal muscle. *Gene Ther* 9: 372-80

278. Lunsford L, McKeever U, Eckstein V, Hedley ML. 2000. Tissue distribution and persistence in mice of plasmid DNA encapsulated in a PLGA-based microsphere delivery vehicle. *J Drug Target* 8: 39-50

279. Schmidt-Wolf GD, Schmidt-Wolf IG. 2003. Non-viral and hybrid vectors in human gene therapy: an update. *Trends Mol Med* 9: 67-72

280. Hirko A, Tang F, Hughes JA. 2003. Cationic lipid vectors for plasmid DNA delivery. *Curr Med Chem* 10: 1185-93

281. Ewert K, Ahmad A, Evans HM, Safinya CR. 2005. Cationic lipid-DNA complexes for non-viral gene therapy: relating supramolecular structures to cellular pathways. *Expert Opin Biol Ther* 5: 33-53

282. Verma IM, Weitzman MD. 2004. Gene Therapy: Twenty-First Century Medicine. *Annu Rev Biochem*

283. Yang Y, Li Q, Ertl HC, Wilson JM. 1995. Cellular and humoral immune responses to viral antigens create barriers to lung-directed gene therapy with recombinant adenoviruses. *J Virol* 69: 2004-15

284. Zhang Y, Chirmule N, Gao GP, Qian R, Croyle M, Joshi B, Tazelaar J, Wilson JM. 2001. Acute cytokine response to systemic adenoviral vectors in mice is mediated by dendritic cells and macrophages. *Mol Ther* 3: 697-707

285. Schnell MA, Zhang Y, Tazelaar J, Gao GP, Yu QC, Qian R, Chen SJ, Varnavski AN, LeClair C, Raper SE, Wilson JM. 2001. Activation of innate immunity in nonhuman primates following intraportal administration of adenoviral vectors. *Mol Ther* 3: 708-22

286. Mountain A. 2000. Gene therapy: the first decade. *Trends Biotechnol* 18: 119-28

287. Raper SE, Chirmule N, Lee FS, Wivel NA, Bagg A, Gao GP, Wilson JM, Batshaw ML. 2003. Fatal systemic inflammatory response syndrome in a ornithine transcarbamylase deficient patient following adenoviral gene transfer. *Mol Genet Metab* 80: 148-58

288. Chiu TK, Davies DR. 2004. Structure and function of HIV-1 integrase. *Curr Top Med Chem* 4: 965-77

289. Cereseto A, Giacca M. 2004. Integration site selection by retroviruses. *AIDS Rev* 6: 13-21

290. Uhm SJ, Kim NH, Kim T, Chung HM, Chung KH, Lee HT, Chung KS. 2000. Expression of enhanced green fluorescent protein (EGFP) and neomycin resistant (Neo(R)) genes in porcine embryos following nuclear transfer with porcine fetal fibroblasts transfected by retrovirus vector. *Mol Reprod Dev* 57: 331-7

291. Kuriyama S, Sakamoto T, Kikukawa M, Nakatani T, Toyokawa Y, Tsujinoue H, Ikenaka K, Fukui H, Tsujii T. 1998. Expression of a retrovirally transduced gene under control of an internal housekeeping gene promoter does not persist due to methylation and is restored partially by 5-azacytidine treatment. *Gene Ther* 5: 1299-305

292. Ellis J, Yao S. 2005. Retrovirus silencing and vector design: relevance to normal and cancer stem cells? *Curr Gene Ther* 5: 367-73

293. Hacein-Bey-Abina S, Von Kalle C, Schmidt M, McCormack MP, Wulffraat N, Leboulch P, Lim A, Osborne CS, Pawliuk R, Morillon E, Sorensen R, Forster A, Fraser P, Cohen JI, de Saint Basile G, Alexander I, Wintergerst U, Frebourg T, Aurias A,

Stoppa-Lyonnet D, Romana S, Radford-Weiss I, Gross F, Valensi F, Delabesse E, Macintyre E, Sigaux F, Soulier J, Leiva LE, Wissler M, Prinz C, Rabbitts TH, Le Deist F, Fischer A, Cavazzana-Calvo M. 2003. LMO2-associated clonal T cell proliferation in two patients after gene therapy for SCID-X1. *Science* 302: 415-9

294. Wagner JA, Reynolds T, Moran ML, Moss RB, Wine JJ, Flotte TR, Gardner P. 1998. Efficient and persistent gene transfer of AAV-CFTR in maxillary sinus. *Lancet* 351: 1702-3

295. Peden CS, Burger C, Muzyczka N, Mandel RJ. 2004. Circulating anti-wild-type adeno-associated virus type 2 (AAV2) antibodies inhibit recombinant AAV2 (rAAV2)-mediated, but not rAAV5-mediated, gene transfer in the brain. *J Virol* 78: 6344-59

296. McCarty DM, Young SM, Jr., Samulski RJ. 2004. Integration of adeno-associated virus (AAV) and recombinant AAV vectors. *Annu Rev Genet* 38: 819-45

297. Balague C, Kalla M, Zhang WW. 1997. Adeno-associated virus Rep78 protein and terminal repeats enhance integration of DNA sequences into the cellular genome. *J Virol* 71: 3299-306

298. Duan D, Yue Y, Engelhardt JF. 2003. Dual vector expansion of the recombinant AAV packaging capacity. *Methods Mol Biol* 219: 29-51

299. van den Brandt J, Wang D, Kwon SH, Heinkelein M, Reichardt HM. 2004. Lentivirally generated eGFP-transgenic rats allow efficient cell tracking in vivo. *Genesis* 39: 94-9

300. Kafri T. 2004. Gene delivery by lentivirus vectors an overview. *Methods Mol Biol* 246: 367-90

301. Zhong L, Granelli-Piperno A, Choi Y, Steinman RM. 1999. Recombinant adenovirus is an efficient and non-perturbing genetic vector for human dendritic cells. *Eur J Immunol* 29: 964-72

302. Morelli AE, Larregina, A.T., Ganster, A.F., Zahorchak, A.F., Plowey, J.M., Takayama, T., Logar, A.J., Robbins, P.D., Falo, L.D., Thomson, A.W. 2000. Recombinant adenovirus induces maturation of dendritic cells via an NF-kappa-beta dependent pathway. *J Virol* 74: 9617-28

303. Rouard H, Leon A, Klonjkowski B, Marquet J, Tenneze L, Plonquet A, Agrawal SG, Abastado JP, Eloit M, Farcet JP, Delfau-Larue MH. 2000. Adenoviral transduction of human 'clinical grade' immature dendritic cells enhances costimulatory molecule expression and T-cell stimulatory capacity. *J Immunol Methods* 241: 69-81

304. Rea D, Schagen FH, Hoeben RC, Mehtali M, Havenga MJ, Toes RE, Melief CJ, Offringa R. 1999. Adenoviruses activate human dendritic cells without polarization toward a T-helper type 1-inducing subset. *J Virol* 73: 10245-53

305. Tillman BW, de Gruijl TD, Luykx-de Bakker SA, Scheper RJ, Pinedo HM, Curiel TJ, Gerritsen WR, Curiel DT. 1999. Maturation of dendritic cells accompanies high-efficiency gene transfer by a CD40-targeted adenoviral vector. *J Immunol* 162: 6378-83

306. Bergelson JM, Cunningham JA, Droguett G, Kurt-Jones EA, Krithivas A, Hong JS, Horwitz MS, Crowell RL, Finberg RW. 1997. Isolation of a common receptor for Coxsackie B viruses and adenoviruses 2 and 5. *Science* 275: 1320-3

307. Tillman BW, Hayes TL, DeGruijl TD, Douglas JT, Curiel DT. 2000. Adenoviral vectors targeted to CD40 enhance the efficacy of dendritic cell-based vaccination against human papillomavirus 16-induced tumor cells in a murine model. *Cancer Res* 60: 5456-63

308. Pereboev AV, Nagle JM, Shakhmatov MA, Triozzi PL, Matthews QL, Kawakami Y, Curiel DT, Blackwell JL. 2004. Enhanced gene transfer to mouse dendritic cells using adenoviral vectors coated with a novel adapter molecule. *Mol Ther* 9: 712-20

309. Dietz AB, Vuk-Pavlovic S. 1998. High efficiency adenovirus-mediated gene transfer to human dendritic cells. *Blood* 91: 392-8

310. Rozis G, de Silva S, Benlahrech A, Papagatsias T, Harris J, Gotch F, Dickson G, Patterson S. 2005. Langerhans cells are more efficiently transduced than dermal dendritic cells by adenovirus vectors expressing either group C or group B fibre protein: implications for mucosal vaccines. *Eur J Immunol* 35: 2617-26

311. Shayakhmetov DM, Carlson CA, Stecher H, Li Q, Stamatoyannopoulos G, Lieber A. 2002. A high-capacity, capsid-modified hybrid adenovirus/adeno-associated virus vector for stable transduction of human hematopoietic cells. *J Virol* 76: 1135-43

312. Li E, Stupack D, Klemke R, Cheresh DA, Nemerow GR. 1998. Adenovirus endocytosis via alpha(v) integrins requires phosphoinositide-3-OH kinase. *J Virol* 72: 2055-61

313. Wickham TJ, Mathias P, Cheresh DA, Nemerow GR. 1993. Integrins alpha v beta 3 and alpha v beta 5 promote adenovirus internalization but not virus attachment. *Cell* 73: 309-19

314. Machen J, Harnaha, J., Lakomy, R., Styche, A., Trucco, M., Giannoukakis, N. 2004. Antisense oligonucleotides down-regulating costimulation confer diabetes-preventive properties to nonobese diabetic mouse dendritic cells. *J Immunol* 173: 4331-41

315. Tan PH, Yates JB, Xue SA, Chan C, Jordan WJ, Harper JE, Watson MP, Dong R, Ritter MA, Lechler RI, Lombardi G, George AJ. 2005. Creation of tolerogenic human DC via intracellular CTLA4: a novel strategy with potential in clinical immunosuppression. *Blood*

316. Asiedu C, Dong, S.S., Pereboev, A. 2002. Rhesus monocyte-derived dendritic cells modified to over-express TGF-beta1 exhibit potent veto activity. *Transplantation* 75

317. Takayama T, Kaneko, K, Morelli, A.E. 2002. Retroviral delivery of transforming growth factor-B1 to myeloid dendritic cells: Inhibition of T cell priming ability and influence on allograft survival. *Transplantation* 74: 112-9

318. Min WP, Gorczynski, R., Huang, X.Y. 2000. Dendritic cells genetically modified to express Fas ligand induce donor-specific hyporesponsiveness and prolong allograft survival. *J Immunol* 164: 161-7

319. Takayama T, Nishioka Y, Lu L, Lotze MT, Tahara H, Thomson AW. 1998. Retroviral delivery of viral interleukin-10 into myeloid dendritic cells markedly inhibits their allostimulatory activity and promotes the induction of T-cell hyporesponsiveness. *Transplantation* 66: 1567-74

320. Oberholzer A, Oberholzer C, Efron PA, Scumpia PO, Uchida T, Bahjat K, Ungaro R, Tannahill CL, Murday M, Bahjat FR, Tsai V, Hutchins B, Moldawer LL, Laface D, Clare-Salzler MJ. 2005. Functional modification of dendritic cells with recombinant adenovirus encoding interleukin 10 for the treatment of sepsis. *Shock* 23: 507-15

321. Zhu M, Wei MF, Liu F, Shi HF, Wang G. 2003. Interleukin-10 modified dendritic cells induce allo-hyporesponsiveness and prolong small intestine allograft survival. *World J Gastroenterol* 9: 2509-12

322. Coates PT. 2001. Gene therapy studies of adenoviral IL-10 transduced dendritic cells in allotransplantation. *PhD Thesis, Transplantation Immunology Laboratory, The Queen Elizabeth Hospital, South Australia*

323. Lu L, Lee WC, Gambotto A, Zhong C, Robbins PD, Qian S, Fung JJ, Thomson AW. 1999. Transduction of dendritic cells with adenoviral vectors encoding CTLA4-Ig markedly reduces their allostimulatory activity. *Transplant Proc* 31: 797

324. Yang Y, Nunes FA, Berencsi K, Furth EE, Gonczol E, Wilson JM. 1994. Cellular immunity to viral antigens limits E1-deleted adenoviruses for gene therapy. *Proc Natl Acad Sci U S A* 91: 4407-11

325. Kay MA, Holterman AX, Meuse L, Gown A, Ochs HD, Linsley PS, Wilson CB. 1995. Long-term hepatic adenovirus-mediated gene expression in mice following CTLA4Ig administration. *Nat Genet* 11: 191-7

326. Nanji SA, Hancock WW, Anderson CC, Adams AB, Luo B, Schur CD, Pawlick RL, Wang L, Coyle AJ, Larsen CP, Shapiro AM. 2004. Multiple combination therapies involving blockade of ICOS/B7RP-1 costimulation facilitate long-term islet allograft survival. *Am J Transplant* 4: 526-36

327. Gorczynski R, Bransom J, Cattral M, Huang X, Lei J, Min W, Wan Y, Gauldie J. 2001. Dendritic cells expressing TGFbeta/IL-10, and CHO cells with OX-2, increase graft survival. *Transplant Proc* 33: 1565-6

328. Brady JL, Lew AM. 2000. Additive efficacy of CTLA4Ig and OX40Ig secreted by genetically modified grafts. *Transplantation* 69: 724-30

329. Bonham CA, Peng L, Liang X, Chen Z, Wang L, Ma L, Hackstein H, Robbins PD, Thomson AW, Fung JJ, Qian S, Lu L. 2002. Marked prolongation of cardiac allograft survival by dendritic cells genetically engineered with NF-kappa B oligodeoxyribonucleotide decoys and adenoviral vectors encoding CTLA4-Ig. *J Immunol* 169: 3382-91

330. Sachs DH. 2003. Tolerance: Of mice and men. *J Clin Invest* 111: 1819-21

331. Adams AB, Pearson, T.C., Larsen, C.P. 2003. Heterologous immunity provides a potent barrier to transplantation tolerance. *J Clin Invest* 111: 1887-95

332. Cossarizza A, Cooper, E.L., Suzuki, M.M., Salvioli, S., Capri, M., Gri, G., Quaglino, D., Franceschi, C. 1996. CD45 isoforms expression on CD4+ and CD8+ T cells throughout life, from newborns to centenarians: implications for T cell memory. *Mech Ageing Dev* 86: 173-95

333. Blattman JN, Anita, R., Sourdive, D.J., Wang, X., Kaech, S.M., Murali-Krishna, K., Altman, J.D., Ahmed, R. 2002. Estimating the precursor frequency of naive antigen-specific CD8 T cells. *J. Exp. Med.* 195: 657-64

334. Choo JK, Seebach JD, Nickeleit V, Shimizu A, Lei H, Sachs DH, Madsen JC. 1997. Species differences in the expression of major histocompatibility complex class II antigens on coronary artery endothelium: implications for cell-mediated xenoreactivity. *Transplantation* 64: 1315-22

335. Rosengard BR, Ojikutu, C.A., Guzzetta, P.C., Smith, C.V., Sundt, T.M., Nakajima, K., Boorstein, S.M., Hill, G.S., Fishbein, J.M., Sachs, D.H. 1992. Induction of specific tolerance to class I disparate renal allografts in miniature swine with cyclosporin. *Transplantation* 54: 490-7

336. Baecher-Allan C, Viglietta, V., Hafler, D.A. 2004. Human CD4+CD25+ regulatory cells. *Semin Immunol* 16: 89-98

337. Hein WR, Griebel PJ. 2003. A road less travelled: large animal models in immunological research. *Nat Rev Immunol* 3: 79-84

338. Pedersen NC, Morris B. 1974. The role of humoral antibody in the rejection of primary renal allografts in sheep. *J Exp Med* 140: 619-30

339. Patrick GM. 1998. Studies of cytokine in alloimmune responses. *PhD Thesis, Transplantation Immunology Laboratory, The Queen Elizabeth Hospital, South Australia*

340. Goodman S, Check E. 2002. The great primate debate. *Nature* 417: 684-7

341. Chomczynski P, Sacchi, N. 1987. Single-step method of RNA isolation by acid guanidinium thiocyanate-phenol-chloroform extraction. *Analyt. Biochem.* 162: 156-9

342. Graham FL, Smiley J, Russell WC, Nairn R. 1977. Characteristics of a human cell line transformed by DNA from human adenovirus type 5. *J Gen Virol* 36: 59-74

343. Banchereau J, Steinman RM. 1998. Dendritic cells and the control of immunity. *Nature* 392: 245-52

344. Lu LM, D. Starzl, T.E. Thomson, A.W. 1995. Bone marrow-derived dendritic cell progenitors (NLDC 145+, MHC class II+, B7-1dim, B7-2-) induce alloantigen-specific hyporesponsiveness in murine T lymphocytes. *Transplantation* 60: 1539-45

345. Rastellini CL, L. Ricordi, C. Rao, A.S. Thomson, A.W. 1995. Granulocyte/macrophage colony-stimulating factor-stimulated hepatic dendritic cell progenitors prolong pancreatic islet allograft survival. *Transplantation* 60: 1366-70

346. Caux C, Massacrier C, Vanbervliet B, Barthelemy C, Liu YJ, Banchereau J. 1994. Interleukin 10 inhibits T cell alloreaction induced by human dendritic cells. *Int Immunol* 6: 1177-85

347. Kirk AD, Harlan DM, Armstrong NN, Davis TA, Dong Y, Gray GS, Hong X, Thomas D, Fechner JH, Jr., Knechtle SJ. 1997. CTLA4-Ig and anti-CD40 ligand prevent renal allograft rejection in primates. *Proc Natl Acad Sci U S A* 94: 8789-94

348. Zhou L, Tedder, T. 1996. CD14 blood monocytes can differentitate into functionally mature CD83 dendritic cells. *Proc Natl Acad Sci U S A* 93: 2588-92

349. Sallusto F, Lanzavecchia, A. 1994. Efficient presentation of soluble antigens by cultured human dendritic cells is maintained by granulocyte/macrophage colony-stimulating factor plus interleukin 4 and downregulated by tumour necrosis factor alpha. *J Exp Med* 179: 1109-18

350. Kato M, Neil TK, Fearnley DB, McLellan AD, Vuckovic S, Hart DN. 2000. Expression of multilectin receptors and comparative FITC-dextran uptake by human dendritic cells. *Int Immunol* 12: 1511-9

351. Forster R, Schubel A, Breitfeld D, Kremmer E, Renner-Muller I, Wolf E, Lipp M. 1999. CCR7 coordinates the primary immune response by establishing functional microenvironments in secondary lymphoid organs. *Cell* 99: 23-33

352. Hock BD, Fearnley, D.B., Boyce, A., et al. 1999. Human dendritic cells express a 95 kDa activation/differentiation antigen defined by CMRF-56. *Tissue Antigens* 53: 320-34

353. Cao W, Lee, S.H., Lu, J. 2005. CD83 is preformed inside monocytes, macrophages and dendritic cells, but it is only stably expressed on activated dendritic cells. *Biochem J* 385: 85-93

354. Chang CH, Furue M, Tamaki K. 1995. B7-1 expression of Langerhans cells is up-regulated by proinflammatory cytokines, and is down-regulated by interferon-gamma or by interleukin-10. *Eur J Immunol* 25: 394-8

355. Allavena P, Piemonti L, Longoni D, Bernasconi S, Stoppacciaro A, Ruco L, Mantovani A. 1998. IL-10 prevents the differentiation of monocytes to dendritic cells but promotes their maturation to macrophages. *Eur J Immunol* 28: 359-69

356. Morel AS, Quaratino S, Douek DC, Londei M. 1997. Split activity of interleukin-10 on antigen capture and antigen presentation by human dendritic cells: definition of a maturative step. *Eur J Immunol* 27: 26-34

357. Punnonen J, de Waal Malefyt R, van Vlasselaer P, Gauchat JF, de Vries JE. 1993. IL-10 and viral IL-10 prevent IL-4-induced IgE synthesis by inhibiting the accessory cell function of monocytes. *J Immunol* 151: 1280-9

358. Groux H, Bigler M, de Vries JE, Roncarolo MG. 1996. Interleukin-10 induces a long-term antigen-specific anergic state in human CD4+ T cells. *J Exp Med* 184: 19-29

359. Peguet-Navarro J, Moulon C, Caux C, Dalbiez-Gauthier C, Banchereau J, Schmitt D. 1994. Interleukin-10 inhibits the primary allogeneic T cell response to human epidermal Langerhans cells. *Eur J Immunol* 24: 884-91

360. Sakaguchi S. 2003. The origin of FOXP3- expressing regulatory T cells: thymus or periphery. *J Clin Invest.* 112: 1310-2

361. Ferlazzo G, Semino C, Melioli G. 2001. HLA class I molecule expression is up-regulated during maturation of dendritic cells, protecting them from natural killer cell-mediated lysis. *Immunol Lett* 76: 37-41

362. Piccioli D, Sbrana S, Melandri E, Valiante NM. 2002. Contact-dependent stimulation and inhibition of dendritic cells by natural killer cells. *J Exp Med* 195: 335-41

363. Karre K. 2002. Immunology. A perfect mismatch. *Science* 295: 2029-31

364. Karre K. 2002. NK cells, MHC class I molecules and the missing self. *Scand J Immunol* 55: 221-8

365. Fernandez NC, Lozier A, Flament C, Ricciardi-Castagnoli P, Bellet D, Suter M, Perricaudet M, Tursz T, Maraskovsky E, Zitvogel L. 1999. Dendritic cells directly trigger NK cell functions: cross-talk relevant in innate anti-tumor immune responses in vivo. *Nat Med* 5: 405-11

366. Gerosa F, Gobbi A, Zorzi P, Burg S, Briere F, Carra G, Trinchieri G. 2005. The reciprocal interaction of NK cells with plasmacytoid or myeloid dendritic cells profoundly affects innate resistance functions. *J Immunol* 174: 727-34

367. Hanna J, Fitchett J, Rowe T, Daniels M, Heller M, Gonen-Gross T, Manaster E, Cho SY, LaBarre MJ, Mandelboim O. 2005. Proteomic analysis of human natural killer cells: insights on new potential NK immune functions. *Mol Immunol* 42: 425-31

368. Zingoni A, Sornasse T, Cocks BG, Tanaka Y, Santoni A, Lanier LL. 2004. Cross-talk between activated human NK cells and CD4+ T cells via OX40-OX40 ligand interactions. *J Immunol* 173: 3716-24

369. Assarsson E, Kambayashi T, Schatzle JD, Cramer SO, von Bonin A, Jensen PE, Ljunggren HG, Chambers BJ. 2004. NK cells stimulate proliferation of T and NK cells through 2B4/CD48 interactions. *J Immunol* 173: 174-80

370. Li ZL, K.L., Mahesh S.P., Liu B., Nussenblatt R.B. 2005. Cutting Edge: In vivo blockade of human IL-2 receptor induces expansion of $CD56^{bright}$ regulatory NK cells in patients with active uveitis. *J. Immunol* 174: 5187-91

371. Farag SS, VanDeusen JB, Fehniger TA, Caligiuri MA. 2003. Biology and clinical impact of human natural killer cells. *Int J Hematol* 78: 7-17

372. Biron C, Nguyen, K.B., Pien, G.C., Cousens, L.P., Salazar-Mather, T. 1997. Natural Killer cells in antiviral defence: function and regulation by innate cytokines. *Annu Rev Immunol* 17: 189-220

373. Robertson MJ, Ritz, J. 1990. Biology and clinical relevance of human natural killer cells. *Blood*: 2421

374. Uehara S, Chase CM, Colvin RB, Russell PS, Madsen JC. 2005. Further evidence that NK cells may contribute to the development of cardiac allograft vasculopathy. *Transplant Proc* 37: 70-1

375. Maier S, Tertilt C, Chambron N, Gerauer K, Huser N, Heidecke CD, Pfeffer K. 2001. Inhibition of natural killer cells results in acceptance of cardiac allografts in CD28-/- mice. *Nat Med* 7: 557-62

376. Westerhuis G, Maas WG, Willemze R, Toes RE, Fibbe WE. 2005. Long-term mixed chimerism after immunological conditioning and MHC-mismatched stem cell transplantation is dependent on NK cell tolerance. *Blood* 106: 2215-20

377. Maraskovsky E, Daro, E., Roux, E., Teepe, M., Maliszewski, C.R., Hoek, J. 2000. In vivo generation of human dendritic cell subsets by Flt3 ligand. *Blood* 96: 878-84

378. Huang YM, Xiao, B.G., Westerlung, I., Link, H. 1999. Phenotype and functional properties of dendritic cells isolated from human peripheral blood in comparison with mononuclear cells and T cells. *Scand J Immunol* 49: 177-83

379. Bujdoso R, Hopkins J., Dutia B.M., Young P., McConnell I. 1989. Characterisation of Sheep Afferent Lymph Dendritic Cells and their Role in Antigen Carriage. *J Exp Med* 170: 1285

380. Johansson C, Kelsall BL. 2005. Phenotype and function of intestinal dendritic cells. *Semin Immunol* 17: 284-94

381. Jan de Heer H, Hammad, H, Kool, M., Lambrecht, B.N. 2005. Dendritic cell subsets and immune regulation in the lung. *Semin Immunol* 17: 295-303

382. Howard CJ, Hope, J.C. 2000. Dendritic cells, implications on function from studies of the afferent lymph veiled cell. *Vet Immunol Immunopathol* 77: 1-13

383. Valladeau J, Saeland S. 2005. Cutaneous dendritic cells. *Semin Immunol* 17: 273-83

384. Roake JA, Rao AS, Morris PJ, Larsen CP, Hankins DF, Austyn JM. 1995. Dendritic cell loss from nonlymphoid tissues after systemic administration of lipopolysaccharide, tumor necrosis factor, and interleukin 1. *J Exp Med* 181: 2237-47

385. Issekutz TB. 1984. Kinetics of cytotoxic lymphocytes in efferent lymph from single lymph nodes following immunization with vaccinia virus. *Clin Exp Immunol* 56: 515-23

386. Dandie GW, Watkins FY, Ragg SJ, Holloway PE, Muller HK. 1994. The migration of Langerhans' cells into and out of lymph nodes draining normal, carcinogen and antigen-treated sheep skin. *Immunol Cell Biol* 72: 79-86

387. Haig DM, Percival A, Mitchell J, Green I, Sargan D. 1995. The survival and growth of ovine afferent lymph dendritic cells in culture depends on tumour necrosis factor-alpha and is enhanced by granulocyte-macrophage colony-stimulating factor but inhibited by interferon-gamma. *Vet Immunol Immunopathol* 45: 221-36

388. Hall JG. 1967. Studies of the cells in the afferent and efferent lymph of lymph nodes draining the site of skin homografts. *J Exp Med* 125: 737

389. Scollay RG, Hall, J.G., Orlans, E. 1976. Studies on lymphocytes in sheep. II. Some properties of cells in various compartments of the recirculating lymphocyte pool. *Eur J Immunol* 6: 121

390. Carpenter CB, Glassock RJ, Gleason R, Corson JM, Merrill JP. 1966. The application of the normal lymphocyte transfer reaction to histocompatibility testing in man. *J Clin Invest* 45: 1452-66

391. Hopkins J, Dutia BM, Bujdoso R, McConnell I. 1989. In vivo modulation of CD1 and MHC class II expression by sheep afferent lymph dendritic cells. Comparison of primary and secondary immune responses. *J Exp Med* 170: 1303-18

392. Lascelles AK, Morris, B. 1961. Surgical techniques for the collection of lymph from unanaesthetized sheep. *Q J Exp Physiol* 46: 199-205

393. Ragg SJ, Dandie GW, Woods GM, Muller HK. 1995. Abrogation of afferent lymph dendritic cell function after cutaneously applied chemical carcinogens. *Cell Immunol* 162: 80-8

394. Brent L, Medawar, P.B. 1963. Tissue Transplantation: a new approach to the typing problem. *Br Med J* 2: 269

395. Johnson GJ, Russell PS. 1967. Normal lymphocyte transfer and lymphocyte stimulation as practical histocompatibility tests. *Br Med J* 2: 202-5

396. Saha K, Mittal MM. 1977. Normal lymphocyte transfer reaction in humans and its possible mechanism. *Vox Sang* 32: 300-10

397. Johnson GJ, Chir, B., Russell, P.P. 1967. Normal lymphocyte and lmphocyte stimulation as practical histocompatibility tests. *Br Med J* 2: 202-5

398. Streilein JW, Billingham, R.E. 1969. An analysis of the genetic requirements for delayed cutaneous hypersensitivity reactions to transplantation in mice. 409-27

399. Zakarian S, Billingham RE. 1972. Studies on normal and immune lymphocyte transfer reactions in guinea pigs, with special reference to the cellular contribution of the host. *J Exp Med* 136: 1545-63

400. Ramseier H, Streilein JW. 1965. Homograft Sensitivity Reactions in Irradiated Hamsters. *Lancet* 17: 622-4

401. Hornick DN, Sensenig DM. 1968. Applicability of the normal lymphocyte transfer test to the dog. *Am Surg* 34: 457-60

402. Emery D, McCullagh P. 1980. Immunological reactivity between chimeric cattle twins. II. Normal lymphocyte transfer. *Transplantation* 29: 10-6

403. Cole GJ, Morris B. 1971. The normal lymphocyte transfer reaction in lambs thymectomized in utero. *Aust J Exp Biol Med Sci* 49: 89-99

404. Su M, Young AJ, He C, West CA, Swanson SJ, Mentzer SJ. 2001. Biphasic response of the regional lymphatics in the normal lymphocyte transfer reaction. *Transplantation* 72: 516-22

405. Aboul-Enein A, el-Kharadely M. 1969. Histopathological study of lymphocyte transfer in man. *Br J Exp Pathol* 50: 209-12

406. Scollay R, Lafferty, K. 1975. Differences in the graft-versus-host reactivity of cells migrating through nonlymphoid tissue or lymph nodes. *Transplantation* 19: 170-6

407. Mackay CR, Kimpton WG, Brandon MR, Cahill RN. 1988. Lymphocyte subsets show marked differences in their distribution between blood and the afferent and efferent lymph of peripheral lymph nodes. *J Exp Med* 167: 1755-65

408. Haig DM, Hopkins J, Miller HR. 1999. Local immune responses in afferent and efferent lymph. *Immunology* 96: 155-63

409. Mackay CR, Marston WL, Dudler L. 1990. Naive and memory T cells show distinct pathways of lymphocyte recirculation. *J Exp Med* 171: 801-17

410. Chan SS, McConnell I, Blacklaws BA. 2002. Generation and characterization of ovine dendritic cells derived from peripheral blood monocytes. *Immunology* 107: 366-72

411. Zhou LJ, Fedder, T.F. 1995. Human blood dendritic cells selectively express CD83, A member of the immunoglobulin superfamily. *J Immunol* 154: 3821-35

412. Steinman RM, Swanson, J. 1995. The endocytic activity of dendritic cells. *J Exp Med* 182: 283-8

413. Stahl PD. 1992. The mannose receptor and other macrophage lectins. *Curr Opin Immunol* 4: 49-52

414. Yanagihara S, Komura E, Nagafune J, Watarai H, Yamaguchi Y. 1998. EBI1/CCR7 is a new member of dendritic cell chemokine receptor that is up-regulated upon maturation. *J Immunol* 161: 3096-102

415. Dieu-Nosjean MC, Vicari, A., Lebecque, S., Caux, C. 1999. Regulation of dendritic cell trafficking: a process that involves the participation of selective chemokines. *J Leukoc Biol* 66: 252-62

416. Martin-Fonteche A, Sebastiani, S., Hopken, U.E., Uguccioni, M., Lipp, M., Lanzavecchia, A., Sallusto, F. 2003. Regulation of dendritic cell migration to the draining lymph node: Impact on T lymphocyte traffic and priming. *J Exp Med* 198: 615-21

417. Bernhard H, Huseby ES, Hand SL, Lohmann M, Batten WY, Disis ML, Gralow JR, Meyer zum Buschenfelde KH, Ohlen C, Cheever MA. 2000. Dendritic cells lose ability to present protein antigen after stimulating antigen-specific T cell responses, despite upregulation of MHC class II expression. *Immunobiology* 201: 568-82

418. Lacerda JF, Ladanyi, M., Louie, D.C., Fernandez, J.M., Papadopoulos, E.B., O'Reilly, R.J. 1996. Human Epstein-Barr virus (EBV)-specific cytotoxic T lymphocytes home preferentially to and induce selective regressions of autologous EBV-induced B cell lymphoproliferations in xenografted C.B-17 scid/scid mice. *J Exp Med* 183: 1215-28

419. Hendrikx PJ, Martens, C.M., Hagenbeek, A., Keij, J.F., Visser, J.W. 1996. Homing of fluorescently labeled murine hematopoietic stem cells. *Exp Hematol* 24: 129-40

420. Beavis AJ, Pennline, K.J. 1994. Tracking of murine spleen cells in vivo: detection of PKH-26-labeled cells in the pancreas of non-obese diabetic (NOD) mice. *J Immunol Methods* 170: 57-65

421. Watkins C, Lau, S., Thistlethwaite, J., Hopkins, J., Harkiss, G.D. 1999. Analysis of reporter gene expression in ovine dermis and afferent lymph dendritic cells in vitro and in vivo. *Vet Immunol Immunopathol* 72: 125-33

422. Jones MAS, Lafferty, K.J. 1969. Characteristics of lymphocyte transfer reactions in sheep. *Aust J Exp Biol Med Sci* 47: 159-69

423. Takahito S, Taichi, E., Michio, O., Kenjiro, M. 2001. Trafficking of host- and donor-derived dendritic cells in rat cardiac transplantation: Allosensitization in the spleen and hepatic nodes. *Transplantation* 71: 1806-15

424. Pearson TC, Alexander, D.Z, Winn, K.J., Linsley, P.S., Lowry, R.P., Larsen, C.P. 1994. Transplantation tolerance induced by CTLA4-Ig. *Transplantation* 57: 1701-6

425. Lu L, Gambotto A, Lee WC, Qian S, Bonham CA, Robbins PD, Thomson AW. 1999. Adenoviral delivery of CTLA4Ig into myeloid dendritic cells promotes their in vitro tolerogenicity and survival in allogeneic recipients. *Gene Ther* 6: 554-63

426. Zhang G, Gurtu V, Kain SR. 1996. An enhanced green fluorescent protein allows sensitive detection of gene transfer in mammalian cells. *Biochem Biophys Res Commun* 227: 707-11

427. Cormack BP, Valdivia, R.H., Falkow, S. 1996. FACS-optimised mutants of the Green Fluorescent Protein (GFP). *Gene* 173: 33-8

428. Skosyrev VS, Rudenko NV, Yakhnin AV, Zagranichny VE, Popova LI, Zakharov MV, Gorokhovatsky AY, Vinokurov LM. 2003. EGFP as a fusion partner for the expression and organic extraction of small polypeptides. *Protein Expr Purif* 27: 55-62

429. Chapdelaine P, Moisset PA, Campeau P, Asselin I, Vilquin JT, Tremblay JP. 2000. Functional EGFP-dystrophin fusion proteins for gene therapy vector development. *Protein Eng* 13: 611-5

430. He XH, Xu LH, Liu Y, Cai XC, Zeng YY. 2004. [Expression of CTLA4-EGFP fusion protein in K562 cells and its subcellular localization]. *Xi Bao Yu Fen Zi Mian Yi Xue Za Zhi* 20: 135-9

431. Zawitkowski M, Russ G, Krishnan R. 2002. Cloning and expression of the ovine CD40 molecule and the inhibition of the mixed lymphocyte reaction by the ovine CD40(e)-EGFP fusion protein. *Vet Immunol Immunopathol* 89: 37-45

432. He TC, Zhou S, da Costa LT, Yu J, Kinzler KW, Vogelstein B. 1998. A simplified system for generating recombinant adenoviruses. *Proc Natl Acad Sci U S A* 95: 2509-14

433. Eto Y, Gao JQ, Sekiguchi F, Kurachi S, Katayama K, Mizuguchi H, Hayakawa T, Tsutsumi Y, Mayumi T, Nakagawa S. 2004. Neutralizing antibody evasion ability of

adenovirus vector induced by the bioconjugation of methoxypolyethylene glycol succinimidyl propionate (MPEG-SPA). *Biol Pharm Bull* 27: 936-8

434. Croyle MA, Chirmule N, Zhang Y, Wilson JM. 2001. "Stealth" adenoviruses blunt cell-mediated and humoral immune responses against the virus and allow for significant gene expression upon readministration in the lung. *J Virol* 75: 4792-801

435. Jooss K, Turka LA, Wilson JM. 1998. Blunting of immune responses to adenoviral vectors in mouse liver and lung with CTLA4Ig. *Gene Ther* 5: 309-19

436. Nakagawa I, Murakami M, Ijima K, Chikuma S, Saito I, Kanegae Y, Ishikura H, Yoshiki T, Okamoto H, Kitabatake A, Uede T. 1998. Persistent and secondary adenovirus-mediated hepatic gene expression using adenovirus vector containing CTLA4IgG. *Hum Gene Ther* 9: 1739-45

437. Paillard F. 1998. Adenoviral vector persistence in vivo with a soluble form of CTLA4. *Hum Gene Ther* 9: 1699-700

438. Clarkson CA, Beale, D., Coadwell, J.W., Symons, D.B. 1993. Sequence of ovine Ig gamma 2 constant region heavy chain cDNA and molecular modelling of ruminant IgG isotypes. *Mol Immunol* 30: 1195-204

439. Kanegae Y, Makimura, M., Saito, I. 1994. A simple and efficient method for the purification of infectious recombinant adenovirus. *Jpn J Med Sci Biol* 47: 157-66

440. Nyberg-Hoffman C, Shabram, P, Li, W., Giroux, D., Aguilar-Cordova, E. 1997. Sensitivity and reproducibility in adenoviral infectious titer determination. *Nature Med* 3: 808-11

441. Lee WC, Zhong C, Qian S, Wan Y, Gauldie J, Mi Z, Robbins PD, Thomson AW, Lu L. 1998. Phenotype, function, and in vivo migration and survival of allogeneic dendritic cell progenitors genetically engineered to express TGF-beta. *Transplantation* 66: 1810-7

442. Darlington PJ, Kirchhof, M.G., Criado, G., Sondhi, J., Madrenas, J. 2005. Hierarchical regulation of CTLA-4 dimer-based lattice formation and its biological relevance for T cell inactivation. *J Immunol* 175: 996-1004

443. Harrington KJ, Spitzweg, C., Bateman, A.R., Morris, J.C., Vile, R.G. 2001. Gene therapy for prostate cancer: current status and future prospects. *J Urology* 166: 1220-33

444. Tan PH, Beutelspacher SC, Xue SA, Wang YH, Mitchell P, McAlister JC, Larkin DF, McClure MO, Stauss HJ, Ritter MA, Lombardi G, George AJ. 2005. Modulation of human dendritic cell function following transduction with viral vectors; implications for gene therapy. *Blood*

445. Baird GS, Zacharias DA, Tsien RY. 2000. Biochemistry, mutagenesis, and oligomerization of DsRed, a red fluorescent protein from coral. *Proc Natl Acad Sci U S A* 97: 11984-9

446. Maksimow M, Hakkila K, Karp M, Virta M. 2002. Simultaneous detection of bacteria expressing GFP and DsRed genes with a flow cytometer. *Cytometry* 47: 243-7

447. Sacchetti A, Subramaniam V, Jovin TM, Alberti S. 2002. Oligomerization of DsRed is required for the generation of a functional red fluorescent chromophore. *FEBS Lett* 525: 13-9

448. Murray AG, Petzelbauer P, Hughes CC, Costa J, Askenase P, Pober JS. 1994. Human T-cell-mediated destruction of allogeneic dermal microvessels in a severe combined immunodeficient mouse. *Proc Natl Acad Sci U S A* 91: 9146-50

449. Berney T, Molano, R.D., Pileggi, A. 2001. Patterns of engraftment in different stains of immunodeficient mice reconstituted with human peripheral blood lymphocytes. *Transplantation* 72: 133-40

450. Thomsen M, Yacoub-Youssef H, Marcheix B. 2005. Reconstitution of a human immune system in immunodeficient mice: models of human alloreaction in vivo. *Tissue Antigens* 66: 73-82

451. Prochazka M, Gaskins, H.R., Shultz, L.D., Leiter, E.H. 1992. The non-obese diabetic scid mouse: model for spontaneous thymomagenesis associated with immunodeficiency. *Proc Natl Acad Sci U S A* 89: 3290-4

452. Shultz LD, Schweitzer PA, Christianson SW, Gott B, Schweitzer IB, Tennent B, McKenna S, Mobraaten L, Rajan TV, Greiner DL, et al. 1995. Multiple defects in innate and adaptive immunologic function in NOD/LtSz-scid mice. *J Immunol* 154: 180-91

453. Bosma GC, Custer RP, Bosma MJ. 1983. A severe combined immunodeficiency mutation in the mouse. *Nature* 301: 527-30

454. Dorshkind K, Keller GM, Phillips RA, Miller RG, Bosma GC, O'Toole M, Bosma MJ. 1984. Functional status of cells from lymphoid and myeloid tissues in mice with severe combined immunodeficiency disease. *J Immunol* 132: 1804-8

455. Custer RP, Bosma GC, Bosma MJ. 1985. Severe combined immunodeficiency (SCID) in the mouse. Pathology, reconstitution, neoplasms. *Am J Pathol* 120: 464-77

456. Serreze DV, Gaskins HR, Leiter EH. 1993. Defects in the differentiation and function of antigen presenting cells in NOD/Lt mice. *J Immunol* 150: 2534-43

457. Baxter AG, Cooke A. 1993. Complement lytic activity has no role in the pathogenesis of autoimmune diabetes in NOD mice. *Diabetes* 42: 1574-8

458. Serreze DV, Leiter EH. 1988. Defective activation of T suppressor cell function in nonobese diabetic mice. Potential relation to cytokine deficiencies. *J Immunol* 140: 3801-7

459. Greiner DL, Shultz LD, Yates J, Appel MC, Perdrizet G, Hesselton RM, Schweitzer I, Beamer WG, Shultz KL, Pelsue SC, et al. 1995. Improved engraftment of human spleen cells in NOD/LtSz-scid/scid mice as compared with C.B-17-scid/scid mice. *Am J Pathol* 146: 888-902

460. Murray AG, Schechner JS, Epperson DE, Sultan P, McNiff JM, Hughes CC, Lorber MI, Askenase PW, Pober JS. 1998. Dermal microvascular injury in the human peripheral blood lymphocyte reconstituted-severe combined immunodeficient (HuPBL-SCID) mouse/skin allograft model is T cell mediated and inhibited by a combination of cyclosporine and rapamycin. *Am J Pathol* 153: 627-38

461. Sultan P, Schechner JS, McNiff JM, Hochman PS, Hughes CC, Lorber MI, Askenase PW, Pober JS. 1997. Blockade of CD2-LFA-3 interactions protects human skin allografts in immunodeficient mouse/human chimeras. *Nat Biotechnol* 15: 759-62

462. Briscoe DM, Dharnidharka VR, Isaacs C, Downing G, Prosky S, Shaw P, Parenteau NL, Hardin-Young J. 1999. The allogeneic response to cultured human skin equivalent in the hu-PBL-SCID mouse model of skin rejection. *Transplantation* 67: 1590-9

463. McCune JM. 1996. Development and applications of the SCID-hu mouse model. *Semin Immunol* 8: 187-96

464. Dvorak HF, Mihm, M.C., Dvorak, A.M., Barnes, B.A., Manseau, E.J., Galli, S.J. 1979. Rejection of first-set skin allografts in man. The microvasculature is the critical target of the immune response. *J Exp Med* 150: 322-37

465. Papalois BE, Wahoff, D.C., Aasheim, T.C., Griffin, R.J., Jessurun, J., Clemmings, S.M., Field, J.M., Leone, J.P., Sutherland, D.E. 1996. Total lymphoid irradiation, without intrathymic injection of donor cells, induces indefinate acceptance of heart but not islet or skin allografts in rats. *Transpl Int* 9: S372-S8

466. Alegre ML, Peterson LJ, Jeyarajah DR, Weiser M, Bluestone JA, Thistlethwaite JR. 1994. Severe combined immunodeficient mice engrafted with human splenocytes have functional human T cells and reject human allografts. *J Immunol* 153: 2738-49

467. Mosier DE, Gulizia RJ, Baird SM, Wilson DB. 1988. Transfer of a functional human immune system to mice with severe combined immunodeficiency. *Nature* 335: 256-9

468. del Real G, Llorente M, Bosca L, Hortelano S, Serrano A, Lucas P, Gomez L, Toran JL, Redondo C, Martinez C. 1998. Suppression of HIV-1 infection in linomide-treated SCID-hu-PBL mice. *Aids* 12: 865-72

469. Somasundaram R, Jacob L, Herlyn D. 1995. Tetanus toxoid-specific T cell responses in severe combined immunodeficiency (SCID) mice reconstituted with human peripheral blood lymphocytes. *Clin Exp Immunol* 101: 94-9

470. Hasui M, Miyawaki T, Ichihara T, Niida Y, Iwai K, Yachie A, Seki H, Taniguchi N. 1994. Mature helper T cell requirement for immunoglobulin production by neonatal native B cells injected intraperitoneally into severe combined immunodeficient (SCID) mice. *Clin Exp Immunol* 95: 357-61

471. Murray A, Schechner, J.S., Epperson, D.E., Sultan, P., McNiff, J.M., Hughes, C.C., Lorber, M.I., Askenase, P.W., Pober, J.S. 1998. Dermal microvascular injury in the human peripheral blood lymphocyte reconstituted-severe combined immunodeficient (HuPBL-scid) mouse/skin allograft model is T cell mediated and is inhibited by a combination of cyclosporin and rapamycin. *Am J Pathol* 153: 627-38

472. Shultz LD, Banuelos SJ, Leif J, Appel MC, Cunningham M, Ballen K, Burzenski L, Greiner DL. 2003. Regulation of human short-term repopulating cell (STRC) engraftment in NOD/SCID mice by host CD122+ cells. *Exp Hematol* 31: 551-8

473. Christianson SW, Greiner DL, Hesselton RA, Leif JH, Wagar EJ, Schweitzer IB, Rajan TV, Gott B, Roopenian DC, Shultz LD. 1997. Enhanced human CD4+ T cell engraftment in beta2-microglobulin-deficient NOD-scid mice. *J Immunol* 158: 3578-86

474. Tary-Lehmann M, Lehmann, P.V., Schols, D., Roncarolo, M.G., Saxon, A. 1994. Anti-SCID mouse reactivity shapes the human CD4+ T cell repertiore in hu-PBL-SCID chimeras. *J Exp Med* 180: 1817-27

475. Sandhu J, Shpitz B, Gallinger S, Hozumi N. 1994. Human primary immune response in SCID mice engrafted with human peripheral blood lymphocytes. *J Immunol* 152: 3806-13

476. Cao T, Leroux-Roels G. 2000. Antigen-specific T cell responses in human peripheral blood leucocyte (hu-PBL)-mouse chimera conditioned with radiation and an antibody directed against the mouse IL-2 receptor beta-chain. *Clin Exp Immunol* 122: 117-23

477. Murphy WJ, Bennett M, Anver MR, Baseler M, Longo DL. 1992. Human-mouse lymphoid chimeras: host-vs.-graft and graft-vs.-host reactions. *Eur J Immunol* 22: 1421-7

478. Takayama T, Kaneko, K., Morelli, A.E., Li, W., Tahara, H., Thomson, A.W. 2002. Retroviral delivery of transforming growth factor-beta1 to myeloid dendritic cells: inhibition of T-cell priming ability and influence on allograft survival. *Transplantation* 74: 112-9

479. Gorczynski RM, Bransom J, Cattral M, Huang X, Lei J, Xiaorong L, Min WP, Wan Y, Gauldie J. 2000. Synergy in induction of increased renal allograft survival after portal vein infusion of dendritic cells transduced to express TGFbeta and IL-10, along with

administration of CHO cells expressing the regulatory molecule OX-2. *Clin Immunol* 95: 182-9

Thesis Erratum

The following changes to the thesis were made after final printing...

Amendments to text

- P4 2nd line: 'best' should be added before 'characterised'.
- P5 2nd paragraph, line 1: agonists should be antagonists.
- P12 section 1.5.3.4: 'high levels of CD80/86 on activated T cells' should read 'high levels of CD80/86 on APC'
- P16 4th last line: 'deceased' should be 'decreased'.
- P19 last sentence: should read 'While IL10 is able to have **a** direct inhibitory effect **on** $CD4^+$ T cells...'
- P20 line 12: The word 'as' should be omitted from 'however, as anti-CD3...'.
- P21 last paragraph: NKκβ should read NFκB.
- P23 3rd paragraph: 'IL-12 secretion promoting...' should read 'IL-2 secretion and IL-12 receptor expression promoting...'
- P35: The following sentence has been added to Table 1.2; 'Lentiviral vectors have been developed from Retroviral vectors to overcome the requirement of cell division for transfection'.
- P37 last sentence: 'CDs' should read 'DCs'.
- P39 line 17: 'be' should be inserted in 'may **be** ineffective...'.
- P39 line 18: 'duel' should read 'dual'.
- P45 'MHC Class II DP' should read 'MHC Class II DQ/DR'
- P46: CC21 acknowledged as an anti-bovine antibody that cross-reacts with sheep.
- P48 catalogue numbers have been added for MEM (61100-061), RPMI (1060120), methionine/cysteine deficient PRMI (16464).
- P54: 'guanidine thiocyantate' should be 'guanidine thiocyanate'.
- P55: 'Dnase' should read 'DNase'
- P69 2.3.2.10: Kanamycin should be deleted from this entire paragraph.
- P95: 'Epstien-Barr' should read 'Epstein-Barr'.
- P100: The following sentence has been added to line 15; 'While this study has provided some mechanisms by which NK cells influence the interactions between DC and T cells, the extent to which cell-contact or cytokines are involved has not been investigated.'
- P103 4.2.3: 'SBUT6' should be '20.27'.
- P113: '(5×10^6)' has been added to the first paragraph as the quantity of DC injected in 4.3.3.
- P113. The last two sentences of 4.3.3. should read 'Compared with cells isolated prior to the injection, a significant shift in fluorescence was observed within 4 h, peaking at 24 h (**figure 4.3.c.**). The presence of PKH26 labeled cells began to dissipate after 40 h.'
- P114 line 2: '($p < 0.05$, paired student T test)' has been added.
- P135: The following sentences have been added... 'Cloning of CTLA4-Ig into the pSecTagB vector inadvertently led to the presence of two signal peptides, however given the functionality of the condictioned media of transfected cells in the MLR (**figure 5.4**), this does not appear to have influenced the secretion or activity of

CTLA4-Ig. Furthermore, cloning of CTLA4-Ig from pSecTagB into an adenoviral construct will exclude the Igκ leader sequence.'

- P135 2nd last line: The words 'The higher level of' has been deleted.
- P153: 'prokoking' should read 'provoking'.

General amendments

- Where 'DNTPs' is written, should be 'dNTPs'.
- Where 'Rnase A' is written, should be 'RNase A'.
- Where 'spleenocyte' is written, should be 'splenocyte'.
- Where '*E.Coli*' is written, should be '*E.coli*'.

Amendments to figure legends

- Figure 1.2 legend: 'signaling' removed, duplicated in text.
- Figure 3.3 legend: 'anti-CTLA4-Ig antibody' should read 'anti-CTLA4 antibody'
- Figures 3.7 and 3.8: DC used were mature DC.
- Figure 4.6: Histology sections should be labeled D2 and D7 not D7 and D14.
- Figure 5.2: 'Tg1α E.Coli' should read 'TG1α *E.coli*'.
- Figure 5.9: The sentence 'FITC conjugated antibodies were used to amplify the signal of the bound protein' was added to the figure legend.
- Figure 5.11: 'Histograms are representative of two independent experiments.' Has been added to the legend.
- Figure 6.7 legend: The sentence 'PCR amplification with β-Actin housekeeping primers confirmed the equivalent amount of cDNA in each sample (data not shown).' has been added.